

**Maynooth
University**

National University
of Ireland Maynooth

Coupled Models of Structured Ecological Systems: Patch Dynamics, Population Demography, and Stochastic Interactions

*A thesis submitted in fulfillment of the requirements
for the degree of Doctor of Philosophy by*

Blake McGrane-Corrigan

Department of Mathematics and Statistics
National University of Ireland, Maynooth
Ollscoil na hÉireann, Má Nuad

Supervisors:

Dr. Rafael de Andrade Moral

Prof. Oliver Mason

October 2024

A Wind that rose
Though not a Leaf
In any Forest stirred
But with itself did cold engage
Beyond the Realm of Bird —
A Wind that woke a lone Delight
Like Separation's Swell
Restored in Arctic Confidence
To the Invisible —

- Emily Dickinson [74]

Declaration

I declare that the work in this thesis is my own. I confirm that:

- This work was done entirely while in candidature for a research degree at the Department of Mathematics and Statistics of Maynooth University.
- This thesis has been prepared in accordance with the PhD regulations of Maynooth University and is subject to copyright. For more information, see PhD Regulations (December 2022).
- This work was supported by a Taighde Éireann – Research Ireland, Government of Ireland Postgraduate Scholarship (GOIPG/2020/939).



- Where I have consulted the published work of others, this is always clearly attributed.

Blake McGrane-Corrigan

29th October 2024

Contributions

Parts of this thesis appeared in the following:

Book Chapter

McGrane-Corrigan, B. and Mason, O., 2023. On Matrix Stability and Ecological Models. In *Modelling Insect Populations in Agricultural Landscapes* (pp. 115-147). Springer, Cham.

Journal Article

McGrane-Corrigan, B., Mason, O. and de Andrade Moral, R., 2024. Inferring stochastic group interactions within structured populations via coupled autoregression. *Journal of Theoretical Biology*, p.111793.

· Code: https://github.com/blakeacorrigan/group_interactions.git

de Godoy, I.B.S., McGrane-Corrigan, B., Mason, O., de Andrade Moral, R. and Godoy, W.A.C., 2023. Plant-host shift, spatial persistence, and the viability of an invasive insect population. *Ecological Modelling*, 475, p.110172.

· Code: https://github.com/blakeacorrigan/plant_host_shift.git

Pre-Print

McGrane-Corrigan, B., de Andrade Moral, R. and Mason, O., 2024. A density-dependent metapopulation model: Extinction, persistence and source-sink dynamics.

Conference or Seminar Presentation

2024

Robust Diffusive Stability and Common Lyapunov Functions — SIAM Conference on Applied Linear Algebra (LA24), Sorbonne University, Paris, France.

Stability for a discrete-time nonlinear dispersal model — 15th Conference on Dynamical Systems Applied to Biology and Natural Sciences, Lisbon University. Lisbon, Portugal.

2023

Persistence for Unimodal Population Maps via Dispersal — Mathematical Ecology Conference, University of Pittsburgh., Pittsburgh, Pennsylvania, USA.

Inferring Predator-Prey Interactions — 43rd Conference of Applied Statistics in Ireland, Limerick, Ireland.

Diagonal Stability and Lotka-Volterra Systems — Graduate Seminar Series, Department of Mathematics and Statistics, Maynooth University.

2022

Time Series, Coupled Autoregression and Community Dynamics — Young Irish Statistical Association Conference, University of Limerick, Limerick, Ireland (winner of the poster competition).

Robust Diffusive Stability, Common Lyapunov Functions and Leslie Matrices — 24th Conference of the International Linear Algebra Society, University of Galway, Galway, Ireland.

Quantifying the temporal interactions of animal groups via coupled log-linear autoregression — 42nd Conference of Applied Statistics in Ireland, Cork, Ireland.

Nonlinear Matrix Models, Dispersal-Driven Growth and Patch Persistence — Student Seminar Series, Hamilton Institute, Maynooth University, Maynooth, Kildare, Ireland.

Stability and Persistence for Matrix Models — Graduate Seminar Series, Department of Mathematics and Statistics, Maynooth University, Maynooth, Kildare, Ireland.

Contents

Declaration	ii
Contributions	iii
Abstract	ix
Acknowledgements	x
List of Figures	xi
List of Tables	xvi
1 Introduction	1
1.1 What is a Structured Population?	1
1.2 Why Ecological Models?	2
1.3 Thesis Outline	3
2 Preliminaries	5
2.1 Notation and Definitions	5
2.2 Discrete-Time Dynamical Systems	7
2.2.1 Equilibria and Lyapunov Stability	7
2.2.2 Positive Systems	7
2.2.3 Lyapunov Functions	9
2.2.4 Periodic Solutions and Chaotic-Type Dynamics	12
2.2.5 Bifurcation Analyses	12
2.2.6 The Logistic Map	13
2.3 Persistence	14
2.4 Positive Integer-Valued Time Series	16
2.4.1 The Markov Property	17
2.4.2 Bayesian Inference	17
2.5 Summary	20
3 Structured Population Models	21
3.1 Linear Systems	21
3.1.1 D-Stability	22
3.1.2 Stage Structure	23

3.2	Density Dependence	27
3.2.1	Nonlinear Systems	28
3.2.2	A Biennial Plant Model	29
3.2.3	The LPA Model	30
3.3	Quiescence	31
3.3.1	Host-Parasitoid Dynamics	33
3.4	Diffusion	34
3.4.1	Turing Instability	34
3.4.2	Diffusively Coupled Systems	35
3.5	Patchy Dispersal	37
3.6	Dispersal-Driven Growth	39
3.7	Stochasticity and Interactions	41
3.7.1	Community Dynamics	42
3.7.2	Observation-Driven Models	44
3.8	Summary	45
4	Costless and Density-Dependent Movement of Invasive Populations	46
4.1	Motivation	46
4.2	The Two-Patch Model	47
4.3	Patch Dynamics	48
4.4	Movement Dynamics	50
4.4.1	Passive Invasion	51
4.4.2	Density-Dependent Invasion	52
4.5	Outbreak and Conservation Examples	56
4.5.1	The Rescue Effect	57
4.5.2	Boom-Bust Dynamics	59
4.5.3	Spatial Synchrony	59
4.5.4	Transience	60
4.6	Plant Host-Shift: A Case Study	62
4.6.1	Focal Species	62
4.6.2	Experimental Setting	62
4.6.3	The Prout and McChesney Model	63
4.6.4	Numerical Simulations	63
4.6.5	Bifurcation Analysis	64
4.7	Summary	68
5	Costly and Density-Dependent Movement of Heterogeneous Metapopulations	70
5.1	Motivation	70
5.2	The Metapopulation Model	71

5.2.1	Regional Maps	71
5.2.2	Dispersal Costs	72
5.2.3	The Coupled System	73
5.3	Stability and Persistence	75
5.3.1	Extinction	75
5.3.2	Coexistence	77
5.4	Sources and Sinks: A Numerical Study	82
5.4.1	Regional Dynamics	83
5.4.2	Density-Dependent Dispersal	83
5.4.3	Global Stability Dichotomy	85
5.4.4	Positive Fixed Point Existence	86
5.4.5	The Total Population Size	87
5.4.6	Bifurcation Analyses	89
5.5	Summary	93
6	Diffusive Stability and Growth for Populations with Demographic Structure	94
6.1	Motivation	94
6.2	The Diffusive Dispersal Model	96
6.3	Common Lyapunov Functions	98
6.3.1	Copositive Lyapunov Functions	98
6.3.2	The Lyapunov Inequality	99
6.3.3	Quadratic Lyapunov Functions	101
6.3.4	Diagonal Lyapunov Functions	102
6.4	Applications	106
6.4.1	Commuting Matrices	106
6.4.2	Planar Systems	108
6.5	Diffusive Growth	109
6.5.1	Convex Hull	110
6.5.2	Asymmetric Dispersal	113
6.6	Stage-Structured Diffusion	114
6.6.1	Leslie Matrices	114
6.6.2	The LPA Model	118
6.6.3	An Invasive Bullfrog Model	120
6.7	Summary	121
7	Stochastic Group Interactions within Social Animal Populations	122
7.1	Motivation	122
7.2	Group Interactions	123
7.2.1	Low Counts and Zero Observations	124

7.3	The Coupled Autoregressive Model	124
7.3.1	The Observation Processes	125
7.3.2	The Intensity Processes	127
7.3.3	Model Fitting	129
7.4	Simulation Studies	129
7.5	Predator-Prey Dynamics: A Case Study	133
7.5.1	Group Formation and Splitting	134
7.5.2	Results and Interpretation	135
7.6	Quantifying Group Interactions	140
7.6.1	Correlation Approximation	141
7.6.2	Theoretical Interpretation	145
7.7	Summary	151
7.8	Appendix	152
8	Future Directions	157
	Bibliography	161

Abstract

In order to study their temporal dynamics, the size, density or abundance of populations are often monitored over discrete time steps. Many of these populations tend to have internal structure or interconnections that affect individuals at various spatiotemporal scales, such as developmental stages, resource preferences, group interactions and movement. In this thesis we are mainly concerned with modelling the dynamics of such structured populations in discrete-time, from both deterministic and stochastic perspectives. In Chapter 1 we motivate the problems we are interested in throughout this thesis. In Chapter 2 we give some technical background needed in order for this thesis to be reasonably self-contained. In Chapter 3 we discuss various existing frameworks and results within the literature related to structured population models, while also demonstrating how matrix stability plays an important role in understanding such systems. In Chapter 4 we propose a costless, density-dependent invasion model, where a population moves between two resources. We explore some of the properties of this model, both theoretically and numerically, in the context of a species expanding its habitat or range. We then apply this model to an pest case study in order to further understand how host switching can affect long-term population viability. In Chapter 5 we propose a model of costly, density-dependent dispersal between a finite number of regions. We study its stability and persistence properties, and numerically show how it relates to various source-sink scenarios. In Chapter 6 we focus on deriving sufficient conditions for the stability of the extinction equilibrium for coupled linear time-invariant systems, which is robust under diffusive couplings, so-called robust diffusive stability (RDS). This model corresponds to demographically-structured populations diffusively dispersing between habitats, such as species migration for example. We discuss the role of the existence/nonexistence of copositive, quadratic and diagonal Lyapunov functions in determining RDS. We then discuss the anthesis of RDS, diffusive growth. Throughout, we apply our results to some commonly used matrix population models. In Chapter 7 we propose a stochastic model that aims to capture the interactions between animal groups within a social population. We conduct simulation scenarios and fit this model to real-world data, to show its applicability. We then discuss the findings of this model fit in the context of ecological theory. We derive an approximation to the marginal group correlation for a simpler model, which describes their net interactions over an observation period. We then theoretically discuss its interpretation in multiple predator-prey scenarios. Finally, in Chapter 8, we conclude by discussing various extensions and open questions suggested by the results presented throughout this thesis.

Acknowledgements

Firstly, I want to thank Rafael and Ollie, for their continued support over the past four years. You both kept with me, even through my indecisiveness, and I am grateful for your diligence, patience, and honesty.

I am beyond grateful to my mam, Jackie, and my dad, Paddy. Your unwavering encouragement and warm support over the years has made all the difference. You have always patiently nurtured my varying passions and interests. I am so thankful for all the ways you have believed in me.

I want to thank Orla for continuing to enrich my life every day. Whenever the work got overwhelming, you always reminded me that "*today is just a day*". If it wasn't for your resilience and compassion I could not have finished this.

I want to thank Akash and YC for encouraging me to not take myself too seriously, for the basketball, talks on the landing, trips, and for making our apartment feel like a home. I want to thank Evan for our too infrequent phone calls and for just being one of the most genuine people I know. I want to thank Fergal and Eleni for the laughs, pints, BBQs, parties, game nights, and that one quiz win. I want to thank Jonny for our chats, for your unguardable hook shot, and for Jeff. I want to thank Ahmed (technically) for our long conversations, walks, and National Concert Hall gigs. I want to thank Podhl for helping me de-stress at all the bouldering sessions we've had over the years.

I owe a big thank you to the rest of my family and friends, both old and new, whose kindness and support have made these past four years so memorable.

I also would like to gratefully acknowledge the financial support of the Irish Research Council. I would finally like to thank my examiners, Kevin Burke and David Malone, for their thorough feedback and insightful comments.

List of Figures

2.1	A matrix $A \in \mathbb{R}^{n \times n}$ is Hurwitz if $\sigma(A) \subset \mathbb{C}_-$ and Schur if $\sigma(A) \subset \mathbb{D}_1$. Here \mathcal{R} and \mathcal{I} respectively denote the real and imaginary axis.	6
2.2	x^* is Lyapunov stable if, for any $\epsilon > 0$ we choose there is some $\delta > 0$ so that for any $x(0) = x_0$ within δ of x^* , the trajectory, $x(t)$, remains within ϵ of x^* for all $t \geq 0$	8
2.3	Illustration of the logistic map $y = ax(1-x)$, where $a > 0$ (solid). This map has a unique maximum at $x = 1/2$ (dotted) which is $y = a/4$ (dashed). . . .	14
2.4	One-parameter bifurcation diagram for $a \in [0, 4]$ vs solutions, x , of (2.2.4).	14
4.1	Conceptual diagram of system (4.2.1), where $f_i(x_i)$ and $d_i(x_i)$ respectively describe the dynamics on and dispersal from patch i . The proportion of individuals remaining on patch i is $1 - d_i(x_i)$	48
4.2	Illustration of a Ricker map $y = \alpha x \exp(-\beta x)$, where $\alpha, \beta > 0$ (solid line). This map has a unique maximum at $x = \beta^{-1}$ (dashed line) which is $y = \alpha/(e\beta)$ (dotted line).	49
4.3	Illustration of a map of the form (4.5.1), where $r \in (0, 1)$ and $u > 0$. The solid black curve, $y = 1 - r \exp(-ux)$, represents positive density-dependent dispersal, with the dashed black curve, $y = r \exp(-ux)$, representing the proportion of individuals remaining. The grey line represents $y = 1$	57
4.4	Simulations of (4.3.2) for $i = 1, 2$ (Isolated) and (4.2.1) (Coupled), for 30 time steps. In both simulations we set $x_0 = (13.7, 31.6)$, $\beta_1 = 0.01, \beta_2 = 0.044, \alpha_1 = 0.7$ and $\alpha_2 = 16.5$. For the coupled model we also set $\mu_1 = 0.05, \mu_2 = 0.03, r_1 = 0.5, r_2 = 0.7$. In each plot, the grey and black lines respectively represents trajectories for region 1 and 2.	58
4.5	Simulation of (4.2.1) for 50 time steps. We set $x_0 = (0, 60), \beta_1 = 0.01, \mu_1 = 0.05, \beta_2 = 0.04, \mu_2 = 0.03, \alpha_1 = 41.44, \alpha_2 = 0.86, r_1 = 0.5,$ and $r_2 = 0.7$. In each plot, the grey and black lines respectively represents trajectories for region 1 and 2.	59
4.6	Simulations of (4.2.1) for 20 time steps. In all simulations we set $x_0 = (94, 56), \beta_1 = 0.01, \mu_1 = 0.01, \beta_2 = 0.06, \mu_2 = 0.05, \alpha_1 = 0.6, \alpha_2 = 25$. For $r_1 = r_2 = r$, we let $r = 0.1$ (Low), $r = 0.5$ (Moderate) and $r = 0.9$ (High). In each plot, the black and grey lines respectively represents trajectories for region 1 and 2.	60

4.7	Simulations of (4.2.1) for 150 time steps. In both simulations we set $x(0) = (65, 51)$, $\beta_1 = 0.01$, $\beta_2 = 0.06$, $\mu_1 = 0.21$, $\mu_2 = 0.34$, $r_1 = 0.5$, $r_2 = 0.7$. In the top plot we set $\alpha_1 = 16.7$ and $\alpha_2 = 13.5$. In the bottom plot we set $\alpha_1 = 21.3$ and $\alpha_2 = 10.7$. In each plot, the grey and black lines respectively represents trajectories for region 1 and 2.	61
4.8	Simulations of (4.2.1) for 52 (weekly) time steps, for strawberry (right) and raspberry (left) patches. In all simulations we set $x(0) = (20, 56)$. We let $\mu_1, \mu_2 \in \{0.001, 0.250, 0.500, 0.750, 1.000\}$ for three scenarios: $\alpha_i = R_i F_i S_i$ (top), $\alpha_i = R_i F_i S_i / 2$ (middle) and $\alpha_i = 10 R_i F_i S_i$ (bottom)1.	65
4.9	Bifurcation diagram for the $(R_1 F_1 S_1, R_2 F_2 S_2)$ -parameter space, showing the number of unique population sizes according to the colour gradient (stable fixed point for values of 1 and periodic orbits for higher values than 1). We considered the last 100 observations after iterating our model for 100,000 generations. Initial conditions where $x(0) = (76, 42)$	66
4.10	Simulations of (4.2.1) for 52 (weekly) time steps, for strawberry (black) and raspberry (grey) patches. We set $x(0) = (76, 42)$, with all other parameters as in Fig. 4.9 for the following scenarios: $\alpha_1 = 5, \alpha_2 = 6$ (Coexistence); $\alpha_1 = 10.3, \alpha_2 = 12.6$ (Period 2); $\alpha_1 = 13, \alpha_2 = 7$ (Period 4); and $\alpha_1 = 30, \alpha_2 = 25$ (Chaotic).	67
4.11	Bifurcation diagram for the (μ_1, μ_2) -parameter space, showing the number of unique population sizes according to the colour gradient (stable fixed point for values of 1 and periodic orbits for higher values than 1). We considered the last 100 observations after iterating our model for 100,000 generations. Initial conditions where $x(0) = (73, 25)$	68
5.1	Illustration of the functions h_1 (dotted), h_2 (solid) and h_3 (dashed).	73
5.2	Conceptual diagram of system (5.2.3) when $n = 3$, where $f_i(x_i)$ and $d_{ij}(x_j)$ respectively describe the dynamics on and dispersal from patch j to i for $i \neq j$. When $i = j$ each d_{ii} describes the proportion of individuals remaining on patch i	74
5.3	Illustration of Ω_1 in the proof of Theorem 5.3.5 for $n = 2$	80
5.4	Illustration of $y = d(x) := a(1 + \exp(-b(x - c)))^{-1}$ (grey solid curve) for $a \in (0, 1)$ and $b, c \geq 0$. The dotted grey line is the curve $y = a$. The dashed grey line is the curve $y = d(0) = a(1 + \exp(bc))^{-1}$. The dashed black line is the curve $y = d(c) = a/2$. The dotted black line is the curve $x = c$	84

5.5 Simulated periodic dynamics of (5.4.1) for (left) $a_1 = 50$ and (right) $a_1 = 750$. We plot the last 10 out of $T = 500,000$ time steps. Here, dark grey is region 1 and black is region 2. In both simulations we let $a_2 = 0.4, b_1 = 0.04, b_2 = 0.01, r_{11} = 0.2, r_{22} = 0.3, r_{12} = 0.6, r_{21} = 0.7, k_{11} = k_{22} = k_{12} = k_{21} = 0.5, s_{11} = 10, s_{22} = 6, s_{12} = 3$ and $s_{21} = 12$. Initial conditions in both were $(x_1(0), x_2(0)) = (92, 103)$ 86

5.6 Simulations of (5.4.1) for various positive initial conditions $x(0) \in [1, 30]^2$, where dark grey (left) and black (right) trajectories respectively correspond to regions 1 and 2. We let $a_1 = 4, a_2 = 0.9, b_1 = 0.04, b_2 = 0.01, r_{12} = r_{21} = 0.1, r_{11} = r_{22} = 0.75, k_{12} = k_{21} = k_{11} = k_{22} = 1$ and $s_{12} = s_{21} = s_{11} = s_{22} = 1$. We increased the number of iterations for each plot to 100,000 to ensure convergence to the fixed point approximately given by $(x_1^*, x_2^*) \approx (28.17, 9.52)$ 87

5.7 Plot of $x_1(T) + x_2(T)$ when patches are connected by dispersal (solid dark grey) and when isolated (dashed black) after $T = 10,000$ time steps. Initial conditions, $(x_1(0), x_2(0)) = (55, 54)$ 88

5.8 Plot of $x_1(T) + x_2(T)$ when two source regions are connected by dispersal (solid dark grey) and when isolated (dashed black) after $T = 10,000$ time steps. Initial conditions, $(x_1(0), x_2(0)) = (55, 54)$, were as in Fig. 5.7. . . . 89

5.9 Simulated dynamics of (5.4.1) for the initial condition $(x_1(0), x_2(0)) = (131, 19)$, where black and dark grey trajectories respectively correspond to region 1 and 2, where $T = 500,000$. We let $a_1 = 90, a_2 = 0.14$, while all other parameters were as in Fig. 5.5. The last 50 time steps are plotted. . . . 90

5.10 Bifurcation diagram for the (a_1, a_2) -plane where regions 1 and 2 were respectively given by Ricker and Hassel-1 maps, for $a_1 \in (1, 300], a_2 \in (0, 1)$. Initial conditions were given by $(x_1(0), x_2(0)) = (131, 19)$. Other parameter values were as in Fig. 5.5. The colour-number legend shows the period of the various periodic trajectories (with periods 2-8), with 1 representing convergence to a unique fixed point (either extinction or a positive equilibrium), and > 8 representing periods higher than 8 and possibly chaotic dynamics. Parameter grid resolution was 150×150 91

5.11 Bifurcation diagrams of $a_2 \in (0, 1)$ versus x_1 (dark grey) and x_2 (black), where regions 1 and 2 were respectively Ricker and Hassell-1 maps. We considered the last 100 observations after 10,000 iterations when (left) $a_1 = 10$ and (right) $a_1 = 100$. Initial conditions where $(x_1(0), x_2(0)) = (20, 10)$ for both scenarios. 92

5.12 Bifurcation diagrams of $a_1 \in (1, 150)$ versus x_1 (dark grey) and x_2 (black), where regions 1 and 2 were respectively Ricker and Hassell-1 maps. We considered the last 100 observations after 10,000 iterations when (left) $a_2 = 0.1$ and (right) $a_2 = 0.9$. Initial conditions where $(x_1(0), x_2(0)) = (20, 10)$ in both scenarios. 92

6.1 Conceptual diagram of system (6.2.1), where A and B describe the linear dynamics of each regional population and D describes the diffusive movement between each of the demographic classes. 97

6.2 Directed graph corresponding to the extended Leslie matrix (6.6.2). 115

7.1 Conceptual diagram of how X and Y are coupled, which includes intraspecific components (7.3.7), auxiliary components (7.3.8), and a interspecific component (7.3.11). 128

7.2 Three randomly selected time series of three groups (main) and the auxiliary population (inset) for scenarios 2, 4 and 5. 131

7.3 Wolf pack (main) and elk (inset) abundances in YNP from 1996-2016. Each grey line represents one pack abundance time series. 134

7.4 Prior- posterior overlap for fixed effects and hyperparameters. The black curve is the prior distribution and grey curve is estimated posterior density. We set $\theta_\mu \sim \mathcal{N}(0, 100^2)$ for $\theta_\mu \in M \cup \{\omega^Y, \lambda^Y, \gamma\}$ and $\theta_\sigma \sim \mathcal{N}^+(0, 100^2)$, for $\theta_\sigma \in \Sigma$ 138

7.5 Violin plots for $\omega^X := \{\omega_1^X, \dots, \omega_{42}^X\}$, $\lambda^X := \{\lambda_1^X, \dots, \lambda_{42}^X\}$, $\psi := \{\psi_1, \dots, \psi_{42}\}$ and $\delta := \{\delta_1, \dots, \delta_{42}\}$. Each plot shows the posterior density estimates for realisations of the random effects for all 42 wolf packs, with the respective 0.5-quantiles. 140

7.6 Illustration of the μ_ψ - μ_δ parameter space for some fixed $i \in \{1, \dots, g\}$, treating all parameters except μ_ψ and μ_δ as known and fixed. Dark (light) grey shaded areas indicate where $\tilde{\rho} > 0$ ($\tilde{\rho} < 0$). The grey dotted line represents the line $-A_i - \mu_\delta B_i - \mu_\psi C_i = 0$. The black dashed line indicates that $\mu_\psi \neq 0$ (by assumption). The white circle is the point $(\mu_\psi, \mu_\delta) = (-A_i/C_i, 0)$. 147

7.7 Contour plot of $(\mu_1^X, \mu_2^X) \in (1, 2.25]^2$ which result in $\tilde{\rho} \in (0, 1)$ (black) and $\tilde{\rho} \in (-1, 0)$ (dark grey), where $\mu_\delta = 0.0001$, $\mu_\psi = -0.62$, $\mu_\lambda = 1$, $\mu_\omega = 0.001$ and $\mu_Y = 100$ 149

7.8 Boxplots of bias and relative bias for $\theta \in M \cup \Sigma \cup \{\gamma, \lambda^Y, \omega^Y\}$ for S1. . . . 152

7.9 Boxplots of bias and relative bias for $\theta \in M \cup \Sigma \cup \{\gamma, \lambda^Y, \omega^Y\}$ for S2. . . . 153

7.10 Boxplots of bias and relative bias for $\theta \in M \cup \Sigma \cup \{\gamma, \lambda^Y, \omega^Y\}$ for S3. . . . 153

7.11 Boxplots of bias and relative bias for $\theta \in M \cup \Sigma \cup \{\gamma, \lambda^Y, \omega^Y\}$ for S4. . . . 154

7.12 Boxplots of bias and relative bias for $\theta \in M \cup \Sigma \cup \{\gamma, \lambda^Y, \omega^Y\}$ for S5. . . . 154

7.13 Bivariate plots for $\{\omega^Y, \lambda^Y, \mu_\psi, \mu_\delta\}$ from simulation No. 20 for S1. 155

7.14 Bivariate plots for $\{\omega^Y, \lambda^Y, \mu_\psi, \mu_\delta\}$ from simulation No. 20 for S2. 155

7.15 Bivariate plots for $\{\omega^Y, \lambda^Y, \mu_\psi, \mu_\delta\}$ from simulation No. 20 for S3. 156

List of Tables

4.1	Empirical parameters estimates.	64
7.1	True parameter values chosen for simulation scenarios S1—S5.	130
7.2	RMSE for posterior mean estimates in scenarios 1 – 5 calculated across 100 different simulations.	132
7.3	Example of how A and B allow for group formation and splitting, where X_t is a count random variable at time $t \geq 0$	136
7.4	Parameter posterior mean estimates, with their respective 95% credible inter- val (CI), prior-posterior overlap (PPO) and interpretations for YNP wolf-elk case study.	137

1. Introduction

The natural world has been profoundly shaped by centuries of human activity, which has unfortunately led to habitat fragmentation, ecological degradation, and the spread of zoonotic diseases [47, 216, 250]. Although these actions have inadvertently benefitted certain species, particularly through the introduction and proliferation of invasive populations, they have also had devastating impacts on vulnerable and endangered populations [14, 27, 33, 96]. Many of these species, after enduring decades of eradication and decline, now require reintroduction into their native habitats, as well as additional conservation efforts to ensure persistence [254]. To effectively conserve indigenous populations, eradicate pests, and keep pandemics at bay, it is crucial to understand the internal processes of species, including their demographic makeup, movement dynamics, and ecological interactions [240]. By doing so, we can make informed decisions that have the potential to help promote biodiversity, support ecosystem resilience, and ensure a sustainable coexistence between humans and wildlife.

1.1. What is a Structured Population?

Within a population, individuals may form clusters, such as herds, packs or colonies. They can also be distributed across localised regions in space or categorised into different life stages or demographic groups. To understand how this internal population structure emerges, we will explore various models of structured population dynamics. Specifically, we will discuss three key types of population structure: spatial, demographic, and social.

By spatial structure we mean the arrangement of individuals in different geographic areas. Spatial models can represent movement processes such as dispersal from natal groups and can also illustrate fragmented landscapes where individuals navigate between distinct geographic areas. By analysing these spatial dynamics, we can gain insights into how environmental features affect population viability and connectivity [93]. Understanding these spatial patterns not only helps in predicting how populations will respond to changes in habitat but also can inform conservation strategies aimed at ensuring long-term sustainability.

Demographic structure concerns the composition of a population in terms of age, sex, and other demographic factors. Understanding how these populations develop over time

is essential. For example, variations in birth and death rates across different age groups can lead to significant shifts in population dynamics, affecting growth rates and ecological stability [62]. By examining demographic models, we can better predict population trends and develop effective management plans that account for life cycle changes and environmental pressures [114, 256]. This understanding can ultimately aid in tailoring conservation efforts to specific population needs, ensuring that vulnerable groups are supported and maintained within their ecosystems.

Finally, social structure concerns the relationships and interactions among individuals within a population. Many social species not only move between subgroups but also engage with these groups and other populations through cooperation, competition, and predation [217]. Understanding these dynamics is crucial, as they can significantly influence individual behaviour and overall population dynamics. By exploring such structure, we can uncover the complexities of social interactions and their effects on population resilience. Additionally, recognising the role of social dynamics can inform management practices, allowing us to develop interventions that enhance cooperation and reduce conflict within populations, ultimately contributing to their stability and success in changing environments [254].

1.2. Why Ecological Models?

In [290] the author explains that an ecosystem can be viewed as a collection of subsystems and that the dynamics of each subsystem can be meaningfully analysed on its own. A population may be thought of in this way. However, in reality these subsystems do not exist in isolation, but involve many complex interconnected processes and structures that contribute to population fitness and survival. While theoretical models may overlook some nuances of real-world ecological systems, they provide insights into the potential mechanisms that drive population changes and qualitative behaviour. In addition to helping understand these population's dynamics, they also play a crucial role in informing natural resource management, laboratory experiments, and field studies, which sometimes face challenges such as negligent practices and ethical concerns, including animal welfare issues [42, 203, 230]. Thus models can serve as a valuable starting point for understanding the dynamics of fragile biological systems. They also provide insights that help shape conservation policies and offer additional perspectives alongside empirical findings, deepening our understanding of the many ecological systems that surrounds us [182].

1.3. Thesis Outline

In Chapter 2 we will introduce notation and discuss some background that is referred to in the rest of this thesis. In Chapter 3 we will discuss some models and results for modelling structured populations in discrete time. This is to give some context to the ideas presented in the rest of this thesis and to highlight some of the theoretical and ecological concepts encountered. In particular we will review concepts such as diffusively coupled systems, quiescence, diffusion, stage-structure, stochastic interactions and count time series.

In Chapter 4 we will investigate, both analytically and numerically, the qualitative dynamics of a discrete-time model of density-dependent, costless dispersal between two regions, in the context of an invasive species colonising a new area, where the dynamics on each patch is of the same form. We first explain the model setup, including regional and dispersal dynamics. We prove some results related to stability and persistence. We then describe some real-world phenomena that our model can capture, including transience and the rescue effect. Finally we apply the model, as a first port of call, to an empirical case study, to investigate the long term viability of an insect pest switching between resource hosts.

In Chapter 5 we will investigate a discrete-time model of density-dependent, costly dispersal between multiple patches, where regional dynamics are defined by a general class of maps and dispersal has a cost across the overall population. In particular, we will give sufficient conditions for the stability/instability of the extinction equilibrium; the existence of a positive equilibrium; and finally uniform strong persistence. We will then numerically explore this model in the context of dispersal between declining and growing patch population, to show some of the qualitative behaviour that it can capture.

In Chapter 6 we will investigate the stability of the zero equilibrium of a two-patch, discrete-time population model, where each patch population is partitioned into demographic classes, and there is arbitrary diffusive dispersal between patch classes. In particular we will show how the existence of different types of common Lyapunov function relate to this problem. We will briefly investigate the antithesis of this idea, i.e. when one can diffusively couple sink regions to induce overall population growth. Throughout this chapter we also discuss how our results apply to a variety of matrix classes used when modelling population dynamics.

In Chapter 7 we will take a data-driven perspective on structured population dynamics. In particular, we will investigate a stochastic discrete-time framework for inferring interactions among animal groups and how an auxiliary population may affect these associations. To do so, we will first outline our general methodology. We will then validate

this framework under various simulation scenarios to evaluate the performance of the parameter estimation procedure. Then, we will derive, under reasonable assumptions, an approximation to the marginal correlation between groups, which we call the net group interaction strength. Lastly, we will interpret this in the context of predator-prey theory to demonstrate its potential applicability.

In Chapter 8 we will review the work within each chapter and present avenues for future work.

2. Preliminaries

In this chapter we will establish some notation and terminology, and state key definitions and known results related to the material presented throughout this thesis.

2.1. Notation and Definitions

We begin by discussing the notation and definitions used throughout the majority of this thesis. Denote the nonnegative integers by $\mathbb{Z}_+ := \{0, 1, 2, \dots\}$. For $x \in \mathbb{R}^n$ we write $x \geq 0$ (> 0) to mean that $x_i \geq 0$ (> 0) $\forall i \in \{1, \dots, n\}$. Denote by

$$\mathbb{R}_+^n := \{x \in \mathbb{R}^n : x \geq 0\}$$

the standard *nonnegative cone* in \mathbb{R}^n . A similar notation is used for matrices in $\mathbb{R}^{n \times n}$ and $\mathbb{R}_+^{n \times n}$. For $A, B \in \mathbb{R}^{n \times n}$ we write $A \geq B$ if $A - B \geq 0$. Denote by A^T the transpose of A . Denote by $\text{Tr}(A) := \sum_i^n a_{ii}$ the trace of A . For $A \in \mathbb{R}^{n \times n}$ we say A is *symmetric* if $A = A^T$. A symmetric matrix A is said to be positive (negative) semi-definite if, for all nonzero $x \in \mathbb{R}^n$, $xAx^T \geq 0$ ($xAx^T \leq 0$) and this is denoted as $A \geq 0$ ($A \leq 0$). Similarly A is said to be positive (negative) definite if, for all nonzero $x \in \mathbb{R}^n$, $xAx^T > 0$ ($xAx^T < 0$) and this is denoted as $A > 0$ ($A < 0$).

A matrix $A \in \mathbb{R}^{n \times n}$ is said to be *irreducible* if there exists no permutation matrix P such that PAP^{-1} is of the form

$$Q = \begin{pmatrix} B & C \\ 0 & D \end{pmatrix}.$$

A is reducible if it is not irreducible. $A \in \mathbb{R}^{n \times n}$ is *column substochastic* if $\mathbb{1}^T A \leq \mathbb{1}^T$, where $\mathbb{1} := (1, \dots, 1)^T$. A matrix $A \in \mathbb{R}^{n \times n}$ is said to be *primitive* if there exists $s \in \mathbb{N}$ such that $A^s > 0$.

Denote by $\sigma(A)$ the spectrum of $A \in \mathbb{R}^{n \times n}$ (the set of its eigenvalues). Denote by $\mathcal{R}(z)$ the real part of $z \in \mathbb{C}$. Denote by $\mathbb{C}_- := \{z \in \mathbb{C} : \mathcal{R}(z) < 0\}$ the *open left halfplane* and $\mathbb{D}_1 := \{z \in \mathbb{C} : |z| < 1\}$ the *open unit disc*. The *spectral radius* and the *spectral abscissa* of $A \in \mathbb{R}^{n \times n}$ are respectively defined as

$$\begin{aligned} \rho(A) &:= \max\{|\lambda| : \lambda \in \sigma(A)\}, \\ \mu(A) &:= \max\{\mathcal{R}(\lambda) : \lambda \in \sigma(A)\}. \end{aligned}$$

A matrix $A \in \mathbb{R}^{n \times n}$ is Schur if $\rho(A) < 1$, i.e. $\sigma(A) \subset \mathbb{D}_1$, and Hurwitz if $\mu(A) < 0$, i.e. $\sigma(A) \subset \mathbb{C}_-$ (see Fig. 2.1).

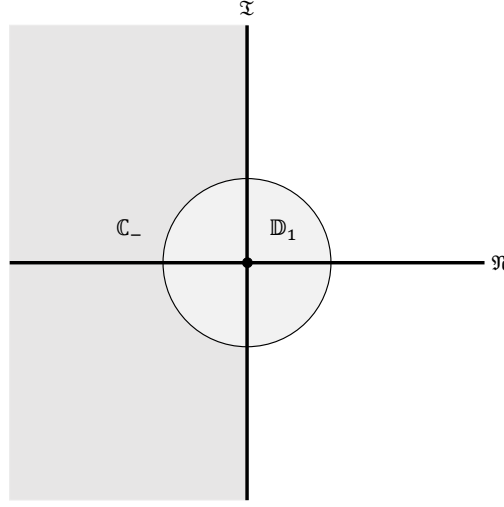


Figure 2.1: A matrix $A \in \mathbb{R}^{n \times n}$ is Hurwitz if $\sigma(A) \subset \mathbb{C}_-$ and Schur if $\sigma(A) \subset \mathbb{D}_1$. Here \mathcal{R} and \mathcal{I} respectively denote the real and imaginary axis.

A matrix $A = (a_{ij}) \in \mathbb{R}^{n \times n}$ is *Metzler* if $a_{ij} \geq 0$ for all $i \neq j$. Given that $A \in \mathbb{R}^{n \times n}$ is Metzler, we can write $A = N - \gamma I$ for $N \in \mathbb{R}_+^{n \times n}$ and $\gamma \geq 0$. If a matrix $B \in \mathbb{R}^{n \times n}$ is a *Z-matrix*, i.e. $b_{ij} \leq 0$ for $i \neq j$, and $B = sI - C$, where C is Metzler and $s \geq \rho(C)$, then B is called an *M-matrix* [26]. It is well known that A is an *M-matrix* if and only if $-A$ is Metzler and Hurwitz.

The l_1 -norm and l_∞ -norm of a vector $x \in \mathbb{R}^n$ are respectively defined as

$$\|x\|_1 := \sum_{i=1}^n |x_i|,$$

$$\|x\|_\infty := \max_i \{|x_i|\}.$$

Given a norm on \mathbb{R}^n , the induced/operator/matrix norm of a matrix $A \in \mathbb{R}^{n \times n}$ is defined as

$$\|A\| := \sup_{x \neq 0} \left\{ \frac{\|Ax\|}{\|x\|} \right\}.$$

The induced l_1 and l_∞ norms of a matrix $A \in \mathbb{R}^{n \times n}$ can be shown to respectively be given by $\|A\|_1 := \max_j \sum_{i=1}^m |a_{ij}|$ and $\|A\|_\infty := \max_i \sum_{j=1}^n |a_{ij}|$ [137].

Denote the m -fold composition of a map $F : \mathbb{R}^n \rightarrow \mathbb{R}^n$ with itself by

$$F^m := \underbrace{F \circ F \circ \dots \circ F}_{m \text{ times}},$$

for $m \in \mathbb{N}$. The *Jacobian* of a smooth vector-valued function $F : \mathbb{R}^n \rightarrow \mathbb{R}^n$ at a point $a \in \mathbb{R}^n$, for $i, j \in \{1, \dots, n\}$, is given by the matrix

$$F'(a) := \left(\frac{\partial F_i(a)}{\partial x_j} \right).$$

2.2. Discrete-Time Dynamical Systems

The systems we deal with in the majority of this thesis are discrete-time (potentially nonlinear) systems of the general form

$$\begin{aligned} x(t+1) &= F(x(t)), \\ x(0) &\in \mathbb{R}^n, \end{aligned} \tag{2.2.1}$$

where $F : \mathbb{R}^n \rightarrow \mathbb{R}^n$ is smooth and x_0 is called an *initial condition*. A trajectory or solution of (2.2.1) at time $t \geq 0$, with initial condition x_0 , is denoted by $x(t, x_0)$. The state space and time set of interest are respectively \mathbb{R}^n and \mathbb{Z}_+ . In this case the trajectory/solution of (2.2.1) defines what is known as a *semiflow*. See [255] for more on dynamical systems theory.

2.2.1. Equilibria and Lyapunov Stability

An *equilibrium* of (2.2.1) is a solution of $F(x) = x$. An equilibrium, x^* , is (*Lyapunov stable*) if for any $\epsilon > 0$ there exists a $\delta > 0$ such that

$$\|x_0 - x^*\| < \delta \implies \|x(t, x_0) - x^*\| < \epsilon$$

for all $t \geq 0$ (see Fig. 2.2). If, in addition, there exists some $R > 0$, such that $x(t, x_0) \rightarrow x^*$ as $t \rightarrow \infty$ for any solution with $\|x_0\| < R$, the equilibrium is *locally asymptotically stable (LAS)*. If this holds for any $R > 0$, it is said to be *globally asymptotically stable (GAS)*. Note that the specification of a norm, $\|\cdot\|$ need not matter, as all norms are equivalent on \mathbb{R}^n [137].

2.2.2. Positive Systems

The system (2.2.1) is called *positive*, if $x(t, x_0) \geq 0$ for all $t \geq 0$ when $x_0 \geq 0$. Put another way, if $F(\mathbb{R}_+^n) \subset \mathbb{R}_+^n$, i.e. \mathbb{R}_+^n is a *forward invariant* set for (2.2.1), then the system is positive.

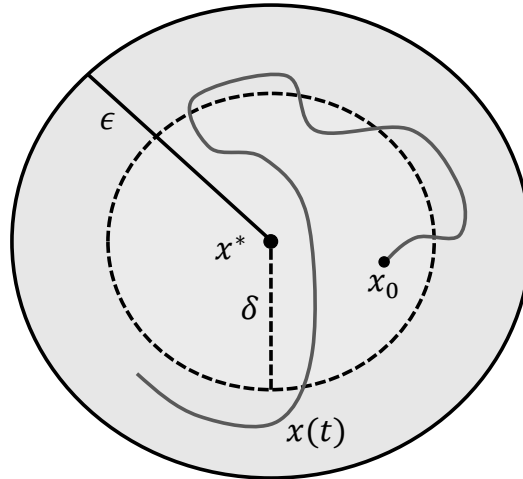


Figure 2.2: x^* is Lyapunov stable if, for any $\epsilon > 0$ we choose there is some $\delta > 0$ so that for any $x(0) = x_0$ within δ of x^* , the trajectory, $x(t)$, remains within ϵ of x^* for all $t \geq 0$.

If the dynamics of our system are linear, we can write (2.2.1) as a *linear time-invariant* (LTI) system given by

$$x(t+1) = Ax(t), \quad (2.2.2)$$

where $x(0) \in \mathbb{R}_+^n$ and $A \in \mathbb{R}^{n \times n}$ [136]. Note that we could arrive at a system of the form (2.2.2) if, for example, we linearise (2.2.1) around some equilibrium x^* . In this case A would be given by the Jacobian of F at x^* . The systems we consider throughout this thesis are positive systems, where the state space is interpreted as population abundances/size/densities and the time set is census/sampling/observation times. In general, it is common for systems of the form (2.2.1), to assume that $F(0) = 0$ and thus 0 is an equilibrium of (2.2.1). In the context of population dynamics, this trivial equilibrium corresponds to extinction. In the rest of this chapter, assume (2.2.1) is a positive system. Note that the system (2.2.2) is positive in discrete-time if $A \in \mathbb{R}_+^{n \times n}$.

Motivated by positive linear systems, the next result is the well-known Perron-Frobenius theorem for irreducible nonnegative matrices.

Theorem 2.2.1. [137] *Let $A \in \mathbb{R}_+^{n \times n}$ be irreducible. Then, $\rho(A) > 0$ is an eigenvalue of A , and there exists a unique (up to scalar multiples) vector $v > 0$ (resp. $w^T > 0$) such that $Av = \rho(A)v$ (resp. $w^T A = \rho(A)w^T$).*

A simple consequence of Theorem 2.2.1 is recalled in the following lemma.

Lemma 2.2.2. *Let $A \in \mathbb{R}_+^{n \times n}$ be irreducible. Then $\rho(A) < 1$ (resp. $\rho(A) = 1$, $\rho(A) > 1$) if and only if there exists $v > 0$ such that $Av < v$ (resp. $Av = v$, $Av > v$).*

These two results will be useful when proving results in Chapters 4, 5 and 6. We next look at how one can prove GAS of an equilibrium using Lyapunov functions.

2.2.3. Lyapunov Functions

In [186] Lyapunov gave a general method to determine GAS of equilibria of (2.2.1), the so-called *Lyapunov's direct method*. It can be used to establish global stability and is summarised well in the next well-known result. First, let $V : \mathbb{R}^n \rightarrow \mathbb{R}_+$ be continuous and $\|\cdot\|$ be any norm on \mathbb{R}^n . Further let the following hold:

1. $V(x^*) = 0$.
2. $V(x) \rightarrow \infty$ as $\|x\| \rightarrow \infty$.
3. $x, F(x) \in \mathbb{R}^n \implies \Delta V(x) := V(F(x)) - V(x) \leq 0$.
4. For $x \neq x^*$, $V(x) > 0$ for all $x \in \{y \in \mathbb{R}^n : \|y - x^*\| < \epsilon\}$ for some $\epsilon > 0$.

Then V is called a (*radially unbounded*) *Lyapunov function* (RULF).

Theorem 2.2.3. [80, 136] *If V is a RULF for (2.2.1) with respect to the equilibrium x^* and $\Delta V(x) < 0$ for all $x > 0$, then x^* is GAS.*

Lyapunov's indirect method is another widely used method to investigate the stability properties of an equilibrium x^* of (2.2.1) that relies on a local linear approximation to the dynamics in a neighbourhood of x^* . The stability properties are then determined by the eigenvalues of the system Jacobian at x^* [136, 255]. The next result is a well known characterisation of global asymptotic stability of the zero equilibrium of the linear system (2.2.2).

Theorem 2.2.4. [165] *0 is a GAS of equilibrium (2.2.2) if and only if A is Schur.*

Therefore $A \in \mathbb{R}^{n \times n}$ being Schur implies that the zero equilibrium of (2.2.2) is GAS. In this case A is said to be (Schur) stable and the stability region of interest is \mathbb{D}_1 . If we linearised (2.2.1) around some equilibrium, x^* , then A being Schur implies that x^* is LAS. Next we will discuss a specific type of Lyapunov function that is considered in the context of positive systems.

2.2.3.1. Copositive Lyapunov Functions

When studying positive systems it is natural to consider so-called copositive Lyapunov functions [114]. Their use can lead to less conservative conditions for positive systems

than those obtained by requiring a traditional Lyapunov function. The linear function $V(x) = v^T x$, $v \in \mathbb{R}^n$, defines a *linear copositive Lyapunov function* (LCLF) for (2.2.2) if and only if $v > 0$ and $A^T v < v$. The class of linear copositive Lyapunov functions has attracted considerable attention over the past two decades [76, 91, 114]. The following characterisation of Schur stability is well known and follows from the Perron-Frobenius Theorem.

Theorem 2.2.5. *Let $A \in \mathbb{R}_+^{n \times n}$. Then the following are equivalent (TFAE):*

1. *A is Schur.*
2. *There exists a LCLF for (2.2.2).*
3. *There exists a vector $v > 0$ with $Av < v$.*

A similar result for Hurwitz stability for Metzler matrices can be shown, which characterises stability in the continuous time case, as we state in the next result.

Theorem 2.2.6. [85] *Let $A \in \mathbb{R}^{n \times n}$ be Metzler. Then the following are equivalent:*

1. $A^{-1} \leq 0$.
2. *A is Hurwitz.*
3. *There exists a vector $v > 0$ with $Av < 0$.*
4. *There exists a vector $w^T > 0$ with $wA^T < 0$.*

From Theorems 2.2.5 and 2.2.6 we can see that, for $A \in \mathbb{R}_+^{n \times n}$ and some $v > 0$,

$$Av < v \iff (A - I)v < 0.$$

Therefore A is Schur if and only if $A - I$ is Hurwitz. This observation, along with Theorem 2.2.5 and 2.2.6 will be used extensively when proving many of the results and for some of the numerical examples in Chapters 4, 5 and 6. In the next section we will look at two other type of Lyapunov function that can be constructed from solutions of linear matrix inequalities.

2.2.3.2. Quadratic and Diagonal Lyapunov Functions

Let $A \in \mathbb{R}^{n \times n}$. We say $P > 0$ is a solution to the *Stein inequality* if

$$A^T P A - P < 0. \tag{2.2.3}$$

A solution of (2.2.3), P , determines a *quadratic Lyapunov function* (QLF), $V(x) := x^T P x$, for (2.2.2). If P is diagonal then V is called a *diagonal Lyapunov function* (DLF) for (2.2.2). If there exists a diagonal Lyapunov function for A , then A is called diagonally (Schur) stable. We will explore these concepts more in Chapter 3. We say $P > 0$ is a solution to the *Lyapunov inequality* if

$$A^T P - P A < 0.$$

The Lyapunov inequality determines a QLF in continuous-time. In Chapters 6 we will be interested in the existence of QLFs/DLFs and their relation to the stability of a coupled linear population model. Next we state a necessary and sufficient condition for the existence of a diagonal solution of the Lyapunov inequality.

Theorem 2.2.7. [19] *A matrix A is diagonally stable if and only if for every nonzero positive semidefinite matrix $B \geq 0$, BA has a negative diagonal element.*

In Chapter 6 we will explore the Lyapunov and Stein inequalities in more detail. Note that these two matrix inequalities are related via

$$C(A) = (A - I)(A + I)^{-1},$$

called the *Cayley transform*, where it is assumed that $\rho(A) < 1$ so that $C(A)$ is well defined.

Theorem 2.2.8. [192] *Let $A \in \mathbb{R}^{n \times n}$ be Schur, and $P = P^T > 0$ be a solution of $A^T P A - P = -Q < 0$. Then P is also a solution of*

$$C(A)^T P + P C(A) = 2(A + I)^{-T} Q (A + I)^{-1} > 0.$$

Quasidominance is one criterion used to check if a matrix is diagonally Schur stable. A matrix $A = (a_{ij}) \in \mathbb{R}^{n \times n}$ is *quasidominant* if there exists a $p > 0$ such that $a_{ii} p_i \geq \sum_{j \neq i} |a_{ij}| p_j$ for all $i \in \{1, \dots, n\}$. The following result is a characterisation of Schur diagonal stability for nonnegative matrices.

Lemma 2.2.9. [152] *Let $A \in \mathbb{R}_+^{n \times n}$. Then TFAE:*

1. *There exists a diagonal matrix D such that $\|D^{-1} A D\|_\infty < 1$.*
2. *There exists a diagonal solution to the Stein inequality.*
3. *$I - A$ is quasidominant.*
4. *$I - A$ is an M -matrix.*
5. *A is Schur.*

Next we will discuss other types of asymptotic behaviour other than the convergence to or stability of fixed points of (2.2.1).

2.2.4. Periodic Solutions and Chaotic-Type Dynamics

In the majority of this thesis our focus is either on the asymptotic stability/instability of equilibria and other qualitative dynamics of systems of the form (2.2.1). Other types of asymptotic qualitative behaviour include periodic trajectories. Given the system (2.2.1) we say that $x_p \in \mathbb{R}_+^n$ is a periodic point of F if, for some $k \in \mathbb{N}$, $F^k(x_p) = x_p$ [80]. In other words x_p is k -periodic if it is a fixed point of $x(t+1) = F^k(x(t))$, $x(0) = x_0 \in \mathbb{R}_+^n$. Clearly an equilibrium is 1-periodic.

In ecological systems the presence or absence of chaos has garnered significant interest over the years [128, 238, 283]. The term *chaos* has been used in many different contexts and its precise definition varies depending on the field of interest. In [258] the author describes chaos as

"aperiodic long-term behaviour in a deterministic system that exhibits sensitive dependence on initial conditions".

In Chapter 4 and 5, we will encounter systems exhibiting behaviour that is suggestive of this, informal, characterisation of chaos. Various mathematical definitions of chaos exist, such as *Devaney's chaos* and *Li-Yorke chaos* [73, 172, 173, 269]. We do not work with a formal definition of chaos, as this is not our focus. However, we will simply identify where chaotic type behaviour seems to occur in the specific ecological systems we are interested in.

2.2.5. Bifurcation Analyses

The qualitative dynamics of solutions of systems of the form (2.2.1) may change depending on what parameterisations we choose. As one varies certain parameters of a model, fixed points may appear/disappear and periodic trajectories or chaotic-type dynamics may emerge. Such transitions between dynamical behaviours take place are called bifurcations and they can be numerically studied using so-called bifurcation diagrams.

To construct a bifurcation diagram, we simulate some parameterisation of a system of the form (2.2.1) for some sufficiently long time $T > 0$ and some given initial condition. We can then take the last $L \in [0, T)$ time steps and calculate if any equilibria or periodic trajectories exists within these $T - L$ time steps. If none are observed this suggests the trajectory is aperiodic. To test if this aperiodic trajectory is sensitive to initial conditions, we perturb our initial condition, x_0 , by various sufficiently small $\epsilon > 0$ and observe if another aperiodic trajectory is obtained. If this occurs then this suggests that such a system

exhibits chaotic-type dynamics. Further analysis would have to be carried out to conclude if a system exhibits chaos, in the sense of [73].

In Chapters 4 and 5 we construct what are known as one- and two-parameter (planar) bifurcation diagrams. One-parameter bifurcation diagrams show the parameter of interest on the x -axis and the value of the trajectory on the y -axis. Two-parameter bifurcation diagrams show the first parameter of interest on the x -axis and second parameter of interest on the y -axis. Points are then assigned a colour based on what type of dynamics are observed over the $T - L$ time steps. Bifurcation diagrams are particularly useful for investigating the association of ecological patterns of population oscillations with changing values of model parameters, allowing one to quantify this contribution to changes in model outputs [275]. It is possible to also analytically study bifurcations, which we will not pursue. See [11, 166] for more on bifurcation analyses.

2.2.6. The Logistic Map

To demonstrate some of the above concepts we will briefly look at the (one-dimensional) logistic map (see Fig. 2.3) as an example, which is a discrete-time analogue of the continuous-time logistic equation used in demographic modelling [258].

First proposed by Lorenz in [183] for modelling climate dynamics, the logistic difference equation was given a first in-depth study in [196]. The logistic difference equation is given by

$$\begin{aligned} x(t+1) &= F(x(t)) := ax(t)(1-x(t)), \\ x(0) &\in \mathbb{R} \end{aligned} \tag{2.2.4}$$

for $a > 0$ (see Fig. 2.3). For modelling populations, it has been shown that (2.2.4) is a positive system once $a \in [0, 4]$ and we restrict the domain of the logistic map, F , to be in $[0, 1]$. The state variable, x , can then be interpreted, in an ecological context, as population density (population abundance per unit inhabited area).

For $a < 1$ the extinction equilibrium is GAS. For $1 < a < 3$ there exists a GAS positive equilibrium given by $x^* = 1 - 1/a$. At $a = 3$ a period 2 solution emerges. If we denote by a_n the value of a where a period 2^n trajectory first appears, in [88] Feigenbaum showed that $\lim_{t \rightarrow \infty} a_t = a_\infty \approx 3.57$. For $a > a_\infty$, when one plots a one-parameter bifurcation diagram, we can observe so-called *periodic windows*, parameter intervals where periodic trajectories emerge, between which chaotic type dynamics can be observed (see Fig. 2.4).

More precisely at $a = 1$ we observe a so-called *transcritical bifurcation*, where the origin goes from being GAS to unstable and a positive fixed point, $x^* > 0$, emerges and is GAS up until $a = 3$. At $a = 3$ we undergo a so-called *flip bifurcation*, where periodic trajectories with increasing periods emerge and period-doubling occurs as a increases. We refer the reader to [258] and references therein for more details on the logistic map.

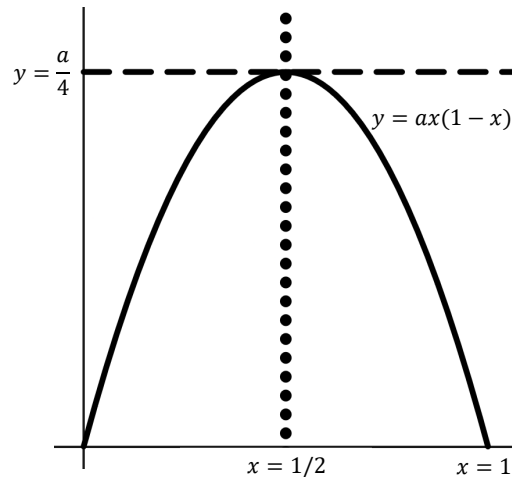


Figure 2.3: Illustration of the logistic map $y = ax(1 - x)$, where $a > 0$ (solid). This map has a unique maximum at $x = 1/2$ (dotted) which is $y = a/4$ (dashed).

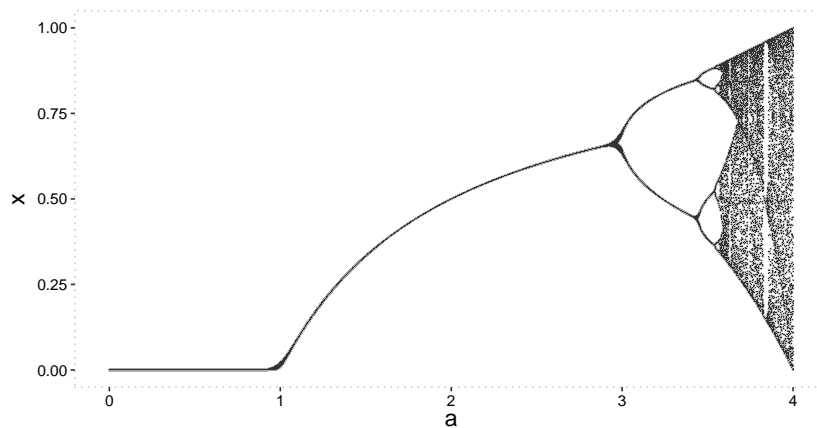


Figure 2.4: One-parameter bifurcation diagram for $a \in [0, 4]$ vs solutions, x , of (2.2.4).

2.3. Persistence

Given a discrete-time dynamical system (2.2.1) that is positive, we can define what is known as persistence. Given a *persistence function* $\eta : \mathbb{R}_+^n \rightarrow [0, \infty)$, the system (2.2.1) is *uniformly weakly η -persistent*, if there exists some $\epsilon > 0$, such that

$$\eta(x_0) > 0 \implies \limsup_{t \rightarrow \infty} \eta(x(t, x_0)) > \epsilon. \quad (2.3.1)$$

and *uniformly strongly η -persistent*, if there exists some $\epsilon > 0$, such that

$$\eta(x_0) > 0 \implies \liminf_{t \rightarrow \infty} \eta(x(t, x_0)) > \epsilon. \quad (2.3.2)$$

The term *uniform* in the above definitions is to highlight the fact that ϵ is independent of the initial condition x_0 . The interpretation for weak persistence is that however far forward in time you look, there will be some later time at which $\eta(x(t, x_0))$ exceeds such a persistence threshold. Strong persistence means that there exists some time point, T , beyond which $\eta(x(t, x_0))$ exceeds some persistence threshold for all $t > T$.

For population vectors $x \in \mathbb{R}_+^n$, examples of possible persistence functions include

- the weighted total population size: $\eta(x) = \sum_i \alpha_i x_i$, where $\alpha_i \geq 0$;
- the minimum population component: $\eta(x) = \min_i x_i$;
- the maximum population component: $\eta(x) = \|x\|_\infty$; and
- the weighted product of population components: $\eta(x) = \prod_i x_i^{p_i}$, where $p_i \geq 0$.

We will now state two results on persistence from [255] that will be useful when proving some of the persistence results in Chapters 4 and 5. We first state a particular case of Proposition 3.16 from [255].

Proposition 2.3.1. [255] *Consider the system (2.2.1) and let $\eta : \mathbb{R}_+^n \rightarrow [0, \infty)$. Assume that $\eta(x) > 0$ implies that $\eta(F(x)) > 0$. Further assume that there exists $\delta > 0$ such that*

$$\inf \left\{ \frac{\eta(F(x))}{\eta(x)} : 0 < \eta(x) < \delta \right\} > 1.$$

Then $\eta(x_0) > 0$ implies that

$$\limsup_{t \rightarrow \infty} \eta(x(t, x_0)) \geq \delta.$$

We next state a result on uniform strong persistence.

Theorem 2.3.2. [255] *Consider the system (2.2.1) and assume the map F is C^1 . Let $\eta(x) = \|x\|$, where $\|\cdot\|$ is any norm on \mathbb{R}_+^n . Suppose that the following hold:*

1. $F(\mathbb{R}_+^n \setminus \{0\}) \subset \mathbb{R}_+^n \setminus \{0\}$;
2. there exists $r_0 > 1$ and $v > 0$ such that $F'(0)^T v \geq r_0 v$;
3. there exists $M > 0$ such that $\forall x(0) \in \mathbb{R}_+^n$ there exists $T \in \mathbb{N}$ such that $\|x(t, x_0)\| \leq M \forall t \geq T$.

Then, F is uniformly strongly η -persistent. Let $\hat{\eta}(x) = \min_i x_i$ and define

$$X_0 := \{x_0 \in \mathbb{R}_+^n : \hat{\eta}(x(t, x_0)) = 0, \forall t \geq 0\}.$$

In addition, if for all $c > 0$ there exists some $s > 0$ such that $F^s(x) > 0 \forall x \in \mathbb{R}_+^n, 0 < \|x(s)\| \leq c$, then there exists some $\epsilon > 0$ such that

$$\liminf_{t \rightarrow \infty} \hat{\eta}(x(t, x_0)) \geq \epsilon$$

for any $x_0 \in \mathbb{R}_+^n \setminus X_0$.

In Chapter 3 we will discuss persistence in more detail for a specific type of population model. For more background on persistence theory we recommend the monograph of [255], as well as the papers of [95, 146, 239, 266] and references therein.

2.4. Positive Integer-Valued Time Series

For ease of exposition, in this section and in Chapter 7, we will use subscripts for indexing time and omit the dependence on initial conditions. That is, instead of writing $x(t, x_0)$ we will simply write x_t , where the dependence on the initial condition is assumed.

Given a random variable X , define the expected value of X as $\mathbb{E}[X] := \sum x\mathbb{P}(X = x)$, the variance of X as $\text{Var}(X) := \mathbb{E}[X^2] - \mathbb{E}[X]^2$ and the covariance of X and another random variable Y as $\text{Cov}(X, Y) := \mathbb{E}[XY] - \mathbb{E}[X]\mathbb{E}[Y]$. We define a *positive integer-valued, discrete-time stochastic process* as $(Z_t)_{t \in \mathbb{Z}_+} := \{Z_t, t \in \mathbb{Z}_+\}$, where, for a given time $t \in \mathbb{Z}_+$, each Z_t is a discrete random variable, assumed to have finite moments. Each Z_t thus has some corresponding probability mass function. Some common distributions for modelling positive integer-valued random variables include the *Poisson* and *Negative-Binomial*, and extensions of these such as the so-called *zero-inflated* and *hurdle models* [135, 202]. In this thesis we are concerned with finite-time stochastic processes, that is stochastic processes of the form

$$(Z_t)_{[0, T]} := \{Z_t, t \in [0, T] \subset \mathbb{Z}_+\},$$

where we write $[0, T]$, in slight abuse of notation, to denote the set of positive integers between 0 and T . When modelling time series one can specify that $X_0 = x_0 \in \mathbb{Z}_+$ or assume that X_0 has some initial distribution, p_0 . We employ the former, as in many ecological studies initial abundances are usually known, which is indeed the case in experimental or conservation monitoring programs for example.

2.4.1. The Markov Property

If for all $t \in [0, T]$ and all $z_0, z_1, \dots, z_{t-1}, z \in \mathbb{Z}_+$, we say $(Z_t)_{[0, T]}$ is first-order Markovian, $(Z_t)_{[0, T]}$ is a first-order *Markov chain* or $(Z_t)_{[0, T]}$ satisfies the *Markov property*, if

$$\mathbb{P}(Z_{t+1} = z | Z_t = z_t, Z_{t-1} = z_{t-1}, \dots, Z_0 = z_0) = \mathbb{P}(Z_{t+1} = z | Z_t = z_t).$$

If we wanted to incorporate additional temporal dependence between states we could condition on earlier observations. Moreover, Markov chains, despite their apparent simplicity, have proven effective in modelling a wide variety of ecological systems [106, 181].

2.4.2. Bayesian Inference

In a Bayesian setting we are interested in the distribution of θ , a model parameter of interest. To quote from [102], in Bayesian inference

"the posterior distribution is centered at a point that represents a compromise between the prior information and the data, and the compromise is controlled to a greater extent by the data as the sample size increases".

This perspective is especially useful in ecological studies when one has hierarchical structures such as observation (observed) and latent (unobserved) processes [18]. Letting the (observed) data y , which depends on θ , have a probability density or mass function $f(y|\theta)$, we can then write the joint distribution of θ and y as $p(\theta, y) = q(\theta)f(y|\theta)$ [102]. The distributions $q(\theta)$ and $f(y|\theta)$ are respectively known as the *prior* and the *sampling/data distribution*. Using Bayes' rule we can then write the so-called *posterior density* of θ given y as

$$r(\theta|y) = \frac{p(\theta, y)}{s(y)} = \frac{q(\theta)f(y|\theta)}{s(y)},$$

where $s(y) = \sum_{\theta} q(\theta)f(y|\theta)$ in the discrete case and $s(y) = \int q(\theta)f(y|\theta)d\theta$ in the continuous case. By treating $s(y)$ as a constant with respect to the unknown θ , i.e. it only depends on the known data y , the so-called *unnormalised posterior density* is given by $r(\theta|y) \propto q(\theta)f(y|\theta)$, where $f(y|\theta)$ is a function of θ . In many contexts the posterior distribution does not have an analytic expression or is intractable to compute. Thus when making inferences, after assigning priors to our parameters of interest, we then use some sampling algorithm to estimate our posterior distribution. In the next section we will discuss how one can choose such priors.

2.4.2.1. Prior Specification

Before fitting Bayesian models, there are many ways to specify priors for our parameters of interest. If one has prior knowledge of the system in question they may set what is known as an *informative prior*, where one can restrict the majority of the distribution to specific regions of the parameter space [102]. If one has less knowledge of the system they may specify a *non-informative prior*, where there are relatively equal weights given to every region of the parameter space, thus allowing the data to greatly inform the posterior distribution. Generally, when deciding on a prior one typically wants to choose proper priors, which are priors chosen so that the posterior density integrates or sums to one. This is so these are valid probability distributions. In Chapter 7 our interest is in assigning non-informative priors to the mean and variance terms of some random effects (as we want the data to provide more information when predicting the posterior density), a concept we will discuss later in Chapter 3. We will now briefly discuss how one would choose such non-informative priors for model parameters representing variances, which are strictly positive quantities.

Let $\text{Inv-}\Gamma(\alpha, \beta)$ be an inverse Gamma distribution, which has probability density function

$$g(x, \alpha, \beta) = \frac{\beta^\alpha}{\Gamma(\alpha)} (1/x)^{\alpha+1} \exp(-\beta/x),$$

for $\alpha, \beta, x > 0$ and where $\Gamma(a)$ denotes the gamma function [102]. According to [100] if we set an $\text{Inv-}\Gamma(\epsilon, \epsilon)$ prior for variance parameters, for ϵ sufficiently small, then there may not exist a proper posterior distribution. The form of this distribution's probability density function is also quite sensitive to changes in values of ϵ . Let $\mathcal{N}^+(0, \sigma^2)$ denote a half-Gaussian distribution, whose probability density function is given by

$$h(x, \sigma) = \frac{\sqrt{2}}{\sigma\sqrt{\pi}} \exp\left(-\frac{x^2}{2\sigma^2}\right),$$

for $\sigma > 0$ and $x \geq 0$. In [100] the author recommends using $\mathcal{N}^+(0, \sigma^2)$ with large σ^2 when choosing non-informative proper priors. This will give more weight to lower values of the estimated variance parameters, while still allowing larger values to be estimated. Note that if we wanted to give more weight to the tails, we could use truncated t-distributions as priors for variance parameters. The inclusion of heavier-tailed distributions as proper priors may result in our model being robust to outlying observations [281], but as noted in [213] the utility of heavy-tailed models in complex settings is not so clear.

2.4.2.2. Hamiltonian Monte Carlo

To fit a Bayesian model one could implement Metropolis Hastings or Gibbs sampling algorithms, using many existing packages, such as Nimble [70], JAGS [225] or WinBUGS [185]. An alternative approach, which has been shown to be more efficient for more complex or high-dimensional models, is Hamiltonian Monte Carlo (HMC) [267]. According to [267]

"HMC tends to converge to regions of higher posterior density more quickly in comparison with Metropolis-Hastings".

We implemented our HMC model fitting in R [263] using the R package rstan [44]. We will next give a short summary of HMC when estimating some posterior distribution of interest. We will not discuss the HMC algorithm implementation in detail, as this is not our focus. However, if one is interested in this and for a discussion on topics such as detailed balance, time-reversibility, the no-U-turn sampler and leapfrog integration, see [28, 267].

Let $\theta \in \mathbb{R}^n$ be a parameter vector of interest, which has posterior density $r(\theta|y)$, where y is a vector of observed data. Let m be a parameter generated from a k -dimensional multivariate normal distribution, i.e. $m \sim \mathcal{N}_k(0, M)$, where $M \geq 0$ is a user-specified covariance matrix. Define the so-called *Hamiltonian function*

$$H(\theta, m) := -\log(r(\theta|y)) + \frac{1}{2}m^T M^{-1}m,$$

assuming that M^{-1} exists. Over time, the HMC process travels along trajectories that are governed by the so-called Hamiltonian equations

$$\begin{aligned} \frac{dm}{dt} &= \frac{-\partial H}{\partial \theta} = \frac{-\partial U}{\partial \theta} = \nabla_{\theta} \log(r(\theta|y)), \\ \frac{d\theta}{dt} &= \frac{\partial H}{\partial m} = \frac{\partial K}{\partial m} = M^{-1}m, \end{aligned}$$

where $\nabla_{\theta} \log(r(\theta|y))$ is the gradient of the log-posterior density. A solution to the Hamiltonian equations is a function that defines the path of (θ, m) . Within each MCMC iteration, a value θ is then sampled from this path. To sample from the posterior distribution, the HMC process generates trajectories of (θ, m) by starting with a chosen $\theta(0)$ and sampling $m(0) \sim \mathcal{N}(0, M)$. Then one integrates the Hamiltonian equations over a time interval, $[0, h]$, using numerical methods. This then gives a sequence $(\theta(t), m(t))$. Finally, for a specified time horizon, the final value of $\theta(t)$ at time h is taken as a sample from the posterior distribution $r(\theta(h)|y)$. In Chapter 7 we use the R package rstan, using R, for

carrying out our Bayesian model fitting, which uses HMC by default to make parameter inferences.

2.4.2.3. *Weak Identifiability*

Let θ be a parameter of interest, with prior and posterior distributions respectively given by p_θ and $p_{\theta|y}$. Following the estimation of the posterior density, $p_{\theta|y}$, when making inferences about θ , an important aspect to investigate is the notion of identifiability. In a Bayesian setting an analogous concept to near-redundancy in frequentist statistics is weak identifiability [97, 99]. A parameter θ is said to be *weakly identifiable* if $p_\theta \approx p_{\theta|y}$ [53]. One typically assesses weak identifiability of θ using its prior-posterior overlap (PPO) statistic. The PPO for θ is given by

$$\tau_\theta = \int \min(p_\theta, p_{\theta|y}) d\theta.$$

Note that $\tau_\theta \in [0, 1]$. The value of τ_θ can be estimated using kernel-density estimation or graphically by plotting the prior and estimated posterior distributions of θ . In ecological applications an ad-hoc threshold of $\tau_T = 0.35$ was proposed in [97] to assess weak identifiability. If one has that the prior-posterior overlap for a given parameter is above τ_T , then that parameter is weakly identifiable. Weakly identified parameters may suggest that a model is parameter redundant or non-identifiable [53]. More work would be needed to mathematically assess if a (potentially nonlinear) model is non-identifiable. This concept has been used in ecological studies to assess so-called practical identifiability, where we are interested in knowing if the data provides us with more information than the priors alone [20, 104, 167]. This is especially important if we are interested in specific parameter estimates for inferential reasons, as is the case in Chapter 7.

2.5. Summary

In this chapter we have introduced the main notation and terminology used throughout this thesis, namely in the context of positive systems and integer-valued time series. We have discussed concepts such as stability, Lyapunov functions, persistence, the Markov property, Bayesian inference and weak-identifiability. We have also recalled the statements of some key results that will be needed later. These concepts and definitions will resurface throughout this thesis in relation to modelling the dynamics of various structured populations.

3. Structured Population Models

In this chapter we will survey various existing discrete-time models of structured populations. We will first look at some deterministic systems to accompany the work in Chapters 4, 5 and 6. We will then look at some stochastic frameworks to accompany the work in Chapter 7. Many of the known results in this chapter are either applied to specific ecological examples or are stated due to their application in other chapters in this thesis.

*Parts of this chapter appeared in: McGrane-Corrigan, B. and Mason, O., 2023. On Matrix Stability and Ecological Models. In *Modelling Insect Populations in Agricultural Landscapes* (pp. 115-147). Springer, Cham.*

3.1. Linear Systems

In practice, populations are not censused continuously: there is typically an interval between each measurement and the next. Many species have non-overlapping generations [107]. For such setups, discrete time models are more appropriate. Furthermore, many species have structured life stages, ages or discrete sub-population structure like male or female groups, for example. This means that higher dimensional matrix models are more appropriate as simple 1-dimensional models cannot capture such structure. The qualitative properties of such models in this context play a vital role when studying the suppression of pests, maintenance of mutualists and conservation of endangered species [94, 208, 260].

We first consider the simplest class of models for such structured populations, where we assume the dynamics are linear. In this case, we can use (2.2.2) to model such an ecological system, where A is commonly called a population projection matrix [256]. As previously discussed, the stability of the extinction equilibrium of (2.2.2) is equivalent to determining when $\rho(A) < 1$, with A being then termed a Schur stable matrix. More general concepts of matrix stability have also been proposed, some inspired by ecological questions [165, 180]; for instance, stability regions, \mathcal{S}_D , other than \mathbb{D}_1 (or \mathbb{C}_- in continuous time) can be considered, where A is said to be \mathcal{S}_D -stable if

$$\sigma(A) \subset \mathcal{S}_D \subset \mathbb{C}.$$

For more on these and related problems, see [165]. We next discuss another type of matrix stability, D -stability, and the so-called net reproduction number in the context of linear

structured population models. The notion of D -stability is closely related to diagonal stability, a concept we will explore in the next section, and also in Chapter 6 in relation to a model of diffusive dispersal between populations with demographic structure.

3.1.1. D -Stability

First introduced in [12] to study market price dynamics, the authors of [190] view D -stability as a form of system stability that is

"robust with respect to parametric uncertainties given by diagonal scaling."

The concept of diagonal stability, or what some authors call *Volterra-Lyapunov stability* [57] or *Volterra dissipativeness* [109], is closely related to D -stability (see [177]).

A matrix $A \in \mathbb{R}^{n \times n}$ is *Schur D -stable* if DA is Schur for all diagonal $D = (d_{ij})$ such that $|D| := (|d_{ij}|) \leq I$. Denote by \mathcal{S} the set of all Schur stable matrices, \mathcal{D}_D the set of all Schur D -stable matrices and \mathcal{D}_d the set of all diagonally Schur stable matrices. Then the following holds [29, 180]:

$$\mathcal{D}_d \subset \mathcal{D}_D \subset \mathcal{S}.$$

Many results exist for D -stability in the continuous-time case. However, we will only discuss Schur D -stability as the focus of the of this thesis is in discrete-time models. For more on D - and diagonal stability we refer the reader to [19, 66, 147, 152, 165, 192].

We will now state some results for general Schur D -stability, where $A \in \mathbb{R}^{n \times n}$. We first recall a result from [89].

Theorem 3.1.1. [89] *Let $A \in \mathbb{R}^{n \times n}$. Let $C_{ii} \geq 0$ be a square matrix and $C_{ij} \leq 0$ for $i, j \in \{1, 2\}, i \neq j$. Assume there exists a permutation matrix $P \in \mathbb{R}^{n \times n}$ such that*

$$PAP^{-1} = \begin{pmatrix} C_{11} & C_{12} \\ C_{21} & C_{22} \end{pmatrix}.$$

Then A is Schur D -stable if and only if A is Schur.

Before we state the next result, let us recall the definition of a monotone norm from [137]. An induced operator norm $\|\cdot\|$ on $\mathbb{R}^{n \times n}$ is called *monotone* if $|A| \leq |B|$ implies that $\|A\| \leq \|B\|$. We now state a version of a result of [89] using induced matrix norms on $\mathbb{R}^{n \times n}$.

Proposition 3.1.2. [89] *For $A \in \mathbb{R}^{n \times n}$, the following each imply that A is Schur D -stable.*

1. There exists a norm $\|\cdot\|$ such that $\|A\| < 1$ and $\|D\| \leq 1$, whenever D is diagonal and $|D| \leq I$.
2. There exists a monotone norm $\|\cdot\|$ on \mathbb{R}^n such that $\|A\| < 1$.
3. There exists a monotone norm $\|\cdot\|$ on \mathbb{R}^n such that $\|AD\| < 1$ whenever D is diagonal and $|D| = I$.

Given $A \in \mathbb{R}^{n \times n}$, the *Frobenius norm*, $\|\cdot\|_F := \text{Tr}(A^T A)^{\frac{1}{2}}$, and *spectral norm*, $\|\cdot\|_S := (\rho(A^T A))^{\frac{1}{2}}$ are two examples of monotone norms.

In the previous results we discussed D -stability for general matrices $A \in \mathbb{R}^{n \times n}$. For positive systems, the definition of Schur D -stability reduces to: $A \in \mathbb{R}_+^{n \times n}$ is Schur D -stable if DA is Schur stable for all nonnegative diagonal matrices $D \leq I$. If $A \in \mathbb{R}_+^{n \times n}$ is Schur stable then one has that

$$\rho(DA) \leq \rho(A) < 1,$$

for all $D \leq I$, which follows from, for example, Corollary 3.3 of [26]. Hence Schur stability implies Schur D -stability. Also, if we have that $A \in \mathbb{R}_+^{n \times n}$ is Schur D -stable, then if we let $D = I$ we have that A is Schur stable. Hence we have simply proved the following result.

Theorem 3.1.3. *Let $A \in \mathbb{R}_+^{n \times n}$. Then A is Schur stable if and only if A is Schur D -stable.*

Next we will briefly explore some Schur stability results related to linear stage structured populations models.

3.1.2. Stage Structure

The asymptotic dynamics of positive linear time-invariant systems are well known [62, 85, 177]. In Chapter 2 we highlighted some properties of such positive systems. In the context of population biology, the following result, known as the *fundamental theorem of demography*, highlights the appeal of studying stability problems related to nonnegative matrices in ecology [62]. Recall from [137] that $A \in \mathbb{R}^{n \times n}$ is primitive if there exists $k \in \mathbb{N}$ such that $A^k > 0$.

Theorem 3.1.4. [61, 62] *Suppose $A \in \mathbb{R}_+^{n \times n}$ is primitive, with left and right eigenvectors corresponding to $\rho(A)$, given respectively by v and w (normalised so $v^T w = 1$). Then*

$$\lim_{t \rightarrow \infty} \frac{x(t, x_0)}{\rho(A)^t} = (v^T x_0)w.$$

Moreover, we have that

$$\lim_{t \rightarrow \infty} \|x(t, x_0)\| = \begin{cases} 0, & \text{if } \rho(A) < 1; \\ \|(v^T x_0)w\|, & \text{if } \rho(A) = 1; \\ \infty, & \text{if } \rho(A) > 1. \end{cases}$$

Many population projection matrices used in population ecology are primitive. Thus the asymptotic dynamics of the corresponding linear models is a trichotomy: either a population goes extinct, grows unbounded or approaches a so-called *stable stage-distribution* given by $(v^T x_0)w$. We will discuss the concepts of primitivity and irreducibility in more detail later, when we look at Leslie matrices. Another way of characterising stability for such models is using a so-called potential-growth indicator. As mentioned in [178]:

"the potential-growth indicator (PGI) problem means to find an explicit function (an indicator) of the parameters whose value can indicate whether the model population grows, declines, or remains steady."

Let \diamond denote one of the relations $<$, $=$ or $>$. We call a (not necessarily unique) function $P_G : \mathbb{R}^{n \times n} \rightarrow \mathbb{R}_+$ a *potential-growth indicator* for (2.2.2) if $P_G(A) \diamond 1$ if and only if $\rho(A) \diamond 1$ [178, 179]. It is easy to show when such a function exists, as we will demonstrate next.

As mentioned in Chapter 2, we can model populations using matrix models. Partition a population of interest into predefined stage classes, corresponding to fecundity (number of offspring produced in each class) or transition rates (between the different classes), $x_i \in \mathbb{R}_+$, $i \in \{1, \dots, n\}$. Let $F = (f_{ij}) \in \mathbb{R}^{n \times n}$ be a *fecundity matrix* and $T = (t_{ij}) \in \mathbb{R}^{n \times n}$ a *transition matrix*, such that

$$f_{ij} \geq 0, \quad t_{ij} \in (0, 1], \quad \text{and} \quad \sum_{k=1}^n t_{kj} \leq 1, \quad (3.1.1)$$

for $i, j \in \{1, \dots, n\}$. We can then model such a population using (2.2.2) with $A = F + T$, where F and T satisfy (3.1.1). Therefore F takes account of the number of offspring produced by each stage class and T takes account of mortality/survival when one stage class transitions to another.

One can characterise stability for matrix models of this type by looking at the net reproduction number, which is itself a potential growth indicator. Given $A = F + T$ such that F and T satisfy (3.1.1), the *net reproduction number* is given by

$$R_0(A) := \rho \left(F(I - T)^{-1} \right), \quad (3.1.2)$$

Assuming that (3.1.1) holds, it was proven in [60] that if A has a positive, simple (algebraic multiplicity of 1), strictly dominant eigenvalue whose associated right-eigenvector is strictly positive, $1 \notin \sigma(T)$ and $\sum_i t_{ij} < 1$, then $R_0(A)$ as in (3.1.2) is a potential growth indicator. Results related to it can also be found in [171]. A sufficient condition for the so-called *resolvent matrix*, $(I - T)^{-1}$, to exist is that $\|T\|_\infty < 1$, which has been interpreted as mortality affecting each stage over every time step, as such transitions rates account for survival and death [61]. We state a similar result to the one in [60]. However, our proof makes use of Lemma 2.2.2 and shows more clearly the link between the signs of $\rho(A)$ and $R_0(A)$.

Theorem 3.1.5. *Let $A = T + F \in \mathbb{R}_+^{n \times n}$ be irreducible and satisfy (3.1.1). Further assume $\rho(T) < 1$ and $F(I - T)^{-1}$ is irreducible. Let \diamond denote one of the relations in $\{<, >, =\}$. Then*

$$\rho(A) \diamond 1 \iff R_0(A) \diamond 1.$$

Proof. First note that $\rho(T) < 1$ implies that $\det(I - T) \neq 0$. Using the *Neumann series* of the resolvent matrix of T at 1, we can see that

$$(I - T)^{-1} = \sum_{k=0}^{\infty} T^k \geq 0 \implies (I - T)^{-1}F \geq 0.$$

(\implies) Assume $\rho(A) \diamond 1$. It follows from Perron-Frobenius that there exists $v^T > 0$ such that

$$\begin{aligned} v^T A = \rho(A)v^T &\iff v^T(T + F) = v^T - (1 - \rho(A))v^T \\ &\iff v^T F = v^T(I - T) - (1 - \rho(A))v^T \\ &\iff v^T F(I - T)^{-1} = v^T - v^T(I - T)^{-1}(1 - \rho(A)). \end{aligned}$$

Thus we have that

$$v^T F(I - T)^{-1} \diamond v^T \iff R_0(A) \diamond 1.$$

It then follows from Lemma 2.2.2 that $v^T F(I - T)^{-1} \diamond v^T$ if and only if $\rho(A) \diamond 1$.

(\impliedby) Conversely assume $r := R_0(A) \diamond 1$. By assumption $(I - T)^{-1}$ exists and $F(I - T)^{-1}$ is irreducible. So by the Perron-Frobenius Theorem, there exists a vector $w^T > 0$ such that

$$\begin{aligned} w^T F(I - T)^{-1} = r w^T &\iff w^T F = w^T(I - T)r \\ &\iff w^T F = r w^T - w^T T + w^T(r - 1) \\ &\iff w^T(F + T) = r w^T + w^T(r - 1). \end{aligned}$$

It then follows from Lemma 2.2.2 that $w^T A \diamond w^T$ if and only if $\rho(A) \diamond 1$. \square

Assume that F and T satisfy (3.1.1) and $\rho(T) < 1$. In [62] the author interprets $F(\sum_{k=0}^{\infty} T^k)x_0$ as the distribution of accumulated newborns for which the initial distribution, x_0 , are responsible for. As $\rho(T) < 1$ we have that

$$F\left(\sum_{k=0}^{\infty} T^k\right) = F(I - T)^{-1}$$

and therefore the matrix $F(I - T)^{-1}$

"maps a generation of newborns to the next generation of newborns".

Note that in the fundamental theorem of demography, one of the assumptions is primitivity. In Theorem 3.1.5 we assumed that A was irreducible. Irreducibility and primitivity are related via the order of cyclicity. The *order of cyclicity* of an irreducible matrix $A \in \mathbb{R}^{n \times n}$ is the number of its eigenvalues whose modulus is $\rho(A)$. An irreducible matrix $A \in \mathbb{R}_+^{n \times n}$ is primitive if and only if its order of cyclicity is 1. The majority of the nonnegative matrices we encounter in this thesis are either irreducible or primitive.

An example of F and T that satisfy (3.1.1) are Leslie matrices [170]. $A \in \mathbb{R}_+^{n \times n}$ is a *Leslie matrix* if

$$A = F + T := \begin{pmatrix} f_{11} & f_{12} & f_{13} & \cdots & f_{1n} \\ 0 & 0 & 0 & \cdots & 0 \\ 0 & 0 & 0 & \cdots & 0 \\ \vdots & \vdots & \vdots & \ddots & \vdots \\ 0 & 0 & 0 & 0 & 0 \end{pmatrix} + \begin{pmatrix} 0 & 0 & 0 & \cdots & 0 \\ t_{21} & 0 & 0 & \cdots & 0 \\ 0 & t_{32} & 0 & \cdots & 0 \\ \vdots & & \ddots & \ddots & \vdots \\ 0 & 0 & 0 & t_{nn-1} & 0 \end{pmatrix}, \quad (3.1.3)$$

where $f_{1i} \geq 0$ and $t_{jj-1} \in (0, 1]$ are respectively the stage-specific fecundity and survival rates for stage classes $i \in \{1, \dots, n\}$ and $j \in \{2, \dots, n\}$. Each f_{1i} quantifies the number of newborns in class i and t_{jj-1} denotes the proportion of individuals in class $j - 1$ that survives and moves into class j . We will investigate Leslie matrices and their generalisation in more detail in Chapter 6 in the context of stage-structured diffusive dispersal.

It is common to assume that A is irreducible and also that $A^k \neq 0$ for some $k \in \mathbb{N}$, i.e. A is not nilpotent. Irreducibility is a reasonable ecological assumption and is interpreted in [256] as ensuring that

"the associated life cycle graph contains the necessary transition rates to facilitate pathways from all stages to all other stages."

Out of the 652 different population projection matrices evaluated in [256], which were used to model 171 different species in the literature, the authors found that only 24.7% of them were reducible. Nilpotency ensures that we can study the asymptotic dynamics of such systems, as if A is nilpotent then we would have what could be termed finite-time extinction. For a matrix A of the form (3.1.3) we have that A is irreducible when $f_{1n} > 0$. This condition also ensures that A is not nilpotent.

The net reproduction number for (3.1.3) can be derived as in [61]

$$R_0(A) = \sum_{i=1}^n f_{1i} \prod_{j=1}^{i-1} t_{jj-1}.$$

Although for positive systems Schur stability, Schur diagonal stability and Schur D -stability are equivalent, we will demonstrate how the results in the previous section apply to Leslie matrices.

Let A be a Leslie matrix of the form (3.1.3). It follows from Lemma 2.2.9 that A is diagonally Schur stable if and only if $I - A$ is quasidominant. Let the $P = \text{diag}(p_1, \dots, p_n) > 0$ denote a diagonal solution to (2.2.3). Thus A is diagonally Schur stable if and only if $\sum_{j \neq 1} f_{1j} p_j \leq f_{11} p_1$ and $t_{ii-1} p_{i-1} \leq p_i, i \in \{1, \dots, n\}$. This is in turn equivalent to $A p < p$. Therefore we get that A is Schur diagonally stable if and only if A is Schur. As $A \in \mathbb{R}_+^{n \times n}$ is of the form (3.1.3) then we get that TFAE:

1. A is Schur.
2. $R_0(A) < 1$.
3. A is Schur D -stable.
4. A is Schur diagonally stable.

An obvious extension to linear matrix models is introducing state dependence, i.e. replacing A in (2.2.2) by a nonlinear matrix-valued function. Next we will discuss such nonlinear models, their stability and persistence properties, and two ecological models in the literature used for modelling various population structure in plants and insects.

3.2. Density Dependence

When the dynamics of a population are affected by its size, this is known as density-dependence. One way of modelling this for structured populations is using nonlinear matrix models, where the linear time-invariant system described in the previous section

is replaced by a nonlinear matrix valued function. We expand on these model classes to show how they can be used to model real-world population dynamics.

3.2.1. Nonlinear Systems

Many species have discrete life stages, corresponding to morphological and physiological changes and matrix models provide a way of capturing such structure [62]. Despite the wide applicability of linear models, they do have some limitations. In many ecological systems, the dynamics of a population are affected by the size or density of itself or another population. Density-dependence is widely observed across a wide variety of species [39]. Examples of density dependent processes include, among others, resource/territory competition, predation and dispersal. Thus there is also a need to include more realistic, nonlinear functions of growth and dispersal into modelling population dynamics.

Recall that for linear models we partition the population of interest into predefined classes, with the density or population size in class i given by $x_i \in \mathbb{R}_+$, $i \in \{1, \dots, n\}$. These define a state vector $x \in \mathbb{R}_+^n$ and the nonlinear population dynamics are described by a *nonlinear matrix model*

$$\begin{aligned} x(t+1) &= G(x(t)) := A(x(t))x(t), \\ x(0) &\in \mathbb{R}_+^n, \end{aligned} \tag{3.2.1}$$

where $A : \mathbb{R}_+^n \rightarrow \mathbb{R}_+^{n \times n}$ is a C^1 matrix-valued function [61]. This model accounts for density-dependent processes like competition and predation, among many others, and generalises the linear matrix population models discussed in the previous chapter. The general model form (3.2.1) will arise again in Chapters 4 and 5. There has been a lot of interest in these models from the perspective of *uniform persistence*, where one aims at keeping some positive function of a population above a threshold after some sufficiently long time [95, 146, 239, 266]. Before discussing some persistence properties of nonlinear matrix models, we will briefly restate some results from [255], which describe how matrix stability relates to the dynamics of (3.2.1).

We can first see when extinction is inevitable (Proposition 3.12 of [255]). Assume that $\rho(A(0)) < 1$ and $A(x) \leq A(0)$ for all $x \geq 0$. It then follows that for $x(0) = x_0 \in \mathbb{R}_+^n$, a solution of (3.2.1) satisfies

$$x(t, x_0) = \prod_{s=1}^t A(x(t-s))x_0 \leq A(0)^t x_0 \tag{3.2.2}$$

for $t \geq 1$. As $\rho(A(0)) < 1$, it follows that $A(0)^t \rightarrow 0$ as $t \rightarrow \infty$. Thus, $x(t, x_0) \rightarrow 0$ as $t \rightarrow \infty$. In this case the extinction equilibrium is GAS. We now state a sufficient condition for the existence of a positive fixed point of G .

Theorem 3.2.1. [255] Let $G : \mathbb{R}_+^n \rightarrow \mathbb{R}_+^n$ be continuous and assume that there exists $R > 0$, $y \in \mathbb{R}_+^n$ and some $D \in \mathbb{R}_+^{n \times n}$ such that $\rho(D) < 1$ and $G(x) \leq y + Dx$, for $x \in \mathbb{R}_+^n$ and $\|x\| \geq R$. Let G be differentiable at 0 and further assume that either $G'(0)$ is irreducible, or $G(x) = A(x)x$ with $A(x)$ nonnegative, and $\rho(G'(0)) > 1$. Then, there exists some nonzero $x \in \mathbb{R}_+^n$ such that $G(x) = x$.

In Theorem 3.2.1 one of the assumptions is that $\rho(G'(0)) > 1$. In a lot of cases one can show that $G'(0) = A(0)$ and so this condition implies that the extinction equilibrium is unstable, as is the case with all of the nonlinear matrix models we study in Chapters 4 and 5. This then motivates us to investigate if there exists a positive equilibrium, as proved in Theorem 3.2.1. In [255], they did not explore the uniqueness or stability properties of such a positive fixed point, but instead focused on population persistence. We will now restate some persistence results, the application of which will be demonstrated in the examples that follow.

Theorem 3.2.2. [255] Let $\|\cdot\|$ be any norm on \mathbb{R}^n and let $\eta(x) = \|x\|$. Suppose $G(\mathbb{R}_+^n) \subseteq \mathbb{R}_+^n$, there exists $r_0 > 1$ and $v > 0$ such that $G'(0)v \geq r_0v$, and for every $\epsilon > 0$ there exists some $\delta > 0$ such that $\|G(x)\| \geq \delta$ when $\|x\| \geq \epsilon$. Then (3.2.1) is uniformly strongly η -persistent.

In Theorem 7.17 of [255] the authors give sufficient conditions for the existence of an $\epsilon > 0$ such that $\liminf_{t \rightarrow \infty} \min_j x_j(t, x_0) \geq \epsilon$ for any $x(0) = x_0$. They call this *stage-persistence*. Next we will discuss two ecological applications of the persistence results above and of stage-persistence, taken from [255], which make use of the assumption that $\rho(A(0)) > 1$.

3.2.2. A Biennial Plant Model

Consider a population that reproduces in the second year of its life and then does not survive to its third year. An example of such a species is a biennial plant [255]. Let x_1 denote the density of the juvenile/seedling class and x_2 denote the density of the adult/plant class. One possible model for the dynamics of such a population is given by the system

$$\begin{aligned} x_1(t+1) &= ax_2(t), \\ x_2(t+1) &= \frac{x_1(t)}{b + cx_1(t)}, \\ x(0) &\in \mathbb{R}_+^2, \end{aligned} \tag{3.2.3}$$

where $a, b, c > 0$. The right-hand side (RHS) of the second equation in (3.2.3) is an example of a Hassell map, which we will encounter again in Chapter 5. We can rewrite

(3.2.3) as a nonlinear matrix model (3.2.1) with

$$A(x) = \begin{pmatrix} 0 & a \\ (b + cx_1)^{-1} & 0 \end{pmatrix}.$$

Recall that the Jacobian of a smooth function $H : \mathbb{R}^n \rightarrow \mathbb{R}^n$ at a point $a \in \mathbb{R}^n$ is written as $H'(a)$ (see Section 2.1). Let $F(x) = A(x)x$. We can see from the form of $A(x)$ that

$$F'(0) = A(0) = \begin{pmatrix} 0 & a \\ b^{-1} & 0 \end{pmatrix}.$$

Using the characteristic polynomial of $A(0)$ we can compute the two eigenvalues of $A(0)$ as $\lambda_{\pm} = \pm\sqrt{a/b}$. Therefore $\rho(A(0)) = \sqrt{a/b}$. We can see that $A(0)$ is irreducible, and so by Theorem 2.2.2 there exists $v > 0$ such that $A(0)v = (\sqrt{a/b})v$.

Let $\epsilon > 0$ and suppose $\|x\|_{\infty} > \epsilon$. Then either $x_1 > \epsilon$ or $x_2 > \epsilon$. In the first case, we have that $ax_2 > a\epsilon$. In the second case, we can see that $x/(b + cx)$ is an increasing function of x . We then have that $x_1 > \epsilon$ implies that

$$\frac{x_1}{b + cx_1} > \frac{\epsilon}{b + c\epsilon}.$$

Therefore we have that

$$\|F(x)\|_{\infty} \geq \delta := \min \left\{ a\epsilon, \frac{\epsilon}{b + c\epsilon} \right\},$$

for all $x \in \mathbb{R}_+^2$ with $\|x\|_{\infty} > \epsilon$. Therefore, if $a > b$, then $\rho(A(0)) > 1$ and so Theorem 3.2.2 holds. The system (3.2.3) is then uniformly strongly persistent with respect to any norm on \mathbb{R}^n .

3.2.3. The LPA Model

Arguably, one of the most widely known nonlinear stage-structured models is the Larvae-Pupae-Adult (LPA) model, first proposed in [55] to explain the population dynamics of the cannibalistic flour beetle *Tribolium castaneum*.

If we denote by $x = (x_1 \ x_2 \ x_3)^T \in \mathbb{R}_+^3$ the abundance vector of larval, pupal and adult sub-populations, then the *LPA model* is given by (3.2.1) with

$$A(x) := \begin{pmatrix} 0 & 0 & p \exp(-ax_1 - bx_3) \\ q & 0 & 0 \\ 0 & r \exp(-cx_3) & s \end{pmatrix}, \quad (3.2.4)$$

where $s \in [0, 1]$ is the adult survival probability, $q \in [0, 1]$ is the larvae to the pupae transition probability, and $r \in [0, 1]$ is the pupae to the adult transition probability. The

parameters $a > 0$, $b > 0$, and $c > 0$ are related to cannibalism and $p > 0$ is the adult fecundity parameter. The stability of this system is partially determined by the spectral properties of $A(0)$. The net reproduction number for the LPA model can be computed as $R_0(A(0)) := qrp(1-s)^{-1}$. If the dynamics of the LPA model were assumed to be linear, i.e. $A(x) \equiv A(0)$, then $R_0(A(0))$ defines a potential growth indicator. One can show that system (3.2.1) with system matrix (3.2.4) is stage-persistent. We omit the details of this result for brevity, as it involves several technical results (Corollary 7.3 and Example 7.4) from [255]. In [255], the authors stated the following dichotomous result for the LPA model.

Theorem 3.2.3. [255] *Let system (3.2.1) be such that $A(x)$ is given by (3.2.4). Then*

1. $R_0(A(0)) < 1$ *implies the extinction equilibrium of F is GAS; and*
2. $R_0(A(0)) > 1$ *implies that (3.2.1) is stage-persistent.*

It can be shown that for $s \in [0, 1)$, for $y = (pa^{-1} 0 0)^T$ (with $a, p > 0$) and $D = A(0)$ there exists a nontrivial fixed point of (3.2.1) by Theorem 3.2.1. In Chapter 6, we will revisit the LPA model in the context of dispersal-driven growth for structured population models. Next, we will discuss another type of matrix model, proposed in [117], to model species that exhibit dormancy within their life cycle. The model and robust stability type that we explore in the next section is closely related to the material in Chapter 6.

3.3. Quiescence

Quiescence, as defined in [77], is

"a type of irregular dormancy (non-seasonal) characterised by slowed metabolism and directly resulting from unfavourable environmental conditions."

Quiescence is not dependent on physiology, but on external stimuli and thus is not inherent in a species life-cycle [65]. It is a widely observed mechanism of survival found in many invertebrate, microbial and plant species [63]. It is also a widespread feature of many cancer cell populations [199]. In this section we will discuss the work of [117] concerning the population dynamics of a species that enters atypical phases of dormancy. For more on mathematical models of quiescence see [10, 115, 116, 118, 119, 120, 187].

We will now discuss several results related to quiescence for discrete-time models. In [117] the author starts from a general coupled model of the form

$$\begin{aligned} v(t+1) &= (I - P)f(v(t)) + Qg(w(t)) \\ w(t+1) &= Pf(v(t)) + (I - Q)g(w(t)). \end{aligned} \tag{3.3.1}$$

with $(v(0) \ w(0))^T \in \mathbb{R}_+^{2n}$. Here $v, w \in \mathbb{R}_+^n$ are abundance vectors and $f, g : \mathbb{R}_+^n \rightarrow \mathbb{R}_+^n$ are smooth maps that respectively describe two discrete time systems on \mathbb{R}^n . The diagonal elements of the matrices $P = \text{diag}(p_1, \dots, p_n)$ and $Q = \text{diag}(q_1, \dots, q_n)$ are assumed to satisfy $p_i, q_i \in [0, 1]$ for each $i \in \{1, \dots, n\}$. Hadeler calls $v(t+1) = f(v(t))$ the *simple system* and defines the *quiescent system* on \mathbb{R}_+^{2n} to be (3.3.1) with $g(w) = w$ for all w . Here v is the population abundance vector for the *active phase* and w represents the *quiescent phase*. The diagonal elements of P and Q describe the transition rates between quiescent and active phases.

With these simplifying assumptions, we can rewrite (3.3.1) as

$$\begin{pmatrix} v(t+1) \\ w(t+1) \end{pmatrix} = \begin{pmatrix} I - P & Q \\ P & I - Q \end{pmatrix} \begin{pmatrix} f(v(t)) \\ w(t) \end{pmatrix}. \tag{3.3.2}$$

with $(v(0) \ w(0))^T \in \mathbb{R}_+^{2n}$. Note that if v^* is an equilibrium of the simple system, then $x^* = (v^*, Q^{-1}Pv^*)$ is an equilibrium of the quiescent system (3.3.1) with $g(w) = w$. Let A denote the Jacobian of f at v^* . We assume that $\rho(A) < 1$, so that v^* is locally asymptotically stable. The Jacobian of (3.3.1) at v^* is

$$J = \begin{pmatrix} (I - P)A & Q \\ PA & I - Q \end{pmatrix} \tag{3.3.3}$$

Assuming $P \neq pI$ and $Q \neq qI$ for any $p, q > 0$, one calls A *strongly stable with respect to quiescent phases* or *quiescently Schur* if (3.3.3) is Schur for all diagonal $0 \leq P, Q \leq I$. This means that, regardless of the choice of feasible transitions rates, our linearised quiescent system remains stable. Therefore, along with D -stability, this form of quiescent Schur stability can be thought of as another form of robust matrix stability.

The next proposition is from [117]. Note that, in that paper, the author uses the term strong stability for what we are calling, in line with common practice, Schur D -stability.

Proposition 3.3.1. [117] *If $A \in \mathbb{R}^{n \times n}$ is Schur D -stable then A is quiescently Schur.*

As noted in [117] it is more difficult to characterise quiescent stability when $n > 2$. This is why we will now present some low-dimensional results for quiescent systems in discrete time. Using the Schur-Cohn criterion (see [136, 80]) for stability, in [117] the author proved the following result when $n = 2$.

Corollary 3.3.2. [117] Let $A \in \mathbb{R}^{2 \times 2}$ and assume that

$$\begin{aligned} \det(A) \pm (a_{11} + a_{22}) + 1 &> 0 \\ -\det(A) \pm (a_{11} - a_{22}) + 1 &> 0. \end{aligned} \tag{3.3.4}$$

Then A is quiescently Schur.

It was also shown in [117] that there is an equivalence between Schur D -stability and quiescent Schur stability when $n = 2$.

Proposition 3.3.3. [117] Let $A \in \mathbb{R}^{2 \times 2}$. Then the inequalities in (3.3.4) hold if and only if A is Schur D -stable.

3.3.1. Host-Parasitoid Dynamics

The Nicholson-Bailey model is frequently used in entomology to study the dynamics of an insect host and a parasitoid [200, 210]. We will now discuss stability in discrete time for such a host-parasitoid system with quiescence, as outlined in [117].

Denote by $x \in \mathbb{R}_+$ and $y \in \mathbb{R}_+$ the size of host and parasitoid populations, respectively. Let $f : \mathbb{R}_+^2 \rightarrow \mathbb{R}_+$ be a smooth function that represents the proportion of hosts that are not parasitised by y . The parameter $\mu > 0$ is interpreted as the host rate of reproduction and parameter $c > 0$ the average number of viable eggs laid by a parasitoid on a single host egg. The dynamics of such populations can be modelled as

$$\begin{aligned} x(t+1) &= \mu x(t) f(x(t), y(t)) \\ y(t+1) &= cx(t)(1 - f(x(t), y(t))), \end{aligned}$$

with $(x(0) \ y(0))^T \in \mathbb{R}_+^2$. We assume that ay is the average number of encounters over one time interval [80]. Parasitoid escape is modelled by the exponentially decreasing function $f(x, y) := e^{-ay}$. As noted in [80], this model does not take account of prey saturation (inclusion of resource limitations). Modifying the growth equation for the host by including a carrying capacity, $K > 0$, we get the well studied host-parasitoid system

$$\begin{aligned} x(t+1) &= x(t) \exp \left(r \left(1 - \frac{x(t)}{K} \right) - ay(t) \right) \\ y(t+1) &= cx(t) (1 - \exp(-ay(t))), \end{aligned} \tag{3.3.5}$$

with $(x(0) \ y(0))^T \in \mathbb{R}_+^2$. By scaling (3.3.5), one can let $K = 1$ and then see that the equilibrium given by $(x_1^*, y_1^*) = (1, 0)$ is stable for $r < 2$ and $a < 1$ [80]. For any $r > 0$ and $a > 1$ there is a unique equilibrium point (x_2^*, y_2^*) .

An extended version of system (3.3.5), called a "react first, then go quiescent" model, was introduced in [117], which can be written as

$$\begin{aligned}
 x(t+1) &= (1-p_1)x(t)\exp\left(r\left(1-\frac{x(t)}{K}\right)-ay(t)\right)+q_1w(t) \\
 y(t+1) &= (1-p_2)x(t)(1-\exp(-ay(t)))+q_2z(t) \\
 w(t+1) &= p_1x(t)\exp\left(r\left(1-\frac{x(t)}{K}\right)-ay(t)\right)+(1-q_1)w(t) \\
 z(t+1) &= p_2x(t)(1-\exp(-ay(t)))+(1-q_2)z(t),
 \end{aligned} \tag{3.3.6}$$

with $(x(0) y(0) w(0) z(0))^T \in \mathbb{R}_+^4$. The author proved that if $r \in (0, 2)$, then there exists $\bar{a}(r) > 1$ such that there exists a positive coexistence equilibrium and the Jacobian of (3.3.6) at this coexistence equilibrium is Schur for $a \in (1, \bar{a}(r))$ and not Schur for $a > \bar{a}(r)$.

3.4. Diffusion

Population composition and size change over time, but also across a habitat or observation region of interest. Thus taking account of such spatial structure is important in order to understand how processes like habitat fragmentation affects such populations. In the next section we will discuss mathematical models with spatial structure. In particular we will discuss some common discrete-time models of diffusion and dispersal, and how matrix theory can be applied to prove some stability/instability results related to these models. This is to complement the work in Chapter 6, where we will look at a population diffusion model.

3.4.1. Turing Instability

A concept closely related to quiescent stability, which we discuss later, is Turing instability, first detailed in [274] in relation to pattern formation in morphogenesis. We will briefly outline this problem from a matrix theoretic perspective, where one is modelling the diffusion of populations around some habitat. This problem is of interest when using partial differential equation models, so called reaction-diffusion systems. However, as our interest in this study is discrete-time difference equation models, we will not pursue the PDE formulation. The details of such studies can be found in [243] and references therein.

Consider $n \geq 2$ species, $x \in \mathbb{R}_+^n$, diffusing across some habitat. Given a so-called reaction function, $f : \mathbb{R}_+^n \rightarrow \mathbb{R}_+^n$, which describes how such species grow over time, let $A \in \mathbb{R}^{n \times n}$ be the Jacobian of f at 0. Turing instability corresponds to determining the existence of

a diagonal $P \in \mathbb{R}_+^{n \times n}$ such that $A - tP$ has a real and positive eigenvalue for some $t > 0$. In [243] the authors briefly discussed when a Hurwitz matrix A exhibits Turing instability for the case $n = 4$. In [121] the authors proved the following result.

Theorem 3.4.1. [121] *Let S_n be the minimal number of nonzero entries that an irreducible matrix $A \in \mathbb{R}^{n \times n}$ must have in order for it to exhibit Turing instability. If $n \geq 3$, then $S_n \leq 2n + 1 - \lfloor \frac{n}{3} \rfloor$, where $\lfloor x \rfloor$ is the greatest integer less than or equal to $x \in \mathbb{R}$. In particular the equality holds when $n = 3$, with $S_3 = 6$.*

We refer the reader to [121] for more details. If the Jacobian of f at 0, namely A , corresponds to a linearisation of such a system around the extinction equilibrium, then Theorem 3.4.1 gives an upper bound for the number of entries in A that are nonzero for it to be unstable following perturbation by some scaled diagonal matrix. In the context of reaction-diffusion systems, Turing instability means that the previously isolated (reaction) system has a stable extinction equilibrium, but this can be destabilised via diffusion. Other authors have investigated this problem for particular cases and applications, for example see [197, 284].

3.4.2. Diffusively Coupled Systems

A related problem to Turing instability and quiescent stability was outlined in [69]. In this paper the author considered diffusively coupled continuous-time linear time-invariant systems defined on a proper cone, and determined sufficient conditions for GAS of the trivial equilibrium following diffusive coupling. We will outline this general framework for continuous-time systems and pose an analogous problem in discrete-time and when our state space is the nonnegative orthant. We will also demonstrate its application when modelling diffusive dispersal between demographically-structured populations. In Chapter 6 we will discuss the properties of this model in more detail.

A set $C \subset \mathbb{R}^n$ is a closed convex *cone* if $\alpha x + \beta y \in C$ for all $\alpha, \beta \geq 0$, $x, y \in C$. Let ∂C be the *boundary* of C and $\text{Int}(C)$ the *interior* of C . A cone C is *solid* if $\text{Int}(C)$ is non-empty, and *pointed* if $x \in C$ and $-x \in C$ both imply that $x = 0$. A cone C is *proper* if it is non-empty, closed, convex, solid and pointed. Given a proper cone C in \mathbb{R}^n , C^m is also a proper cone in \mathbb{R}^{nm} for $m \in \mathbb{N}$. Given a vector space V over \mathbb{R} , a *linear functional* is an element of the *dual space*, V^* , i.e. a linear map from V to \mathbb{R} . The Riesz Representation Theorem allows one to identify every $\lambda \in (\mathbb{R}^n)^*$ with a unique v in \mathbb{R}^n such that $\lambda(x) = \langle x, v \rangle$ for all $x \in \mathbb{R}^n$, where $\langle \cdot, \cdot \rangle$ is the usual Euclidean inner product [16]. Using this identification, for a convex cone C , we can consider its *dual cone*

$$C^* := \{v \in \mathbb{R}^n : \langle x, v \rangle \geq 0 \text{ for all } x \in C\},$$

which is always a non-empty closed convex cone. Denote by $\mathcal{L}(\mathbb{R}^n)$ the set of all linear maps from \mathbb{R}^n to \mathbb{R}^n . For $i, j \in \{1, \dots, m\}$, $m \in \mathbb{N}$, we say that the map $D \in \mathcal{L}(\mathbb{R}^n)$ acts diffusively on a proper cone C , if we have that $D(C) \subset C$, $(x, v) \in \partial C \times C^*$ and $\langle x, v \rangle = 0$ implies that $\langle Dx, v \rangle = 0$.

In [69] the author looked at the continuous-time, diffusively coupled system on \mathbb{R}^{nm}

$$\begin{aligned} \frac{dx_i}{dt} &= A_i x_i + \sum_{j \neq i} D_{ij} (x_j - x_i), \\ x_i(0) &\in \mathbb{R}_+^n, \end{aligned} \tag{3.4.1}$$

where $x_i \in C$, each $D_{ij} = D_{ji}$ acts diffusively on C and $A_i \in \mathcal{L}(\mathbb{R}^n)$ are quasi-monotone for C . i.e. $\langle x, v \rangle = 0$ for $(x, v) \in \partial C \times C^*$ implies that $\langle A_i x, v \rangle \geq 0$, for $i \in \{1, \dots, m\}$. We briefly discuss the formulation of [69] in continuous time so to show how it relates with the model and results we obtain in Chapter 6. Quasi-monotonicity implies that $A_i(C) \subset C$ [69]. One can rewrite the system (3.4.1) as

$$\begin{aligned} \frac{dX}{dt} &= M_1 X, \quad X(0) \in \mathbb{R}^{nm}, \\ M_1 &:= \begin{pmatrix} A_1 - \sum_{j \neq 1} D_{1j} & D_{12} & \cdots & D_{1m} \\ D_{21} & A_2 - \sum_{j \neq 2} D_{2j} & \cdots & D_{2m} \\ \vdots & \vdots & \ddots & \vdots \\ D_{m1} & D_{m2} & \cdots & A_m - \sum_{j \neq m} D_{mj} \end{pmatrix}, \end{aligned} \tag{3.4.2}$$

where $X = (x_1^T \ x_2^T \ \cdots \ x_m^T)^T \in \mathbb{R}^{nm}$. If M is Hurwitz in continuous-time then (3.4.1) has a GAS extinction equilibrium for all $\{D_{ij}\}$ that act diffusively on C . A reasonable question to ask then is what assumptions do we need on $\{A_1, \dots, A_m\}$ so that M_1 is Hurwitz for all $\{D_{ij}\}$ that act diffusively on C ? An answer to this problem for proper cones was given by [69]. Note that a Lyapunov function, V , is a *common Lyapunov function* for a finite set of linear operators $\mathcal{A} = \{A_1, \dots, A_m\} \subset \mathcal{L}(\mathbb{R}^n)$ if V is a Lyapunov function for each $A \in \mathcal{A}$.

Theorem 3.4.2. [69] *Given a proper cone C in \mathbb{R}^n , assume that $A_1, \dots, A_m \in \mathcal{L}(\mathbb{R}^n)$ are quasi-monotone for C . Further assume that $\{D_{ij}\}$ is nonempty and acts diffusively on C . If $\{A_1, \dots, A_m\}$ admit a common linear copositive Lyapunov function (CLCLF) on C , then M_1 is Hurwitz for all $\{D_{ij}\}$ that act diffusively on C .*

One can define a discrete time version of (3.4.2), which, like its continuous-time analogue, mimics Fick's first law of diffusion [21], where there is a flow from high to low states, determined by the coupling matrices. We will now consider a discrete-time, diffusively coupled system similar to the above case, but when specifically modelling population densities, meaning we are working with the particular case where the cone, C , is the nonnegative orthant, \mathbb{R}_+^n .

Let $C \equiv \mathbb{R}_+^n$. The boundary of \mathbb{R}_+^n is $\partial\mathbb{R}_+^n := \{x \in \mathbb{R}_+^n : \prod_{i \in \bar{n}} x_i = 0\}$ and \mathbb{R}_+^n is *self-dual*, i.e. $(\mathbb{R}_+^n)^* = \mathbb{R}_+^n$. The only set of linear operators $\{D_{ij}\}$ that act diffusively on \mathbb{R}_+^n are diagonal nonnegative matrices [69]. Also note that when $C \equiv \mathbb{R}_+^n$ quasi-monotonicity implies that the matrices A_1, \dots, A_m are Metzler [69].

For $m \in \{2, 3, \dots\}$ patches within some landscape, let $x_i \in \mathbb{R}_+^n$ denote the density vector on patch $i \in \{1, \dots, m\}$, where each component of x_i is a demographic class, such as age, hierarchy level, stage etc. Let $A_i \geq 0$ be a population projection matrix that describes how patch i reproduces and recruits individuals from each stage class. For $i, j \in \{1, \dots, m\}$ with $i \neq j$, let $D_{ij} = D_{ji}$ be a nonnegative diagonal matrix such that $A_i - D_{ij} \geq 0$. The matrix $D_{ij} = D_{ji}$ describes the diffusive movement of individuals in and out of each class between patches i and j . The model is

$$X(t+1) = M_1 X(t), \quad X(0) \in \mathbb{R}_+^{nm}, \quad (3.4.4)$$

where we specify that $C^m = \mathbb{R}_+^{nm}$. Here M_1 is the same as in (3.4.3), but is nonnegative because $A_i \geq 0$ and each $D_{ij} = D_{ji} \geq 0$ satisfies $A_i - D_{ij} \geq 0$. Assume that $\rho(A_i) < 1$ for $i \in \{1, \dots, m\}$, so each patch goes extinct in isolation. Can we find criteria for $\{A_1, \dots, A_m\}$ that ensure stability of M_1 for any set of coupling matrices $\{D_{ij}\} \subset \mathcal{D}$? In Chapter 6 we will investigate this problem further. Next we will discuss metapopulations, where populations are spread amongst a patchy landscape with asymmetric and potentially nonlinear movement between patches.

3.5. Patchy Dispersal

When ecological invasions occur it is often in the presence of an interacting resident community. However, in Chapter 4 we will focus on the situation when a single species is expanding its range from one patch/region to another. In the past, many authors have investigated how dispersal affects the overall dynamics of two coupled populations. In the papers of [93, 113, 279] the authors studied the planar model

$$\begin{aligned} x_1(t+1) &= (1-d) f_1(x_1(t)) + d f_2(x_2(t)), \\ x_2(t+1) &= (1-d) f_2(x_2(t)) + d f_1(x_1(t)), \\ x(0) &\in \mathbb{R}_+^2. \end{aligned} \quad (3.5.1)$$

In [93] the authors assumed that $f_i(x) = r_i x g_i(x)$, where $g_i : \mathbb{R}_+ \rightarrow (0, \infty)$ was strictly decreasing, $g_i(0) = 1$ and $d \in [0, 1]$. They showed that, when the spectral radius of the Jacobian of system (3.5.1) at 0 is less than 1, any initial population is driven to extinction. On the other hand, they showed that (3.5.1) is permanent (there is a compact set $K \subset \text{Int}(\mathbb{R}_+^2)$ and $t_0 > 0$ such that any solution $x(t, x_0)$ remains in K for all $t \geq t_0$) if the

spectral radius of the Jacobian of the system at the extinction equilibrium is greater than 1. The model was investigated numerically for various parameter scenarios when regional dynamics are given by either a Ricker or Hassell-1 map. In [279] the authors assumed that $d \in [0, 0.5]$ and $f_1 = f_2 = f$, where f was given by an extension of the Ricker map. They found that the appearance and disappearance of attractors of their coupled system is dependent on how strong the level of dispersal is, quantified by d . They also explored how transient phenomena emerged within such a simple coupled system. More recently, in [113] the authors assumed that each f_i was given by a Hassell-1 map, with each patch being a so-called source, and $d \in [0, 1]$. They investigated how changing the dispersal rate in various scenarios affected the asymptotic total population size and discussed the biological interpretations of their results. In Chapter 4 we will extend such models to include density-dependent dispersal. Chapter 5, we will look at a dispersal model between arbitrarily finite many regions, where there is heterogeneous dynamics on each patch. The rest of this section explores similar multi-patch models, where dispersal is assumed to be passive/constant.

The authors of [288] investigated the system

$$\begin{aligned} x_i(t+1) &= \left(1 - \sum_{j=1}^n d_{ij}\right) f_i(x_i(t)) + \sum_{j=1}^n d_{ji} f_j(x_j(t)), \\ x_i(0) &\in \mathbb{R}_+, \end{aligned} \tag{3.5.2}$$

where for each $i \neq j$, $0 < d_{ij}, d_{ji} < 1$, $\sum_{j=1}^n d_{ij} \in (0, 1)$ and $d_{ii} = 0$. Each d_{ij} is the proportion of individuals dispersing from region i to j . They also assumed that each f_i was given by a so-called α -concave monotone map, for $\alpha \in (0, \infty]$. A positive C^2 map, f , is α -concave monotone if $f'(x) > 0$ and $f''(x) < 0$ for all $x \in [0, \alpha]$. Examples of such maps can be generated by choosing appropriate parameterisations of *Ricker*, *Smith-Slatkin* and *Beverton-Holt* maps [288]. The authors then went to give a sufficient condition for the existence and global stability of a positive fixed point of (3.5.2).

In [156] the authors proposed the following n -patch model

$$\begin{aligned} x(t+1) &= S_p \Gamma(x(t)) x(t), \\ x(0) &\in \mathbb{R}_+^n \end{aligned} \tag{3.5.3}$$

where $p \in (0, 1]^n$ is a vector of such that p_i is the dispersal probability of an individual on patch i , $S = (s_{ij}) \in \mathbb{R}_+^{n \times n}$ is a primitive column substochastic matrix such that s_{ji} is the probability that a dispersing individual from patch i survives to patch j , $\Gamma : \mathbb{R}_+^n \rightarrow \mathbb{R}_+^{n \times n}$ is given by $\Gamma(x) = \text{diag}(g_1(x_1), \dots, g_n(x_n))$, which contains the regional growth functions of each patch. Furthermore they defined $S_p := I - \text{diag}(p) + S \text{diag}(p)$. Each $g_i : \mathbb{R}_+ \rightarrow \mathbb{R}_+$

is a positive, continuous, decreasing map such that $\lim_{x_i \rightarrow \infty} g_i(x_i) < 1$ and $f_i(x) = g_i(x)x$ is increasing. In relation to (3.5.3), the authors stated the following result, the proof of which relied heavily on the strong monotonicity properties of their system class. A map F is *strongly monotone* if $F(x) \geq F(y)$ ($F(x) > F(y)$) whenever $x \geq y$ ($x > y$).

Theorem 3.5.1. [156] *If $\rho(S_p\Gamma(0)) \leq 1$ then the extinction equilibrium for (3.5.3) is GAS. If $\rho(S_p\Gamma(0)) > 1$ then there exists a GAS positive equilibrium for (3.5.3).*

A variation of the models in [156, 288] were studied in [241, 242]. In these papers, the model studied is of the form

$$x_i(t+1) = \sum_{j=1}^n d_{ji} f_j(x_j(t)), \quad (3.5.4)$$

where $x_i(0) \in \mathbb{R}_+^n$. In [241] the author assumed that $f_1 = f_2 = \dots = f_n = f$, where $f(x) = g(x)x$ for $g : \mathbb{R}_+ \rightarrow \mathbb{R}_+$. The author also assumed that $\sum_j d_{ij} = 1$. Under the additional assumption that $d_{ij} = d_{ji}$ for all $i, j \in \{1, \dots, n\}$, they proved that if $x^* \geq 0$ is GAS for f then $(x^*, \dots, x^*) \in \mathbb{R}_+^n$ is GAS for (3.5.4). In [242] the author looked at (3.5.4), but where $f_i(x)$ comes from a family of continuous, one-parameter, positive maps. The author then looked numerically at various scenarios involving different dispersal mechanisms when restricted to two regions, and where sources were connected to sinks. An early instance of a model of the form in (3.5.4) can be found in [151], where the local stability properties of a planar system in the applied context of mathematical genetics were studied. The above n -patch systems provide some context to the work we present in Chapter 5, where we consider nonlinear, asymmetric dispersal between n regions.

3.6. Dispersal-Driven Growth

Recently one concept that has garnered considerable interest in relation to dispersal is dispersal-driven growth (DDG). Roughly speaking, DDG corresponds to the situation wherein isolated populations are predicted to become extinct, but the act of coupling leads to population persistence or growth. DDG can be likened to the classical Diffusion-Driven Instability of Turing from the 1950s [274], and is, to quote from [153],

"[...] an interesting example of an emergent dynamical phenomenon which arises from the combination of several elementary mechanisms, and which cannot occur if any of the mechanisms are excluded."

A closely related phenomena to DDG occurs in source-sink dynamics, which trace their roots back to [229]. A source (sink) is a patch where a population exhibits asymptotic growth (extinction). We will explore sources and sinks more in Chapter 5.

Much attention has been devoted to the study of DDG and source-sink dynamics, although often for scalar valued population models [22, 153]. However, the life cycles of numerous species involve transitions through distinct developmental stages, such as instars in insects. This motivates the use of structured population models, which are popular in mathematical/theoretical ecology as they allow for consideration of such within-population demographic variation. Knowledge of how dispersal affects these stage classes is vital in order to understand the effect of habitat fragmentation and biodiversity loss on vulnerable and endangered species [94].

In [114] the authors investigated DDG from the perspective of stage-structured population models. Following reproduction/recruitment, we will assume that the state variable in patch i , denoted $x_i(t) \in \mathbb{R}_+^n$, evolves according to

$$\begin{aligned} x_i(t+1) &= A_i x_i(t) - D_{ii} x_i(t) + \sum_{j \neq i} \gamma_{ij} D_{ij} x_j(t), \\ x_i(0) &\in \mathbb{R}_+^n. \end{aligned} \tag{3.6.1}$$

Here $i \in 1, \dots, m$, and the nonlinear matrix-valued function $A_i : \mathbb{R}_+^n \rightarrow \mathbb{R}_+^{n \times n}$ models density-dependent recruitment and survival/growth on patch i . Here $D_{ij} \in \mathbb{R}_+^{n \times n}$ accounts for the effect of dispersal of patch j on patch i . The parameters $\gamma_{ij} \in [0, 1]$ are such that $\sum_{j=1} \gamma_{ij} \in [0, 1]$, and account for mortality or cost of dispersal from patch j . In ecological applications when managing species of conservation concern, researchers frequently use regional (non)linear matrix models, A_i , of so-called Leslie, Leftkovich or LPA form, as we discussed for linear models in Chapter 2.

Note that to ensure solutions of system (3.6.1) are nonnegative we assume that $A_i(x) - D_i \geq 0$ for all $x \geq 0$. Note that (3.6.1) is closely related to the diffusively coupled model of [69], and represents a general, heterogeneous patch topology, where dispersal is asymmetric, there are interactions among dispersing stage classes, and there is a risk attached to dispersal, such as mortality. In the context of (3.6.1), before connection via dispersal, the authors of [114] assumed that patch i is a sink, i.e. $\rho(A_i(0)) < 1$ and $A(x) \geq A(0)$ for all $x \leq 0$, so that the extinction equilibrium is GAS. They then proved the following necessary condition for DDG.

Theorem 3.6.1. [114] *If $A_1, \dots, A_m \in \mathbb{R}_+^{n \times n}$ admit a common linear Lyapunov function (CLLF), then the zero equilibrium of the dispersal model (3.6.1) is globally exponentially stable, for all feasible dispersal matrices $\{D_{ij}\}$ and for all feasible weightings $\{\gamma_{ij}\}$. Consequently, that $\{A_1, \dots, A_m\}$ does not admit a CLLF is a necessary condition for DDG.*

In relation to stage structured dispersal, we will investigate DDG in further detail in

Chapter 6 in relation to stage-structured diffusion, Leslie matrices and the LPA model. In the next section we finish by investigating some stochastic models of population dynamics in the context of modelling social interactions, which is a preface to the work presented in Chapter 7.

3.7. Stochasticity and Interactions

In reality ecological systems are random/stochastic. Deterministic systems have merit in the fact that they can represent conceptual idealistic situations where one can study the core aspects of inherently complex ecological systems. Throughout this thesis we have varying perspectives of within-population structure. The final structure we will investigate is social structure, albeit from a stochastic perspective. This is to complement the work in Chapter 7, where we will look at a stochastic model of social group dynamics. Note that in this chapter and in Chapter 7 we make a change to the notation we use to denote time dependence. Instead of indexing time using brackets will use subscripts, to make expressions easier to read.

When populations are censused/sampled in the field or in ecological experiments they are typically measured by abundance or population size, which are nonnegative and integer-valued, i.e. taking values in \mathbb{Z}_+ . These *counts* are observed over time, thus creating a time series of such a population's density or abundance over some finite observation window or time horizon.

Abundance or counts are typically modelled using discrete probability distributions, such as the Poisson and Negative-Binomial distributions [135]. We refer the reader to Section 2.4 of Chapter 2 for a more general discussion of positive integer-valued time series modelling. For example, let Y , the abundance of a population or group of interest, have a Poisson distribution, $Y \sim \mathcal{P}(\lambda)$, with intensity parameter $\lambda \in \mathbb{R}_+$, i.e. $\mathbb{P}[Y = y] = e^{-\lambda} \lambda^y / y!$. If we observe a population over some time period, i.e. Y above is a stochastic process, we may specify that for a fixed time $t \geq 0$ we have that $Y_t \sim \mathcal{P}(\lambda_t)$, where λ_t is called an *inhomogenous intensity process*. We may specify particular forms for λ_t that allows us to take account of demographic/environmental covariates or past observations of Y_t , for example. Later in this chapter we will discuss this further in the context of observation-driven models. In Chapter 7 we will also delve into inhomogenous intensities in more detail. Next, we will discuss population interactions in ecology and how we could model these in a stochastic setting.

3.7.1. Community Dynamics

When modelling pairwise interactions between species within a community, in [249] the author proposed using Poisson Lotka-Volterra (PLV) processes. Let $x_t = (x_{1,t}, \dots, x_{n,t})^T \in \mathbb{R}_+^n$ be a vector of $n \in \{2, 3, \dots\}$ interacting species at time $t \geq 0$, where the subscripts denote the identity of species i . Let $A = (a_{ij}) \in \mathbb{R}_+^{n \times n}$ be the interaction matrix, where a_{ij} is the “per-capita” effect of species j on species i . Let the vector $r = (r_1, \dots, r_n)^T \in \mathbb{R}_+^n$ be a vector of the “intrinsic per-capita growth rates” for all species. The discrete-time Lotka-Volterra model is given by

$$\begin{aligned} x_{i,t+1} &= L_i(x_t) := x_{i,t} \exp\left(r_i + \sum_j a_{ij} x_{j,t}\right), \\ x_{i,0} &= x_i^{(0)} \in \mathbb{R}_+, \end{aligned}$$

where $i \in \{1, 2, \dots, n\}$. In a PLV model we assume that $x_{i,t}$ is a count random variable, where

$$\mathbb{P}[x_{i,t+1} = k | x_{i,t} = x] = \frac{e^{-L_i(x)} L_i(x)^k}{k!},$$

i.e. $x_{i,t+1}$ is Poisson distributed with intensity given by $L_i(x_t)$. In other words, the deterministic Lotka-Volterra system describes the mean dynamics of the stochastic PLV system. In [249] the author investigated the asymptotic dynamics of such a stochastic model, deriving conditions for persistence and coexistence. We omit the explicit results shown in [249] as it would require us to define a stochastic version of persistence and asymptotic stability.

When modelling interactions between a small number of species, such as between predators and their prey, we could also consider more complex model paramterisations, in order to elucidate specific mechanisms of species interactions. For example, in [20] the authors fitted a stochastic model to simulated time series of predator-prey densities and kill rate data, in order to investigate how the inclusion of interaction data affects model identifiability.

The stochastic model they considered was given by

$$\begin{aligned} X_{t+1} | G_t, X_t, Y_t &\sim \mathcal{N}(\mu_{1,t}, \sigma_1^2), \\ Y_{t+1} | G_t, X_t, Y_t &\sim \mathcal{N}(\mu_{2,t}, \sigma_2^2), \\ \mu_{1,t} &:= X_t + r - \frac{G_t P_t}{V_t} - \ln(1 + \gamma V_t) \\ \mu_{2,t} &:= Y_t + s - \ln\left(1 + \frac{q P_t}{V_t}\right). \end{aligned} \tag{3.7.1}$$

for $r, \gamma, s, q > 0$, where V_t represents the prey density and P_t the predator density at time $t \geq 0$, taken to be count random variables, $X_t := \ln(V_t)$ and $Y_t := \ln(P_t)$. We assume

$V_t, P_t \neq 0$ for any $t \geq 0$, so X_t and Y_t are well defined. The functional response model, which describes the resource intake rate of V_t , is given by

$$G_t|V_t \sim \mathcal{N}(g(V_t), \sigma_3^2),$$

where we define the so-called *Holling type II functional response* as $g(V_t) = aV_t/(b + V_t)$, for $a, b > 0$, i.e. the intake rate of V_t is an increasing (saturating) function. Assuming that V_t and P_t are now just real numbers for each $t \geq 0$ (and not random variables), the corresponding deterministic system to (3.7.1) is given by

$$\begin{aligned} V_{t+1} &= \frac{V_t e^r}{1 + \gamma V_t} \exp\left(\frac{-g(V_t)P_t}{V_t}\right), \\ P_{t+1} &= \frac{P_t e^s}{1 + qP_t/V_t}, \end{aligned} \tag{3.7.2}$$

with $(V_0, P_0)^T = (V, P)^T \in \mathbb{R}_+^2$ [20]. In the stochastic model we are essentially taking the mean process for X_t and Y_t to be the natural logarithm of the respective RHS of (3.7.2) with V_t and P_t being count random variables. In [20] the authors found that when the deterministic component of the model, i.e. (3.7.2), was parametrised so that solutions either converge to a stable fixed point or a stable limit cycle, adding Gaussian noise to this system, i.e. (3.7.1), results in more accurate parameter estimation, when they took account of known kill rate data than without it. They also assessed the practical identifiability of their stochastic model in a Bayesian setting, using the prior-posterior overlap, as discussed in Chapter 2, to conclude weak identifiability. In Chapter 7 we will be interested in predation, inferring interactions and assessing weak parameter identifiability, albeit from a structured population perspective.

A single definition of interaction, be it between individuals, groups or populations, is not so easy to state when studying complex ecological systems. The difficulty of measuring interactions within food webs is that co-occurrence of species does not imply that they interact with one another, with higher-order effects and various abiotic processes also blurring how explicit or implicit these interactions are [30, 291]. In [25] the authors give a list of possible interaction metrics that can be used in the context of community interactions. One that stands out as a simple but useful interaction strength metric, in the stochastic context, is the standard Pearson's correlation coefficient

$$\text{Corr}(X, Y) := \frac{\text{Cov}(X, Y)}{\sqrt{\text{Var}(X)\text{Var}(Y)}}, \tag{3.7.3}$$

where X and Y are count random variables with finite moments, which could represent the abundance of two populations. The magnitude of the correlation between changes of one species' abundance and changes in another is a simple way of measuring a food-web's

response to temporal abundance changes, especially when using observational data. As noted in [25], these metrics can sometimes be difficult to interpret, but they do however allow for the inclusion of indirect interactions, for example. In Chapter 7 we will investigate a general stochastic framework, with the aim of being able to quantify interaction strengths from time series data of groups within a population using (3.7.3) as a measure of interaction strength. Next, we will outline the general setting for observation-driven count models.

3.7.2. Observation-Driven Models

Many count time series models can be classified into two types, observation-driven and parameter-driven models [161], which was first introduced in [56]. For the former, the parameter values are written as deterministic functions of previous dependent variables, as well as current and past external variables. For the latter, the current parameters change over time via dynamic processes that incorporate random, unique shocks or disturbances specific to each time period [161]. Later in Chapter 7, we will be using an observation-driven approach. See [68] for other formulations of observation- and parameter-driven models.

Given a positive integer-valued time series $(Y_t)_{t \in [0, T]}$, for some finite time horizon $[0, T] \subset \mathbb{Z}_+$, we gather all the past observations up to a time $s \geq 0$, $\mathcal{F}_s := \{Y_1, \dots, Y_s\}$. At time t we assume that for a specific set of unknown parameters $\theta_t \in \mathbb{R}$ and $\phi_t \in \mathbb{R}$, and for known smooth functions $\psi : \mathbb{R} \rightarrow \mathbb{R}$ and $c : \mathbb{Z}_+ \times \mathbb{R} \rightarrow \mathbb{R}$,

$$\mathbb{P}(Y_t = y | \mathcal{F}_{t-1}, \theta_t, \phi_t) = p(y, \theta_t, \phi_t) := \exp\left(\frac{y\theta_t - \psi(\theta_t)}{\phi_t} + c(y, \phi_t)\right), \quad (3.7.4)$$

i.e. p is a discrete *exponential family* PMF [157, 205, 206]. The parameters θ_t and ϕ_t are respectively the *natural/canonical parameter* and *scale parameter*, at time $t \geq 0$. We also define the state process that describes the evolution of

$$Z_t := \mathbb{E}(Y_t | \mathcal{F}_{t-1}, \theta_t, \phi_t) = \psi'(\theta_t)$$

over time, which may depend on lagged versions of θ_t and Y_t . Z_t may be partially observed and describes the system's dynamics, inducing temporal dependencies in the data. For count time series one typically uses the so-called *canonical log-link* $\ln(Z_t) = g(Z_1, \dots, Z_{t-1}, Y_1, \dots, Y_{t-1})$, where g is some smooth function. We may also derive $\text{Var}(Y_t | \mathcal{F}_{t-1}, \theta_t, \phi_t) = \phi_t \psi''(\theta_t)$ [205].

These models are natural extensions of general linear models that have been classically used to analyse count data in the past (see [90] for a more theoretical exploration of observation-driven modelling). In Chapter 7 we will use this general framework in the

context of modelling groups, where each group count process is of the form (3.7.4), and where each intensity process is coupled. Examples of discrete distributions (modelling counts or abundances) that fall into the exponential family include the Poisson, Negative-Binomial (with fixed failure rate) and categorical (with fixed number of trials) distributions.

We lastly note that in this framework, we can account for overdispersion, i.e. when the variance is greater than the mean, and also within-population heterogeneity using random effects. Note that the term *overdispersion* in this case does not refer to dispersal or diffusion, but to the fact that the variance of some random variable is greater than its mean. Assume that a random variable, Y , is such that $Y|\eta \sim \mathcal{P}(\eta)$ and η is a random variable, termed *random effect*, where $\mathbb{E}(\eta) = \mu$ and $\text{Var}(\eta) = \sigma^2$. Then it follows respectively from the Law of Total Expectation and Law of Total Variance that

$$\begin{aligned}\mathbb{E}(Y) &= \mathbb{E}[\mathbb{E}(Y|\eta)] = \mathbb{E}(\eta) = \mu, \\ \text{Var}(Y) &= \mathbb{E}[\text{Var}(Y|\eta)] + \text{Var}[\mathbb{E}(Y|\eta)] \\ &= \mathbb{E}(\eta) + \text{Var}(\eta) \\ &= \mu + \sigma^2.\end{aligned}\tag{3.7.5}$$

More generally, the use of compound distributions such as these induces a variance function that can be greater than the mean, and therefore capture some degree of overdispersion. See [205, 206] for more on modelling random effects in various other contexts. The role of such random effects will become apparent in Chapter 7, in the context of modelling the stochastic dynamics of groups of animals within a social population. In Chapter 7, each parameter in our group abundance mean equations will be a random effect with a corresponding population-level mean and variance, which allows one to easily capture heterogeneity between groups.

3.8. Summary

In this chapter we have reviewed various deterministic and stochastic models of population dynamics that account for population structure such as discrete life stages, dormancy, spatiality, density-dependence and interaction strengths. Many of the concepts and model components discussed in this section will resurface throughout this thesis in a variety of contexts. Moreover, several of the results presented later relate directly to the material of this chapter.

4. Costless and Density-Dependent Movement of Invasive Populations

In this chapter, we propose a population model involving sub-populations dynamics in two spatial regions with density-dependent and asymmetric movement, focusing on an invasive species. Our approach assumes dispersal is costless to the overall population and extends existing passive symmetric dispersal models. Our goal is to analyse the long-term dynamics of the model, establishing conditions for extinction or persistence in one and/or both patches. We will also explore various numerical simulations, which capture behaviours observed in conservation or pest management scenarios. Finally, we will apply our findings to an empirical case study, namely the switching of an invasive insect species between two resource hosts.

*Parts of this chapter appeared in: de Godoy, I.B.S., McGrane-Corrigan, B., Mason, O., de Andrade Moral, R. and Godoy, W.A.C., 2023. Plant-host shift, spatial persistence, and the viability of an invasive insect population. *Ecological Modelling*, 475, p.110172.*

4.1. Motivation

The adaptation of non-native species or spread of a native species to new environments is essential for biological range expansion, which involve colonization, establishment, and local or regional dispersal events [134]. In recent years, additional structure has been implicitly and explicitly incorporated into mathematical and computational models of species' dynamics, as an attempt to account for the movement of individuals within a population, at different spatiotemporal scales and life stages [113, 193]. For example, the introduction of spatial structure offers a new perspective when investigating the movement of insects between patches [214, 232], a mechanism that may have significant consequences for integrated pest management and conservation strategies [209].

Range expansions often encompass processes such as encroachment [9], species redistributions [31] and invasive spread [253]. These can be driven by climate change, resource shifts and environmental events such as drought. An aspect that has been little studied is the effect of regional density on movement, as many species are known to disperse from or remain in a region in response to high/low population densities [5]. Landscapes are

also heterogeneous by nature and so dispersing between two specified regions can have varying effects [1].

To take account of this asymmetric movement and density dependence, we will consider a simple nonlinear model of dispersal that aims to capture the dynamics of a population dispersing between two regions within some landscape. We will derive sufficient conditions for global asymptotic extinction when dispersal is constant. When dispersal is density dependent we will derive conditions for population persistence and the existence of a positive fixed point. We will then demonstrate how the modelling framework we consider can be applied to capture various real-world ecological phenomena. Finally we will apply this model to an agricultural case study, to assess the long-term viability of an insect pest switching between hosts.

4.2. The Two-Patch Model

Dispersal can be an asymmetric process and may have significant consequences for population persistence [235], especially when assessing the impacts of climate change and monitoring species range shifts [293]. Many authors also assume invasive spread or range expansion to be density-independent. In many cases these ecological processes are largely density-dependent, with this dependence varying from negative to positive to mixtures of the two [5, 259, 285].

To accommodate dispersal asymmetry and density-dependence, we will now describe the modelling framework that we are interested in for the majority of this chapter. Consider a single-species population that consumes two resource types and inhabits two non-identical patches. Denote the patch population densities, in generation $t \in \mathbb{Z}_+$, by $x_1(t)$ and $x_2(t)$, respectively. Following reproduction on a patch we assume both sub-populations disperse between patches, at a rate which depends continuously on their respective densities. We also assume that the overall population is spatially closed, i.e. individuals reproduce and disperse only on the two specified patches. A general mathematical form for such a system and the model we are interested in throughout this chapter is given by

$$\begin{aligned} x_1(t+1) &= [1 - d_1(x_1(t))]f_1(x_1(t)) + d_2(x_2(t))f_2(x_2(t)) \\ x_2(t+1) &= [1 - d_2(x_2(t))]f_2(x_2(t)) + d_1(x_1(t))f_1(x_1(t)), \\ x(0) &= x_0 \in \mathbb{R}_+^2, \end{aligned} \tag{4.2.1}$$

where $f_i(x_i) = g_i(x_i)x_i$ (see Fig. 4.1). This extends the model in [93] to incorporate asymmetric and nonlinear dispersal. This formulation considers three C^1 maps, given by $f_i : \mathbb{R}_+ \rightarrow \mathbb{R}_+$ and $g_i : \mathbb{R}_+ \rightarrow \mathbb{R}_+ \setminus \{0\}$, that respectively describe the regional growth/recruitment and fitness on patch i , and $d_i : \mathbb{R}_+ \rightarrow (0, 1)$ which describes density-dependent

dispersal from patch i . Note that under this framework one can specify that dispersal from patch i is either constant or density-dependent. Throughout the rest of this chapter, unless stated otherwise, we assume that both patches exhibit density-dependent dispersal. Note that in Chapter 5 we will look an extended model form to (4.2.1), where there are more than two patches. Some of the mathematical results of this chapter can be proved for such a model, but there are distinctions between the two that will become clear in both the mathematical and numerical work.

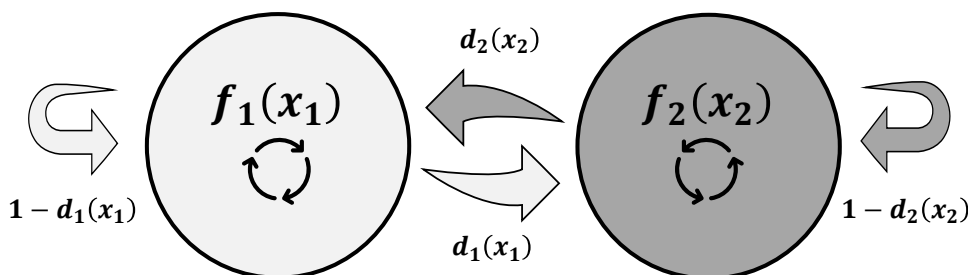


Figure 4.1: Conceptual diagram of system (4.2.1), where $f_i(x_i)$ and $d_i(x_i)$ respectively describe the dynamics on and dispersal from patch i . The proportion of individuals remaining on patch i is $1 - d_i(x_i)$.

4.3. Patch Dynamics

We will assume that the regional growth function takes the form of a Ricker map, i.e.

$$f_i(x_i) := \alpha_i x_i e^{-\beta_i x_i} \quad (4.3.1)$$

for $i = 1, 2$. The parameter α_i is the growth rate of the subpopulation on patch i , while $\beta_i > 0$ is the influence of intra-specific competition on patch i . Note that the difference in each patch is determined by the effects of both the strength of growth and density-dependence, as determined by α_i and β_i respectively. In isolation, each region's dynamics is governed by a Ricker map, which is a widely used nonlinear model of population growth that can describe many real-world population dynamics [126, 159, 234]. It has also been used to describe the dynamics of many invasive insect and fish species [43, 221].

If the two patches are isolated, the dynamics on patch i is given by

$$x_i(t+1) = f_i(x_i(t)) = g_i(x_i(t)) x_i(t), \quad (4.3.2)$$

where $g_i(x) = \alpha_i \exp(-\beta_i x)$ where is known as a recruitment or fitness function [50]. The map f_i is unimodal, meaning it attains a unique highest value or global maximum on its

domain (see Fig. 4.2). This occurs at $x_i = \beta_i^{-1}$. The maximum possible population size is then

$$f_i\left(\frac{1}{\beta_i}\right) = \frac{1}{\beta_i} g_i\left(\frac{1}{\beta_i}\right) = \frac{\alpha_i}{e\beta_i}$$

and so the population is bounded from reaching arbitrarily large values. It can also be seen from (4.3.1) that

$$\alpha_i < 1 \implies x_i(t) \rightarrow 0, t \rightarrow \infty.$$

Note that $\alpha_i < 1$ corresponds to patch i being a sink, a habitat where a population asymptotically goes extinct. There exists a unique nontrivial equilibrium for patch i

$$x_i^* := \frac{\ln(\alpha_i)}{\beta_i} > 0 \iff \alpha_i > 1.$$

Note that $\alpha_i > 1$ corresponds to patch i being a source, a habitat that can sustain a population and enable it to grow. As f_i is continuously differentiable at x_i^* , the local stability properties can be determined by linearisation [80]. Local asymptotic stability is guaranteed once

$$|f_i'(x_i^*)| < 1.$$

From the form of f_i we can see that x_i^* is locally asymptotically stable if

$$|1 - \ln(\alpha_i)| < 1 \iff 1 < \alpha_i < e^2 \quad (4.3.3)$$

and x_i^* is unstable for $\alpha_i > e^2$.

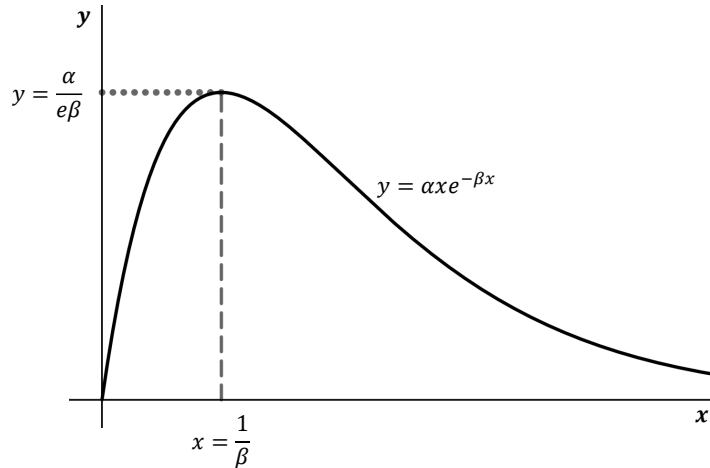


Figure 4.2: Illustration of a Ricker map $y = \alpha x \exp(-\beta x)$, where $\alpha, \beta > 0$ (solid line). This map has a unique maximum at $x = \beta^{-1}$ (dashed line) which is $y = \alpha/(e\beta)$ (dotted line).

4.4. Movement Dynamics

For the rest of this chapter we assume dispersal is asymmetric, i.e. $d_i(x) \neq d_j(x)$ for $i \neq j$, and bidirectional, i.e. $d_i(x) \notin \{0, 1\}$, for all $x \geq 0$. We can rewrite (4.2.1) as a nonlinear matrix model of the form (3.2.1), i.e. $F(x) := A(x)x$, where $x \in \mathbb{R}_+^2$ and $A : \mathbb{R}_+^2 \rightarrow \mathbb{R}_+^{2 \times 2}$ is the matrix-valued function given by

$$A(x) = \underbrace{\begin{pmatrix} 1 - d_1(x_1) & d_2(x_2) \\ d_1(x_1) & 1 - d_2(x_2) \end{pmatrix}}_{D(x)} \underbrace{\begin{pmatrix} g_1(x_1) & 0 \\ 0 & g_2(x_2) \end{pmatrix}}_{G(x)}. \quad (4.4.1)$$

As g_i and d_i are C^1 it follows that A is C^1 . As $F(x) = A(x)x$, we can see that F is also C^1 and so we can compute the Jacobian of F as

$$F'(0) = \begin{pmatrix} [1 - d_1(0)] f'_1(0) + d'_1(0) f_1(0) & d_2(x_2) f'_2(0) + d'_2(x_2) f_2(0) \\ d_1(0) f'_1(0) + d'_1(0) f_1(0) & [1 - d_2(0)] f'_2(0) + d'_2(0) f_2(0) \end{pmatrix}. \quad (4.4.2)$$

We can observe that

$$f_i(x) = \alpha_i x e^{-\beta_i x} \implies f'_i(x) = \alpha_i e^{-\beta_i x} (1 - \beta_i x).$$

We can thus conclude that

$$F'(0) = A(0) = \begin{pmatrix} [1 - d_1(0)] \alpha_1 & d_2(0) \alpha_2 \\ d_1(0) \alpha_1 & [1 - d_2(0)] \alpha_2 \end{pmatrix}. \quad (4.4.3)$$

If we were to linearise our nonlinear dispersal model around 0 we could approximate the iterated dynamics using a linear system with system matrix given by $F'(0) = A(0)$. The form of the matrix (4.4.3) will be important when we prove some stability and persistence results later in this chapter.

In many models of species movement, it is assumed that dispersal has no cost to the population dispersing from a patch [93, 113, 279]. In other words, costless dispersal is when the proportion of individuals remaining on a patch is exactly the proportion left following dispersal. Mathematically, in the context of (4.2.1), this means that the proportion of individuals dispersing from and remaining on a single patch sums to unity. This is the case with our model, as can be seen from the form of $A(x)$. For a fixed $x \in \mathbb{R}_+^2$, it is clear to see that $D(x) := (d_{ij}(x))$ is column stochastic, as for a given $j \in \{1, 2\}$ we have that

$$\sum_{i=1}^2 d_{ij}(x_i) = 1 - d_i(x_i) + d_i(x_i) = 1,$$

which in turn implies that $\|D(x)\|_1 = 1$. Although we assume costless dispersal, this does not exclude the fact there could be mortality due to dispersal, as the proportion dispersing,

$d_i(x_i)$, is state-dependent. In Chapter 5 we will explore a different model where we assume that there are dispersal costs. We will now look at the simpler case of passive, costless dispersal.

4.4.1. Passive Invasion

If we assume that we have passive/constant dispersal, i.e. $d_i(x_i) \equiv d_i \in (0, 1)$, for $i \in \{1, 2\}$, then it is clear to see from the form of $A(x)$ that

$$e^{-\beta_i x_i} \leq 1 \implies A(x) \leq A(0)$$

for all $x \geq 0$. It now follows that for $x(0) = x_0 \in \mathbb{R}_+^2$, our solution satisfies (3.2.2) for $t \geq 1$. Recall that $\rho(A(0)) < 1$ implies that $A(0)^t \rightarrow 0$ as $t \rightarrow \infty$. Therefore, we can conclude that the extinction equilibrium is GAS. This gives a sufficient condition for ensuring that we have patch extinction for any initial condition, as is shown in [255] for general nonlinear matrix models.

The model of the form (4.2.1) with passive dispersal is similar in form to (3.5.1), the model in [93] as seen in Chapter 3, albeit with asymmetric dispersal proportions. The next result is a generalisation of their main result, in the context of (4.2.1), when we have passive (asymmetric) dispersal. The proof of this is the same as in [93].

Proposition 4.4.1. *Assume $f_i(x) = g_i(x)x$, where g_i is given by (4.3.1). Further assume that $d_i(x) = d_i \in (0, 1)$ for all $x \geq 0$. Then, system (4.2.1) is persistent if $\rho(A(0)) > 1$, whereas any initial population is driven to extinction when $\rho(A(0)) \leq 1$.*

For any $A = (a_{ij}) \in \mathbb{R}^{n \times n}$ we have that $\rho(A) \leq \|A\|_1 = \max_{j \in \{1, \dots, n\}} \{\sum_{i=1}^n |a_{ij}|\}$. It then follows that $\rho(A(0)) < 1$ if all column sums of $A(0)$ are less than 1. It is clear then that

$$\alpha_i < 1 \implies \rho(A(0)) < 1.$$

Growth rates less than unity could arise in a scenario where each patch population has high fertility but low survival probability due to high intra-population competition for resources, which intuitively would lead to the decline of the population in the long run.

As $x \in \mathbb{R}_+^2$, we can derive a simple expression that characterises global stability of the extinction equilibrium in terms of our model parameters, which is more general than just assuming that $\alpha_i < 1$ as above. To do so, we first restate the following well-known result.

Theorem 4.4.2. [80] *Let $a > 0, b > 0$. The roots of the polynomial*

$$q(x) = x^2 - ax + b \tag{4.4.4}$$

lie in \mathbb{D}_1 if and only if $a - 1 < b < 1$.

The characteristic polynomial of $A(0)$ is given by

$$\det(A(0) - \lambda I) = \lambda^2 - \text{Tr}(A(0))\lambda + \det(A(0)). \quad (4.4.5)$$

By observing that (4.4.4) and the RHS of (4.4.5) have the same form, we can see then that

$$\rho(A(0)) < 1 \iff \text{Tr}(A(0)) < 1 + \det(A(0)) < 2.$$

It then follows that that $\rho(A(0)) < 1$ if and only if

$$\alpha_1(1 - d_1) + \alpha_2(1 - d_2) < 1 + \alpha_1\alpha_2(1 - d_1 - d_2) < 2. \quad (4.4.6)$$

From (4.4.6) we can see that the global stability of the extinction equilibrium for (4.2.1) is independent to choices of the density-dependent terms β_1 and β_2 . From (4.4.6) we can interpret these inequalities as suggesting that eventual extinction is guaranteed once the sum of the proportion of individuals remaining on a patch, i.e. the LHS of (4.4.6), is sufficiently low. For example, if both α_1 and α_2 are sufficiently low, the incentive to disperse from either patch is lower, thus enabling extinction to occur on both patches. If resource quality was higher on patch 1 and lower on patch 2, for example, then we would expect a higher value of α_1 and lower value of α_2 . This could promote dispersal from patch 2 to 1, with (4.4.6) also being violated. Thus the trade off between dispersal rate and regional growth determines the incentive to disperse from a patch and in turn the conditions for global extinction and persistence. We next move on to the more complex case of nonlinear or density-dependent dispersal.

4.4.2. Density-Dependent Invasion

We will now consider (4.2.1), where we assume that dispersal is a bidirectional, asymmetric and density-dependent process. Therefore instead of d_i being constant, it is state-dependent. We will first note that $F(x) = A(x)x$ is strongly positive.

Lemma 4.4.3. *Let $A(x)$ be given by (4.4.1) and patch dynamics given by (4.3.1), with $\alpha_i, \beta_i > 0$ and $d_i(x) \in (0, 1)$ for all $x \geq 0$ and $i = 1, 2$. Then for any $x \in \mathbb{R}_+^2 \setminus \{0\}$ we have that $F(x) > 0$.*

Proof. It is clear to observe that for all $x = (x_1 \ x_2)^T \geq 0$ one has that $f_i(x_i) > 0$ and $d_i(x_i) > 0$ implies that $A(x) > 0$. Therefore $F(x) = A(x)x > 0$ for all nonzero $x \in \mathbb{R}_+^2$. \square

In the following lemma, we show that solutions to system (4.2.1) are bounded. This simple fact is needed for the results on persistence that follow.

Lemma 4.4.4. *Let $A(x)$ be given by (4.4.1) and patch dynamics given by (4.3.1), with $\alpha_i, \beta_i > 0$ and $d_i(x) \in (0, 1)$ for all $x \geq 0$ and $i = 1, 2$. Then there exists some $M > 0$ such that for any $x(0) = x_0 \in \mathbb{R}_+^2$, $\|x(t, x_0)\|_1 \leq M$ for all $t \geq 1$.*

Proof. It follows from Lemma 4.4.3 that $\mathbb{R}_+^2 \setminus \{0\}$ is forward invariant under F , i.e.

$$x(0) = x_0 \in \mathbb{R}_+^2 \setminus \{0\} \implies F(x(t, x_0)) \in \mathbb{R}_+^2 \setminus \{0\}$$

for all $t \geq 0$. Thus the l_1 -norm of $x(t, x_0)$ is given by $\|x(t, x_0)\|_1 = \mathbb{1}^T x(t, x_0)$. For any $t \geq 1$, our solution $x(t, x_0)$ is of the form $A(x(t-1))x(t-1)$ for some $x(t-1) \in \mathbb{R}_+^2$. From the form of $A(x)$, we can see that for $x = (x_1 \ x_2)^T$,

$$\mathbb{1}^T A(x) = (\alpha_1 \exp(\beta_1 x_1) \ \alpha_2 \exp(\beta_2 x_2)) \implies \|A(x)x\|_1 = \sum_{i=1}^2 \alpha_i x_i \exp(\beta_i x_i).$$

As (4.4.8) holds for all $x \geq 0$, we have that

$$\|A(x)x\|_1 = \sum_{i=1}^2 \alpha_i x_i \exp(\beta_i x_i) \leq \sum_{i=1}^2 \frac{\alpha_i}{e\beta_i} \forall x \geq 0.$$

Our solution $x(t)$ is of the form $A(z)z$, for $z \geq 0$ and $t \geq 1$. This proves the lemma with $M := \alpha_1/(e\beta_1) + \alpha_2/(e\beta_2)$. \square

In our next result, we give a sufficient condition for the existence of a positive equilibrium.

Proposition 4.4.5. *Let $A(x)$ be given by (4.4.1) and patch dynamics given by (4.3.1), with $\alpha_i, \beta_i > 0$ and $d_i(x) \in (0, 1)$ for all $x \geq 0$ and $i = 1, 2$. Suppose that $\rho(A(0)) > 1$. Then there exists some $x > 0$ with $F(x) = x$.*

Proof. First note that for $x \geq 0$

$$F(x) = A(x)x = \begin{pmatrix} (1 - d_1(x_1))\alpha_1 e^{-\beta_1 x_1} + d_2(x_2)\alpha_2 e^{-\beta_2 x_2} \\ (1 - d_2(x_2))\alpha_2 e^{-\beta_2 x_2} + d_1(x_1)\alpha_1 e^{-\beta_1 x_1} \end{pmatrix} \quad (4.4.7)$$

We can see that

$$x_i e^{-\beta_i x_i} \leq \frac{1}{e\beta_i} \quad (4.4.8)$$

for $x_i \geq 0, i = 1, 2$. We can then see that there exists $y > 0$ such that $F(y) \leq y$ for all $x \in \mathbb{R}_+^2$. As $F(x)$ is continuous, it follows from Theorem 3.2.1 that there exists a nonzero $z \in \mathbb{R}_+^2$ such that $F(z) = z$. As $F(x) > 0$ for any non-zero x , by Lemma 4.4.3, this implies that $z > 0$. \square

Deriving criteria for the local or global stability of a positive equilibrium in Proposition 4.4.5 is not as tractable as when dispersal is constant, as the interplay between the Ricker maps, f_1 and f_2 , and in the choice of nonlinear maps d_1 and d_2 , can alter the expression of such an equilibrium. Instead of exploring when this equilibrium is unique or when it is locally/globally stable, we will restrict the problem to when one can guarantee that the population remains persistent. The next result gives a sufficient condition for weak persistence with respect to either one of the patches (see Chapter 2 for a definition).

Theorem 4.4.6. *Let $A(x)$ be given by (4.4.1) and patch dynamics given by (4.3.1), with $\alpha_i, \beta_i > 0$ and $d_i(x) \in (0, 1)$ for all $x \geq 0$ and $i = 1, 2$. Further let $\eta_1(x) := x_1$ and $\eta_2(x) := x_2$. Assume that $\alpha_i > 1$ and there exists $\gamma_i \in (1, \alpha_i)$ such that*

$$d_i(x_i) < 1 - \frac{\gamma_i}{\alpha_i} \quad (4.4.9)$$

for all $x_i \geq 0$ and some $i \in \{1, 2\}$. Then there exists $\delta > 0$ such that $x_i < \delta$ implies that

$$\limsup_{t \rightarrow \infty} \eta_i(x(t, x_0)) \geq \delta.$$

Proof. Assume $x \geq 0$. From the form of F we have that, for $i, j \in \{1, 2\}$ and $i \neq j$,

$$\eta_i(x) = x_i > 0 \implies \eta_i(F(x)) = (1 - d_i(x_i))\alpha_i x_i e^{-\beta x_i} + d_j(x_j)\alpha_j x_j e^{-\beta x_j} > 0.$$

We also have that

$$\eta_i(x) = x_i > 0 \implies \frac{\eta_i(F(x))}{\eta_i(x)} \geq (1 - d_i(x_i))\alpha_i \exp(-\beta_i x_i).$$

It follows from (4.4.9) that

$$(1 - d_i(x_i))\alpha_i > \gamma_i > 1.$$

Therefore there exists some $\delta > 0$ such that

$$\frac{\eta_i(F(x))}{\eta_i(x)} > \gamma_i > 1, 0 < x_i < \delta.$$

The result then follows from Proposition 2.3.1. □

Condition (4.4.9) in Theorem 4.4.6 implies that there is a balance to the dispersal rate and the growth rate on patch i . By ensuring that dispersal is sufficiently low relative to the growth rate, this condition allows for the possibility that the population in patch i can grow and not deplete the patch if growth is not fast enough to compensate for dispersing individuals leaving. Note that this is only for one patch. There may be sufficient inflow from patch $j \neq i$ that allows the proportion on patch i to be higher than this threshold.

Example 4.4.1. A dispersal function satisfying (4.4.9) is $d_i(x_i) = a_i \exp(-(x_i - r_i)^2)$ with $a_i < 1 - (\gamma_i/\alpha_i)$, for $\alpha_i > 1$, $r_i > 0$ and $\gamma_i \in (1, \alpha_i)$, which could describe a population that has highest dispersal proportions at densities that are neither too low nor too high, and low dispersal proportions at relatively extreme low/high densities. This may describe a situation where dispersal peaks at such intermediate population densities where there is a balance between intraspecific competition and habitat quality [82].

The next result gives a sufficient condition for uniform strong persistence with respect to two different persistence functions.

Theorem 4.4.7. *Let $A(x)$ be given by (4.4.1) and patch dynamics given by (4.3.1), with $\alpha_i, \beta_i > 0$ and $d_i(x) \in (0, 1)$ for all $x \geq 0$ and $i = 1, 2$. For $x \in \mathbb{R}_+^2$, let $\eta_1(x) = \|x\|_1$ and $\eta_2(x) = \min\{x_1, x_2\}$. Suppose $\rho(A(0)) > 1$. Then, system (4.2.1) is uniformly strongly persistent with respect to η_1 and η_2 .*

Proof. It follows from Lemma 4.4.3 that F is strongly positive. Therefore $\mathbb{R}_+^n \setminus \{0\}$ is forward invariant under F . Also $\rho(A(0)) > 1 \implies \rho(A(0)^T) > 1$ and so there exists $v > 0$ such that $A(0)^T v > v$. Therefore we can choose $r_0 > 1$ with $A(0)^T v \geq r_0 v$. Finally, Lemma 4.4.4 implies that there exists some $M > 0$ such that for any $x(0) \in \mathbb{R}_+^2$, $|x(t)|_1 \leq M$ for all $t \geq 1$. Then, by Theorem 2.3.2 there exists $\epsilon_1, \epsilon_2 > 0$ such that

$$\begin{aligned} \liminf_{t \rightarrow \infty} \eta_1(x(t, x_0)) &> \epsilon_1, \\ \liminf_{t \rightarrow \infty} \eta_2(x(t, x_0)) &> \epsilon_2 \end{aligned}$$

for all $x(0) = x_0 \in \mathbb{R}_+^2 \setminus \{0\}$. □

Note that even though $\rho(A(0)) > 1$ in Theorem 4.4.7, the value of ϵ_1 and ϵ_2 may be different, as uniform persistence is dependent on the choice of persistence function. As well as this, for ϵ_i , the asymptotic time, T_i , where $x(t, x_0) \geq \epsilon_i$ for all $t \geq T_i$ could be different for $i \in \{1, 2\}$, i.e. we may have that $T_1 \neq T_2$.

We will now state a sufficient condition for $\rho(A(0)) > 1$, in terms of the regional growth rates and initial dispersal proportions. These conditions are in turn sufficient for both the existence of a positive fixed point and for strong uniform persistence, as per Theorems 4.4.5 and 4.4.7.

Proposition 4.4.8. *Let $A(0) \in \mathbb{R}_+^{2 \times 2}$ be given by (4.4.3). Assume that the following hold:*

- (a) $d_1(0) + d_2(0) = 1$, and
- (b) $\alpha_1(1 - d_1(0)) > 1 - \alpha_2(1 - d_2(0))$.

Then $\rho(A(0)) > 1$.

Proof. As $A(0) \in \mathbb{R}_+^{2 \times 2}$ and $d_i(x) \neq 1$ for all $x \geq 0$, we have that

$$\text{Tr}(A(0)) = \alpha_1(1 - d_1(0)) + \alpha_2(1 - d_2(0)) > 1.$$

As $A(0)$ is nonnegative and is a 2×2 matrix, it can be shown that the eigenvalues of $A(0)$ must be real. From assumption (b) we have that $\text{Tr}(A(0)) > 1$. Assumption (a) directly implies the

$$\det(A(0)) = \alpha_1\alpha_2(1 - d_1(0) - d_2(0)) = 0.$$

Therefore we have that $\rho(A(0)) = \text{Tr}(A(0)) > 1$. □

An interpretation of Proposition 4.4.8 is that if, in the first generation, the total proportion of individuals dispersing is 1 and the sum of the total number of individuals remaining is greater than 1, then we have strong uniform persistence with respect to the total population size.

Example 4.4.2. Assume both patches have identical growth rates, i.e. $\alpha_1 = \alpha_2 = \alpha > 0$, and the assumptions of Proposition 4.4.8 hold. It follows from (a) and (b) in Proposition 4.4.8 that

$$\alpha_1(1 - d_1(0)) + \alpha_2(1 - d_2(0)) = \alpha(1 + 1 - d_1(0) - d_2(0)) > 1 \iff \alpha > 1.$$

In this case we only get uniform strong persistence with respect to the total population size when each patch is a source with identical growth rates. Note the difference in the patches is then determined by β_i . This could be interpreted as each patch being of the same high quality resource. A real-world example of such a scenario could be a monoculture system, where the same crop or plantation is grown across multiple areas [244].

To complement the mathematical results in this section we will now move on to numerically explore system (4.2.1) in several ecologically important scenarios.

4.5. Outbreak and Conservation Examples

In this section we will numerically explore how the model we consider can be used in the context of modelling a population invading another habitat or expanding its home range. In this context, we are primarily interested in how the presence/absence of dispersal influences persistence over time and what drives the population on either patch to extinction (eradication). All numerical computations and simulations were conducted in R [263].

For the purpose of simulating model (4.2.1), we must specify a form for $d_i(x_i)$, as this is an arbitrary function taking values in $(0, 1)$. We therefore assume that density-dependent dispersal from patch i is given by

$$d_i(x_i) = 1 - r_i e^{-\mu_i x_i}, \quad (4.5.1)$$

where μ_i is the strength of density-dependent dispersal and $r_i \in (0, 1)$ is a scaling factor that can be interpreted as the minimum amount of dispersal that is permitted. As we have costless dispersal and assume the dispersal functions are of the form (4.5.1), we can interpret this scenario as positive density-dependent dispersal, that is movement away from each patch increases with increasing patch density, with the number of remaining individuals decreasing with increasing patchy density (see Fig. 4.3). This form of dispersal could be induced via overcrowding and competitive interactions on the patch where individuals are dispersing from [195]. We will now investigate how our model can capture four ecological phenomena typically observed in many empirical studies.

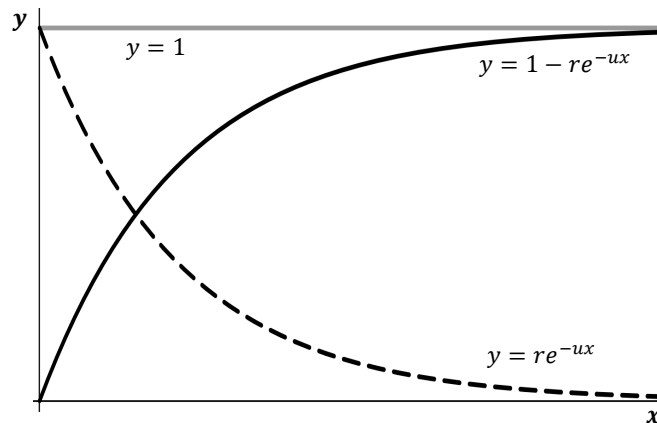


Figure 4.3: Illustration of a map of the form (4.5.1), where $r \in (0, 1)$ and $u > 0$. The solid black curve, $y = 1 - r \exp(-ux)$, represents positive density-dependent dispersal, with the dashed black curve, $y = r \exp(-ux)$, representing the proportion of individuals remaining. The grey line represents $y = 1$.

4.5.1. The Rescue Effect

Say one was interested in reversing the decline of one patch population after allowing movement to and from a more suitable patch. This phenomenon is known as the *rescue effect* [83]. This may be of interest in a conservation management scenario where one's aim is to conserve a population of natural residents, for example. Let us look at the scenario when $\alpha_1 < 1$ and $\alpha_2 > 1$, so on patch 1 the population tends to extinction and on patch 2 there is high survival and fertility. From the form of $A(0)$ we can see that for α_2 sufficiently large, we can ensure that both uniform strong persistence and patch-persistence

occur. We simulated this scenario for the case where both patches are in isolation and for the case where they are coupled (see Fig. 4.4). For the chosen parameter values, we find that $\rho(A(0)) \approx 11.7 > 1$. By Theorem 4.4.7, this implies that, even though on one patch extinction may be inevitable, by allowing dispersal one can not only rescue the declining patch from extinction and help the overall population to recover, but also ensure that each individual patch population also persists. In Fig. 4.4 we can see that in isolation, patch 1 tends to extinction whereas patch 2 remains persistent, albeit with rapid fluctuations in population size. Once these patches are coupled via dispersal as in (4.2.1) we can see that both patches tend toward a positive equilibrium, the existence of which is guaranteed by Proposition 4.4.5, and thus the total coupled population is persistent. Not only does dispersal rescue the declining population on patch 1, but it also stabilises the dynamics on patch 2.

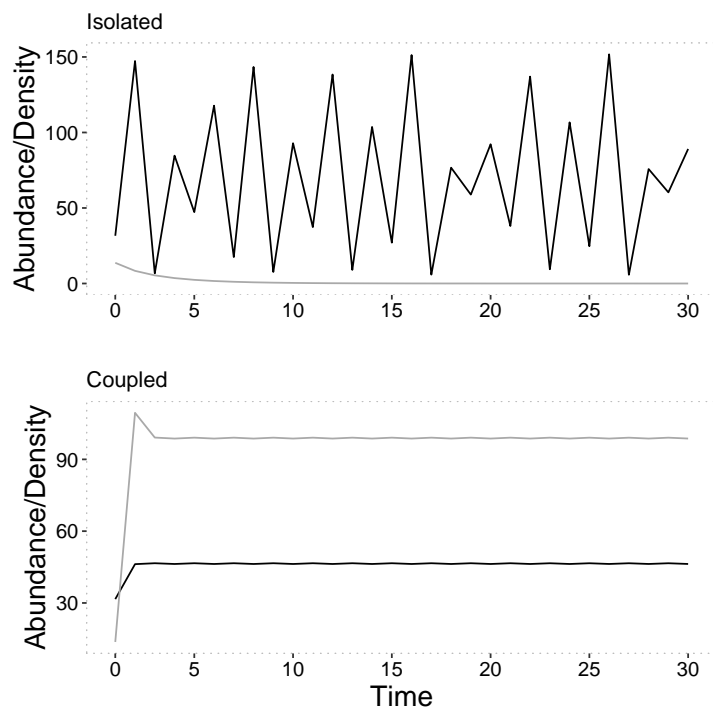


Figure 4.4: Simulations of (4.3.2) for $i = 1, 2$ (Isolated) and (4.2.1) (Coupled), for 30 time steps. In both simulations we set $x_0 = (13.7, 31.6)$, $\beta_1 = 0.01$, $\beta_2 = 0.044$, $\alpha_1 = 0.7$ and $\alpha_2 = 16.5$. For the coupled model we also set $\mu_1 = 0.05$, $\mu_2 = 0.03$, $r_1 = 0.5$, $r_2 = 0.7$. In each plot, the grey and black lines respectively represents trajectories for region 1 and 2.

A region may become a sink in the absence of immigration or source patches, but dispersal from a source can allow the overall population the opportunity to recover. For fast-growing species with short life cycles and for those that exhibit boom-bust dynamics (also called irruptive dynamics), like for example insect species, populations can reach (and exceed) their carrying capacity very quickly, likely leading to high intraspecific competition and density-dependent dispersal [111, 226]. Low quality habitat (sinks) can be distributed

among higher quality habitat (sources), which in turn can limit the movement of organisms in space. Therefore identifying when extinction or growth occurs for certain habitat types following connectance via dispersal is important to take account of [133].

4.5.2. Boom-Bust Dynamics

It is well known that dispersal is an important factor in producing boom-bust type dynamics for pests and founder populations (a small population established by individuals from a larger population following displacement). This is where the invading population increases rapidly in an initial outbreak (boom) phase, before rapidly declining to a much lower density (bust) [111, 257]. As an example, we will look at a scenario where $x_1(0) = 0$, with $\alpha_1 > 1$, and $x_2(0) \gg 0$, with $\alpha_2 < 1$. Thus we want to determine how immigration from a crowded sink patch to an initially empty source patch affects the overall dynamics of our coupled system. From Fig. 4.5 we can see that even though patch 1 is initially empty with patch two destined for extinction, once we couple these through density-dependent dispersal we can induce (chaotic-type) boom-bust dynamics on both patches. This parametrisation results in the rescue effect. Even though $x_1(0) = 0$, we can see that $\rho(A(0)) \approx 20.98 > 1$ and $\|x(0)\|_1 > 0$. It then follows from Theorem 4.4.7 that our population is uniformly strongly persistent with respect to the total population size across two patches, as measured by the l_1 -norm.

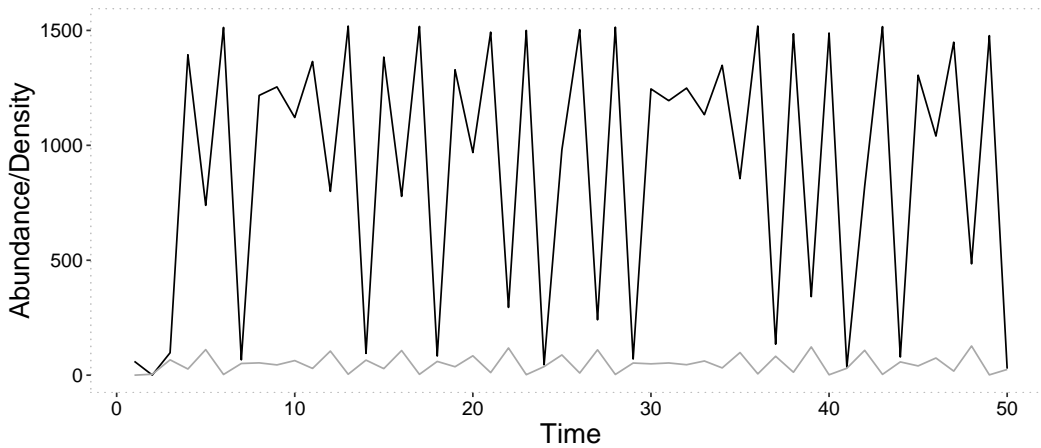


Figure 4.5: Simulation of (4.2.1) for 50 time steps. We set $x_0 = (0, 60)$, $\beta_1 = 0.01$, $\mu_1 = 0.05$, $\beta_2 = 0.04$, $\mu_2 = 0.03$, $\alpha_1 = 41.44$, $\alpha_2 = 0.86$, $r_1 = 0.5$, and $r_2 = 0.7$. In each plot, the grey and black lines respectively represents trajectories for region 1 and 2.

4.5.3. Spatial Synchrony

We will now investigate how varying r_1 and r_2 can affect the dynamics of (4.2.1). This could, for example, be of interest to agricultural field managers who want to induce

dispersal from a vulnerable crop to some neighbouring land/matrix, or when one wants to promote dispersal of natural enemies/predators to enter a region where there is a crop of interest, in order to predate upon the pests present there [268]. As mentioned previously, r_i can be interpreted as the minimum proportion of individuals that are allowed to disperse from patch i . This could be interpreted in the context of promoting dispersal through application of pesticide or introduction of natural enemies on patch i , thus raising the value of r_i .

We simulated (4.2.1) for three different management scenarios, when r_i was low, moderate and high. At values of r_i close to 0 we get that $d_i(x)$ slowly increases toward 1. At values of r_i closer to 1 we get that $d_i(x)$ is a near constant function of x . In Fig. 4.6 we can see as r_i is increased from low to high values a dynamical change from smooth convergence to a positive fixed point, to oscillatory convergence to the same fixed point and finally the emergence of a periodic trajectory. In each simulation the initial condition was fixed at $(x_1(0), x_2(0)) = (94, 56)$. Therefore we can see that under certain parameterisations, increasing r_i can induce synchrony across the two patches, where the peaks and troughs of one patch matches that of the other. This is in line with some empirical studies that have shown that rapid dispersal can induce spatial synchrony [278].

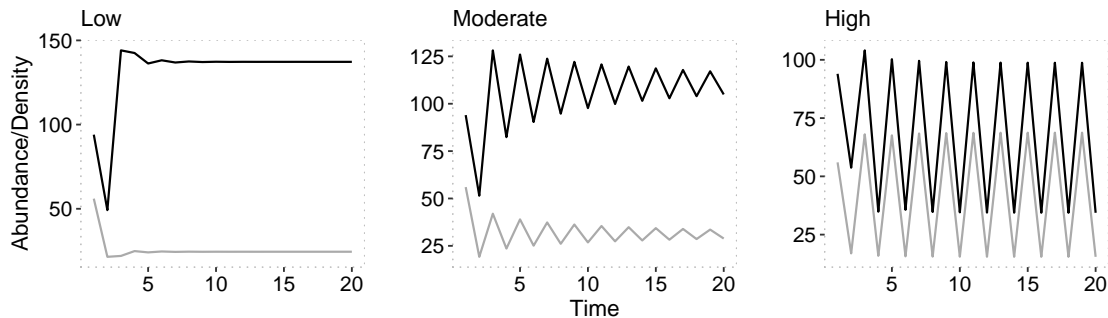


Figure 4.6: Simulations of (4.2.1) for 20 time steps. In all simulations we set $x_0 = (94, 56)$, $\beta_1 = 0.01$, $\mu_1 = 0.01$, $\beta_2 = 0.06$, $\mu_2 = 0.05$, $\alpha_1 = 0.6$, $\alpha_2 = 25$. For $r_1 = r_2 = r$, we let $r = 0.1$ (Low), $r = 0.5$ (Moderate) and $r = 0.9$ (High). In each plot, the black and grey lines respectively represents trajectories for region 1 and 2.

4.5.4. Transience

Finally, we will now show how our model can exhibit short-term transient dynamics. When one is modelling the dynamics of a species, such as an invasive population, there are relevant timescales of interest, that can be the scale of days to years depending on how the population is censused. The term transience refers to dynamics that are on so-called ecological timescales (finite times that are of interest to the specific case study in question, like days, months and years, for example) and so depend on the specific system in question.

For example, one may want to infer when a population undergoes a regime shift or when outbreaks have ceased during some year of crop production. These type of dynamics have been observed in many empirical studies, as noted in [130]. A pest species that has been shown to exhibit transient dynamics is the spruce budworm, for example, where one observes extended periods of low budworm density followed by large outbreaks or boom-bust type dynamics.

In Fig. 4.7 (Top) not only do we observe transient dynamics followed by convergence to a fixed point, but the difference in positive fixed points is quite large. The positive equilibrium on patch 2 is quite low with respect to patch 1. A major concern in agricultural management is when, for small periods of time, say between crop rotations, a small numbers of individuals persist on low-quality habitat and then exhibit rapid growth when favourable conditions arise [232]. It is also a problem when boom-bust dynamics continue indefinitely and cease to settle. Thus it is important to know when/if on either patch, both assumed to differ in resource quality, the subpopulations persist, but also do oscillations or chaotic-type dynamics continue for long enough timescales.

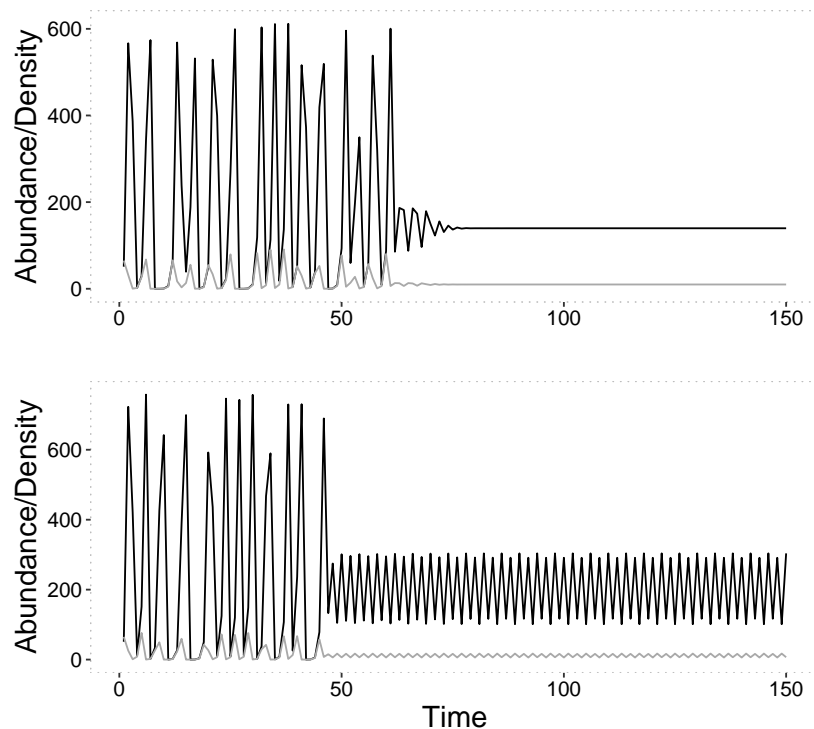


Figure 4.7: Simulations of (4.2.1) for 150 time steps. In both simulations we set $x(0) = (65, 51)$, $\beta_1 = 0.01$, $\beta_2 = 0.06$, $\mu_1 = 0.21$, $\mu_2 = 0.34$, $r_1 = 0.5$, $r_2 = 0.7$. In the top plot we set $\alpha_1 = 16.7$ and $\alpha_2 = 13.5$. In the bottom plot we set $\alpha_1 = 21.3$ and $\alpha_2 = 10.7$. In each plot, the grey and black lines respectively represents trajectories for region 1 and 2.

In both figures in Fig. 4.7 we see what is called a regime shift. The chaotic-type dynamics

observed for approximately the first 50 generations is followed by either positive fixed point dynamics or the emergence of a periodic trajectory on both patches (of differing periods). As seen above there are boom-bust type dynamics for dozens of generations but these fluctuations settle somewhat into predictable periodic or positive fixed point trajectories. The initial outbreak phase in both simulations is a transient phenomenon. If we stopped our simulation during the chaotic regime, we may conclude that this species will exhibit chaotic-type dynamics. We may also stop the simulation when abundance is low/high and conclude that this population is persisting at low values, or we have observed a population outbreak. However, if we run such a simulation for more time steps, we can observe that the invader population can establish a more stable, and thus predictable, long-term coexistence across the two patches, as alluded to by [257], where initial chaotic-type dynamics are followed by either periodic behaviour or convergence to a positive equilibrium. We extended the simulations in Fig. 4.7 to longer time steps and observed similar behaviour. In reality the length of time a simulation is run for depends on the ecological context, whether it be days, months or years for example. The simulations in this section were to demonstrate the different type of phenomena that can be captured by our model. In the next section the length of simulations is considered in the context of monitoring the daily density observations of an insect pest dispersing between two agricultural regions.

4.6. Plant Host-Shift: A Case Study

4.6.1. *Focal Species*

Drosophila suzukii is an example of an invader species that has had a significant negative economic and environmental impact around the world. It originated in Asia and was first observed outside its native range in 1980 in Hawai'i, and then later in Europe, the United States and Mexico [108]. Compared to other fruit flies, it can cause serious damage to fruit plants, resulting in significant losses in crop production, with its potential to consume multiple resources making it a harmful and pervasive pest of many agricultural species.

4.6.2. *Experimental Setting*

In [108] the authors reared a population of *D. suzukii* on raspberries and conducted an experimental assay where two generations were produced on either strawberry or raspberry. The fruits were replaced daily, and the number of eggs and daily mortality of adults were recorded over the 1st and 2nd generations. They observed the total number of eggs laid in each replicate, egg-adult viability, total period whereby eggs are laid (in days), and

survival time of the adults (in days). Since they only observed up to the F2 generation in their experiment, the model proposed at the beginning of this chapter was used to simulate the effects of host-shift and the long-term behaviour of *D. suzukii*, based on estimates of fecundity and survival obtained from the laboratory experimental data. Quasi-Poisson models were used to analyse the data on total number of eggs [71]. To study the association between oviposition behaviour over time and survival times of the insects, a joint model for longitudinal outcomes (oviposition) and time-until-event outcomes (survival times) was fitted to the data [236]. We refer the reader to [108] for more details.

4.6.3. The Prout and McChesney Model

In [228] the authors used a difference equation to describe intraspecific competition among an immature *Drosophila melanogaster* population, a very ecologically similar species to *D. suzukii*, and ultimately how this affected adult fertility and survival. Their model took the form of a Ricker map. They also assumed egg survival and fertility were decreasing functions of adult density, and further included a sex ratio of a half. For our application one can consider subscripts 1 and 2 in (4.2.1) as representing dispersal from strawberry to raspberry and raspberry to strawberry, respectively. In the context of modelling host switching, and as in [228], we let $\alpha_i = R_i F_i S_i$, where $R_i \in (0, 1)$ is the sex-ratio (male:female), $F_i > 0$ is the average fecundity and $S_i \in (0, 1)$ is the average number of individuals surviving on host i . We keep this growth rate as fixed, as if we also let F_i and S_i be functions of density our model becomes difficult to both analyse and parameterise. An estimate for $\beta_1 = \beta_2 = \beta$ was obtained from [228], who used an intraspecific competition term of 0.0064, which was the sum of fertility, f , and survival, s , in their demographic model. See [228] for more details. We assumed an a priori sex ratio of a half, i.e. $R_1 = R_2 = 1/2$, as this accurately reflects the ratio in the models in [228] and the biology of the focal species.

4.6.4. Numerical Simulations

In order to model the dynamics of *D. suzukii*, we will now outline our numerical framework using empirically estimated growth rates. For simplicity, we let the density-dependent terms be equal so that each patch population only differs in its growth rate α_i . For the dispersal function given by (4.5.1) and patch dynamics given by (4.3.1), we simulated our model for 52 generations for a variety of scenarios, where each sub-population is censused each week over a one year time-horizon. The empirical parameter values are given in Table 4.1. F_i and S_i were taken from the experiments conducted. All numerical computations and simulations were done in R [263].

Parameter	R_1	F_1	S_1	R_2	F_2	S_2	β
Estimate	0.5	9.43	0.335	0.5	21.7	0.216	0.0064

Table 4.1: Empirical parameters estimates.

We will now look at what dynamics occur for various choices of dispersal strengths. Let $r_1 = 0.95$ and $r_2 = 0.1$, which corresponds to permitting a minimum of 5% and 90% dispersal from patch 1 and 2 respectively. We simulated (4.2.1) with empirical parameter values, as seen in Fig. 4.8 (top). We can observe that both patches are sources, with $1 < R_i F_i S_i < e^2$, i.e. both patches also have a LAS positive equilibrium. We can further notice that $\rho(A(0)) \approx 1.62 > 1$, which implies that we have the existence of a positive patch coexistence equilibrium. We also can ensure uniform strong persistence with respect to the minimum of both patches. In Fig. 4.8 (top) we can observe that both trajectories converge to a positive equilibrium.

Given that simulations under the empirical parameter estimates suggest global convergence to a unique positive fixed point for a variety of dispersal strengths, we simulated (4.2.1) for two additional scenarios, where we scale the growth rates, while leaving all other parameters fixed as above. These scenarios will respectively correspond to perturbing both patches, by respectively reducing or improving resource quality. Let $\alpha_i = R_i F_i S_i / 2$. In this case patch 1 is a sink and patch 2 a source with stable positive equilibrium. We can see in Fig. 4.8 (middle) that both patches go extinct in the long run. In this case we can compute $\rho(A(0)) \approx 0.81 < 1$ and so extinction is inevitable. Now let $\alpha_i = 10R_i F_i S_i$. In this case both patches are sources with unstable positive equilibrium. We can see in Fig. 4.8 (bottom) that both patches either tend to a positive equilibrium or enter periodic regimes. In this case we can compute $\rho(A(0)) \approx 16.2 > 1$ and so we can ensure strong uniform persistence for each patch.

4.6.5. Bifurcation Analysis

Different methods have been proposed to analyze the sensitivity of parameters in population growth models. Among the approaches used for sensitivity analysis, bifurcation analysis stands out. Bifurcation analysis aims to study changes in the qualitative behaviour of a dynamical system under parameter variation, such as the stability of fixed points, emergence of periodic solutions or chaos [258]. This is particularly useful for investigating the association of ecological patterns of oscillation in populations with changing values of demographic parameters. This approach allows one to quantify the contribution from changes in parameter values to changes in model outputs [275].

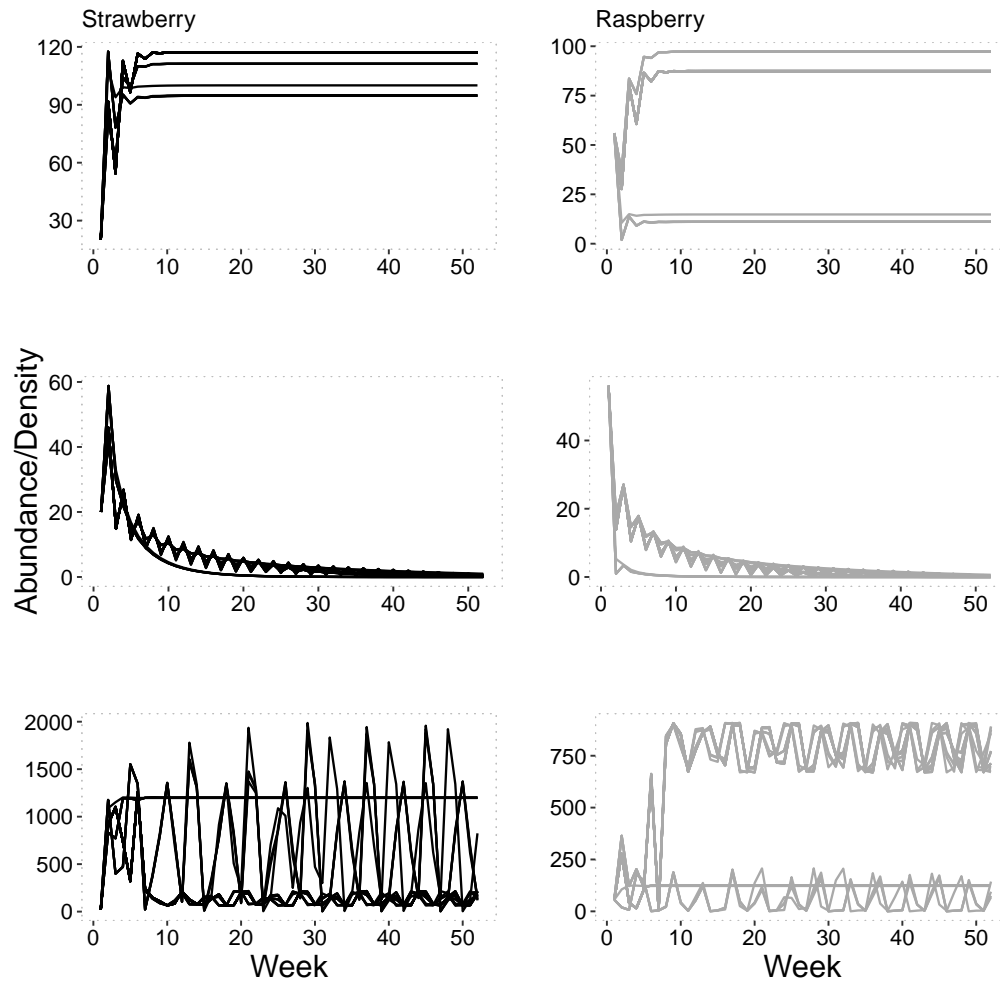


Figure 4.8: Simulations of (4.2.1) for 52 (weekly) time steps, for strawberry (right) and raspberry (left) patches. In all simulations we set $x(0) = (20, 56)$. We let $\mu_1, \mu_2 \in \{0.001, 0.250, 0.500, 0.750, 1.000\}$ for three scenarios: $\alpha_i = R_i F_i S_i$ (top), $\alpha_i = R_i F_i S_i / 2$ (middle) and $\alpha_i = 10 R_i F_i S_i$ (bottom)1.

We conducted a bifurcation analysis to explore the stability our model within the $R_i F_i S_i$ and μ_i parameter spaces (see Fig. 4.9 and Fig. 4.11). All numerical computations and simulations were conducted in R [263]. Bifurcation diagrams emerge from relationships between parameter values and population sizes [72]. Usually, the parametric space on the one axis determines significant changes on the other axis, expressing long-term population behaviour. As a result of this relationship, it is possible to observe stable trajectories, periodic cycles with fixed maximum and minimum limiting values and chaotic-type dynamics, a regime characterized by total unpredictability, that is, by the apparent absence of fixed cycles [258]. As mentioned in Chapter 2, chaotic-type dynamics are long term trajectories that do not exhibit fixed point convergence or periodic behaviour, with such dynamics being sensitive to the choice of initial conditions. The computational method to

distinguish between the different dynamical behaviour is outlined in Subsection 2.2.5.

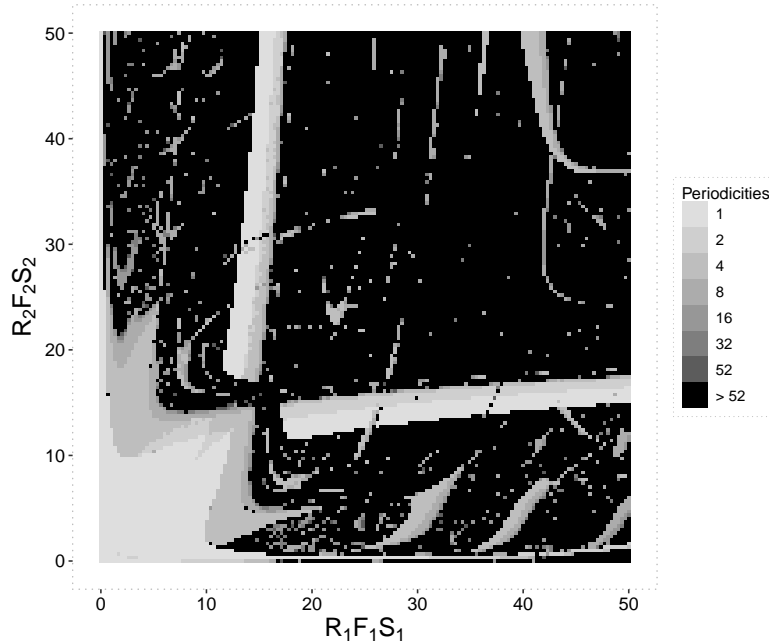


Figure 4.9: Bifurcation diagram for the $(R_1F_1S_1, R_2F_2S_2)$ -parameter space, showing the number of unique population sizes according to the colour gradient (stable fixed point for values of 1 and periodic orbits for higher values than 1). We considered the last 100 observations after iterating our model for 100,000 generations. Initial conditions were $x(0) = (76, 42)$.

We chose to use the product of the demographic parameters, $R_iF_iS_i$ in our bifurcation analysis as they play an important role in determining conditions for strong persistence and the presence of a positive equilibrium. For the $R_iF_iS_i$ bifurcation diagram we set $\mu_1 = 0.2$ and $\mu_2 = 0.3$, to reflect low-moderate density dependence (see Fig. 4.9). We then simulated trajectories for 4 different points in the $(R_1F_1S_1, R_2F_2S_2)$ -parameter space that correspond to varying periodic trajectory periodicities (see Fig. 4.10). In Fig. 4.9 we see that at low values of $R_iF_iS_i$ we have stable equilibria. As we allow demographic parameters to reach values above 10, trajectories are quite unpredictable, in that the period of these periodic trajectories begin to increase to values greater than 52. Since R_i and S_i can be maximally 1, these larger $R_iF_iS_i$ values are driven by the magnitude of F_i being large. It would be interesting for further work to further elucidate the different dynamical behaviour of our model when one varies fecundity on each patch.

Many discrete models exhibit similar complex dynamic behaviour like that seen in Fig. 4.9 [103, 125]. Trajectories may seem predictable for some parameter ranges, either stabilising or fluctuating after initial increases, but outside these ranges the behaviour we observe is more suggestive of a form of deterministic chaos. Note that the empirical parameter estimates, as in Table 4.1 give $R_iF_iS_i$ within the stable region of the parameter space.

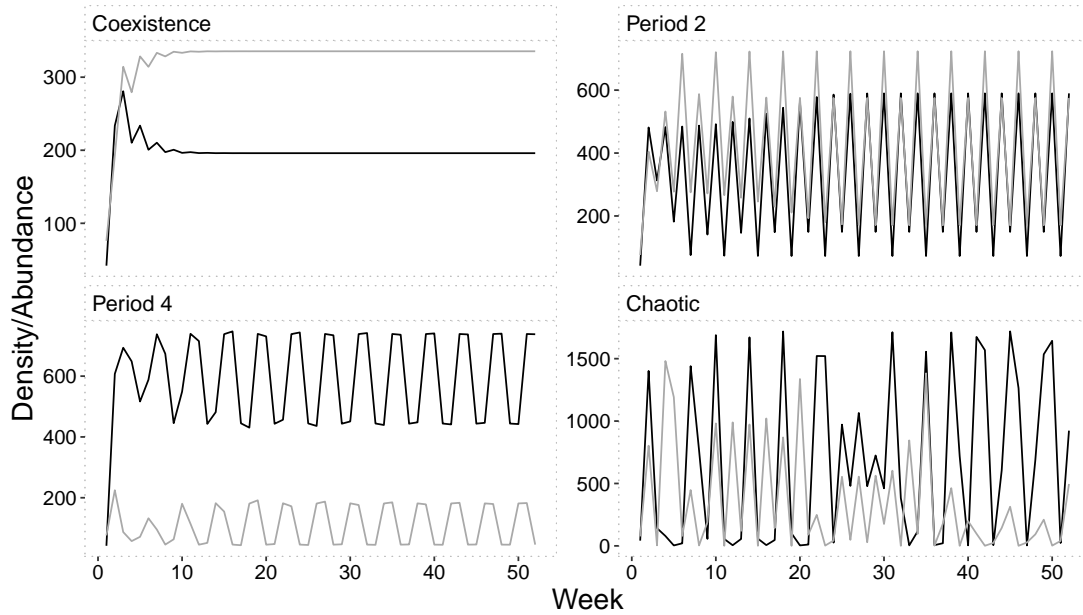


Figure 4.10: Simulations of (4.2.1) for 52 (weekly) time steps, for strawberry (black) and raspberry (grey) patches. We set $x(0) = (76, 42)$, with all other parameters as in Fig. 4.9 for the following scenarios: $\alpha_1 = 5, \alpha_2 = 6$ (Coexistence); $\alpha_1 = 10.3, \alpha_2 = 12.6$ (Period 2); $\alpha_1 = 13, \alpha_2 = 7$ (Period 4); and $\alpha_1 = 30, \alpha_2 = 25$ (Chaotic).

The $R_i F_i S_i$ product obtained from empirical estimates resulted in stable trajectories for all chosen values of μ_i , for $i \in \{1, 2\}$. For the μ_i bifurcation diagram we therefore set $R_1 F_1 S_1 = 20$ and $R_2 F_2 S_2 = 24$. In this case both patches are sources with unstable regional positive equilibria. We are thus interested to explore what happens when both patches exhibit higher survival and fertility. The narrow range within the (μ_1, μ_2) -parameter space (see Fig. 4.11), where trajectories seem to approach a stable fixed point, shows how sensitive density-dependent dispersal can be. As we increase both parameter values, more complex dynamical behaviour occurs, which may allude to increased density dependent effects on individuals who remain on each patch. This may be because $R_i F_i S_i$ is sufficiently large, for $i = 1, 2$, meaning sub-populations have higher survival probabilities or increased fertility on their respective patches, which could lead to increased regional competitive interactions for resources. Each patch also has a nonzero influx/outflow of individuals to/from it, and this may permit sufficient genetic mixing, with dispersal being one of the main drivers of genetic variation in insect species [231]. It would be interesting to investigate further the interplay between regional growth rates and the dispersal parameters, for example by fixing $\alpha_1 = \alpha_2 = \alpha$ and $\mu_1 = \mu_2 = \mu$, and conducting bifurcation analyses on α and μ together.

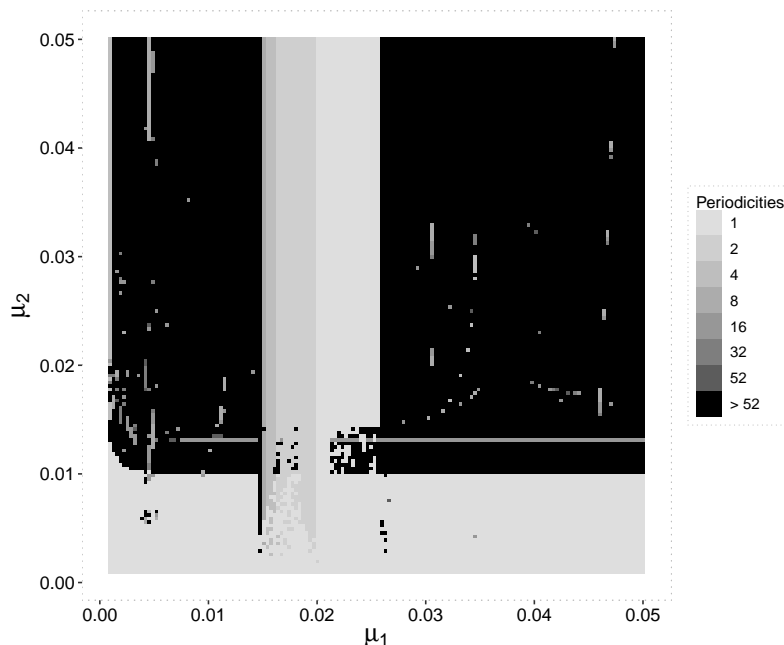


Figure 4.11: Bifurcation diagram for the (μ_1, μ_2) -parameter space, showing the number of unique population sizes according to the colour gradient (stable fixed point for values of 1 and periodic orbits for higher values than 1). We considered the last 100 observations after iterating our model for 100,000 generations. Initial conditions where $x(0) = (73, 25)$.

The demographic parameters considered in Table 2 determine the conditions for the existence of a patch coexistence equilibrium. For values of μ_i within the narrow band in Fig. 4.11 one can observe that we always have $\rho(A(0)) > 1$. Proposition 4.4.5 then implies that we have existence of a positive equilibrium and by Theorem 4.4.7 we have strong uniform persistence with respect to both patches.

4.7. Summary

In order to understand the dynamics of invasive populations, important factors to consider are spatiality and resource availability. Dispersal has been suggested as a possible mechanism for supporting survival or persistence for populations that inhabit local sinks. Our model results further support this hypothesis for spatially-structured populations, by showing that costless and density-dependent dispersal may rescue a species from extinction within a two-patch environment, even when fertility and survival proportions are low on one of the patches. We have also shown clearly the differences between passive and density-dependent dispersal. In model simulations we found that, including density-dependent dispersal and intraspecific competition, trajectories exhibit a range of behaviour and are highly sensitive to changes in parameter values. It must be kept in mind that these simulations excluded demographic or environmental stochasticity, which may

cause a previously deterministic dynamics to fluctuate, and may even allow trajectories to get arbitrarily close to the basin of attraction of the extinction equilibrium [129]. It is important to quantify the range of behaviour of complex and nonlinear ecological systems. In our model we took account of such nonlinearities through allowing both local growth and dispersal to be density-dependent functions, while also applying our model to various pest invasion dynamics. Recognising the explicit movement and within population interactions of pest species will prove to be important for both natural and invading species who inhabit fragmented landscapes.

5. Costly and Density-Dependent Movement of Heterogeneous Metapopulations

In this chapter, we propose a nonlinear dispersal model, where sub-populations move between a arbitrarily finite number of regions. The model form is an extension of the two-patch model in Chapter 4 to more than two regions. Each population's dynamics can be a different map that comes from a class of bounded population maps, with dispersal being both density-dependent and costly. We focus on the asymptotic qualitative dynamics of the model, proving various stability and persistence results. We also perform extensive numerical simulations for populations moving between regions of decline and growth, so to highlight the similarities and differences between our model and passive dispersal models. We finally conduct numerous numerical bifurcation analyses in order to assess parameter sensitivity in a variety of scenarios.

Parts of this chapter appeared in: McGrane-Corrigan, B., Mason, O. and Moral, R.D.A., 2024. A density-dependent metapopulation model: Extinction, persistence and source-sink dynamics. arXiv preprint arXiv:2405.04505.

5.1. Motivation

Habitat destruction, caused by processes such as deforestation, urbanisation and agriculture, is a major cause for species to become so-called *metapopulations*, sub-groups within a population spread out across many regions in a patchy landscape [47, 216, 250, 262]. A key ecological question is then how dispersal between these regions impacts such species' population dynamics and if this can promote coexistence among regions. For example, given that a subpopulation on one or more of the isolated regions goes extinct asymptotically, one may be interested in knowing if the coupled system is persistent, if such a system possesses a positive equilibrium or if there exists a locally/globally stable positive equilibrium. In population dynamics, coupling regional dynamics via dispersal has attracted a lot of attention in recent literature, albeit primarily in continuous time. Recently there has been interest in discrete-time dispersal models [17, 108, 156, 241, 242]. In many models the proportion dispersing is assumed to be constant. However it

has been found that this can also largely depend on the population density of the region from where such movement is taking place [204, 271].

In this chapter we will consider a model related to that in [241, 242, 288]. In their models, the authors investigated constant, costless dispersal, where the maps that describe regional population dynamics were both of Ricker or Hassell-1 form. We however will look at nonlinear dispersal rates, where each regional map can be a different map from a family of bounded population maps and where there is an overall cost to dispersal. This was motivated by the work of Chapter 4, where we considered a planar Ricker model with density-dependent and cost-free dispersal in the context of invasion dynamics. Here, we will consider an arbitrary, finite number of regions, where regional dynamics can be non-identical and come from a more general class of population maps than in Chapter 4. We will derive conditions that ensure local and global stability, and instability, of the extinction equilibrium, the existence and global stability of a positive (coexistence) equilibrium, and finally strong uniform persistence, after regions are connected by dispersal. We will first give some preliminary results and background. We will then introduce our model and state our main theoretical and numerical results.

5.2. The Metapopulation Model

Consider a population that inhabits $n \in \{2, 3, \dots\}$ regions within some patchy landscape and denote the population density in region $i \in \{1, \dots, n\}$, at time $t \in \mathbb{Z}_+$, by $x_i(t) \in \mathbb{R}_+$. We assume that all regions are accessible by all individuals.

5.2.1. Regional Maps

Let $f_i : \mathbb{R}_+ \rightarrow \mathbb{R}_+$ be a map which describes population growth on region i . Denote \mathcal{M} the set of maps $f : \mathbb{R}_+ \rightarrow \mathbb{R}_+$ such that f is a *Kolmogorov-type map*, i.e. $f(x) := g(x)x$ where $g : \mathbb{R}_+ \rightarrow (0, \infty)$ is C^1 [160]; and there exists $m \in [0, \infty)$ such that $f(x) \leq m$ for all $x \geq 0$. The last condition is based on the assumption that there is a maximum the population size can reach at any given time.

Throughout the rest of the chapter we will assume that $\{f_1, \dots, f_n\} \subset \mathcal{M}$. The class \mathcal{M} contains many of the commonly used maps for discrete time modeling of ecological systems. In particular, the following maps all belong to \mathcal{M} :

- Generalised Beverton-Holt: $f(x) = \frac{ax}{1 + (x/b)^c}$ [92],
- Hassell: $f(x) = \frac{ax}{(1 + bx)^c}$ [126],

- Ricker: $f(x) = ax \exp(-bx)$ [234], and
- Ricker with Allee effect: $f(x) = x \exp\left(a\left(1 - \frac{x}{b}\right)\left(\frac{x}{m} - 1\right)\right)$ [279],

where $a, b, s > 0$, $c \geq 1$ and $0 < m < b$. The maps discussed above are single-humped maps, i.e. either increase to a maximum and decrease after this maximum (unimodal), or are non-decreasing and saturating as $x \rightarrow \infty$. The set \mathcal{M} also contains the logistic map, given by $f(x) = ax(1-x)$, where $a \in [0, 4]$ and the domain of f is restricted to $x \in [0, 1]$, so that we do not get negative densities [196]. Also note that \mathcal{M} contains multi-modal maps such as $f(x) = ax \sum_{i=1}^m \exp\left(-b_i(x - c_i)^2\right)$, for $a > 0$, $b_i, c_i \geq 0$ and $m \in \mathbb{N}$.

5.2.2. Dispersal Costs

Following reproduction/recruitment, sub-populations from region j move to region i , with the proportion given by the C^1 map $d_{ij} : \mathbb{R}_+ \rightarrow (0, 1)$, where, for a given $i \in \{1, \dots, n\}$, we assume

$$\sum_{j=1}^n d_{ji}(x) < 1 \quad \forall x \geq 0. \quad (5.2.1)$$

The map d_{ij} can be different for each i and j , thus allowing for various dynamics for dispersing and remaining individuals in each region. Note that if $\sum_{j=1}^n d_{ji}(x) = 1 \quad \forall x \geq 0$, then this could be interpreted as there being no cost to dispersal [17, 241]. However, in this chapter we assume (5.2.1) holds, so that

$$d_{ii}(x) \neq 1 - \sum_{j \neq i} d_{ji}(x), \quad (5.2.2)$$

which allows one to incorporate dispersal costs, i.e. the sum of the proportions of individuals remaining and leaving patch i is less than unity. This may be, for example, due to factors such as *departure* or *transfer costs* that respectively occur at the initial and final stages of movement from a region [32]. With appropriate parameterisations so that (5.2.1) holds, examples of d_{ij} include (see Fig. 5.1):

- Exponential decay: $h_1(x) = \exp(-a(x + b))$,
- Unimodal: $h_2(x) = \exp\left(-\left((ax - b)^2 + c\right)\right)$, and
- Generalised logistic: $h_3(x) = \frac{r}{(1 + b \exp(-cx))^{\frac{1}{p}}}$,

where $a, b, c, p > 0$ and $r \in (0, 1)$.

5.2.3. The Coupled System

A general form for the metapopulation model we consider can be written as

$$x_i(t+1) = \sum_{j=1}^n d_{ij}(x_j(t)) f_j(x_j(t)), \quad (5.2.3)$$

where $x_i(0) \in \mathbb{R}_+$, $i \in \{1, \dots, n\}$ (see Fig. 5.2). System (5.2.3) is the same form as system (4.2.1) in Chapter 4. The differences are that we assume that we have $n \geq 2$ regions, dispersal is costly, and that each f_i can be a different map from \mathcal{M} . We can rewrite (5.2.3) as a nonlinear matrix model of the form $F(x) = A(x)x$, as in Chapter 3, where the matrix valued function $A : \mathbb{R}_+^n \rightarrow \mathbb{R}_+^{n \times n}$ in this chapter is defined as

$$A(x) := D(x)G(x), \quad (5.2.4)$$

where $D(x) := (d_{ij}(x_j))$ and $G(x) := \text{diag}(g_1(x_1), \dots, g_n(x_n))$. As g_i and d_{ij} are continuous, A is also continuous. Note that for a fixed $x \in \mathbb{R}_+^n$, as (5.2.1) holds we have that $D(x)$ is a column substochastic matrix.

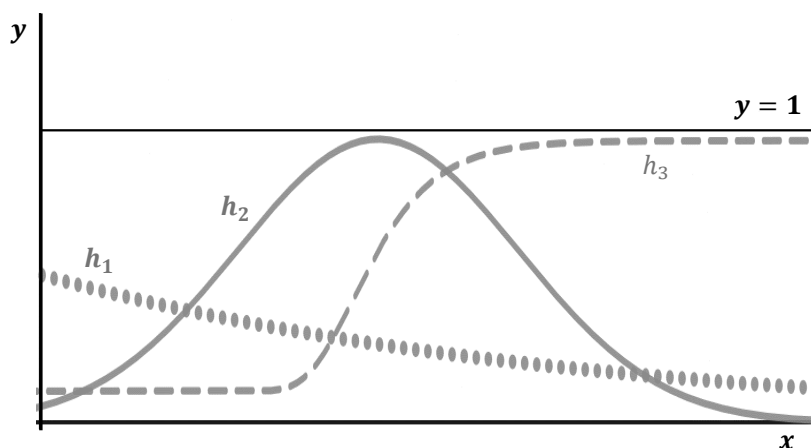


Figure 5.1: Illustration of the functions h_1 (dotted), h_2 (solid) and h_3 (dashed).

Assumption (5.2.1), along with $\{f_1, \dots, f_n\} \subset \mathcal{M}$, further highlights the difference between our coupled model and the models of [156, 241, 242, 288]. Note that the model in Chapter 4 does not consider dispersal costs, as in that case $d_{ii} = 1 - d_{ij}$ for $i, j \in \{1, 2\}$. Further note that, as is similarly the case in Chapter 4, each d_{ij} being a function of x means that one can incorporate density-dependent effects like competition, mortality and other ecological processes that may affect individuals both during the process of remaining on a patch and/or dispersing between patches.

In [156, 288] the authors assumed dispersal was constant. In [156] the authors also had three additional assumptions on g_i and f_i , as seen in Chapter 2. In [288] the authors

assumed each region was modelled by an α -concave monotone map. However, we note that our regional maps are different.

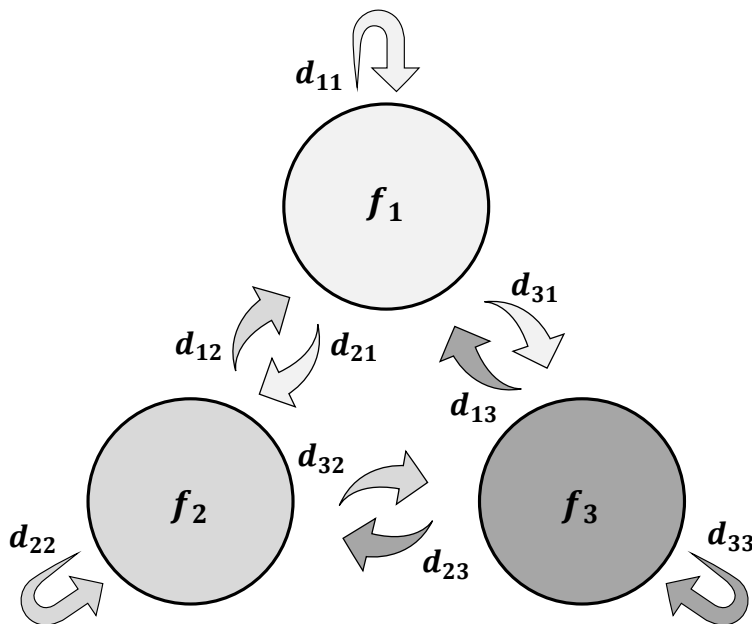


Figure 5.2: Conceptual diagram of system (5.2.3) when $n = 3$, where $f_i(x_i)$ and $d_{ij}(x_j)$ respectively describe the dynamics on and dispersal from patch j to i for $i \neq j$. When $i = j$ each d_{ii} describes the proportion of individuals remaining on patch i .

Example 5.2.1. Consider the function $f(x) = \gamma x \exp(-(x-1)^2)$, where $\gamma > e$. Clearly f is C^1 , $f(x) > 0$ for $x > 0$, $f(0) = 0$, and f is of the form $g(x)x$ with $g(x) = \gamma \exp(-(x-1)^2)$. We can also see that f has a unique global maximum at $m = (1 + \sqrt{3})/2$. Therefore we can conclude that $f \in \mathcal{M}$. One can verify that

$$\begin{aligned} f'(x) &= \gamma \exp(-(x-1)^2)(1 + 2x - 2x^2) \\ f''(x) &= 2\gamma \exp(-(x-1)^2) (2 - x - 4x^2 + 2x^3). \end{aligned}$$

From this we can see that $f'(x) > 0 \forall x \in (0, m)$, but for $m_1 \approx 0.223$ we have that $f''(x) > 0 \forall x \in (0, m_1)$. Therefore there does not exist an $\alpha \in (0, \infty]$ such that $f''(x) < 0$ for all $x \in (0, \alpha]$ and so the definition of α -concave monotonicity is violated. Hence we have found $f \in \mathcal{M}$ such that f is not α -concave monotone.

A family of maps closely related to the maps in \mathcal{M} are unimodal population maps. Let $f : \mathbb{R}_+ \rightarrow \mathbb{R}_+$ be a C^1 map such that $f(0) = 0$ and $f(x) > 0$ for all $x > 0$; f has fixed points $\{0, K\}$, such that $K \in (0, \infty)$, $f(x) > x$ for $x \in (0, K)$ and $f(x) < x$ for $x \in (K, \infty)$; and f has a unique critical point $L < K$ such that $f'(x) > 0$ for all $x \in (0, L)$, $f'(x) < 0$ for all $x \in (L, \infty)$, and $f'(0) > 0$. Such maps are known as *unimodal population maps* [92]. Let \mathcal{U} be the set of unimodal population maps. It is clear, by definition, that $\mathcal{U} \subset \mathcal{M}$. Maps

in \mathcal{U} , by assumption, have an unstable extinction equilibrium and a positive equilibrium. They also have a unique global maximum. The stability of systems with maps in \mathcal{U} has attracted much interest in the past. For examples, see [58, 247, 248, 251].

The maps in \mathcal{U} are also closely related to α -concave monotone maps considered in [288].

Example 5.2.2. Maps in \mathcal{U} must possess a positive equilibrium that is greater than $L > 0$. One must also have that they are increasing and concave up to this maximum, and decreasing and concave down after it. In [288] the authors assumed that the dynamics on each region was modelled by an α -concave monotone map of the form $f(x) := g(x)x$, where g is a strictly decreasing, positive, C^2 map. Clearly if f is α -concave monotone then it is positive-definite. We also have that $f \in \mathcal{U}$ is unimodal. The authors also assume $f'(x) > 0$ up to $x = \alpha > 0$. This does not require that $\alpha < K$ and so an α -concave monotone map is not necessarily unimodal. If we let $\alpha = L$ as in the definition of \mathcal{U} then we can see that f is concave in $[0, \alpha]$.

In the next section we will discuss some of the qualitative properties of (5.2.3).

5.3. Stability and Persistence

5.3.1. Extinction

We first state a sufficient condition for local asymptotic stability of the extinction equilibrium.

Proposition 5.3.1. *Suppose $\{f_1, \dots, f_n\} \subset \mathcal{M}$ and $F(x) = A(x)x$, where $A(x)$ is given by (5.2.4). Further assume that $\max_{i \in \{1, \dots, n\}} g_i(0) < 1$. Then, $x^* = 0$ is a LAS equilibrium of system (5.2.3) for all d_{ij} satisfying (5.2.1).*

Proof. Assume that $\max_{i \in \{1, \dots, n\}} g_i(0) < 1$. As f_i is a Kolmogorov-type map, i.e. $f_i(x) = g_i(x)x$, we have that $f_i(0) = 0$ for all $i \in \{1, \dots, n\}$. The Jacobian of $F(x) = A(x)x$ at 0 can be written as

$$F'(0) := \begin{pmatrix} d_{11}(0)f'_1(0) & d_{12}(0)f'_2(0) & \cdots & d_{1n}(0)f'_n(0) \\ d_{21}(0)f'_1(0) & d_{22}(0)f'_2(0) & \cdots & d_{2n}(0)f'_n(0) \\ \vdots & & \ddots & \vdots \\ d_{n1}(0)f'_1(0) & d_{n2}(0)f'_2(0) & \cdots & d_{nn}(0)f'_n(0) \end{pmatrix}. \quad (5.3.1)$$

As each f_i is of Kolmogorov type we have that

$$f'_i(x) = g'_i(x)x + g_i(x), \quad x \geq 0 \implies f'_i(0) = g_i(0).$$

As $g_i(0) > 0$ and $d_{ij}(0) \in (0, 1)$, we have that $F'(0) = A(0) > 0$. Recall that $\rho(B) \leq \|B\|_1$ for $B \in \mathbb{R}^{n \times n}$. Therefore, as (5.2.1) holds, we have that

$$\begin{aligned} \rho(A(0)) \leq \|A(0)\|_1 &= \max_{i \in \{1, \dots, n\}} \left\{ f'_i(0) \sum_{j=1}^n d_{ji}(0) \right\} \\ &< \max_{i \in \{1, \dots, n\}} f'_i(0) \\ &= \max_{i \in \{1, \dots, n\}} g_i(0). \end{aligned}$$

We thus have that $\rho(A(0)) < 1$ and so $x^* = 0$ is a LAS equilibrium of (5.2.3), which follows from standard Lyapunov stability results [136]. \square

Note that a sufficient condition for $x^* = 0$ to be a LAS equilibrium of the system (2.2.1) is that $|f'(0)| < 1$. This then implies that the sufficient condition in Proposition 5.3.1 for LAS of extinction for each isolated system, with $f_i \in \mathcal{M}$, i.e. $\max_{i \in \{1, \dots, n\}} g_i(0) < 1$, is also sufficient for LAS of the extinction equilibrium for (5.2.3). Local asymptotic stability of the extinction equilibrium for each patch means that if there are sufficiently small abundances on each patch, these patch populations would tend to extinction in isolation. The result above then can be interpreted as ensuring that, at small population values, these patches would still tend to extinction when they are all connected by density-dependent dispersal. This may arise in a situation where habitat quality is poor, or resources are scarce. In such cases, density-dependent dispersal alone is not enough to sustain the system, leading to extinction across all the patch populations.

Our next result concerns the global stability of the extinction equilibrium.

Theorem 5.3.2. *Suppose $\{f_1, \dots, f_n\} \subset \mathcal{M}$, (5.2.1) holds, $F(x) = A(x)x$, where $A(x)$ is given by (5.2.4), and $d_{ij}(x)$ satisfies (5.2.1). Further assume that the following hold:*

1. *either $d_{ij}(x) \equiv d_{ij} \in (0, 1)$ or $d_{ij}(x)$ is decreasing in x ;*
2. *$g_i(x)$ is decreasing in x ;*
3. *$\rho(A(0)) < 1$.*

Then, $x^ = 0$ is a GAS equilibrium of (5.2.3).*

Proof. Assume $\rho(A(0)) < 1$. In the proof of Proposition 5.3.1 we saw that $F'(0) = A(0) > 0$ and so it follows from Lemma (2.2.5) that there exists $v^T > 0$ such that $v^T A(0) < v^T$. Define the function $V : \mathbb{R}^n \rightarrow \mathbb{R}$ as $V(x) := v^T x$. As $g_i(x)$ and either $d_{ij}(x)$

are decreasing in x or $d_{ij}(x) \equiv d_{ij} \in (0, 1)$ we have that $v^T A(x) \ll v^T A(0)$ for all $x \geq 0$. As (5.2.3) is a positive system, it follows that for $t \in \mathbb{N}$

$$\begin{aligned} V(x(t+1)) - V(x(t)) &= V(F(x(t))) - V(x(t)) \\ &= v^T (A(x(t)) - I) x(t) \\ &< v^T (A(0) - I) x(t) \\ &< 0. \end{aligned}$$

Hence V is decreasing along non-zero trajectories of F . Clearly V is positive-definite, i.e. $V(0) = 0$ and $V(x) > 0$ for all $x > 0$. For $x \in \mathbb{R}_+^n$ we can see that V is radially unbounded, i.e. $\lim_{\|x\| \rightarrow \infty} V(x) \rightarrow \infty$. Thus V defines a radially unbounded copositive Lyapunov function for F with respect to $x^* = 0$ [136]. This then implies that $\lim_{t \rightarrow \infty} x(t, x_0) = 0$. \square

Example 5.3.1. If we had that $d_{ii}(x) \equiv d_{ii} \in (0, 1)$ and $d_{ij}(x)$ is decreasing in x for $i \neq j$, this can be interpreted as there being a fixed number of remaining individuals over time on each region, but dispersal from each patch exhibits negative density-dependence. Positive (negative) density-dependent dispersal is where, for large population densities, the proportion of individuals dispersing from (remaining on) a region is high. As mentioned in Chapter 4, positive density-dependent dispersal may be due to factors such as competition/crowding, or dominance hierarchies [195]. On the other hand, negative density dependence may be due to factors such as aggressive interactions due to territoriality or mate searching, for example.

We will now investigate when sub-populations may coexist on their respective patches.

5.3.2. Coexistence

We can show that there exists a positive equilibrium of system (5.2.3). Before we do this we will prove two results. First we will show that F is strongly positive.

Lemma 5.3.3. *Suppose $\{f_1, \dots, f_n\} \subset \mathcal{M}$, (5.2.1) holds and $F(x) = A(x)x$, where $A(x)$ is given by (5.2.4). Then, $F(x) > 0$ for all $x \in \mathbb{R}_+^n \setminus \{0\}$ and for all d_{ij} satisfying (5.2.1).*

Proof. As each f_i is a Kolmogorov-type map and (5.2.1) hold, clearly $A(x) > 0 \implies F(x) > 0$ for all $x \geq 0$. \square

Our next result establishes the boundedness of the map F .

Proposition 5.3.4. *Suppose $\{f_1, \dots, f_n\} \subset \mathcal{M}$, (5.2.1) holds, $F(x) = A(x)x$, where $A(x)$ is given by (5.2.4), and $d_{ij}(x)$ satisfies (5.2.1). Then, $\exists M > 0$ such that $\forall x \in \mathbb{R}_+^n$*

$$\|F(x)\|_1 \leq M.$$

Proof. For $x \in \mathbb{R}_+^n$, the l_1 norm of x is given by

$$\|x\|_1 = \sum_{i=1}^n x_i = 1^T x,$$

where $1 := (1, \dots, 1)^T$. It follows from Lemma 5.3.3 that $F(x) > 0 \forall x \geq 0$. As (5.2.1) holds we therefore have that

$$\|F(x)\|_1 = 1^T F(x) \leq \sum_{i=1}^n f_i(x_i) \leq \sum_{i=1}^n m_i, \forall t > 0.$$

Thus define the upper bound $0 < M := \sum_{i=1}^n m_i$. □

It follows from Lemma 5.3.3 and Proposition 5.3.4 that $F(\mathbb{R}_+^n) \subset \mathbb{R}_+^n$ and the sequence $\{F^t(x)\}_{t \geq 0}$ has no unbounded trajectory. It is immediate that for any $x_0 \in \mathbb{R}_+^n$, $\|x(t, x_0)\|_1 \leq M$ for all $t \geq 1$.

We now state our first main result of this section, which gives a sufficient condition for the existence of a positive fixed point of F .

Theorem 5.3.5. *Suppose $\{f_1, \dots, f_n\} \subset \mathcal{M}$, (5.2.1) holds, $F(x) = A(x)x$, where $A(x)$ is given by (5.2.4), and $d_{ij}(x)$ satisfies (5.2.1). If $\rho(A(0)) > 1$, then $\exists x^* \in \text{Int}(\mathbb{R}_+^n)$ such that $F(x^*) = x^*$.*

Proof. We will prove this by showing that we can find a nonempty, convex and compact set, $\Omega_1 \subset \text{Int}(\mathbb{R}_+^n)$, such that

$$F(\Omega_1) \subset \Omega_1,$$

which allows us to invoke Brouwer's Fixed Point Theorem [264].

Step 1: We first construct Ω_1 and show it is nonempty and compact. It follows from Proposition 5.3.4 that there exists a constant $M > 0$, such that $\|F(x)\|_1 \leq M$ for all $x \in \mathbb{R}_+^n$. If $\rho(A(0)) > 1$, it follows from Lemma (2.2.5) that $\exists v > 0$ such that

$$v^T A(0) > v^T.$$

As $A : \mathbb{R}_+^n \rightarrow \mathbb{R}_+^{n \times n}$ is a continuous matrix-valued function there exists a constant $0 < \delta < M$ such that

$$v^T A(x) \geq v^T, \|x\|_1 \leq \delta.$$

For any such $x \geq 0$ ($x \neq 0$) we then can see that

$$v^T F(x) = v^T A(x)x \geq v^T x.$$

If we define

$$\Omega_0 := \{x \in \mathbb{R}_+^n : \delta \leq \|x\|_1 \leq M\}$$

we then have that $F(x) > 0$ for $x \in \Omega_0$ and hence

$$x \in \Omega_0 \implies v^T F(x) > 0. \quad (5.3.2)$$

As A is continuous, F is also continuous. It then follows from the Extreme Value Theorem that $v^T F(x)$ attains its minimum and maximum Ω_0 . Therefore there exists $\kappa_1 > 0$ such that

$$\min \{v^T F(x), x \in \Omega_0\} = \kappa_1.$$

Now choose some $\bar{x} > 0$ with $\|\bar{x}\|_1 \leq M$. Set $\kappa_2 = v^T \bar{x}$. Then $\kappa_2 > 0$. Let $\kappa = \min\{\kappa_1, \kappa_2\}$ and define

$$\Omega_1 := \{x \in \mathbb{R}_+^n : v^T x \geq \kappa, \|x\|_1 \leq M\}.$$

By construction Ω_1 is non-empty. Clearly Ω_1 is closed and bounded, so therefore compact

Step 2: We will now show that Ω_1 is convex. Let $x, y \in \Omega_1$ and let $\alpha \in [0, 1]$ be arbitrary. Then, we have that

$$v^T((1 - \alpha)x + \alpha y) \geq (1 - \alpha)\kappa + \alpha\kappa = \kappa,$$

and by the triangle inequality

$$\begin{aligned} \|(1 - \alpha)x + \alpha y\| &\leq (1 - \alpha)\|x\| + \alpha\|y\| \\ &\leq (1 - \alpha)M + \alpha M \\ &= M. \end{aligned}$$

Therefore

$$x, y \in \Omega_1 \implies (1 - \alpha)x + \alpha y \in \Omega_1$$

for all $\alpha \in [0, 1]$, i.e. Ω_1 is convex.

Step 3: Finally we will show that F maps elements of Ω_1 into Ω_1 . Let $z \in \Omega_1$. There are two cases to consider for $\|z\|_1$.

Case 1: Consider $\delta \leq \|z\|_1 \leq M$. We saw in (5.3.2) that

$$\delta \leq \|z\|_1 \leq M \implies v^T F(z) \geq \kappa \implies F(z) \in \Omega_1.$$

Case 2: Consider $\|z\|_1 \leq \delta$. As $\delta \leq M$ we must then have that

$$\|z\|_1 \leq \delta \implies v^T F(z) \geq v^T z \geq \kappa \implies F(z) \in \Omega_1.$$

In both cases we have that

$$x \in \Omega_1 \implies F(x) \in \Omega_1.$$

Hence we have found a non-empty, compact, convex set in $\mathbb{R}_+^n \setminus \{0\}$, given by Ω_1 , such that F maps Ω_1 into itself. Therefore, as F is C^1 on Ω_1 , it follows from Brouwer's Fixed Point Theorem [264] that there exists $x^* \in \Omega_1$ such that $F(x^*) = x^*$. It follows from Lemma 5.3.3 that $x^* = F(x^*) > 0$. \square

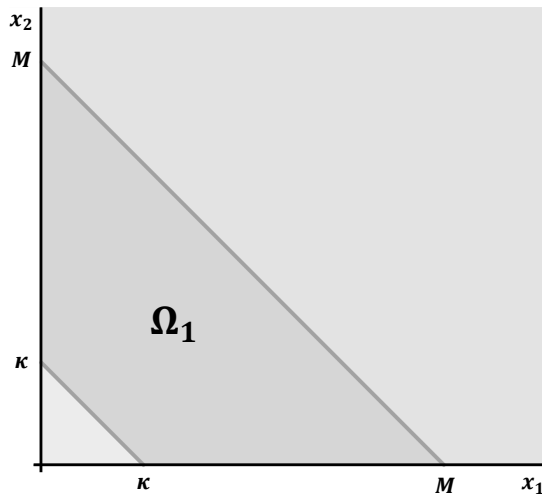


Figure 5.3: Illustration of Ω_1 in the proof of Theorem 5.3.5 for $n = 2$.

It should be noted that Theorem 7.5 of [255] could be used to give an alternative proof of the last result, as in the proof of Proposition 4.4.5 in Chapter 4. However, our proof above directly uses the specific properties of the system (5.2.3) rather than relying on more general conditions. Moreover, it clarifies that the positive equilibrium is contained in the region Ω_1 . An illustration of the region Ω_1 is given in Fig. 5.3 for when $n = 2$.

As is the case in Chapter 4, to derive sufficient conditions for either uniqueness or the local/global stability of a positive equilibrium of (5.2.3) is not as tractable as when dispersal is constant/passive. In Theorem 3.5.1 [156] the authors used the fact that their system was strongly monotone, which allowed them to prove both uniqueness and global asymptotic stability of a positive equilibrium of their coupled system. A map $F : \mathbb{R}^n \rightarrow \mathbb{R}^n$ is *strongly monotone* if $F(x) \geq F(y)$ (resp., $F(x) > F(y)$) whenever $x \geq y$ (resp., $x > y$). As there are many different choices of regional maps in \mathcal{M} and for each dispersal function d_{ij} , in the current context our model is not in general strongly monotone, as we can demonstrate with a simple example.

Example 5.3.2. Let $n = 2$. Consider

$$f_1(x) = f_2(x) = ax \exp(-bx) \quad (5.3.3)$$

for $a, b > 0$. Further let $d_{ii}(x) \equiv d_{ii} \in (0, 1)$ and $d_{ij}(x) \equiv d_{ij} \in (0, 1)$, for $i, j \in \{1, 2\}$, $i \neq j$. Each $d_{ij}(x)$ is constant for all $x \geq 0$. Recall from Chapter 4 that the Ricker map of the form (5.3.3) is increasing in x up to the point $x = 1/b$ and is decreasing after this point. Therefore in this simple illustrative example, F cannot be strongly monotone.

An alternative perspective to asymptotic stability is that of uniform persistence. Note that as $F'(0) = A(0) > 0$ we have that $F'(0)$ is irreducible, as already shown in the proof of Proposition 5.3.1. It then follows from Corollary 3.18 in [255], that if $\rho(A(0)) > 1$, then the system (5.2.3) is uniformly weakly $\|\cdot\|$ -persistent for $\|\cdot\|$ any norm on \mathbb{R}^n . We will now show that $\rho(A(0)) > 1$ is also sufficient for (5.2.3) to be uniformly strongly persistent with respect to two different persistence functions, for arbitrary choices of both $f_i \in \mathcal{M}$ and d_{ij} satisfying (5.2.1).

Theorem 5.3.6. *Suppose $\{f_1, \dots, f_n\} \subset \mathcal{M}$ and $F(x) = A(x)x$, where $A(x)$ is given by (5.2.4) and $d_{ij}(x)$ satisfies (5.2.1). Let $\|\cdot\|$ be any norm on \mathbb{R}^n . Define $\eta_1(x) := \min_{i \in \{1, \dots, n\}} x_i$ and $\eta_2(x) := \|x\|$. If $\rho(A(0)) > 1$, then F is uniformly strongly η_i -persistent.*

Proof. Assume $\rho(A(0)) > 1$. It follows from Lemma 5.3.3 that

$$F(\mathbb{R}_+^n \setminus \{0\}) \subset \text{Int}(\mathbb{R}_+^n).$$

Clearly $\rho(A(0)) > 1$ implies that $\rho(A(0)^T) > 1$. In the proof of Proposition 5.3.1 we saw that $F'(0) = A(0) > 0$. It then follows from Lemma 2.2.2 that there exists $v > 0$ such that

$$F'(0)^T v = A(0)^T v > v \implies F'(0)^T v \geq r_0 v$$

for some suitably chosen $r_0 > 1$. It follows from Proposition 5.3.4 that there exists $M > 0$ such that $\|F(x)\|_1 \leq M$ for all $x > 0$. As noted in [255], the set

$$X_0^{(i)} := \{x_0 \in \mathbb{R}_+^n : \eta_i(x(t, x_0)) = 0, \forall t \geq 0\}$$

is equal to $\{0\}$ precisely when $F(0) = 0$ and for all $c > 0$ there exists $s \in \mathbb{N}$ such that

$$F^s(x) > 0, \quad 0 < \|x\| \leq c, \quad (5.3.4)$$

for $i \in \{1, 2\}$, where $\|\cdot\|$ is any norm on \mathbb{R}^n . We can see from the form of F that

$$f_i(0) = 0 \forall i \in \{1, \dots, n\} \implies F(0) = 0.$$

As F is strongly positive we can also see that (5.3.4) holds for all $c > 0$, with $s = 1$. Therefore we have that $X_0^{(k)} = \{0\}$, $k \in \{1, 2\}$. We have thus verified the assumptions of Theorem 2.3.2. We can thus conclude that there exists $\epsilon_1, \epsilon_2 > 0$ such that

$$\begin{aligned} \min_{i \in \{1, \dots, n\}} x_i(0) > 0 &\implies \liminf_{t \rightarrow \infty} \min_{i \in \{1, \dots, n\}} x_i(t) \geq \epsilon_1, \\ \|x(0)\| > 0 &\implies \liminf_{t \rightarrow \infty} \|x(t)\| > \epsilon_2, \end{aligned}$$

i.e. (5.2.3) is uniformly strongly η_i -persistent, $i \in \{1, 2\}$. □

5.4. Sources and Sinks: A Numerical Study

In this section we will use numerical methods to investigate several questions suggested by the results of the previous section. All numerical computations and simulations were conducted in R [263]. This section also illustrates how the model class we consider either supports or exhibits behaviours that are distinct from some of the other metapopulation models discussed earlier. Let us consider the simplest case of (5.2.3) when $n = 2$. Therefore (5.2.3) reduces to

$$\begin{aligned} x_1(t+1) &= d_{11}(x_1(t))f_1(x_1(t)) + d_{12}(x_2(t))f_2(x_2(t)) \\ x_2(t+1) &= \underbrace{d_{22}(x_2(t))f_2(x_2(t))}_{\text{remaining}} + \underbrace{d_{21}(x_1(t))f_1(x_1(t))}_{\text{dispersing}}, \end{aligned} \quad (5.4.1)$$

for $x(0) \in \mathbb{R}_+^2$. This is similar in form to system (4.2.1) in Chapter 2, but in this case we have that (5.2.2) holds and so each d_{ij} can be a different map for the remaining and dispersing components. We also have that f_1 and f_2 do not have to be the same map (in Chapter 4 both were Ricker maps), but can be two different maps in \mathcal{M} .

In this section we will investigate the following:

- Does an analagous result to Theorem 3.5.1 hold for (5.2.3)?
- Is $\rho(A(0)) > 1$ necessary for the existence of a positive equilibrium?
- How does varying parameters of the parameterised dispersal maps d_{ij} affect the total population size over time?
- How does varying parameters of system (5.2.3) affect its asymptotic behaviour?

Note that the following example is a simple consequence of Theorem 5.3.1.

Example 5.4.1. Consider (5.4.1) with each f_i given by a Generalised Beverton-Holt, Hassell, Ricker or Logistic map. Then, if $a_i \in (0, 1)$ for $i = 1, 2$, it follows from Proposition 5.3.1 that extinction for (5.4.1) is at least LAS for any choice of $d_{ij}(x)$.

Given a C^1 Kolmogorov type map, $f(x) = g(x)x$, in [247] the author states that

- a) $g(x) < 1 \forall x \geq 0 \implies x(t, x_0) \rightarrow 0$ as $t \rightarrow \infty$ for all $x(0) = x_0 > 0$, and
- b) $g(0) > 1 \implies x(t, x_0) \rightarrow 0$ as $t \rightarrow \infty$ for some $x(0) = x_0 > 0$.

For $f_i \in \mathcal{M}$, we call region i a *sink* if it is a low quality habitat where an isolated population would go extinct, i.e. a) holds for g_i . On the other hand, region i is a *source* if it can sustain an inhabiting population, i.e. b) holds for g_i . Throughout the rest of this section we will explore our model in the context of source-sink dynamics.

5.4.1. Regional Dynamics

To demonstrate the impact and flexibility of our model, let's consider two different classes for local dynamics: Ricker and Hassell maps. Note that other choices of maps in \mathcal{M} are of course possible. Assume that f_1 is given by a Ricker map, i.e. $f_1(x) = a_1x \exp(-b_1x)$ and f_2 is given by what we call a Hassell-1 map (a Hassell map as in Section 5.2.1 with $c = 1$), i.e. $f_2(x) = (a_2x)/(1 + b_2x)$, where $a_i, b_i > 0$ for $i = 1, 2$. In Chapter 4 we outlined some of the qualitative properties of the Ricker map. We will recall these and some properties of the Hassell-1 for ease of exposition in the current context.

For Ricker and Hassell-1 maps, one has that $g_i(0) = a_i < 1$ implying that $g_i(x_i) < 1$ for all $x_i \geq 0$ and so the regional extinction equilibrium is GAS for f_i . If $a_i > 1$, the extinction equilibrium is unstable for f_i . This also implies that there exists a unique positive equilibrium for f_i . For f_1 this is given by $x_R^* := \ln(a_1)/b_1$ and for f_2 this is given by $x_H^* := (a_2 - 1)/b_2$. For the Ricker map, if $1 < a_1 < e$ we have that x_R^* is LAS. If $a_1 > e$ we have that x_R^* is unstable. For the Hassell-1 map, if $a_2 > 1$ we have that x_H^* is GAS [59]. Unless stated otherwise we further assume that region 1 is a source and region 2 is a sink, i.e. $a_1 > 1$ and $a_2 < 1$. Thus we are interested in examining some of the dynamical behaviour of (5.4.1) in various scenarios when a patch destined for extinction is coupled to a patch which exhibits long-term growth.

5.4.2. Density-Dependent Dispersal

Unless stated otherwise, throughout the rest of this section, let the dispersal functions in (5.4.1) be given by

$$d_{ij}(x_j) = \frac{r_{ij}}{(1 + \exp(-k_{ij}(x_j - s_{ij})))}, \quad (5.4.2)$$

where $r_{ij} \in (0, 1)$ and $k_{ij}, s_{ij} \geq 0$ for $i, j \in \{1, 2\}$. Note that this form of dispersal map has considerable biological justification. In the papers of [164, 272, 289] the authors conducted numerical simulations using such a dispersal map for a variety of ecological scenarios. The authors used their models with density-dependent dispersal to investigate various natural phenomena, such as patch-population synchrony, where populations on two disjoint patches exhibit synchronous dynamics over time. We will use such a dispersal map to investigate some of the qualitative behaviour of (5.4.1).

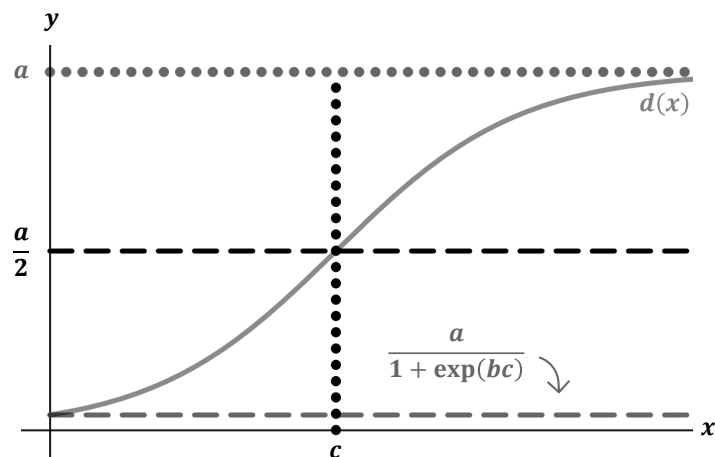


Figure 5.4: Illustration of $y = d(x) := a(1 + \exp(-b(x - c)))^{-1}$ (grey solid curve) for $a \in (0, 1)$ and $b, c \geq 0$. The dotted grey line is the curve $y = a$. The dashed grey line is the curve $y = d(0) = a(1 + \exp(bc))^{-1}$. The dashed black line is the curve $y = d(c) = a/2$. The dotted black line is the curve $x = c$.

The dispersal function (5.4.2) may describe, for example, regional populations that exhibit a mixture of both *negative* and *positive* density-dependent dispersal, which can be controlled through the parameters r_{ij} , k_{ij} and s_{ij} [237]. For instance, one can model positive density-dependent dispersal on both regions by letting both r_{ii} and k_{ii} be sufficiently small, and r_{ij} and k_{ij} be sufficiently large, for $i \neq j$. In other words, $d_{ii}(x_i)$, which models the proportion of individuals remaining on region i , will be relatively small for all values of x_i and is an increasing function of x_i , with the rate of increase being quite gradual. At the same time, d_{ji} rapidly increases toward r_{ji} , which is relatively close to 1, as x_j increases.

Density-dependent dispersal may be positive or negative depending on the specific context. For example, it is known that for many aphid species, when densities become too high, wingless generations can begin to produce winged offspring, which results in increased movement away from their natal region [36]. On the other hand, when densities become sufficiently low, perhaps due to unfavourable conditions, aphid populations will produce winged individuals in order to disperse and occupy other habitats that have the potential to increase fecundity and survival.

The dispersal function (5.4.2) is also a specific form of the *generalised logistic function* or so-called *Richards curve* [233]. An illustration of a function of the form of (5.4.2) is given in Fig. 5.4. We can observe that the following hold:

$$\begin{aligned} d_{ii}(x) + d_{ji}(x) < 1 &\iff r_{ii} + r_{ji} < 1, i \neq j; \\ d_{ij}(0) &= \frac{r_{ij}}{1 + \exp(k_{ij}s_{ij})} > 0; \\ \lim_{x \rightarrow \infty} d_{ij}(x) &= r_{ij} < 1; \text{ and} \\ d_{ij}(s_{ij}) &= \frac{r_{ij}}{2}. \end{aligned}$$

5.4.3. Global Stability Dichotomy

Theorem 5.3.5 gave a sufficient condition for the existence of a positive equilibrium for (5.2.3), the proof of which gave a region in the state space where one can find such an equilibrium. Theorem 3.5.1 stated sufficient conditions for the global stability of the extinction equilibrium and a positive equilibrium, as proved in [156].

In relation to (5.2.3), a natural question to ask is: does an analogous result hold to Theorem 3.5.1 for any choice of appropriate f_i and d_{ij} ? In particular we ask, for $\{f_1, \dots, f_n\} \subset \mathcal{M}$ and d_{ij} satisfying (5.2.1),

- does $\rho(A(0)) < 1 \implies x^* = 0$ is a GAS equilibrium for system (5.2.3); and
- does $\rho(A(0)) > 1 \implies x^* > 0$ is a GAS equilibrium for system (5.2.3)?

The answers to the above questions are in fact no, as we can demonstrate using examples.

First we consider the case when $\rho(A(0)) < 1$.

Example 5.4.2. Let all parameters be as in Fig. 5.5. Let $a_1 = 50$. Then we get that $\rho(A(0)) \approx 0.1051 < 1$. If we simulate this parameterised system we can observe in Fig. 5.5 (left) the existence of a periodic solution of period 2. Hence $x^* = 0$ is not GAS.

Next we consider the case when $\rho(A(0)) > 1$.

Example 5.4.3. Let all parameters be as in Fig. 5.5. Let $a_1 = 750$. Then we get that $\rho(A(0)) \approx 1.058 > 1$. If we simulate this parameterised system we can observe in Fig. 5.5 (right) the existence of a periodic solution of period 2. Hence $x^* > 0$, which exists by Theorem 5.3.5, is not GAS.

Let $x_P^{(1)}$ and $x_P^{(2)}$ respectively be the period-2 trajectories in Examples 5.4.2 and 5.4.3. We numerically checked that, for $i = 1, 2$, $F^2(x_P^{(i)}) = F(F(x_P^{(i)})) = x_P^{(i)}$.

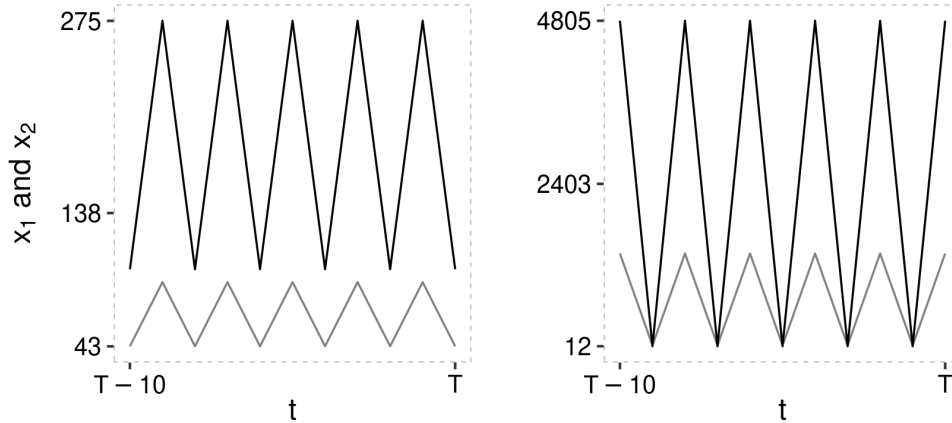


Figure 5.5: Simulated periodic dynamics of (5.4.1) for (left) $a_1 = 50$ and (right) $a_1 = 750$. We plot the last 10 out of $T = 500,000$ time steps. Here, dark grey is region 1 and black is region 2. In both simulations we let $a_2 = 0.4$, $b_1 = 0.04$, $b_2 = 0.01$, $r_{11} = 0.2$, $r_{22} = 0.3$, $r_{12} = 0.6$, $r_{21} = 0.7$, $k_{11} = k_{22} = k_{12} = k_{21} = 0.5$, $s_{11} = 10$, $s_{22} = 6$, $s_{12} = 3$ and $s_{21} = 12$. Initial conditions in both were $(x_1(0), x_2(0)) = (92, 103)$.

5.4.4. Positive Fixed Point Existence

Theorem 5.3.5 shows that $\rho(A(0)) > 1$ is sufficient for the existence of a positive fixed point for (5.2.3). We can numerically show that this is not necessary.

Example 5.4.4. Let $a_1 = 4$ and $a_2 = 0.9$. Further let all other parameters be as in Fig. 5.6. We can then observe that $\rho(A(0)) \approx 0.81 < 1$ but $(x_1^*, x_2^*) \approx (28.17, 9.52)$ is a positive equilibrium of this system (see also Fig. 5.6).

We simulated this system for 400 different positive initial conditions in Fig. 5.6. The results of this simulation suggest this equilibrium is unique and locally stable. We observed convergence to the extinction equilibrium when initial conditions were sufficiently close to the boundary of \mathbb{R}_+^2 . This behaviour is distinct to the dynamical behaviour in [156], as seen via Theorem 3.5.1. As mentioned above, the spectral radius dichotomy for stability does not, in general, hold for the model class we consider. However, when g_i and d_{ij} are decreasing with d_{ii} constant, we can ensure GAS for a positive equilibrium (Theorem 5.3.5).

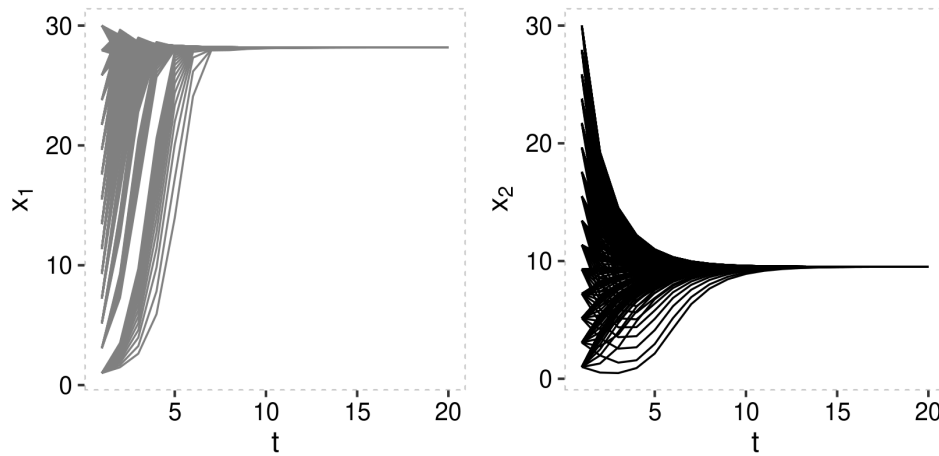


Figure 5.6: Simulations of (5.4.1) for various positive initial conditions $x(0) \in [1, 30]^2$, where dark grey (left) and black (right) trajectories respectively correspond to regions 1 and 2. We let $a_1 = 4$, $a_2 = 0.9$, $b_1 = 0.04$, $b_2 = 0.01$, $r_{12} = r_{21} = 0.1$, $r_{11} = r_{22} = 0.75$, $k_{12} = k_{21} = k_{11} = k_{22} = 1$ and $s_{12} = s_{21} = s_{11} = s_{22} = 1$. We increased the number of iterations for each plot to 100,000 to ensure convergence to the fixed point approximately given by $(x_1^*, x_2^*) \approx (28.17, 9.52)$.

5.4.5. The Total Population Size

In [93] the authors looked at how dispersal affects the total population before and after coupling. They demonstrated that for the specific planar systems with constant dispersal rates, dispersal can have varying effects on the overall population. We will now present two simple examples where one can observe analogous effects, when dispersal is nonlinear and asymmetric, and when regional maps come from different model classes. We will specifically look at the affects of source-sink and source-source dynamics.

5.4.5.1. Source-Sink

To give a simple demonstration of these effects in a source-sink context we will let $r = r_{12} = r_{21}$ vary in $(0, 0.5)$ and fix all other parameters. We also let d_{ii} to be constant, i.e. the proportion remaining in region i stays fixed over time. Note that a sufficient condition for (5.2.1) to hold in this context is that $r_{ij} \in (0, 0.5)$ for $i, j \in \{1, 2\}$, $i \neq j$. Let $a_1 = 65$, $a_2 = 0.4$ and $d_{11}(x) = d_{22}(x) \equiv 0.499$. Further let the remaining parameters be as in Fig. 5.6. We have that

$$A(0) = \begin{pmatrix} r_{11}a_1 & \frac{ra_2}{1 + \exp(k_{12}s_{12})} \\ \frac{ra_1}{1 + \exp(k_{21}s_{21})} & r_{22}a_2 \end{pmatrix},$$

which, for a given r , has characteristic polynomial approximately given by

$$\chi(\lambda) \approx (32.4 - \lambda)(0.2 - \lambda) - 1.9r^2.$$

By solving for λ in the above equation we can observe that $\rho(A(0)) \approx ra_1 \approx 32.4 > 1$ for all $r \in (0, 0.5)$. It follows from Theorem 5.3.6 that (5.2.3) is uniformly strongly persistent with respect to the total population size. Despite this, we can see from Fig. 5.7 that for certain values of r , dispersal can have an increasing, decreasing or neutral effect on the total population size.

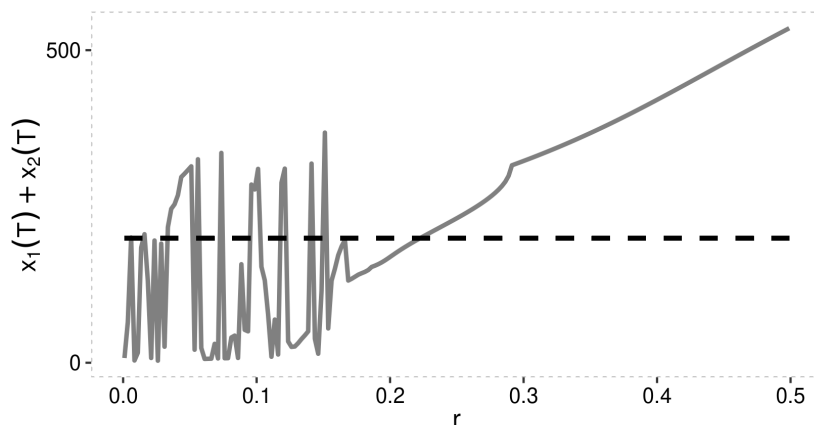


Figure 5.7: Plot of $x_1(T) + x_2(T)$ when patches are connected by dispersal (solid dark grey) and when isolated (dashed black) after $T = 10,000$ time steps. Initial conditions, $(x_1(0), x_2(0)) = (55, 54)$.

In our example we see from Fig. 5.7, that after some critical value, $r_c \approx 0.22$, increasing r has a monotonically increasing effect on the total population size. This may be due to some sort of population buffering, where increased dispersal may lead to greater overall population resilience. If a sink population faces environmental pressures, increasing the dispersal rate beyond some critical value may allow for quicker replenishment from the source patch, maintaining higher effective population sizes across the landscape. Note that while we know the population is uniformly strongly persistent, it is possible that the asymptotic time when this occurs may change when varying r . It is also possible that the persistence threshold ϵ changes when varying r .

5.4.5.2. Source-Source

We also conducted an analogous simulation for the case where both regions were sources (see Fig. 5.8). We kept the initial conditions and all parameters the same as in Fig. 5.7 and set $a_2 = 10$, i.e. region 2 is also a source. We can then see that, although a_1 is the same as in the previous source-sink case, when we connect two sources by dispersal we

can get that the total population size is always below that of the case where the regions are isolated, for identical initial conditions.

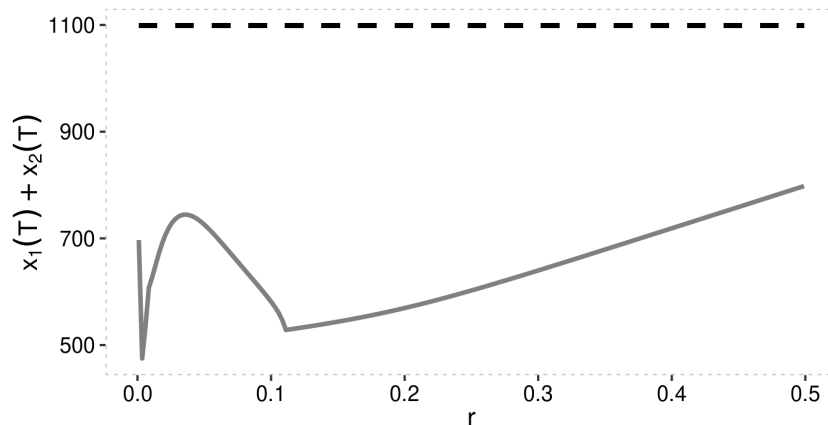


Figure 5.8: Plot of $x_1(T) + x_2(T)$ when two source regions are connected by dispersal (solid dark grey) and when isolated (dashed black) after $T = 10,000$ time steps. Initial conditions, $(x_1(0), x_2(0)) = (55, 54)$, were as in Fig. 5.7.

The importance of studying the effect of dispersal on the total population has been emphasised in [113] for planar systems, where each region was a source and dispersal was constant. We have demonstrated that, as did [93] for the case of constant dispersal, the manner in which two patches are connected can have varying effects on the total population size.

5.4.6. Bifurcation Analyses

In the above numerical simulations we observed that varying dispersal and regional parameter values can result in quite complex dynamical behaviour for trajectories of system (5.4.1). Therefore in order to briefly explore parameter sensitivity we will conclude this section by looking at single- and two-parameter bifurcation diagrams.

As $g_i(0) := a_i$ determines stability (of the extinction and/or positive equilibrium) on region i , we produced a two-parameter bifurcation diagram for a_1 and a_2 , to observe what range of dynamical behaviour can arise. Recall the ad-hoc informal description of chaos [258] given in Chapter 2. Fig. 5.9 shows an example of a numerical simulation of (5.4.1) with $a_1 = 90$ and $a_2 = 0.14$, and all other parameters as in Fig. 5.5. We simulated (5.4.1) for $T = 500,000$ time steps, while also numerically computing the number of unique values attained over $[0, T]$. This resulted in no observed periodic behaviour. We also tested if this aperiodicity is sensitive to choices in initial conditions. In particular, for various sufficiently small $\epsilon_i > 0$, initial conditions given by $(x_1(0), x_2(0)) = (131 \pm \epsilon_1, 19 \pm \epsilon_2)$, resulted in trajectories of (5.4.1) that enter a different aperiodic regime from those observed

in Fig. 5.9. These observations suggest that (5.4.1) may be capable of dynamical behaviour similar to that exhibited by chaotic systems.

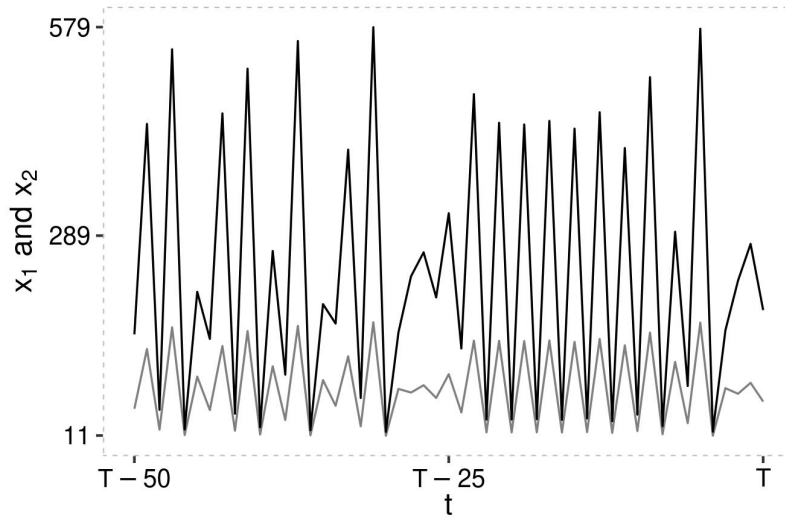


Figure 5.9: Simulated dynamics of (5.4.1) for the initial condition $(x_1(0), x_2(0)) = (131, 19)$, where black and dark grey trajectories respectively correspond to region 1 and 2, where $T = 500,000$. We let $a_1 = 90$, $a_2 = 0.14$, while all other parameters were as in Fig. 5.5. The last 50 time steps are plotted.

In order to produce a two-parameter bifurcation diagram for a_1 and a_2 , we considered the last 100 observations after 100,000 iterations (see Fig. 5.10). All other parameters were fixed as in Fig. 5.5. We produced bifurcation diagrams for various other initial conditions (different from the one in Fig. 5.5) and observed similar asymptotic behaviour. In Fig. 5.10 we let $a_1 \in (1, 300]$ and $a_2 \in (0, 1)$. The colour-number legend in Fig. 5.10 shows the period of the various periodic trajectories, with 1 representing convergence to a unique fixed point (either extinction or a positive equilibrium), and > 8 representing periods higher than 8 and possibly chaotic dynamics, as chosen also in [279]. In Fig. 5.10 we can observe that a large region of the (a_1, a_2) -parameter space consists of trajectories that either converge to a fixed point or enter period-2 periodic trajectories. For $a_2 \in (0, 0.28)$ we see a region where period-2 periodic trajectories emerge from chaotic type dynamics. For sufficiently low values of a_2 we see a portion of the (a_1, a_2) -plane where there is high sensitivity to changes in a_1 . One moves from period-2 periodic trajectories to regions of higher period and potentially chaotic regimes, followed by regions where trajectories converge to extinction for low enough a_2 . This diagram demonstrates the complexity that the model we consider can capture. That is, depending on the appropriate choice of both the dispersal and regional maps, deriving simple criteria for local/global stability of extinction or a positive equilibrium, in terms of a_1 and a_2 , is not so trivial.

We will now observe how varying a_i , with a_j fixed, for $i \neq j$, affects the asymptotic

dynamics of (5.4.1). We will do this by giving a single-parameter bifurcation plot for each a_i vs x_1 and x_2 . First let all parameters except a_1 and a_2 , be as in Fig. 5.5. Similar to Fig. 5.10, we considered the last 100 observations after 100,000 iterations. We first fix a_1 to a relatively low (Fig. 5.11 (left)) and high value (Fig. 5.11 (right)), while varying a_2 within $(0, 1)$. We set $(x_1(0), x_2(0)) = (20, 10)$. We produced single-parameter bifurcation diagrams for various other initial conditions and observed similar asymptotic behaviour. For $a_1 = 10$, Fig. 5.11 (left), we observed (stable) fixed point regimes for all values of a_2 in the interval $(0, 1)$. Once we increased a_1 to 100 for small a_2 we observe stability of the extinction equilibrium and then the appearance of *periodic windows*, where there was period halving bifurcations as a_2 increased. For all values of $a_2 > c_1 \approx 0.24$, we see the appearance of period-2 periodic trajectories. Thus for a low enough range of a_2 values and high enough a_1 we see chaotic-type dynamics. These then undergo a period-halving route to a (seemingly) locally stable period-2 solution.

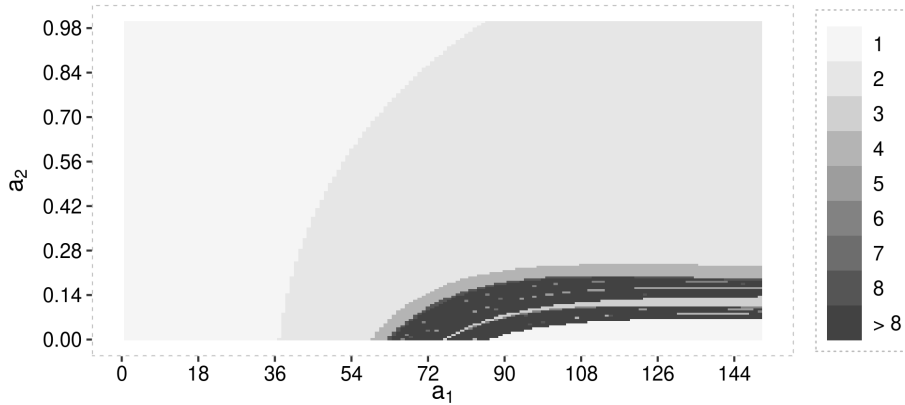


Figure 5.10: Bifurcation diagram for the (a_1, a_2) -plane where regions 1 and 2 were respectively given by Ricker and Hassel-1 maps, for $a_1 \in (1, 300]$, $a_2 \in (0, 1)$. Initial conditions were given by $(x_1(0), x_2(0)) = (131, 19)$. Other parameter values were as in Fig. 5.5. The colour-number legend shows the period of the various periodic trajectories (with periods 2-8), with 1 representing convergence to a unique fixed point (either extinction or a positive equilibrium), and > 8 representing periods higher than 8 and possibly chaotic dynamics. Parameter grid resolution was 150×150 .

We also fixed a_2 to a relatively low (Fig. 5.12 (left)) and high value (Fig. 5.12 (right)), while varying a_1 within $(1, 150)$. We set $(x_1(0), x_2(0)) = (20, 10)$, as in Fig. 5.11. In this case we observed significantly different behaviour than in Fig. 5.11. For $a_2 = 0.1$ we observed that extinction was stable for sufficiently small a_1 values, with a stable positive fixed point emerging, followed by the appearance of periodic windows. As a_1 increased toward 150 we observed period doubling bifurcations. We then enter a chaotic regime for large a_1 values where the dynamics become quite unpredictable. Once we increased a_2 to 0.9 we saw that for low enough values of a_1 extinction is stable, and for sufficiently large

values of a_1 less than $c_2 \approx 75$ we observe stability of a positive equilibrium followed by the emergence of a stable period-2 solution.

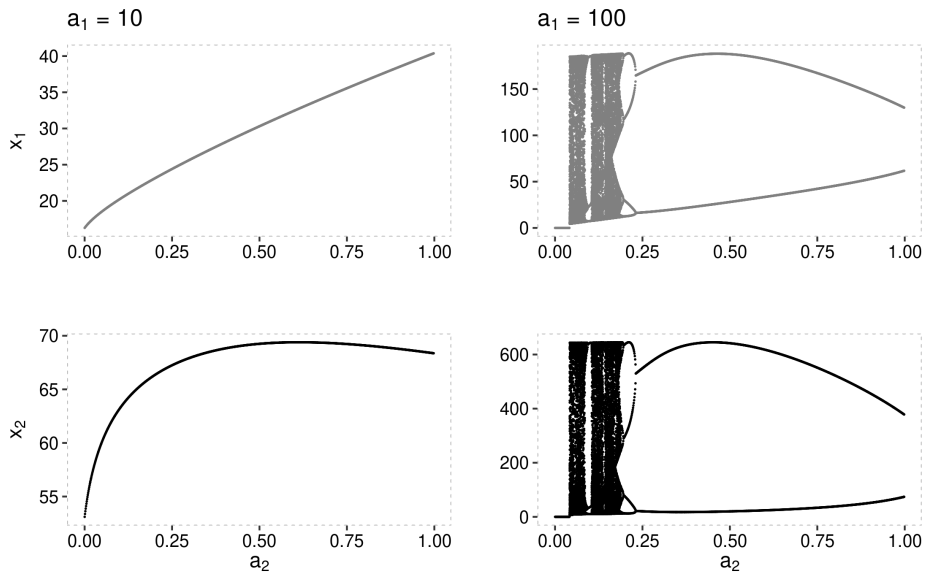


Figure 5.11: Bifurcation diagrams of $a_2 \in (0, 1)$ versus x_1 (dark grey) and x_2 (black), where regions 1 and 2 were respectively Ricker and Hassell-1 maps. We considered the last 100 observations after 10,000 iterations when (left) $a_1 = 10$ and (right) $a_1 = 100$. Initial conditions where $(x_1(0), x_2(0)) = (20, 10)$ for both scenarios.

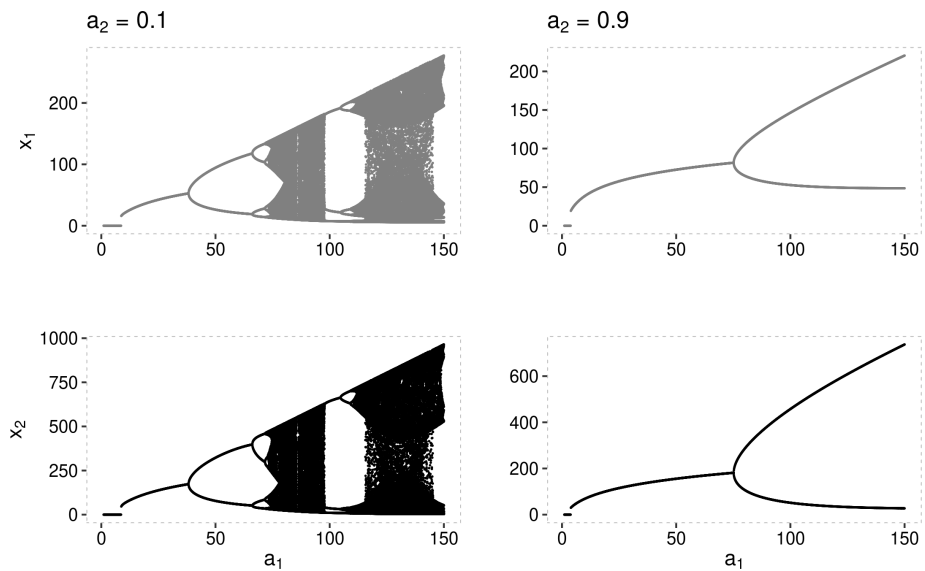


Figure 5.12: Bifurcation diagrams of $a_1 \in (1, 150)$ versus x_1 (dark grey) and x_2 (black), where regions 1 and 2 were respectively Ricker and Hassell-1 maps. We considered the last 100 observations after 10,000 iterations when (left) $a_2 = 0.1$ and (right) $a_2 = 0.9$. Initial conditions where $(x_1(0), x_2(0)) = (20, 10)$ in both scenarios.

5.5. Summary

Understanding the qualitative dynamics of sub-populations following coupling (via dispersal) is important for numerous ecological applications. In this chapter, we considered a nonlinear model of dispersal, giving sufficient conditions for the stability of the extinction equilibrium, uniform persistence, and the existence of a positive fixed point. We also briefly explored how our results, via numerical simulations and bifurcation diagrams, can be used to study the long term dynamics of populations dispersing between sources and sinks. Our numerical results show that introducing density-dependent dispersal can alter the asymptotic dynamics of a previously passive dispersal model. In particular, we observed both periodic dynamics and chaotic-type dynamics, which is different to the behaviour of the passive dispersal models that we mention throughout the chapter. We also saw that the existence of a positive fixed point is possible when $\rho(A(0)) < 1$, showing that $\rho(A(0)) > 1$ is not necessary for this fixed point to exist. We also conducted simulations to demonstrate the overall effect of density-dependent dispersal on the asymptotic total population size, showing that the way two patches are connected via dispersal is highly sensitive to changes in parameter values and choices in regional and dispersal maps. This is important for conservation management, if one wants to know how heterogeneous sub-populations can persist within a fragmented landscape.

6. Diffusive Stability and Growth for Populations with Demographic Structure

In this chapter, we propose a two-patch, discrete-time model of diffusive dispersal between populations with demographic structure. This accompanies the work in Chapters 4 and 5 by considering dispersal between populations that are partitioned into an arbitrarily finite number of compartments or classes, which can correspond to their life cycle, for example. We demonstrate the relation of the existence of various common Lyapunov functions to the global stability of the extinction equilibrium, which is robust to changes in diffusive couplings, what we call robust diffusive stability. Additionally, we explore the opposite scenario, so-called diffusive growth, where we are interested in finding specific diffusive couplings that lead to overall population growth. We apply our results to various matrix classes commonly utilised in structured population modelling. Finally we explore an additional model of stage-structured diffusion and state results related to matrices of Leslie and LPA form.

6.1. Motivation

As demonstrated in the Chapters 4 and 5, dispersal within a patchy environment has important consequences for both invasive species management and metapopulation conservation. Although we have discussed the importance of including density-dependent dispersal, we will now consider a different perspective on dispersal, namely linear diffusion between demographically-structured populations. Diffusion, or diffusive dispersal, means that, at a given time, dispersal/movement occurs from an area of high density to an area of low density. The model we propose in this chapter assumes that the strength of movement between classes is fixed over time, i.e. is passive diffusion. Although we have demonstrated that density-dependent dispersal is important for ecological dynamics, the model in this chapter we focus on a simpler scenario where movement between populations is based only on density gradients. This approach helps us study how diffusion affects the spatial dynamics of demographically-structured populations. The model we consider can describe, for example, migratory species that disperse along some resource or environmental gradient [143].

Individuals within a population transition through distinct developmental stages, as was

discussed in Chapter 3. They can also be partitioned into other demographic classes such as age, sex, kin groups and size. This motivates the use of demographically-structured population models, where individuals are partitioned into distinct compartments/groups [61, 62]. These groups may interact with one another, like for example if we split the populations into male and female. There also may be transitions between such groups corresponding to their life-cycle, like for example with juvenile and adult stages. This class of models in turn allows for the consideration of within-population variation that is common across many species. Knowledge of how the strength and mechanisms of dispersal within such patchy populations is important to consider in order to understand the effects of habitat fragmentation and biodiversity loss on vulnerable and endangered species exhibiting such demographic structure [23].

In this chapter, inspired by the work in [69], we consider a discrete-time linear model for the dynamics of demographically-structured populations subject to diffusive dispersal. In particular we want to investigate when diffusively coupled populations grow unbounded or decline to extinction. As demonstrated in the fundamental theorem of demography (see Chapter 3), this reduces to deriving sufficient conditions for $\rho(A) \diamond 1$, where $A \in \mathbb{R}_+^{n \times n}$ is the system matrix, describing interconnections between demographic classes, and \diamond is one of the relations $>$ or $<$. In this chapter we will derive conditions that ensure that two sink regions can be coupled to ensure that the resulting coupled system has a GAS extinction equilibrium, which is robust to changes in diffusive couplings. This then determines what assumptions are necessary for overall population growth, given that the population in each isolated region goes extinct in the long run. We will also consider the problem of finding diffusive couplings that result in such isolated sinks being coupled so that the overall population grows, what we call *diffusive growth*. Other authors have referred to such a phenomenon as *dispersal-driven growth* [114] or *dispersal-induced growth* [153].

We will first outline our general modelling framework. We will then discuss how common Lyapunov functions relate to robust diffusive stability, while also demonstrating our results using specific matrix classes as examples. Following this analytical work, we will then discuss some numerical examples related to the ecological application in question. In particular we will investigate scenarios involving so-called diffusive growth in this context. Finally we will discuss RDS in relation to an alternative model of diffusive dispersal when one considers common matrix classes used in ecology, such as Leslie matrices. Note that we do not provide numerical simulations in this chapter, as was done in Chapters 4 and 5 as the dynamics of the model we consider is linear. As we are interested in the stability/instability of the extinction equilibrium, the resulting numerical simulations will either show trajectories tending to 0 or tending to ∞ for all initial conditions.

6.2. The Diffusive Dispersal Model

Recall from Chapter 3 the model formulation of diffusively coupled systems as described in [69]. In this chapter we consider the simplest case of (3.4.4), where $m = 2$ and $C = \mathbb{R}_+^{2n}$. Let $A, B \in \mathbb{R}_+^{n \times n}$ be matrices respectively describing the linear population dynamics in two distinct regions, i.e. each isolated population's dynamics is governed by

$$\begin{aligned}x_1(t+1) &= Ax_1(t), \\x_2(t+1) &= Bx_2(t),\end{aligned}$$

where $x_i(0) \in \mathbb{R}^n$ for $i \in \{1, 2\}$. Denote by $\mathcal{D}_{A,B}$ the set of nonnegative diagonal matrices such that, for $D \in \mathcal{D}_{A,B}$, $A - D \geq 0$ and $B - D \geq 0$. Our diffusively coupled system is given by

$$\begin{aligned}x_1(t+1) &= Ax_1(t) + D(x_2(t) - x_1(t)), \\x_2(t+1) &= Bx_2(t) + D(x_1(t) - x_2(t)), \\(x_1(0)^T, x_2(0)^T)^T &\in \mathbb{R}_+^{2n},\end{aligned}\tag{6.2.1}$$

where $D \in \mathcal{D}_{A,B}$ (see Fig. 6.1). This can be thought of as a discrete-time, planar version of the continuous-time model of [69] and a special case of one of the models of [114]. By letting $x := (x_1^T \ x_2^T)^T \in \mathbb{R}_+^{2n}$, we can rewrite (6.2.1) as

$$\begin{aligned}x(t+1) &= Mx(t) \\M &:= \begin{pmatrix} A - D & D \\ D & B - D \end{pmatrix} \\x(0) &= x_0 \in \mathbb{R}_+^{2n}.\end{aligned}\tag{6.2.2}$$

The matrices in $\mathcal{D}_{A,B}$ can be interpreted as describing the diffusive dispersal of individuals between their respective demographic classes, where there is movement from high density to regions of low density. Note that the influx/outflux of individuals can be in different directions. For example, let $n = 2$, $D = \text{diag}(d_1, d_2) \in \mathcal{D}_{A,B}$ and $x_i := (x_{i,1} \ x_{i,2})^T \in \mathbb{R}_+^2$, $i \in \{1, 2\}$. The dispersal components as in (6.2.1), for $j \neq i$, are of the form

$$D(x_j - x_i) = \begin{pmatrix} d_1 & 0 \\ 0 & d_2 \end{pmatrix} \begin{pmatrix} x_{j,1} - x_{i,1} \\ x_{j,2} - x_{i,2} \end{pmatrix}.$$

For a given time, assume that $x_{j,1} > x_{i,1}$ and $x_{j,2} < x_{i,2}$. We would then have that at this instant there is a movement of individuals from region j to region i in the 1st group, while movement in the 2nd group is in the opposite direction. Note that the model we consider can be written as a linear-time invariant system, with system matrix M , it can be interpreted as modelling positive density dependence, as there is a diffusion of a demographic class

from regions of high density to regions of low density. As the diffusion matrices are fixed, we can additionally interpret this as being passive dispersal, where the density-dependence arises due to the difference in regional abundances, perhaps due to competitive effects or variability of resources. The dispersal components of our model are additive. One may also have multiplicative dispersal or diffusion (for example see [114]).

The diffusive dispersal of individuals within certain demographic classes, from areas of high density to areas of low density, can be understood through Charnov's so-called Marginal Value Theorem, which states that an individual should leave a resource patch when the marginal rate of return, i.e. the energy gained per unit of time spent in a patch, falls below the average rate of return across all patches in the environment [49]. In the context of optimal foraging theory, individuals may disperse from crowded or overpopulated areas in search of more favorable conditions [86]. Such behavior reflects the idea of optimising resource use, with organisms foraging for environments that provide the greatest benefits in terms of survival, reproduction, or resource availability for example. This interpretation is not restricted to the current diffusion model, but is an intuitive explanation of positive density-dependent dispersal, both in general and in the context of Chapters 4 and 5 for example.

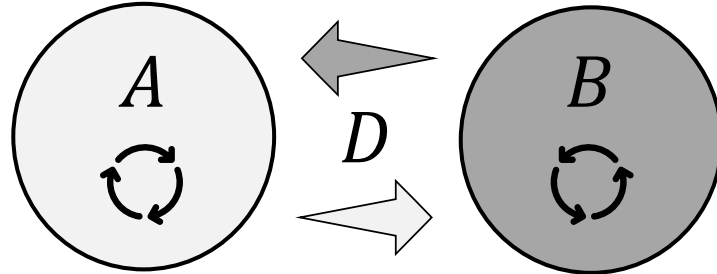


Figure 6.1: Conceptual diagram of system (6.2.1), where A and B describe the linear dynamics of each regional population and D describes the diffusive movement between each of the demographic classes.

If we assume both regions in question are sinks, i.e. both populations go extinct asymptotically, this is characterised mathematically in terms of the spectral radii of A and B as $\rho(A), \rho(B) < 1$. Our first goal is to investigate when these two regions can be coupled via diffusive dispersal such that the resulting system has a GAS extinction equilibrium for any choice of admissible coupling matrix. One may also ask: can we ensure that both these regions are rescued from global extinction, i.e. when do we get an unstable equilibrium for (6.2.1)? As noted in [69], instead of determining

"when destabilization occurs, one can try to restrict the classes of matrices

to which A and B belong to guarantee that the question can be answered affirmatively."

Thus we want to determine conditions on A and B such that $\rho(M) < 1$ for all $D \in \mathcal{D}_{A,B}$, what we will call *robust diffusive stability* (RDS).

The system we are interested in is composed of two linear time invariant (LTI) subsystems which are diffusively coupled. These LTI subsystems may be the result of the linearisation of a nonlinear model around some equilibrium or linearity may be an a priori assumption. The problem we consider is closely related to similar robust matrix stability problems, such as Turing instability and quiescent stability, as discussed in Chapter 3. Note that system (6.2.2) may also arise from linearisation of some nonlinear dispersal model around some equilibrium. Thus sufficient conditions for GAS of the extinction equilibrium for 6.2.2 are then sufficient for the LAS of the equilibrium in question for the nonlinear model.

In [69] the author studied a similar system to (6.2.2), albeit in continuous-time and for arbitrarily many finite subsystems defined on a proper cone. Similar models have been studied in both discrete and continuous time in [114], where the subsystems are restricted to \mathbb{R}_+^n (see Chapter 3). In both [69] and [114] the authors made use of common linear copositive Lyapunov functions to obtain sufficient conditions for the global stability of the extinction equilibrium in the coupled models they studied. We are interested in exploring how other types of common Lyapunov function can ensure RDS. Next we will discuss such ideas in the context of (6.2.2). All numerical examples were computed using MATLAB [142].

6.3. Common Lyapunov Functions

In this section we highlight how the existence of various types of common Lyapunov functions relate to RDS. We refer the reader to Chapter 2 for a more detailed description of the various types of Lyapunov function that arise when studying positive systems. First note that, given m linear time-invariant positive system matrices, $\mathcal{A} := \{A_1, \dots, A_m\} \subset \mathbb{R}_+^{n \times n}$, a Lyapunov function $L : \mathbb{R}^n \rightarrow \mathbb{R}$ is called a common Lyapunov function for \mathcal{A} if it is a Lyapunov function for each system with system matrix A_i , $i \in \{1, \dots, m\}$.

6.3.1. Copositive Lyapunov Functions

Note that, for $D \in \mathcal{D}_{A,B}$, we have that $A - D, B - D \geq 0$. One can then observe that $M \geq 0$ and so system (6.2.2) is positive. We will now state a result analogous to one given in [69] for continuous-time systems defined on proper cones.

Theorem 6.3.1. *Assume $A, B \in \mathbb{R}_+^{n \times n}$ are Schur. If there exists a common linear copositive Lyapunov function (CLCLF), $V(x) := v^T x$, for A and B , then M is Schur for all $D \in \mathcal{D}_{A,B}$.*

Therefore the existence of a CLCLF for A and B is sufficient for RDS. The next result we state is another simple sufficient condition for RDS.

Proposition 6.3.2. *Assume $A, B \in \mathbb{R}_+^{n \times n}$ are Schur. If there exists $v > 0$ such that $Av < v$ and $Bv < v$, then M is Schur for all $D \in \mathcal{D}_{A,B}$.*

Proof. Let diagonal $D \geq 0$ be arbitrary. As A and B are Schur, it follows from Lemma 2.2.2 that $Av = (A - D)v + Dv < v$ and $Bv = (B - D)v + Dv < v$. It is then easy to see that $My < y$ for $y := (v^T \ v^T)^T$. The result then follows from Lemma 2.2.2. \square

Recall that the induced l_∞ -norm of $L = (l_{ij}) \in \mathbb{R}^{n \times n}$ is given by $\|L\|_\infty := \max_{i \in \{1, \dots, n\}} \sum_{j=1}^n |l_{ij}|$ [137]. The next result immediately follows from Proposition 6.3.2.

Corollary 6.3.3. *Let $A, B \in \mathbb{R}_+^{n \times n}$. Assume that $\|A\|_\infty < 1$ and $\|B\|_\infty < 1$. Then M is Schur for all $D \in \mathcal{D}_{A,B}$.*

Proof. Recall that for $L \in \mathbb{R}^{n \times n}$, $\rho(L) \leq \|L\|$ for any induced matrix norm $\|\cdot\|$ on \mathbb{R}^n [137]. Therefore both A and B are Schur. Set $v = \mathbb{1}$ as in Proposition 6.3.2. \square

6.3.2. The Lyapunov Inequality

We will now state how the existence of a common diagonal solution to the Lyapunov inequality relates to RDS.

Theorem 6.3.4. *Let $A, B \in \mathbb{R}_+^{n \times n}$ be Schur. If there exists a $C = \text{diag}(c_1, \dots, c_n) > 0$ satisfying*

$$\begin{aligned} Q_A &:= (A - I)^T C + C(A - I) < 0, \\ Q_B &:= (B - I)^T C + C(B - I) < 0, \end{aligned}$$

then M is Schur for all $D \in \mathcal{D}_{A,B}$.

Proof. Let $D = \text{diag}(d_1, \dots, d_n) \in \mathcal{D}_{A,B}$ be arbitrary. We will show that $P := \text{diag}(C, C) > 0$ defines a diagonal solution to the Lyapunov inequality

$$Q_M := (M - I)^T P + P(M - I) < 0. \tag{6.3.1}$$

A simple calculation involving matrix multiplication yields

$$\begin{aligned} Q_M &= \begin{pmatrix} (A - I - D)^T C + C(A - I - D) & 2CD \\ 2CD & (B - I - D)^T C + C(B - I - D) \end{pmatrix} \\ &= \begin{pmatrix} Q_A - 2CD & 2CD \\ 2CD & Q_B - 2CD \end{pmatrix}. \end{aligned}$$

Define

$$G = (g_{ij}) := \begin{pmatrix} -2CD & 2CD \\ 2CD & -2CD \end{pmatrix}.$$

As C and D are diagonal, we have that $G = G^T$ and therefore its eigenvalues are all real. The i th diagonal entry of G is $-c_i d_i \leq 0$, while the only other non-zero entry in the i th row is $c_i d_i$. It follows from the Gershgorin Circle Theorem that the eigenvalues of G are real and negative [137]. As G is symmetric we have that $G \leq 0$. We also have that

$$Q_A, Q_B < 0 \implies Q := \begin{pmatrix} Q_A & 0 \\ 0 & Q_B \end{pmatrix} < 0.$$

We can then see that for $Q_M = Q + G$ and every $x \neq 0$ we have that

$$x^T Q_M x = x^T (Q + G)x = x^T Q x + x^T G x < 0$$

and so $Q_M < 0$. Therefore P is a diagonal Lyapunov function for $M - I$. It then follows from Theorem 2.2.6 that $M - I$ is Hurwitz. Therefore there exists $v > 0$ such that $(M - I)v < 0$. Then we have that $Mv < v$. It then follows from Theorem 2.2.5 that M is Schur. \square

Recall that an analagous result to the main result of [69] shows that A and B admitting a common linear copositive Lyapunov function, is sufficient for RDS. We will now show that one can find A and B that do not admit a common linear copositive Lyapunov function, but do satisfy the assumptions of Theorem 6.3.4.

Example 6.3.1. Consider

$$A = B^T = \begin{pmatrix} 0.1 & 1 \\ 0 & 0 \end{pmatrix}$$

Clearly A and B are Schur. Assume A and B admit a common linear copositive Lyapunov function $V(x) := w^T x$, where $w > 0$, i.e.

$$A^T w = \begin{pmatrix} 0.1w_1 \\ w_1 \end{pmatrix} < \begin{pmatrix} w_1 \\ w_2 \end{pmatrix}, B^T w = \begin{pmatrix} 0.1w_1 + w_2 \\ 0 \end{pmatrix} < \begin{pmatrix} w_1 \\ w_2 \end{pmatrix}.$$

This implies that $w_1 < w_2$. We then have that $0.1w_1 + w_2 < w_1 < w_2$. This then implies that $0.1w_1 < 0$, which is a contradiction. Hence A and B do not admit a CLCLF. One can show that

$$C = I \implies Q_A = Q_B = \begin{pmatrix} -1.8 & 1 \\ 1 & -2 \end{pmatrix} < 0$$

It then follows from Theorem 6.3.4 that M is Schur for all $D \in \mathcal{D}_{A,B}$.

In [191] the authors gave the following necessary and sufficient condition for the existence of a common diagonal Lyapunov function (CDLF) in continuous time for two positive matrices.

Theorem 6.3.5. [191] *Let $A, B \in \mathbb{R}^{n \times n}$ be Metzler and Hurwitz matrices with no zero entries. Then there exists a diagonal $P > 0$ satisfying*

$$\begin{aligned} A^T P + P A &< 0, \\ B^T P + P B &< 0, \end{aligned}$$

if and only if $A + C B C$ is non-singular for all diagonal $C > 0$.

Using Theorem 6.3.4 we can state the following sufficient condition for RDS.

Corollary 6.3.6. *Let $A, B \in \mathbb{R}_+^{n \times n}$ be Schur matrices such that $a_{ij}, b_{ij} \neq 1$ for all $i, j \in \{1, \dots, n\}$. If $A - I + C(B - I)C$ is non-singular for all diagonal $C > 0$, then M is Schur for all $D \in \mathcal{D}_{A,B}$.*

Proof. As $A = (a_{ij})$ and $B = (b_{ij})$ are Schur and $a_{ij}, b_{ij} \neq 1$ for all $i, j \in \{1, \dots, n\}$, this implies that $A - I$ and $B - I$ are Hurwitz and have no zero entries. It follows from Theorem 6.3.5 that there exists diagonal $P > 0$ satisfying

$$\begin{aligned} (A - I)^T P + P(A - I) &< 0, \\ (B - I)^T P + P(B - I) &< 0. \end{aligned}$$

The result then follows from Theorem 6.3.4. □

6.3.3. Quadratic Lyapunov Functions

In [114] the authors asked: does the existence of a common quadratic Lyapunov function (CQLF) imply that their coupled system has globally stable zero equilibrium? Formally the question asks does the existence of $C > 0$ that satisfies the Stein inequalities

$$\begin{aligned} A^T C A - C &< 0, \\ B^T C B - C &< 0 \end{aligned} \tag{6.3.2}$$

imply that their coupled system matrix is Schur for any feasible coupling? They provided a counterexample to show that this was not true for the system class considered in [114]. However, this is not a counterexample if we ask the same question for the system described by (6.2.2). We can demonstrate, with a different example, that the existence of a common quadratic Lyapunov function for A and B is indeed not sufficient for RDS.

Example 6.3.2. Consider

$$A = \begin{pmatrix} 0.260 & 0.572 & 0.5910 \\ 0.134 & 0.597 & 0.377 \\ 0.195 & 0.055 & 0.493 \end{pmatrix}, B = \begin{pmatrix} 0.563 & 0.150 & 0.323 \\ 0.048 & 0.132 & 0.156 \\ 0.575 & 0.066 & 0.503 \end{pmatrix},$$

and

$$C = \begin{pmatrix} 2.7094 & -2.2095 & -1.3574 \\ -2.2095 & 2.2726 & 1.5634 \\ -1.3574 & 1.5634 & 1.2748 \end{pmatrix}.$$

It can be verified numerically that the eigenvalues of C are positive, so $C > 0$. One can also verify that (6.3.2) holds. Thus $C > 0$ defines a CQLF for A and B . By letting $D = \text{diag}(0.131, 0.066, 0.247)$, we can then compute $\rho(M) \approx 1.001 > 1$. Thus, the system is not robustly diffusively stable even though A and B admit a common solution to the Stein inequality.

6.3.4. Diagonal Lyapunov Functions

Up to now we have shown how the Lyapunov inequality and common quadratic Lyapunov functions relate to RDS. The Lyapunov inequality arises in continuous-time linear systems analysis. An analogous equation in discrete time is the Stein inequality. Recall from Chapter 2 that a solution to the Stein inequality can be used to define a quadratic Lyapunov function (QLF) for a linear time-invariant system. In Example 6.3.2 we saw that the existence of a CQLF for A and B is not sufficient for RDS. This then motivates us to restrict the class of Lyapunov function and therefore to look at diagonal Lyapunov functions. We will next show that the existence of a CDLF for A and B is in fact sufficient for RDS.

Theorem 6.3.7. *Let $A, B \in \mathbb{R}_+^{n \times n}$ be Schur. If there exists a diagonal $C > 0$ satisfying*

$$\begin{aligned} A^T C A - C &< 0, \\ B^T C B - C &< 0, \end{aligned}$$

then M is Schur for all $D \in \mathcal{D}_{A,B}$.

Proof. Suppose $C > 0$ is a diagonal solution of

$$A^T C A - C < 0. \quad (6.3.3)$$

By adding and subtracting CA on the LHS in (6.3.3), we can see that

$$\begin{aligned} A^T C A - C &= (A - I)^T C A + C A - C \\ &= (A - I)^T C A + C(A - I). \end{aligned} \quad (6.3.4)$$

By adding and subtracting $(A - I)^T C$ on the RHS of (6.3.4) to see that

$$(A - I)^T C A + C(A - I) = (A - I)^T C + C(A - I) + (A - I)^T C(A - I). \quad (6.3.5)$$

It then follows from (6.3.4) and (6.3.5) that

$$A^T C A - C = (A - I)^T C + C(A - I) + (A - I)^T C(A - I). \quad (6.3.6)$$

As A is Schur we have that $A - I$ is invertible. Therefore, as $C > 0$, we have that $(A - I)^T C(A - I) > 0$. It follows from (6.3.6) that

$$A^T C A - C < 0 \implies (A - I)^T C + C(A - I) < 0.$$

Using an analogous argument we can show that

$$B^T C B - C < 0 \implies (B - I)^T C + C(B - I) < 0.$$

Therefore it follows from Theorem 6.3.4 that M is Schur for all $D \in \mathcal{D}_{A,B}$. \square

It is well known that the existence of solutions to the Lyapunov and Stein inequalities are linked via the Cayley transform, as discussed in Chapter 3. We can see in the proof of Theorem 6.3.7 that the existence of a common solution to the Stein inequality for A and B implies that there exists a common solution to the Lyapunov inequality for $A - I$ and $B - I$. Together these observations motivate us to investigate if the converse holds, i.e. are the two sufficient conditions for RDS in Theorems 6.3.4 and 6.3.7 equivalent? This is in general not true, as we can demonstrate with an example. Before we do so, we will need the following result which gives a sufficient condition for the non-existence of a common solution to the Stein inequality.

Theorem 6.3.8. *Let $A, B \in \mathbb{R}^{n \times n}$. If there exists nonzero $Y_1, Y_2 \geq 0$ such that*

$$A Y_1 A^T - Y_1 + B Y_2 B^T - Y_2 \geq 0,$$

then there does not exist a common solution to the Stein inequality, i.e. there does not exist $P > 0$ such that

$$\begin{aligned} A^T P A - P &< 0, \\ B^T P B - P &< 0. \end{aligned} \quad (6.3.7)$$

Proof. Let $S_n \subset \mathbb{R}^{n \times n}$ denote the set of symmetric matrices, $S_n^+ \subset S_n$ the set of positive semi-definite matrices and $\text{Int}(S_n^+)$ the set of positive definite matrices. Given $X \in \mathbb{R}^{n \times n}$, define $L_A(X) = A^T X A - X$ and $L_B(X) = B^T X B - X$. Then L_A and L_B map from S_n to S_n . The *Hilbert-Schmidt inner product* on S_n is defined as $\langle A, B \rangle = \text{Tr}(AB)$ [137]. The adjoint mapping of L_A (L_B) with respect to $\langle \cdot, \cdot \rangle$ on S_n is given by $L_A^*(X) = AXA^T - X$ ($L_B^*(X) = BXB^T - X$). To see this, note that

$$\begin{aligned} \langle X, L_A(Y) \rangle &= \text{Tr}(XA^T Y A - XY) \\ &= \text{Tr}(AXA^T Y - XY) \\ &= \langle AXA^T - X, Y \rangle, \end{aligned}$$

where we use the fact that the trace is linear and for $A, B \in \mathbb{R}^{n \times n}$ we have that $\text{Tr}(AB) = \text{Tr}(BA)$.

We prove our result by contradiction. It is well known that S_+^n is self-dual, i.e. $(S_+^n)^* = S_+^n$, and so $\text{Int}((S_+^n)^*) = \text{Int}(S_+^n)$ (see Example 2.24 of [35]). Therefore for $X \in \text{Int}(S_+^n)$ and nonzero $Z \in S_+^n$, we have that $\langle X, Z \rangle > 0$. Suppose there exists $Y_1, Y_2 \geq 0$, with at least one nonzero, such that $L_A^*(Y_1) + L_B^*(Y_2) \geq 0$ and there exists $X > 0$ such that $L_A(X) < 0$ and $L_B(X) < 0$. Therefore we have that

$$L_A^*(Y_1) + L_B^*(Y_2) = AY_1A^T - Y_1 + BY_2B^T - Y_2 \geq 0.$$

We know at least one of Y_1, Y_2 is non-zero and we are assuming that both $L_A(X) < 0$ and $L_B(X) < 0$. This implies that

$$\langle L_A(X), Y_1 \rangle + \langle L_B(X), Y_2 \rangle < 0.$$

This then implies that

$$\langle X, L_A^*(Y_1) + L_B^*(Y_2) \rangle < 0. \quad (6.3.8)$$

We then have that (6.3.8) contradicts the assumption that $L_A^*(Y_1) + L_B^*(Y_2) \geq 0$. \square

Using Theorem 6.3.8 we can show that the existence of a common solution to the Lyapunov inequality (for $A - I$ and $B - I$) does not imply that there is a common solution to the Stein inequality (for A and B).

Example 6.3.3. Consider

$$A = \begin{pmatrix} 0.622 & 1.114 \\ 0.164 & 0.295 \end{pmatrix}, B = \begin{pmatrix} 0.283 & 0.164 \\ 0.766 & 0.223 \end{pmatrix},$$

and $C = \text{diag}(1.049, 2.233)$. One can show that

$$(A - I)^T C + C(A - I) \approx \begin{pmatrix} -0.793 & 1.535 \\ 1.535 & -3.149 \end{pmatrix} < 0,$$

$$(B - I)^T C + C(B - I) \approx \begin{pmatrix} -1.504 & 1.883 \\ 1.883 & -3.470 \end{pmatrix} < 0.$$

Consider the positive definite matrices

$$Y_1 = \begin{pmatrix} 51.054 & 39.958 \\ 39.958 & 43.663 \end{pmatrix} \text{ and } Y_2 = \begin{pmatrix} 74.859 & 13.410 \\ 13.410 & 8.557 \end{pmatrix}.$$

One can then verify that

$$AY_1A^T - Y_1 + BY_2B^T - Y_2 = \begin{pmatrix} 10.869 & -0.107 \\ -0.107 & 5.750 \end{pmatrix} > 0.$$

It follows from Theorem 6.3.8 that there cannot exist a common quadratic solution to (6.3.7), which in turn shows that there cannot exist a common diagonal solution to (6.3.7).

We saw that the existence of a CQLF for A and B is not sufficient for RDS. Theorem 6.3.7 shows that the existence of a CDLF for A and B is sufficient for RDS. This sufficient condition, along with that in Theorem 6.3.4 together provide two distinct sufficient conditions for RDS, as demonstrated using Example 6.3.3. In fact the condition in Theorem 6.3.4 is a weaker assumption, as it implies that there exists a common diagonal solution to the Stein inequality for A and B . Therefore the result of Theorem 6.3.4 is stronger.

If we considered a continuous-time version of (6.2.1), then if A and B are both Metzler and Hurwitz, this would correspond to each isolated system being positive and having a globally stable extinction equilibrium. In this case, as noted in Chapter 3, the set of matrices that act diffusively on \mathbb{R}_+^n are diagonal Metzler matrices. RDS in this continuous time case corresponds to M being Hurwitz for all diagonal $D > 0$. It can be shown that in this continuous-time case, the existence of a CQLF for A and B , is not sufficient for RDS. However, the existence of a CDLF for A and B is sufficient for RDS, the proof of which is the same as that of Theorem 6.3.4, albeit replacing $A - I$ and $B - I$ respectively with A and B in Q_A and Q_B . Therefore we can conclude that in both discrete and continuous time, the existence of a common diagonal Lyapunov function for A and B is sufficient for RDS.

Next, we will look at some applications of Theorem 6.3.4.

6.4. Applications

To demonstrate the applicability of Theorem 6.3.4 we will now show how it relates to specific classes of matrices that may arise when looking at stage-structured population dynamics and provide some ecological interpretations of these results.

One well studied class of matrices are commuting matrices. The matrices $A, B \in \mathbb{R}^{n \times n}$ are said to *commute* if $AB = BA$. To demonstrate the applicability of Theorem 6.3.4 we will first show that if two Schur matrices commute, then we can ensure RDS.

6.4.1. Commuting Matrices

Proposition 6.4.1. *Let $A, B \in \mathbb{R}_+^{n \times n}$ be Schur. If $AB = BA$, then M is Schur for all $D \in \mathcal{D}_{A,B}$.*

Proof. First observe that

$$AB = BA \iff (A - I)(B - I) = (B - I)(A - I).$$

As A and B are Schur, we have that $A - I$ and $B - I$ are Hurwitz. It follows from Theorem 2.2.6 that $(A - I)^{-1} \leq 0$ and $(B - I)^{-1} \leq 0$. By definition we have that

$$\det(A) \neq 0 \iff \text{rank}(A) = n. \quad (6.4.1)$$

Therefore as $A - I$ is Hurwitz we have that $\det(A - I) \neq 0$. Therefore $A - I$, and similarly $B - I$, has no all zero rows or columns. Choose some $x > 0$. We then have that

$$x > 0 \implies y := (A - I)^{-1}(B - I)^{-1}x > 0,$$

as $(A - I)^{-1}(B - I)^{-1} \geq 0$. We can then see that

$$(A - I)y = (B - I)^{-1}x < 0.$$

We also have that $(A - I)(B - I) = (B - I)(A - I)$ implies that

$$\begin{aligned} (B - I)y &= (B - I)(A - I)^{-1}(B - I)^{-1}x \\ &= (A - I)^{-1}(B - I)(B - I)^{-1}x \\ &= (A - I)^{-1}x < 0. \end{aligned}$$

The result follows from Proposition 6.3.2. □

Note that we could simply prove Proposition 6.4.1 using Lemma 9.6 of [162], which can be used to show that any finite set of matrices that commute pairwise admit a CLCLF. However, in our proof of Proposition 6.4.1 we show how one can construct a CLCLF for A^T and B^T . A simple consequence of this result is contained in the following Corollary. For $A \in \mathbb{R}^{n \times n}$, A is circulant if it is of the form $A = \sum_{k=0}^{n-1} a_{k+1} C_n^k$, where $a_1, \dots, a_n \in \mathbb{R}$ and

$$C_n := \begin{pmatrix} 0 & I \\ 1 & 0 \end{pmatrix} \in \mathbb{R}^{n \times n}.$$

Corollary 6.4.2. *Let $A, B \in \mathbb{R}_+^{n \times n}$ be Schur. Further assume that one of the following hold:*

1. *A and B are circulant.*
2. *A and B are simultaneously diagonalisable.*

Then M is Schur for all $D \in \mathcal{D}_{A,B}$.

Proof. The first statement follows from the well-known fact that circulant matrices commute [137]. The second statement follows from the other well-known fact that if two matrices are simultaneously diagonalisable then they commute [137]. In either case the result follows from Proposition 6.4.1. \square

We now present an example that demonstrates the ecological applicability of Corollary 6.4.2.

Example 6.4.1. Consider A and B of the form

$$U = \begin{pmatrix} u_1 & 0 & u_2 \\ u_2 & u_1 & 0 \\ 0 & u_2 & u_1 \end{pmatrix}, \quad (6.4.2)$$

where $u_1, u_2 \in (0, 1)$ are such that $u_1 + u_2 < 1$. The matrix U is a special case of an *Usher matrix*, which are commonly used in size-structured population models [61]. Populations structured by size include many fish and tree species, where such populations are partitioned into size classes that may correspond to developmental stages or sex, which in many cases can be easier to measure than age/stage characteristics in field studies [163, 189]. The matrix U is circulant. We can also compute

$$\sigma(U) = \left\{ u_1 + u_2, \frac{2u_1 - u_2 \pm i\sqrt{3}u_2}{2} \right\}.$$

It is easy to see that

$$x^2 + y^2 - xy < \sqrt{x^2 + y^2 - xy} < x + y \quad \forall x, y \in (0, 1).$$

We can also observe that

$$\left| \frac{2u_1 - u_2 \pm i\sqrt{3}u_2}{2} \right| = \sqrt{u_1^2 + u_2^2 - u_1u_2}.$$

These observations in turn imply that $\rho(U) = u_1 + u_2 < 1$. Note that this more easily follows from the fact that $\rho(U) \leq \|U\|_\infty = u_1 + u_2$. A and B are of the form (6.4.2), and so are both Schur and circulant. It then follows from Corollary 6.4.2 that M is Schur for all $D \in \mathcal{D}_{A,B}$.

We will next state a sufficient condition for RDS for the case when $n = 2$.

6.4.2. Planar Systems

Proposition 6.4.3. *Let $A = (a_{ij}), B = (b_{ij}) \in \mathbb{R}_+^{2 \times 2}$ be Schur. Assume that $a := a_{11} = a_{22}$ and $b := b_{11} = b_{22}$, $(a - 1)^2 - (a_{12} + a_{21})^2 > 0$ and $(b - 1)^2 - (b_{12} + b_{21})^2 > 0$. Then M is Schur for all $D \in \mathcal{D}_{A,B}$.*

Proof. First note that A and B are of Toeplitz form, i.e. have constant diagonal terms [137]. If $a_{12} = a_{21}$ and $b_{12} = b_{21}$, then A and B are both symmetric and circulant. The result then follows from Corollary 6.4.2. Therefore assume that $a_{12} \neq a_{21}$ and $b_{12} \neq b_{21}$. Let $p > 0$, $P = pI$ and

$$Q_A := (A - I)^T P + P(A - I)$$

$$Q_B := (B - I)^T P + P(B - I)$$

By direct calculation one can show that both Q_A and Q_B are Metzler (also see Lemma 3.1. of [191]). We can then see that $S \in \mathbb{R}^{n \times n}$ is Hurwitz if and only if $\det(S) > 0$ and $\text{Tr}(S) < 0$. As A and B are Toeplitz, it follows from (a) and (b) that

$$\det(Q_A) = p^2(4(a - 1)^2 - (a_{12} + a_{21})^2) > 0,$$

$$\det(Q_B) = p^2(4(b - 1)^2 - (b_{12} + b_{21})^2) > 0.$$

As $p > 0$ and $a, b < 0$, we have that $\text{Tr}(Q_1) = 4pa < 0$ and $\text{Tr}(Q_2) = 4pb < 0$. Therefore Q_k is Hurwitz. We also have that Q_A and Q_B being symmetric implies that $Q_A, Q_B < 0$. The result follows from Theorem 6.3.4. \square

Note that in Proposition 6.4.3 not only do we get RDS, but we can see from the proof that 2×2 matrices that are Toeplitz and Schur admit a CDLF given by pI for any $p > 0$. We will now demonstrate the ecological applicability of Proposition 6.4.3.

Example 6.4.2. Consider a coupled two-patch population, where each of the patch sub-populations is partitioned into two age classes, where individuals can transition back and forth between these two given age classes. Let

$$A = \begin{pmatrix} 0.48 & 0.14 \\ 0.12 & 0.48 \end{pmatrix} \text{ and } B = \begin{pmatrix} 0.59 & 0.09 \\ 0.13 & 0.59 \end{pmatrix}$$

One could respectively interpret $a_{11} = a_{22} = a = 0.48$ and $b_{11} = b_{22} = b = 0.59$ as identical intrinsic growth rates or fecundity of each sub-population stage class on patches 1 and 2. One can also interpret a_{ij} and b_{ij} , with $i \in \{1, 2\}$ $i \neq j$, as asymmetric transition rates. We could justify the identical growth rates on each patch by assuming the patches are similar in resource allocation. We can also assume, for simplicity, that these species are living in a closed ecosystem, such as a laboratory environment for example, and so their growth rates can be controlled. This could possibly describe a cnidarian species, such as jellyfish, sea anemones or corals, for example [224]. This species has two age classes, namely the polyp and medusa reproductive ages, which transition between these age classes through what is known as *ontogeny reversal*. We can see that A and B are Toeplitz and Schur. We also have that

$$\begin{aligned} (a - 1)^2 - (a_{12} + a_{21})^2 &= 0.2028 > 0, \\ (b - 1)^2 - (b_{12} + b_{21})^2 &= 0.1197 > 0. \end{aligned}$$

Therefore by Proposition 6.4.3, we have that M is Schur for all $D \in \mathcal{D}_{A,B}$. Therefore in this case, when each demographic class on their respective patch has identical growth rates, with asymmetric transition rates between these classes, we get that diffusive dispersal cannot rescue such declining patches from extinction, under the technical assumptions that $(a - 1)^2 - (a_{12} + a_{21})^2 > 0$ and $(b - 1)^2 - (b_{12} + b_{21})^2 > 0$.

6.5. Diffusive Growth

In previous sections we investigated when the extinction equilibrium of (6.2.2) was GAS for all feasible diffusive couplings, otherwise known as robust diffusive stability. We will now numerically explore the situation when, given that $\rho(A) < 1$ and $\rho(B) < 1$, one can find a diagonal $D \in \mathcal{D}_{A,B}$ $\rho(M) > 1$, what we will call *diffusive growth*, i.e. the extinction equilibrium of (6.2.1) is unstable. This, in the context of demographically-structured populations, corresponds to finding certain diffusive couplings that result in two sink

populations being connected such that overall population growth across the two patches is observed. This concept has been discussed recently for continuous time models in [153, 22] and for discrete-time, stage-structured population models in [114], where it referred to as dispersal-induced growth or dispersal-driven growth. This is a similar concept to the rescue effect, as discussed briefly in Chapter 4, where a declining populations is connected via dispersal to a growing population in order to prevent overall extinction. For diffusive growth however, we are assuming that both patches are sinks. Diffusive growth is particularly relevant if, for example, one was interested in conserving migratory species or constructing ecological corridors [148, 252, 143].

6.5.1. Convex Hull

The convex hull arises frequently when investigating stability in control and systems analysis, and has recently been of interest in relation to stage-structured population models [127, 48]. We will say that the convex hull of A and B , $\{\alpha A + (1 - \alpha)B : \alpha \in (0, 1)\}$, is unstable if $\rho(\alpha A + (1 - \alpha)B) \geq 1$ for some $\alpha \in (0, 1)$.

The existence of a common linear, diagonal, or quadratic Lyapunov function all imply that the convex hull of A and B consists only of Schur matrices. In fact, it can be shown that this is the case for any convex common Lyapunov function [174]. Given the link between common Lyapunov function existence and diffusive growth (or the opposite, RDS), as discussed in previous sections of this chapter, these considerations lead us to investigate the relationship between diffusive growth and the existence of an unstable convex hull. Before we investigate diffusive growth, we first state a result on the potential instability of the convex hull of two Schur matrices.

Proposition 6.5.1. *Let $A, B \in \mathbb{R}_+^{n \times n}$ be Schur. Then TFAE:*

- (a) *there exists $\alpha \in (0, 1)$ such that $\rho(\alpha A + (1 - \alpha)B) \geq 1$.*
- (b) *$(A - I)(B - I)^{-1}$ has a negative real eigenvalue.*
- (c) *$A - I + \gamma(B - I)$ is singular for some $\gamma > 0$.*
- (d) *$A - I + \gamma(B - I)$ is not Hurwitz for some $\gamma > 0$.*

Proof. Let $\hat{A} := A - I$ and $\hat{B} := B - I$.

(a) \iff (b). As A and B are Schur, and $\rho(\cdot)$ is a continuous function of its matrix argument elements, (a) is equivalent to the existence of some $\gamma \in (0, 1)$ such that $\rho(\gamma A +$

$(1 - \gamma)B) = 1$. For such a γ let $C = \gamma\hat{A} + (1 - \gamma)\hat{B}$. We can observe that C is Metzler. It then follows that $0 \in \sigma(C)$. We then have that

$$\det(C) = 0 \iff \det(\gamma\hat{A} + (1 - \gamma)\hat{B}) = 0.$$

\hat{B} is Hurwitz and so $\det(\hat{B}) \neq 0$. Therefore

$$\begin{aligned} \det(\gamma\hat{A} + (1 - \gamma)\hat{B}) = 0 &\iff \det(\gamma\hat{A}\hat{B}^{-1} + (1 - \gamma)I) \det(\hat{B}) = 0 \\ &\iff \det\left(\hat{A}\hat{B}^{-1} + \frac{(1 - \gamma)}{\gamma}I\right) = 0. \end{aligned}$$

It is then immediate that $\mu(C) = 0$ if and only if

$$0 > \frac{\gamma - 1}{\gamma} \in \sigma(\hat{A}\hat{B}^{-1}).$$

(b) \iff (c) \iff (d): Proof as in [191]. \square

Using the above result we can now show that the existence of an unstable convex hull can correspond to diffusive growth.

Example 6.5.1. Consider

$$A = \begin{pmatrix} 0.74 & 0.20 \\ 0.40 & 0.67 \end{pmatrix} \text{ and } B = \begin{pmatrix} 0.73 & 0.08 \\ 0.87 & 0.73 \end{pmatrix}.$$

We can compute that $\rho(A) \approx \rho(B) \approx 0.99$. Therefore A and B are both Schur. One can also verify that $-14.0262 \in \sigma((A - I)(B - I)^{-1})$. It follows from Proposition 6.5.1 that there exists $\alpha \in (0, 1)$ such that $\rho(\alpha A + (1 - \alpha)B) \geq 1$. Therefore it follows that there exists no common Lyapunov function of any type for A and B . We can also see that for $D = \text{diag}(0.73, 0.67)$ one has $\rho(M) \approx 1.009 > 1$.

The fact that it is possible to have diffusive growth when there is an unstable convex combination is not really surprising. However, a natural next question to ask is: for every $\{A, B\} \subset \mathbb{R}_+^{n \times n}$ such that A and B are Schur and there exists $\alpha \in (0, 1)$ such that $\rho(\alpha A + (1 - \alpha)B) \geq 1$, does there exist a $D \in \mathcal{D}_{A,B}$ such that $\rho(M) > 1$, i.e. does the existence of an unstable convex combination of A and B imply diffusive growth? The answer to this is in fact no, as we can demonstrate with a simple example. First we state the following characterisation of Hurwitz stability, as proved more generally in [79]. Let $P, S, R, Q \in \mathbb{R}^{n \times n}$. Further let

$$\Gamma := \begin{pmatrix} P & Q \\ R & S \end{pmatrix}. \tag{6.5.1}$$

The *Schur complement* of Γ with respect to P (resp. S) is defined as $\Gamma \setminus P := S - RP^{-1}Q$ (resp. $\Gamma \setminus S := P - RS^{-1}Q$), provided that P^{-1} (resp. S^{-1}) exists [137].

Proposition 6.5.2. [79] Let $P, S \in \mathbb{R}^{n \times n}$ be Metzler and let $R, Q \in \mathbb{R}_+^{n \times n}$. Let Γ be of the form (6.5.1). Then TFAE:

1. The Metzler matrix Γ is Hurwitz.
2. P is Hurwitz and $\Gamma \setminus P$ is Metzler and Hurwitz.
3. S is Hurwitz and $\Gamma \setminus S$ is Metzler and Hurwitz.

We can now show that there exists Schur $A, B \in \mathbb{R}_+^{n \times n}$ and $\alpha \in (0, 1)$ such that $\rho(\alpha A + (1 - \alpha)B) > 1$, but $\rho(M) < 1$ for all diagonal $D \in \mathcal{D}_{A,B}$.

Example 6.5.2. Consider

$$A = \begin{pmatrix} 0.4 & 0.76 \\ 0.78 & 0 \end{pmatrix} \text{ and } B = \begin{pmatrix} 0.5 & 0.45 \\ 1.01 & 0.07 \end{pmatrix}.$$

We can compute that $\rho(A) \approx \rho(B) \approx 0.99$ and verify that $-5.6501 \in \sigma((A - I)(B - I)^{-1})$. It follows from Proposition 6.5.1 that there exists $\alpha \in (0, 1)$ such that $\rho(\alpha A + (1 - \alpha)B) \geq 1$. Therefore it follows that there exists no common Lyapunov function of any type. As both $A - D \geq 0$ and $B - D \geq 0$, we have that $D = \text{diag}(d_1, 0)$ for $d_1 \in [0, 0.4]$. We therefore have that

$$M - I = \begin{pmatrix} -0.6 - d_1 & 0.76 & d_1 & 0 \\ 0.78 & -1 & 0 & 0 \\ d_1 & 0 & -0.5 - d_1 & 0.45 \\ 0 & 0 & 1.01 & -0.93 \end{pmatrix}.$$

The Schur complement of $M - I$ with respect to $B - I - D$ is

$$(M - I) \setminus (B - I - D) = S := B - I - D - D(A - I - D)^{-1}D.$$

Observe that $M - I$ is Metzler. $B - I - D$ is Metzler and as $A - D$ is Hurwitz, we have that $(A - D)^{-1} \leq 0$. Therefore

$$-D(A - I - D)^{-1}D \geq 0,$$

which implies that S is also Metzler. We can compute that

$$\begin{aligned} S &= \begin{pmatrix} -0.5 - d_1 & 0.45 \\ 1.01 & -0.93 \end{pmatrix} - \begin{pmatrix} d_1 & 0 \\ 0 & 0 \end{pmatrix} \begin{pmatrix} -0.6 - d_1 & 0.76 \\ 0.78 & -1 \end{pmatrix}^{-1} \begin{pmatrix} d_1 & 0 \\ 0 & 0 \end{pmatrix} \\ &= \begin{pmatrix} -0.5 - d_1 & 0.45 \\ 1.01 & -0.93 \end{pmatrix} - \frac{1}{d_1 + 0.6072} \begin{pmatrix} d_1 & 0 \\ 0 & 0 \end{pmatrix} \begin{pmatrix} -1 & -0.76 \\ -0.78 & -0.6 - d_1 \end{pmatrix} \begin{pmatrix} d_1 & 0 \\ 0 & 0 \end{pmatrix} \\ &= \begin{pmatrix} -0.5 - d_1 & 0.45 \\ 1.01 & -0.93 \end{pmatrix} + \frac{d_1^2}{d_1 + 0.6072} \begin{pmatrix} 1 & 0 \\ 0 & 0 \end{pmatrix}. \end{aligned}$$

From the form of the characteristic polynomial of S we can see that it is a Hurwitz matrix if and only if $\text{Tr}(S) < 0$ and $\det(S) > 0$. As $d_1 > 0$ we have that

$$\begin{aligned}\text{Tr}(S) < 0 &\iff -1.4907d_1 - 0.8683 < 0, \\ \det(S) > 0 &\iff 0.5752d_1 + 0.0064 > 0.\end{aligned}$$

Therefore S is Hurwitz. It then follows from Proposition 6.5.2 that $M - I$ is also Hurwitz for all diagonal $D \in \mathcal{D}_{A,B}$. Therefore we have that M is Schur for all diagonal $D \in \mathcal{D}_{A,B}$.

The main aim of this subsection was to demonstrate the link between diffusive growth and the existence of an unstable convex hull. Example 6.5.2 demonstrated that for any pair of system matrices, A and B , that are Schur, the existence of an unstable convex combination, and therefore the nonexistence of a common Lyapunov function, does not imply that we can find a feasible diffusive coupling that results in overall population growth.

6.5.2. Asymmetric Dispersal

As discussed in Chapters 4 and 5, dispersal can also be asymmetric rather than diffusive, i.e. symmetric. We will next show that we can induce diffusive growth if we have asymmetric dispersal rather than diffusion. To define asymmetric dispersal we first rewrite the diffusively coupled system (6.2.2) as

$$\begin{aligned}x(t+1) &= Mx(t) \\ M &:= \begin{pmatrix} A - D_1 & D_2 \\ D_1 & B - D_2 \end{pmatrix} \\ x(0) &= x_0 \in \mathbb{R}_+^{2n},\end{aligned}\tag{6.5.2}$$

where D_1 and D_2 are nonnegative diagonal matrices such that $A - D_1 \geq 0$, $B - D_2 \geq 0$ and $D_1 \neq D_2$. Note that system (6.5.2) is a special case of (3.6.1) with diagonal dispersal matrices, D_1 and D_2 , and setting $\gamma_1 = \gamma_2 = 1$.

Example 6.5.3. Consider

$$A = \begin{pmatrix} 0.413 & 0.668 \\ 0.199 & 0.763 \end{pmatrix}, B = \begin{pmatrix} 0.088 & 0.808 \\ 0.509 & 0.536 \end{pmatrix}.\tag{6.5.3}$$

One can verify that A and B are Schur and that $C = \text{diag}(3.494, 7.713) > 0$ is a common diagonal solution to (6.3.3). Although this is the case, we can see that, for $D_1 = \text{diag}(0.413, 0.763)$ and $D_2 = \text{diag}(0.088, 0.536)$, we have that $\rho(M) \approx 1.003 > 1$. If we were to have diffusion instead of asymmetric dispersal, we can see that the assumptions of Theorem 6.3.4 hold. Therefore we would get RDS. However the example above implies

that the extinction equilibrium in the case of asymmetric dispersal is unstable, i.e. overall population growth occurs. Therefore the existence of a common Lyapunov function for A and B does not imply that we have $\rho(M) < 1$ for all feasible asymmetric dispersal matrices.

We will now discuss some results related to RDS and diffusive growth for two common population matrix models used in ecology, namely the Leslie matrix model and the LPA model.

6.6. Stage-Structured Diffusion

As discussed in Chapter 3, stage-structured models take account of the discrete stages within a species' life cycle. We will now discuss RDS and diffusive growth in this context.

6.6.1. Leslie Matrices

Recall from Subsection 3.1.2 of Chapter 3 that when using population matrix models it is common to decompose the system matrix $A \in \mathbb{R}_+^{n \times n}$ as $A = T + F$, where $T = (t_{ij})$, $F = (f_{ij}) \in \mathbb{R}_+^{n \times n}$ are respectively called *transition* and *fertility matrices* [61]. The entries of these matrices satisfy, for $i, j \in \{1, \dots, n\}$,

$$f_{ij} \geq 0, t_{ij} \in (0, 1], \sum_{i=1}^n t_{ij} \leq 1. \quad (6.6.1)$$

One such class of matrices that satisfies (6.6.1) were introduced in [170], as defined in Chapter 3. In this chapter we consider a generalisation of such matrices. We say that $A \in \mathbb{R}_+^{n \times n}$ is an *extended Leslie matrix* if it takes the form

$$L = \underbrace{\begin{pmatrix} f_{11} & f_{12} & f_{13} & \cdots & f_{1n} \\ 0 & 0 & 0 & \cdots & 0 \\ 0 & 0 & 0 & \cdots & 0 \\ \vdots & \vdots & \vdots & \ddots & \vdots \\ 0 & 0 & 0 & 0 & 0 \end{pmatrix}}_F + \underbrace{\begin{pmatrix} 0 & 0 & 0 & \cdots & 0 \\ t_{21} & 0 & 0 & \cdots & 0 \\ 0 & t_{32} & 0 & \cdots & 0 \\ \vdots & & \ddots & \ddots & \vdots \\ 0 & 0 & 0 & t_{nn-1} & t_{nn} \end{pmatrix}}_T. \quad (6.6.2)$$

where $f_{1i} \geq 0$ and $t_{jj-1} \in (0, 1]$ are respectively called *stage-specific fecundity and survival/transition rates*, for $i \in \{1, \dots, n\}$, $j \in \{2, \dots, n\}$ [62]. The parameter $t_{nn} \in [0, 1]$ corresponds to the proportion of the final stage class that survives to the next generation. This is interpreted as a fixed proportion, t_{nn} , of individuals in final stage class

who survive to the next census. When $t_{nn} = 0$ we have that (6.6.2) reduces to a standard Leslie matrix, as we saw in Chapter 3. We will simply refer to matrices of the form (6.6.2) as Leslie matrices (see Fig. 6.2). Note that (6.6.2) is of the form of a so-called Lefkovich matrix [177].

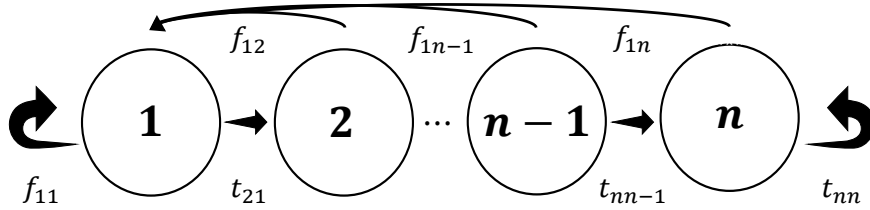


Figure 6.2: Directed graph corresponding to the extended Leslie matrix (6.6.2).

Leslie matrices in the context of patchy dispersal were investigated in [13]. The authors studied the model

$$x_i(t+1) = T_i x_i(t) + \sum_{j=1}^n c_{ij} F_j x_j(t),$$

where F_i and T_i are respectively of the form of F and T in (6.6.2), with $t_{nn} = 0$, and where $C = (c_{ij}) \in \mathbb{R}_+^{n \times n}$ is a dispersal connectivity matrix whose entries correspond to the proportions of successfully dispersed juveniles. The authors looked at how the reproduction number for such Leslie matrices related to metapopulation growth for various types of dispersal networks.

Up to now, we have used diagonal matrices to describe dispersal between patches. However, for several discrete time models, the structure of the matrices describing local dynamics makes diagonal dispersal matrices inappropriate. Leslie matrix models are stage-structured, and as these are also discrete-time models, each time step corresponds to the length of time spent in each stage class. Recall that the nonzero entries of T describe transitions between stage classes and the survival of the adult class to the next generation. This then means that the most appropriate position for our diffusion terms between stage classes would be in the $(i, i-1)$ and (n, n) positions, for $i \in \{2, \dots, n\}$. More formally, assume that $D \in \mathcal{D}_{L(A,B)}$, where $\mathcal{D}_{L(A,B)}$ is the set of lower-triangular, nonnegative matrices of the form

$$D_L = \begin{pmatrix} 0 & 0 & 0 & \cdots & 0 \\ d_{21} & 0 & 0 & \cdots & 0 \\ 0 & d_{32} & 0 & \cdots & 0 \\ \vdots & & \ddots & \ddots & \vdots \\ 0 & 0 & 0 & d_{nn-1} & d_{nn} \end{pmatrix}, \quad (6.6.3)$$

such that $A - D_L \geq 0$ and $B - D_L \geq 0$. Further define the following:

- For $i \in \{2, \dots, n\}$, $\mathcal{D}_{A,B}^i := \{D_L \in \mathcal{D}_{L(A,B)} : d_{ii-1} > 0, d_{jj-1} = d_{nn} = 0, j \neq i\}$, i.e. diffusion only affects the transition class i . This could arise in a scenario where, for example, there is natal/breeding dispersal of one mobile class of juveniles or adults [123].
- $\mathcal{D}_{A,B}^f := \{D_L \in \mathcal{D}_{L(A,B)} : d_{nn} > 0, d_{21} = d_{32} = \dots = d_{nn-1} = 0\}$, i.e. diffusion only affects the remaining/surviving adult class. This could arise in a scenario where there is delayed dispersal of adults only, due to, for example, cooperative breeding [158].

We now state a result about Leslie matrices that makes use of the column selection set of A and B . Given a matrix A , let $A^{[i]}$ denote its i th row. Given a matrix pair $\{A, B\} \subset \mathbb{R}^{n \times n}$ define $S(A, B)$, the so-called *row selection set* of A and B , to be the set of all real matrices, each of which has i th row given by the i th row of either A or B [3].

Let A and B be Leslie matrices of the form (6.6.2). Further let

$$S_A := \begin{pmatrix} a_{11} & a_{12} & a_{13} & \cdots & a_{1n} \\ m_{21} & 0 & 0 & \cdots & 0 \\ 0 & m_{32} & 0 & \cdots & 0 \\ \vdots & & \ddots & \ddots & \vdots \\ 0 & 0 & 0 & m_{nn-1} & m_{nn} \end{pmatrix} \text{ and } S_B := \begin{pmatrix} b_{11} & b_{12} & b_{13} & \cdots & b_{1n} \\ m_{21} & 0 & 0 & \cdots & 0 \\ 0 & m_{32} & 0 & \cdots & 0 \\ \vdots & & \ddots & \ddots & \vdots \\ 0 & 0 & 0 & m_{nn-1} & m_{nn} \end{pmatrix}$$

where we define $m_{ll-1} := \max \{a_{ll-1}, b_{ll-1}\}$, for $l \in \{2, \dots, n\}$, and $m_{nn} := \max \{a_{nn}, b_{nn}\}$.

We will now state a useful result for establishing RDS for Leslie matrices.

Theorem 6.6.1. *Let $A, B \in \mathbb{R}_+^{n \times n}$ be Schur and of form (6.6.2), such that $a_{1n}, b_{1n}, a_{nn}, b_{nn} > 0$. Then there exists $v > 0$ such that $Av < v, Bv < v$ if and only if $\rho(S_A) < 1$ and $\rho(S_B) < 1$.*

Proof. (\implies) Assume that there exists $v > 0$ such that $Av < v, Bv < v$. Each entry in $S_A v$ and $S_B v$ are given by the corresponding entry in one of Av or Bv . We can then conclude $S_A v < v$ and $S_B v < v$. It follows from Lemma 2.2.2 that S_A and S_B are Schur.

(\impliedby) Conversely assume that S_A and S_B Schur. Given $R \in S(A, B)$ we have that $R \leq S_A$ or $R \leq S_B$. As both S_A and S_B are Schur, then R is also Schur. This then implies that every $P \in S(A - I, B - I)$ is Hurwitz. \square

The next two results state sufficient conditions for RDS for Leslie matrices where diffusion only affects the remaining/surviving adult stage class, i.e. $D \in \mathcal{D}_{A,B}^f$.

Corollary 6.6.2. *Let $A = (a_{ij}), B = (b_{ij}) \in \mathbb{R}_+^{n \times n}$ be Leslie matrices of form (6.6.2) such that $a_{1n}, b_{1n}, a_{nn}, b_{nn} > 0$. Assume that S_A and S_B are Schur. Then M is Schur for all $D \in \mathcal{D}_{A,B}^f$.*

Proof. It follows from Theorem 6.6.1 that both $\rho(S_A) < 1$ and $\rho(S_B) < 1$ if and only if both $Av < v$ and $Bv < v$. Hence, by Proposition 2.2.2, M is Schur for all $D \in \mathcal{D}_{A,B}^f$. \square

Corollary 6.6.2 states that if the Leslie matrices A and B only differ in their fertility parameters, i.e. their first rows, then we can ensure RDS. We next state an even stronger result for Schur Leslie matrices.

Theorem 6.6.3. *Let $A = (a_{ij}) = F_1 + T_1, B = (b_{ij}) = F_2 + T_2 \in \mathbb{R}_+^{n \times n}$ be Schur, Leslie matrices of form (6.6.2), such that $a_{1n}, b_{1n}, a_{nn}, b_{nn} > 0$. Then M is Schur for all $D \in \mathcal{D}_{A,B}^f$.*

Proof. $S \in \mathbb{R}^{n \times n}$ is irreducible if and only if the corresponding digraph of S is strongly connected [137]. As $a_{1n}, b_{1n}, a_{nn}, b_{nn} > 0, a_{ii-1}, b_{ii-1} > 0$ for all $i \in \{2, \dots, n\}$, the directed graph corresponding to A and B are strongly connected. Thus both A and B are irreducible. By assumption we have that $D \in \mathcal{D}_{A,B}^f$. Therefore

$$A - D, B - D \geq 0 \implies D = \text{diag}(0, 0, \dots, d),$$

for some $d \in [0, \min\{a_{nn}, b_{nn}\}]$. If $d = 0$ then M is block diagonal and so, if A and B are Schur, then so is M . Assume that $d > 0$. One can observe that from the form of M that its corresponding digraph is strongly connected. Therefore M is irreducible. As $M \geq 0$ it follows from Theorem 2.2.1 that there exists $y > 0$ such that $My = \rho(M)y$.

We prove our result by contradiction. Assume $\rho(M) \geq 1$. As A and B are Schur and because $\rho(L)$ is a continuous function of the entries in $L \in \mathbb{R}^{n \times n}$, there must exist some diagonal $D > 0$ such that $\rho(M) = 1$. For such a D , it follows from Lemma 2.2.2 that $\rho(M) = 1$ if and only if there exists $y := (v \ w)^T > 0$ such that $My = y$. One can then observe that $My = y$ if and only if

$$(A - I)v = D(v - w) = (0 \ 0 \ \dots \ 0 \ d((v_n - w_n))^T \tag{6.6.4}$$

$$(B - I)w = D(w - v) = (0 \ 0 \ \dots \ 0 \ d((w_n - v_n))^T. \tag{6.6.5}$$

The RHS of one of (6.6.4) or (6.6.5) must be nonnegative. This means that either $Av \geq v$ or $Bw \geq w$. Assume that $Av \geq v$. We then have that $(A - I)v \geq 0$ if and only if $Av \geq v$, which contradicts that A is Schur. This holds similarly if we assume $Bw \geq w$. Therefore, in either case, M is Schur for all $D \in \mathcal{D}_{A,B}^f$. \square

Theorem 6.6.3 means that if we allow only adult diffusion, we cannot rescue the two patches from extinction. Using a similar argument as in the proof of Theorem 6.6.3, we can prove the following result, where diffusion only affects one particular transition stage class, i.e. we have that $D \in \mathcal{D}_{A,B}^i$ for some given $i \in \{2, \dots, n\}$.

Theorem 6.6.4. *Let $A = (a_{ij}), B = (b_{ij}) \in \mathbb{R}_+^{n \times n}$ be Schur, Leslie matrices of form (6.6.2), such that $a_{1n}, b_{1n} > 0$. Then, for a given $i \in \{1, \dots, n\}$, M is Schur for all $D \in \mathcal{D}_{A,B}^i$.*

In Theorem 6.6.4 we saw that diffusion is only permitted in transition stage class. In Theorems 6.6.3 and 6.6.4 we can see that allowing diffusion between only one stage class results in RDS. A natural next question to ask is: can we guarantee RDS if we allow diffusion in more than one stage class? The answer to this in general is in fact no, as we can demonstrate with a simple example.

Example 6.6.1. Consider

$$A = \begin{pmatrix} 0.10 & 0.84 & 0.14 \\ 0.93 & 0 & 0 \\ 0 & 0.64 & 0.18 \end{pmatrix}, B = \begin{pmatrix} 0.59 & 0.13 & 0.99 \\ 0.4900 & 0 & 0 \\ 0 & 0.35 & 0.47 \end{pmatrix}.$$

One can verify that A and B are Schur. Letting

$$D = \begin{pmatrix} 0 & 0 & 0 \\ 0.2500 & 0 & 0 \\ 0 & 0.1800 & 0 \end{pmatrix}$$

one can verify that $\rho(M) \approx 1.02 > 1$. Thus diffusive growth occurs once diffusion is permitted to take place between more than one transition stage class.

We will next demonstrate how the above results apply to the LPA model, a nonlinear extension of a 3×3 extended Leslie matrix model.

6.6.2. The LPA Model

As discussed in Chapter 3, a well-known structured population model in ecology is the nonlinear LPA model [55]. We can see from the form of the matrix valued function $A(x)$, given by (3.2.4), that $A(0)$ is of the extended Leslie matrix form

$$A(0) := \begin{pmatrix} 0 & 0 & p \\ q & 0 & 0 \\ 0 & r & s \end{pmatrix}, \tag{6.6.6}$$

where $p > 0$ and $q, r, s \in [0, 1]$. Motivated by the diffusively coupled system (6.2.2), we can write this system as a nonlinear matrix model as follows. Let $A(x)$ and $B(x)$ be of the form (3.2.4). Then our nonlinear diffusively coupled system can be written as

$$\begin{aligned} x(t+1) &= M(x)x(t) \\ M(x) &:= \begin{pmatrix} A(x) - D & D \\ D & B(x) - D \end{pmatrix} \\ x(0) &= x_0 \in \mathbb{R}_+^{2n}, \end{aligned} \tag{6.6.7}$$

for $D \in \mathcal{D}_{L(A,B)}$. As the LPA model is nonlinear, for each patch to be a sink, in the context of (6.6.8), we will assume that $\rho(A(0)), \rho(B(0)) < 1$. We can observe from the form of (3.2.4) that $A(x) \leq A(0)$ and $B(x) \leq B(0)$. It then follows that for $x(0) = x_0 \in \mathbb{R}_+^2$, a solution of (3.2.1) satisfies $x(t, x_0) = \prod_{s=1}^t A(x(t-s))x_0 \leq A(0)^t x_0$ for $t \geq 1$. Therefore we have that $\rho(A(0)) < 1$ implies that $A(0)^t \rightarrow 0$ as $t \rightarrow \infty$. Therefore we can see that $\rho(A(0)), \rho(B(0)) < 1$ implies the extinction equilibrium is GAS on both patches.

In the context of the LPA model, one would expect dispersal to occur at the adult stage, where the species is mobile. Therefore assume $D \in \mathcal{D}_{A,B}^f$, i.e. diffusion occurs in the adult survival stage class. It then follows from Theorem 6.6.3, that if we allow diffusive dispersal from the adult class, we must have that the extinction equilibrium is LAS and in turn we must have that it is also GAS, where dispersal is described by a constant matrix D as $M(x) \leq M(0)$ in this case. Therefore when dispersal is constant and occurs from the adult class we can ensure that diffusive growth can never occur. We can generalise dispersal so that it is nonlinear, by rewriting (6.6.8) as

$$\begin{aligned} x(t+1) &= M(x)x(t) \\ M(x) &:= \begin{pmatrix} A(x) - D(x) & D(x) \\ D(x) & B(x) - D(x) \end{pmatrix} \\ x(0) &= x_0 \in \mathbb{R}_+^{2n}, \end{aligned} \tag{6.6.8}$$

where we assume that $D : \mathbb{R}_+^n \rightarrow \mathbb{R}_+^{n \times n}$ is a matrix valued function of the form (6.6.3). Each d_{ij} is a smooth function describing the density-dependent diffusion of that respective transition stage class. From the form of $A(x)$ and $B(x)$ we must have that $D = \text{diag}(0, 0, d(x))$, where $d : \mathbb{R}_+ \rightarrow \mathbb{R}_+$, such that $r \geq d(x)$ for all $x \geq 0$, so that our system remains positive. We can then see from that if $\rho(A(0)), \rho(B(0)) < 1$ then we get that $M(0)$ is LAS. The interplay between $A(x)$ and $D(x)$ would need to be further investigated to conclude a stronger statement about stability. To further demonstrate the ecological applicability of our results, we will show next how they apply to a well-known model of amphibian dynamics.

6.6.3. An Invasive Bullfrog Model

In the context of modelling invasive species, in [112] the authors proposed a model for the stage-structured dynamics of the American bullfrog, a species that has been introduced around the world and which causes great damage to native populations. In this paper the authors proposed the following system matrix for modelling its linear dynamics:

$$A_F := \begin{pmatrix} 0 & 0 & 0 & 0 & a_1 \\ a_2 & 0 & 0 & 0 & 0 \\ 0 & a_3 & 0 & 0 & 0 \\ 0 & a_4 & a_5 & 0 & 0 \\ 0 & 0 & 0 & a_6 & a_7 \end{pmatrix}, \quad (6.6.9)$$

for $a_1 > 0$, $a_i \in (0, 1]$ for $i \in \{2, \dots, 6\}$ and $a_7 \in (0, 1)$. This matrix model describes the fecundity of the adult class, as well as transitions between tadpole, juvenile and adult stage classes. The a_4 entry corresponds to the transition of one year old tadpoles to juveniles. The matrix A_F is very similar in form to an extended Leslie matrix, apart from the $a_4 > 0$ entry. As noted in [62], A_F is irreducible as its associated digraph is strongly connected. One can then observe that the following result holds, the proof of which is identical to that of Theorem 6.6.3.

Theorem 6.6.5. *Let $A, B \in \mathbb{R}_+^{5 \times 5}$ be Schur matrices of the form in (6.6.9). Then M is Schur for all $D \in \mathcal{D}_{A,B}^f$.*

We will now demonstrate the use of Theorem 6.6.5 using an empirical example.

Example 6.6.2. In [112] the authors estimated the entries of A_F for a suburban population of American bullfrog in Victoria in British Columbia, Canada as

$$A_F = \begin{pmatrix} 0 & 0 & 0 & 0 & 2080 \\ 0.070 & 0 & 0 & 0 & 0 \\ 0 & 0.078 & 0 & 0 & 0 \\ 0 & 0.016 & 0.020 & 0 & 0 \\ 0 & 0 & 0 & 0.129 & 0.318 \end{pmatrix}. \quad (6.6.10)$$

Let A be given by (6.6.10) and further let

$$B = \begin{pmatrix} 0 & 0 & 0 & 0 & 2080 \\ 0.02 & 0 & 0 & 0 & 0 \\ 0 & 0.318 & 0 & 0 & 0 \\ 0 & 0.129 & 0.078 & 0 & 0 \\ 0 & 0 & 0 & 0.016 & 0.070 \end{pmatrix}. \quad (6.6.11)$$

As the authors only give one parameterised population projection matrix, we assumed that the entries in B were given by (6.6.11), which is the matrix A with transition rates shuffled. We based this on the fact that factors like temperature or resource quality could induce different survival rates across transition stages on the two patches. Although this is an oversimplification, this example is merely to demonstrate the applicability of the concepts in this chapter. One can numerically check that $\rho(A) = \rho(A_F) \approx 0.855 < 1$ and $\rho(B) \approx 0.599 < 1$. It then follows from Theorem 6.6.5 that M is Schur for all $D \in \mathcal{D}_{A,B}^f$. Thus, in this case, if one's goal was to ensure eradication of such an invasive pest, then only permitting diffusive dispersal in the adult stage class will result in the overall extinction of two sink patches.

6.7. Summary

In this chapter, we considered a number of matrix theoretic questions related to structured population dynamics, where there is movement between demographic classes in two regions. In particular, we investigated how one can guarantee that the extinction equilibrium is stable for all feasible diffusive couplings (robust diffusive stability or RDS). We demonstrated how various types of Lyapunov functions relate to RDS. In particular we demonstrated that the existence of a CQLF for our system matrices is not sufficient for RDS, but the existence of a CDLF is sufficient. We described some variations of this problem and also gave some examples of when RDS does not hold, what we termed diffusive growth. We also briefly explored how our results applied to a range of matrix classes that arise in stage-structured modelling, such as Leslie matrix models, the LPA model and using a bullfrog model. The results and examples in this chapter highlight the importance of taking account of the demographic makeup of a population, as the effect of dispersal on sub-groups within populations is an important factor to understand when trying to project future ecological population dynamics under varying habitat characteristics.

7. Stochastic Group Interactions within Social Animal Populations

In this chapter, we take a stochastic perspective when modelling structured populations. In particular, we propose a time series model that couples the dynamics of animal groups within a population with social structure and an additional auxiliary population. This framework is proposed in order to infer the temporal associations/interactions among such groups and the influence of such auxiliary population. We first outline our methodology. We validate it through various simulation scenarios, to assess parameter estimation and bias. We then apply our model to a well-known predator-prey case study to assess how various parameters can be interpreted and how they can be used to infer associations. Finally, we derive, under a new simpler time series model, an approximation of the marginal correlation structure between groups, termed the net group interaction strength, and interpret this within the context of predator-prey theory to highlight its potential applicability.

Parts of this chapter appeared in: McGrane-Corrigan, B., Mason, O. and de Andrade Moral, R., 2024. Inferring stochastic group interactions within structured populations via coupled autoregression. Journal of Theoretical Biology, 584, p.111793.

7.1. Motivation

Many animals have a tendency to congregate into clusters or distinct groups across space and time. This within-population structure in turn affects the ability of such populations to compete for resources, occupy home-ranges and participate in community interactions [217]. Dispersal events also greatly influence such populations, as was theoretically demonstrated in Chapters 4, 5 and 6 in relation to invasion, metapopulations and demographically-structured populations. In the evolutionary theory proposed in [122], living in groups has major benefits for group members, as well as the overall population. These include, for example, alloparenting, where non-parental individuals care for young [184], along with many costs, such as inter-group competition and free-riding [270]. Thus, trade-offs balance such intra- and inter-group factors which can lead to higher group fitness and perhaps to the detriment of individual members. As noted in [4], other important factors influencing group dynamics include predation risk, as well as diet and the spa-

tiotemporal heterogeneity of resources in many large animal populations [105, 245]. Many studies have investigated the efficiency of group living [15, 40, 110, 194]. For example, in [84] the authors analysed a mathematical model of wolf-pack hunting, concluding that larger packs reduce the effectiveness of group hunting, which explains why hunting success tends to peak at small pack sizes. Other authors have focused on how group size may impact disease spread [38] or theoretical aspects such as the evolution of cooperation [155, 211].

In the previous chapters we have looked at various mathematical models of within-population dynamics such as metapopulation dispersal and stage-structure. In this chapter our specific interest is to model the stochastic dynamics of animal groups that are monitored over some observation window, in order to better understand how these groups interact with one another and how the presence of an additional auxiliary population could alter these interactions over time. We will first discuss our model formulation and how we can fit the model in a Bayesian setting. We then discuss different simulation scenarios that show how well our model performs. We then present an implementation of our model for inferring associations within a real-world predator-prey system, namely wolf-elk interactions in Yellowstone National Park (YNP). We then show, under common assumptions, how we can derive an approximation to the net group correlation structure of a social population. Finally we describe possible interpretations of this approximation in the context of predator-prey theory.

7.2. Group Interactions

As outlined in Chapter 3 for modelling interactions among populations, we could fit a PLV model to the time series of g subgroups within a population. However, we would need to estimate each component of the intrinsic growth rate vector, r , and each element of the interaction matrix, A . Therefore the number of parameters to estimate over all the groups would be $g(g + 1)$. This does not include the number of parameters that would need to be estimated when an auxiliary population model is also considered, which depends on the chosen model parameterisation. Therefore for inferring pairwise group interactions, it would be beneficial to explicitly deduce which groups are strongly/weakly associated to one another. A disadvantage of this approach in the group context would be that for short observation periods, which are common in ecological time series [144], the resolution of data is too low to accurately estimate such parameters, with parameter estimation becoming difficult as g gets large. The model we consider in this chapter does not involve specifying any specific interaction type, as in the example outlined in Chapter 3 for modelling predator-prey dynamics. This is because parametrising such systems would be difficult, if perhaps the number of groups was large. We would also need good high

resolution group-specific data such as kill rates, mortality rates, along with assuming a specific form for the functional response for example, in order to fit such a model.

When dealing with groups within a population, we can safely assume that groups interact with one another either through a variety of processes such as dispersal, resource competition and hunting cooperation, among others [217]. Therefore we will use the standard Pearson's correlation coefficient as a metric of interaction in our group context, which we will discuss further in later sections, along with interpreting our model parameters as indicators of interaction also. In the following section we will present our coupled autoregressive model for modelling group dynamics and later describe how the (pairwise) correlation, as in (3.7.3), between such groups can possibly be used to measure interaction strengths among a set of subgroups within a population.

7.2.1. *Low Counts and Zero Observations*

Many count time series models used in ecology often assume normality on the log scale, which means that density or abundance is considered multiplicative on the log scale. This can be valid when counts are large enough to be effectively modelled by autoregressive models (such as the Gompertz model) with white noise error structure [218]. However, for low counts, this might not fully capture the dynamics in the same way it does for larger counts. Additionally, these models often rely on the assumption of a direct linear relationship between covariates and the response variable [212]. Applying log transformations to raw data may also affect how model outputs are interpreted. Finally, zero observations may not be addressed in the most straightforward way. In certain cases, such as modelling social groups in large mammals, where group sizes typically remain small (often fewer than ten individuals), low counts may be a common occurrence [37].

We next describe our coupled autoregressive model, where we use an observation-driven approach, as outlined more generally in Chapter 3. We also discuss how our general framework may address some attributes of modelling social group dynamics, such as short-observation periods, low counts and zero-inflation.

7.3. **The Coupled Autoregressive Model**

Consider $g \in \{2, 3, \dots\}$ groups within some finite population, X , and an auxiliary population, Y , both of which are observed/censused over $T \in \mathbb{Z}_+$ time steps. The random variables under consideration are discrete counts (abundances) of all groups, $X_t := \{X_{1,t}, \dots, X_{g,t}\}$, and an auxiliary population, Y_t , at time $t \in [0, T] \subset \mathbb{Z}_+$. Thus $(X_{i,t})_{[0,T]}$ and $(Y_t)_{[0,T]}$ are

respectively realisations of the temporal point processes. In our context these are abundance time series respectively for animal group $i \in \{1, \dots, g\}$ and an auxiliary population over the finite time horizon $[0, T]$. Examples of social populations that our framework could model include:

- Predator-prey systems: X is a population of predator groups, such as orca pods, and Y their main prey population, such as Atlantic herring [149];
- Consumer-resource systems: X is a population of consumer groups, such as vervet monkey troops and Y one of their main seasonal food resource, such as pink ivory [246];
- Host-parasite systems: X is a population of host groups, such as ant colonies, and Y their parasitoid, such as parasitic wasps [87];
- Predator-competitor systems: X is a population of predator groups, such as North American grey wolf packs, and Y a competitor population, such as North American cougars [81].

7.3.1. The Observation Processes

Let $\mathcal{G}_r := \{X_s, Y_s : s = 0, \dots, r\}$ to be the set of counts for all groups and the auxiliary population up to and including a given time $r \geq 0$ and $\mathcal{H}_t := \{X_t, Y_t\}$ be the set of all groups and the auxiliary population at a given time $t \geq 0$. We first assume that

$$\begin{aligned}\mathbb{P}(X_{i,t}|\mathcal{G}_{t-1}) &= \mathbb{P}(X_{i,t}|\mathcal{H}_{t-1}), \\ \mathbb{P}(Y_t|\mathcal{G}_{t-1}) &= \mathbb{P}(Y_t|\mathcal{H}_{t-1}),\end{aligned}$$

for all $i \in \{1, \dots, g\}$ and any fixed $t \in \{1, \dots, T\}$. In other words, $(X_{i,t})_{[0,T]}$ and $(Y_t)_{[0,T]}$ are discrete-time Markov chains. Similar to the models in previous chapters, here we are assuming that the current observation only depends on the initial past values of the group and auxiliary population counts.

Further let

$$w := \{\omega_i^X, \lambda_i^X, \psi_i, \delta_i; i \in \{1, \dots, g\}\}. \quad (7.3.1)$$

The elements of w are random variables given by

$$\omega_i^X \sim \mathcal{N}(\mu_\omega, \sigma_\omega^2), \lambda_i^X \sim \mathcal{N}(\mu_\lambda, \sigma_\lambda^2), \psi_i \sim \mathcal{N}(\mu_\psi, \sigma_\psi^2), \delta_i \sim \mathcal{N}(\mu_\delta, \sigma_\delta^2), \quad (7.3.2)$$

for $i \in \{1, \dots, g\}$, where

$$\begin{aligned}M &:= \{\mu_\omega, \mu_\lambda, \mu_\psi, \mu_\delta\} \subset \mathbb{R}^4, \\ \Sigma &:= \{\sigma_\omega^2, \sigma_\lambda^2, \sigma_\psi^2, \sigma_\delta^2\} \subset \mathbb{R}_+^4\end{aligned} \quad (7.3.3)$$

are assumed to be known a priori. The elements of w are called random effects, with M being a set of population-level means and Σ being a set of population-level variances. We will discuss these in more detail later in this section. Here $\mathcal{N}(\mu, \sigma^2)$ denotes a Gaussian distribution with probability density function given by

$$f(x, \alpha, \beta) := \frac{1}{\sqrt{2\pi\beta^2}} \exp\left(-\frac{(x - \alpha)^2}{2\beta^2}\right),$$

for $\alpha \in \mathbb{R}$ and $\beta > 0$.

With \mathcal{H}_t and w defined as above, we assume that

$$X_{i,t} | \mathcal{H}_{t-1}, w \sim \text{Pois}\left(\mu_{i,t}^X\right), \quad (7.3.4)$$

$$Y_t | \mathcal{H}_{t-1}, w \sim \text{Pois}\left(\mu_t^Y\right), \quad (7.3.5)$$

for $t \in [1, T]$ and $i \in \{1, \dots, g\}$, where we assume that the initial conditions $X_{i,0} = x_{i,0} \geq 0$, $Y_0 = y_0 \geq 0$, $\mu_{i,0}^X > 0$, $\mu_0^Y > 0$ are known a priori. Here $\text{Pois}(\mu)$ denotes a Poisson distribution with probability mass function given by

$$f(k, \mu) = \frac{\mu^k e^{-\mu}}{k!},$$

where $k \in \mathbb{Z}_+$ and $\mu > 0$. Therefore each $X_{i,t}$ and Y_t are conditional Poisson random variables with inhomogenous intensities respectively given by $\mu_{i,t}^X$ and μ_t^Y . In a slight abuse of notation, we are assuming that the elements of \mathcal{H}_{t-1} and w are known in the conditional probabilities (7.3.4) and (7.3.5), but omit writing these for ease of exposition.

The random variables in w are commonly called random effects, with M and Σ respectively being the set of population level means and variances, otherwise known as *hyperparameters*. See Subsection 3.7.2 in Chapter 2 for more on random effects. These random effects are assumed to be mutually independent from one another. At each fixed time $t \geq 0$ we also assume they are independent to the elements of \mathcal{H}_{t-1} . These random effects will be included in the components that make up $\mu_{i,t}^X$ and μ_t^Y , which we will describe in the next section. The inclusion of random effects allows us to account for across-group variability in each of the intensity processes. It is common procedure to monitor individual animals and pool their counts to estimate population-level effects without taking account of group-level variation. However, we explicitly take account of group dynamics, their couplings and the influence of an external auxiliary population. The use of random effects allows us to incorporate the assumption that each group's dynamics are governed by realisations of random variables that describe the global behaviour of a theoretically infinite number of possible groups. We will now outline the various coupling components of our model.

7.3.2. The Intensity Processes

The inhomogenous mean of each conditional Poisson process is a function of $X_{i,t}$ and Y_t . This allows us to couple these processes together to build our coupled autoregressive model (see Fig. 7.1). The log-intensity process for (7.3.4) is given by

$$\ln(\mu_{i,t}^X) = \omega_i^X + \Lambda_{i,t-1}^X + \Psi_{i,t-1} + \Delta_{i,t-1}. \quad (7.3.6)$$

The random intercept parameter for group i , ω_i^X , incorporates density-independent effects for group i in isolation, i.e. intrinsic growth. The autoregressive component,

$$\Lambda_{i,t}^X = \lambda_i^X \ln(x_{i,t} + 1),$$

accommodates temporal correlation in $X_{i,t}$. That is, group i 's abundance at time t depends on λ_i^X and the observed count $x_{i,t}$, with their magnitudes determining how strong this dependence is. This component incorporates within-group density-dependent effects for group i . The intraspecific component,

$$\Psi_{i,t} = \psi_i \ln\left(\sum_{j \neq i} x_{j,t} + 1\right), \quad (7.3.7)$$

describes how cumulative changes in abundances of each group $j \neq i$ affects group i , with ψ_i and the magnitude of each of the observed counts of all of the other groups determining how strong this dependence is. This intraspecific component could, for example, take account of the effects of across-group processes like group predation/foraging or competition for territory. The auxiliary component,

$$\Delta_{i,t} = \delta_i \ln(y_t + 1), \quad (7.3.8)$$

describes how changes in the auxiliary population affect group i , where δ_i and the magnitude of the observed y_t determines how strong this dependence is. The auxiliary component could, for example, take account of the effects of prey availability or indirect competition.

The log-intensity process for (7.3.5) is given by

$$\ln(\mu_t^Y) = \omega^Y + \Lambda_{t-1}^Y + \Gamma_{t-1}. \quad (7.3.9)$$

The intercept parameter, ω^Y , incorporates density-independent effects for the auxiliary population in isolation, i.e. intrinsic growth. The autoregressive component,

$$\Lambda_t^Y = \lambda^Y \ln(y_t + 1), \quad (7.3.10)$$

accommodates temporal correlation in Y_t . That is, the abundance of the auxiliary population at time t also depends on λ^Y and the observed count y_t , with their respective magnitudes determining how strong this dependence is. This component incorporates within-population density-dependent effects for Y_t . The interspecific component,

$$\Gamma_t = \gamma \ln \left(\sum_{j=1}^g x_{j,t} + 1 \right), \quad (7.3.11)$$

accounts for how changes in the overall target population affects Y_t , where γ and the magnitude of each of the other observed counts of groups determine how strong this dependence is. The interspecific component could, for example, take account of the effects of predation or interspecific competition. Note that the inclusion of a natural log-link in (7.3.6) and (7.3.9) is to ensure that $\mu_{i,t}^X$ and μ_t^Y are non-negative. Adding a constant 1 within each ln argument ensures that our model can capture zero abundance observations and so correlations can take values in \mathbb{R} , as noted by [90]. It also to avoid sampled intensity values to increase rapidly when these mean processes are only regressed on $X_{i,t-1}$ and Y_{t-1} [90, 201]. Conditioning on (7.3.2) in the latent processes (7.3.6) and (7.3.9) can allow for the accommodation of overdispersion, i.e. violation of expectation-variance equality [206], a common issue faced when modelling count time series.

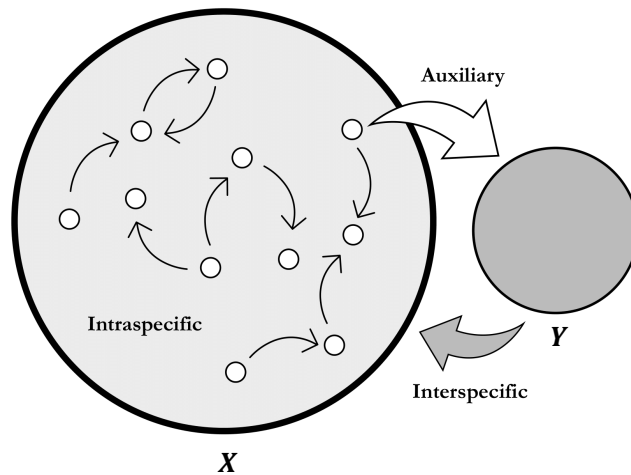


Figure 7.1: Conceptual diagram of how X and Y are coupled, which includes intraspecific components (7.3.7), auxiliary components (7.3.8), and a interspecific component (7.3.11).

Our modelling approach is similar to level-correlated models, which incorporate dependence between components of a count vector via an underlying correlated latent process [2, 52, 67]. Another way of allowing for overdispersion is using quasi-likelihood methods, but we adopt a mixed model approach in order to also account for the grouping behaviour and inter-group variation. In time series models of counts, observational and latent processes are included to account for measurement error [138]. In our hierarchical framework,

the data generating process is given by (7.3.5) and (7.3.4), with the unobserved or latent processes modelled by (7.3.6) and (7.3.9). Therefore we are implicitly assuming perfect detection. We do not explicitly model the measurement process, as we are only concerned with inferential aspects of our model.

7.3.3. Model Fitting

To fit our model we took a Bayesian perspective (see Chapter 3 for a brief overview of Bayesian time series analysis). In all of the analyses below, we employed a Hamiltonian, no-U-turn sampler (NUTS) algorithm to fit our model (see Chapter 3 for a brief explanation of HMC). We implemented this via the probabilistic programming language Stan, using the R package rstan [44]. We used four chains in each of the simulations in the above scenarios and the case study below. For our case study we used 20,000 iterations, a thinning rate of 20 and burn-in of 2000. Convergence was assessed using trace plots, autocorrelation function plots, effective sample size and the Gelman-Rubin statistic [101].

In Chapter 2 we discussed how one may choose to assign priors for variance and mean terms. When fitting our model in this chapter we assigned independent noninformative Gaussian priors to our mean hyperparameters and auxiliary population parameters, $\theta_\mu \sim \mathcal{N}(0, 100^2)$, for $\theta_\mu \in M \cup \{\omega^Y, \lambda^Y, \gamma\}$, where M is given in (7.3.3). For our standard deviation hyperparameters we assigned independent noninformative half-Gaussian priors, $\theta_\sigma \sim \mathcal{N}^+(0, 100^2)$, for $\theta_\sigma \in \Sigma$, where Σ is given in (7.3.3).

7.4. Simulation Studies

Within the ecological literature, count time series may vary from low to high resolution, which reflects the nature of how the data is observed and collected. To evaluate model performance, we simulated synthetic data from (7.3.5) and (7.3.4) for 5 different scenarios. This allows us to validate our estimation procedure outlined in the previous section, independently of uncertainties due to data constraints, or inadequate data resolution which are widespread in empirical abundance time series [64, 144]. It also allows us to show that the parameter estimates can be used to infer group interactions/associations in a stochastic setting. Being able to reliably estimate parameters is also important within the context of our theoretical work later in this chapter.

The scenarios we consider in this section include the following:

1. $g = 10, T = 20$;

2. $g = 42, T = 20$;
3. $g = 50, T = 50$;
4. $g = 42, T = 20, \gamma = -0.15, \mu_\psi = 0.15, \mu_\delta = 0.15$
5. $g = 42, T = 20, \gamma = 0.05, \mu_\psi = -0.05, \mu_\delta = -0.05$.

The remaining parameters were set to the values as given in Table 7.1. For scenarios 1-3 we further set $\gamma = -0.05, \mu_\psi = -0.5$ and $\mu_\delta = 0.2$.

Parameter	ω^Y	λ^Y	μ_ω	μ_λ	σ_ω	σ_λ	σ_δ	σ_ψ
True Value	0.9	0.9	0.9	0.06	0.2	0.2	0.04	0.04

Table 7.1: True parameter values chosen for simulation scenarios S1—S5.

Scenarios 1 - 3 were used to observe how well parameters were estimated when the resolution of the ecological data varies from low to high, due to either the number of groups observed or the length of each time series. In scenario 1 we have a small number of groups and short observation period length, which could arise when modelling elusive social species over a sparse observation period for example. In scenario 2 we have a moderate number of groups and observation period length. This echoes the data structure of our case study in the next section. In scenario 3 we have a large number of groups and long observation period length. This could describe a scenario when monitoring the weekly abundance of a highly mobile species for example. We included the last two scenarios to deduce how well parameters are estimated where a predator population and its prey is monitored, for example.

In scenario 4, as $\gamma < 0$, we are assuming that predator groups have negative effect on prey abundance. This may be due to the direct effect of depletion of the prey by the predators. As $\mu_\delta > 0$, we are assuming that the prey has a net positive effect on predator group abundance. This may be due to the direct effect of prey consumption by the predators. Lastly, as $\mu_\psi > 0$ we are assuming that predator groups have a net positive effect on other predator group abundances. This may be due to, for example, hunting cooperation [7].

In scenario 5, as $\gamma > 0$, we are assuming that predator groups have a positive effect on prey abundance. As $\mu_\delta < 0$, we are assuming that the prey has a net negative effect on predator group abundance. The sign of both γ and μ_δ being positive could arise in a situation where predator satiation is observed for example, where the prey produces a large number of offspring in order to ensure population survival following predation [141]. Predators can also have a net positive effect on prey through so-called predator-induced modifications, where the predator can reduce the foraging time of a prey species, which in turn can lead to an increase in prey resource levels [220]. Lastly, as $\mu_\psi < 0$ we are assuming that predator

groups have a net negative effect on other predator group abundances. This may be due to the direct effect of group competition for prey or territory [254]. We further discuss some of the situations above in more depth in our theoretical work later.

We ran 100 simulations for each scenario. We can interpret these parameter values in a biological context. Observe that $\mu_\omega > 0$, which implies that intrinsic growth for the auxiliary population is positive. We also can infer positive density dependence for the auxiliary population, as $\lambda^Y > 0$. Positivity of the mean parameters, μ_ω and μ_λ , implies that the target population has both positive intrinsic growth and density-dependence. Finally the standard deviation parameters indicate that across groups there is small variation around these mean values, as determined by (7.3.2). For scenarios 1-3 the values of γ , μ_ψ and μ_δ respectively indicate that predator groups have a negative effect on prey abundance, that the prey has a net positive effect on predator group abundance, and that predator groups have a net negative effect on other predator group abundances.

For scenarios 1, 2, 4 and 5 we used 20,000 iterations, a thinning rate of 20 and burn-in of 2000. For scenario 3, as this was the highest resolution of our simulated data scenarios, we used 40,000 iterations, a thinning rate of 40 and burn-in of 4000, so to ensure HMC chain convergence. For each simulation scenario we let $Y_0 = 10,000$ and for each X_{i0} we sampled random values from a discrete uniform distribution $U(1, 20)$. Initial conditions were simulated once and fixed for all simulation scenarios. Three examples of simulated time series are given in Fig. 7.2, for scenarios 2, 4 and 5. In each plot we show time series for 3 groups (main) and the auxiliary population (inset).

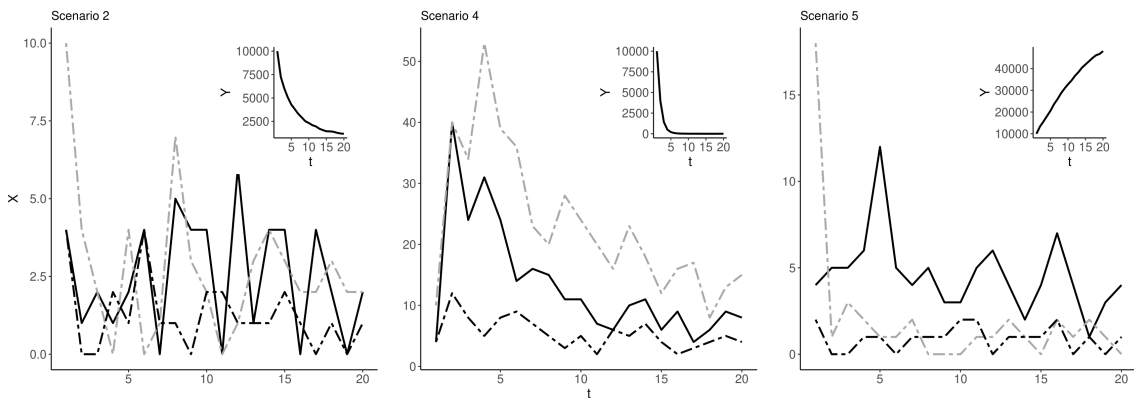


Figure 7.2: Three randomly selected time series of three groups (main) and the auxiliary population (inset) for scenarios 2, 4 and 5.

The accuracy of parameter estimates was assessed by calculating the root mean square error (RMSE), bias and relative bias over all 100 simulations. Let θ be a true (known) parameter and $\hat{\theta}_i$ an estimate of the posterior mean for simulation $i \in \{1, \dots, n\}$. We define

RMSE over n simulations as

$$\text{RMSE} := \sqrt{\frac{\sum_{i=1}^n (\hat{\theta}_i - \theta)^2}{n}}.$$

We respectively define bias (B_i) and relative bias (RB_i) for the i th simulation as

$$\begin{aligned} B_i &:= \hat{\theta}_i - \theta, \\ \text{RB}_i &:= \frac{B_i}{\theta}, \end{aligned}$$

given that $\theta \neq 0$. RMSE assesses how close our predicted values are to the true values. The lower RMSE is the closer our estimates are to the true simulated parameters. We also used bias and relative bias as other accuracy measures. Bias and relative bias, in our context, measure the difference and scaled difference between the mean obtained from a large number of simulations and our true parameter value. Using all three of these measures will help us understand how well our parameters are estimated. For all scenarios the RMSE for parameter estimates can be seen in Table 7.2. We clearly see an improvement of parameter estimation, via lower values of RMSE, as our sample size increases from scenarios 1 to 3, with some possible small exceptions. The RMSE for μ_ω gets smaller as sample size increases but remains relatively large in scenario 3 at 0.406. For scenarios 4 and 5 we see that in general RMSE is quite low, except for μ_ω in scenario 4. This large value could be due to the high variability of our parameter estimates, as indicated by the boxplots in Fig. 7.8 – 7.12, which we will discuss next.

Parameter	Scenario				
	1	2	3	4	5
ω^Y	0.061	0.057	0.059	0.053	0.272
λ^Y	0.009	0.008	0.007	0.004	0.015
γ	0.011	0.008	0.006	0.005	0.025
μ_ω	0.784	0.472	0.406	1.187	0.135
μ_λ	0.129	0.064	0.078	0.068	0.042
μ_ψ	0.120	0.079	0.102	0.099	0.028
μ_δ	0.088	0.055	0.027	0.091	0.007
σ_ω	0.147	0.060	0.069	0.089	0.060
σ_λ	0.109	0.066	0.044	0.069	0.031
σ_δ	0.011	0.012	0.014	0.014	0.007
σ_ψ	0.015	0.015	0.019	0.024	0.012

Table 7.2: RMSE for posterior mean estimates in scenarios 1 – 5 calculated across 100 different simulations.

For bias and relative bias we plotted boxplots, with medians and outliers, as can be seen in Fig. 7.8 – 7.12 in the Appendix. In all the scenarios the boxplots for bias and relative bias have medians close to 0, relative to the boxplot of μ_ω , which has quite a high variance.

Issues arise however with the biases for the intercept mean in scenario 5, as data resolution increases. We therefore plotted bivariate plots of our HMC draws in order to see if there was any confounding between parameters (see Fig. 7.13 – 7.15 in the Appendix for a single simulation for scenarios 1 – 3 as an example of such confounding, as an example). In some simulation runs for scenarios 1 – 3 we saw slight confounding between ω^Y and λ^Y , and between μ_δ and μ_ω , which indicates that these parameters are sometimes slightly biased and there may be slight identifiability issues, as already indicated through the larger RMSE values for μ_ω . We do not include bivariate plots for these in the Appendix. Overall, more work would be needed to further elucidate the causes of such partial confounding. However, we found that such confounding reduced (lower correlation) as the sample size increased, showing that larger resolution of data results in less biased estimation (see Fig. 7.13 – 7.15 for an example).

Bias is relatively low for most of our parameters, indicating that under all of these scenarios of interest our estimation procedure is reasonable accurate in estimating such parameter values. The overall low RMSE values and low bias values indicates that our estimates are somewhat close to their true values, with some issues for specific parameters. In particular, μ_ω and μ_λ stand out as being particularly problematic, which suggests confounding between these parameters within our model. In order to better understand the underlying issues with the estimation procedure, one could look at the coverage of the credible intervals. Where the bias of some parameters is high one may observe that the credible interval coverage is poor. For example, some of the variance components are also slightly biased, based on the relative bias boxplots, especially σ_ψ . To address this further, one could also increase the number of simulations, while altering the HMC set-up so to get better chain convergence. To address confounding, between ω^Y and λ^Y for example (see Fig. 7.13 – 7.15), one could also look at the posterior mean values from each of the simulation replicates and plot these as scatter plots to assess the potential lack of orthogonality in parameter estimates.

7.5. Predator-Prey Dynamics: A Case Study

We will now apply our model to a case study, namely the predator-prey dynamics of grey wolves (*Canis lupus*) and elk (*Cervus canadensis*) in Yellowstone National Park (YNP) over 20 years. Since the reintroduction of grey wolves to YNP and the surrounding areas in 1995, wolf and elk populations have been thoroughly monitored in order to assess ecosystem responses [34]. Thus a lot is known about their predator-prey relationship and, more generally, the ecological processes that affect these populations. We chose this predator-prey system as we can verify our model results with the empirical work that has been undertaken in YNP over this long study period. Predation is one of several regulatory

factors of elk population growth in YNP [254]. By applying predator-prey theory, in [277] the authors predicted that elk abundance would decrease to a low equilibrium state following wolf reintroduction. Many studies have questioned how significant this predation effect has been [222]. However there is general consensus that wolf predation is largely density-dependent, with stronger dependence attributed wolf density [280].

It has been observed that the rate of predation of wolf packs can remain constant even when elk densities are declining, suggesting that at certain times the functional response (the intake rate of a predator as a function of prey density) of wolves may just be a linear function of prey abundance [132]. Intra-pack and inter-pack competition also has a substantial effect on hunting efficiency and prey acquisition by wolf packs [46]. This suggests that studying pack dynamics in this context is vital to understand how social animals behave over time.

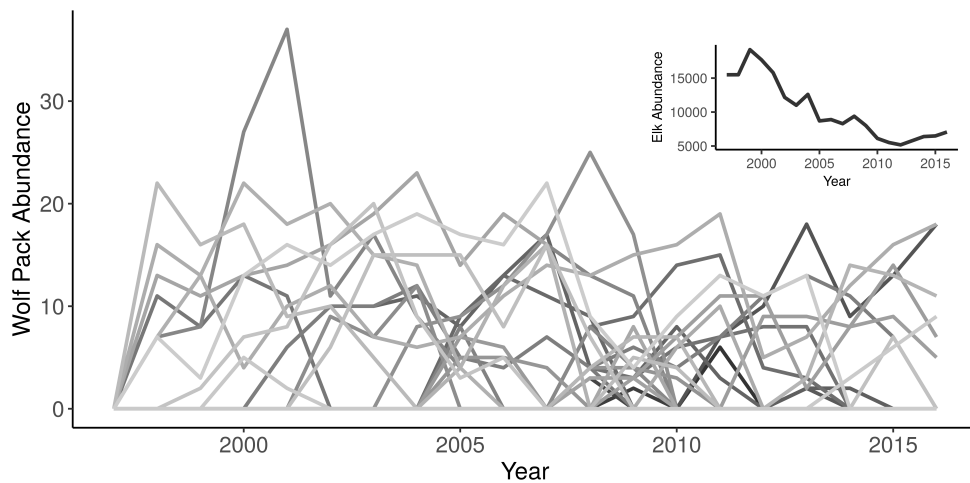


Figure 7.3: Wolf pack (main) and elk (inset) abundances in YNP from 1996-2016. Each grey line represents one pack abundance time series.

Annual predator and prey observational abundance data was obtained from [37] (see Fig. 7.3). Yearly abundance data for grey wolf packs from YNP were collated over 20 years using observational studies and field research. As noted by [37], in the dataset, the group membership and composition of packs is known. For our framework, we therefore assume that we have perfect detection, i.e. we do not have an additional process that explicitly takes account of the uncertainty of abundance measurement. In Chapter 8 we expand on this in more detail.

7.5.1. Group Formation and Splitting

Grey wolf packs are known to form and disband over time via natal or breeding dispersal [254]. They are largely territorial with overlapping spatial ranges. However, wolf

packs tend to avoid neighbouring packs, in order to minimise aggressive interactions and mortality [154]. We assume that once a pack forms, its abundance stays positive until it splits, and thereafter its abundance is zero. Note that this is different to the model in our simulation studies in Section 7.4, where groups have the possibility to reform once they have disbanded. In order to account for pack formation and splitting we modify (7.3.6) to become

$$X_{i,t}|w, \mathcal{H}_{t-1} \sim \mathcal{P}\left(\mu_{i,t}^X C(X_{i,t})\right),$$

$$C(X_{i,t}) := \underbrace{\mathbb{I}_{\mathbb{N}}\{X_{i,t-1}\}}_{A(X_{i,t})} + \underbrace{\mathbb{I}_0\left\{\sum_{k=0}^{t-1} X_{i,k}\right\}}_{B(X_{i,t})},$$

for $t \geq 1$, where $\mu_{i,t}^X$ is the same as in (7.3.6). For $S \subset \mathbb{Z}_+$ and $t \geq 1$ we define

$$\mathbb{I}_S\{Z\} := \begin{cases} 1 & \text{if } Z = S, \\ 0 & \text{if } Z \neq S. \end{cases}$$

We set $A(X_{i,0}) = 1 - B(X_{i,0}) = 1$ so that $C(X_{i,0}) = 1$. Consider $X_{k,t}$ for some fixed $k \in \{1, \dots, g\}$ and $t \geq 1$. Our model is first-order Markovian. So at time t , we assume that we know the state $X_{k,t-1}$. If a pack has not formed up to time t , i.e. $X_{k,s} = 0$ for $s < t$, then there is still opportunity for pack emergence. We thus want to include such zero abundance observations in our extended framework. Instead, if a pack has split at time t , i.e. $X_{k,s} = 0$ for $s > t$, then we know it will not form again. Thus we want to ignore these zero abundance observations. We include an illustrative example of how the indicators A and B respectively correspond to pack formation and splitting in Table 7.3, reflecting the data structure in question.

In the wolf-elk data-set obtained from [37], observations of lone wolves (members of no packs) and transient packs (groups existing for less than two consecutive months) were removed by the authors. Therefore we do not want to model (non-group) events such as these. We will discuss possibilities for extending our model to include such structure in Chapter 8.

7.5.2. Results and Interpretation

Parameter posterior mean estimates can be seen in Table 7.4, along with their respective 95% credible intervals (CIs). We can interpret our parameter estimates in the context of this wolf-elk system as characterising how each group/population is affected by the other over the observation period. Using Bayesian models for inferential purposes means we must test for parameter identifiability. Weakly identifiable models are subsets of

parameter redundant models, and can therefore aid us in knowing when our model is unidentifiable [53]. It is important to know whether parameters are identifiable when the focus is interpreting parameter estimates, for example to infer interaction strengths. This is because we would like to know if these accurately capture the behaviour of the system in question.

t	X_t	$A(X_t)$	$B(X_t)$	$C(X_t)$
0	0	0	1	1
1	0	0	1	1
2	3	0	1	1
3	10	1	0	1
4	5	1	0	1
5	0	1	0	1
6	0	0	0	0
7	0	0	0	0

Table 7.3: Example of how A and B allow for group formation and splitting, where X_t is a count random variable at time $t \geq 0$.

Suppose $f(\theta|y)$ is the marginal posterior distribution for a parameter, θ , and $\pi(\theta)$ the prior distribution assigned to θ . Recall, from Chapter 3, that θ is weakly identifiable if $f(\theta|y) \approx \pi(\theta)$. As also outlined in Chapter 3, by plotting the prior-posterior overlap (PPO), or by computing this overlap via kernel density estimation, we can deduce whether their model is weakly identifiable [53]. For this case study we looked at the prior-posterior overlap for each of our estimates. These can be seen numerically in Table 7.4 and graphically in Fig. 7.4. The largest observed overlap was $7.5\% < \tau$, where $\tau = 35\%$ is the recommended (ad hoc) threshold value given in [97]. If we have that the prior-posterior percentage overlap for each parameter is above this threshold, then that parameter is said to be weakly identifiable, i.e. the data does not provide us with more information than the priors alone, and thus the model is unidentifiable. As all of our parameters have sufficiently small prior-posterior overlap, we can conclude that our model is identifiable, giving us stronger justification for interpreting our parameter estimates.

In YNP, elk undergo habitat selection so as to avoid wolf predation in the summer. In winter, they use other strategies, like grouping, to avoid predation, thus altering their seasonal distribution in direct response to predator presence [188]. For elk, the estimated intercept, $\hat{\omega}^Y$, and autoregressive parameter, $\hat{\lambda}^Y$, suggest that elk intrinsic growth was positive and the net intraspecific effect of changes in elk abundance was also positive over the study period. This suggests a positive coupling between elk abundance and growth. Many mammals, such as ungulates, are known to exhibit irruptive or boom-bust type dynamics, i.e. short term increases in abundance followed by rapid decline [78]. This is in line with our findings, suggesting that elk mean growth was positive with negative

density-dependence hindering this population from increasing in abundance. Perhaps this density dependence played a more significant role as the population reached higher values, when also coupled with other factors, thus reducing the overall population to a much lower level near the end of our study period. Negative density-dependence is known to be caused by predation and competition for resources [222].

Parameter	Estimate	95% CI	PPO (%)	Interpretation
ω^Y	0.85	[0.74, 0.96]	0.20	Elk intrinsic growth
λ^Y	0.91	[0.90, 0.93]	0.00	Elk intraspecific effect
γ	-0.02	[-0.03, -0.02]	0.00	Effect of wolf on elk
μ_ω	10.32	[4.05, 17.70]	7.50	Wolf mean growth rate
μ_λ	0.50	[0.29, 0.69]	0.40	Wolf intra-pack net effect
μ_ψ	1.14	[0.56, 1.84]	0.90	Wolf inter-pack net effect
μ_δ	-1.74	[-2.55, -1.06]	1.20	Net effect of elk on wolves
σ_ω	15.24	[9.93, 21.92]	6.90	Wolf growth rate variability
σ_λ	0.46	[0.28, 0.7]	0.30	Wolf intra-pack variability
σ_ψ	1.41	[1.20, 2.58]	1.10	Wolf inter-pack variability
σ_δ	1.80	[0.83, 2.19]	1.10	Auxiliary net effect variability

Table 7.4: Parameter posterior mean estimates, with their respective 95% credible interval (CI), prior-posterior overlap (PPO) and interpretations for YNP wolf-elk case study.

We interpret $\hat{\gamma}$ as the net effect of changes in wolf abundance on elk. Some authors have suggested that the influence of predation pressure on declining elk population has been overemphasised, with hunting pressure and drought, for example, having a substantially larger effect [222]. Our results suggest that $\hat{\gamma}$ is negative, indicating that increases in the wolf population abundances has had a negative net effect on the elks mean process. The magnitude of this negative effect may suggest that over this 20 year period wolf related processes, such as predation, may not have been the dominant cause of elk abundance reduction.

We can see that $\hat{\mu}_\omega$ and $\hat{\sigma}_\omega$ are both large compared to the other parameter estimates. This may suggest that there was a high wolf population mean growth rate, with large variability, over the study period. The wide credible intervals suggest high variability, as in the simulation studies, suggests that these may be difficult to estimate. Their values suggests that individual wolf pack abundance, across the whole study period, has increased significantly since reintroduction, with increases varying in magnitude across packs. This can be seen by the cyclic rise and fall of wolf pack abundances across the study period. Pack size is known to be a major determinant of hunting success, with this success varying with prey type [254]. Small wolf pack sizes result in low prey consumption, but also low kill rates, meanwhile large pack sizes result in both high kill rates and consumption [286]. Pack composition is also an important aspect, due to quantitative benefits such as hunting

success and negative consequences when acquiring resources, such as free-riding. For example, packs with a larger proportion of older members or adult males have a greater chance of winning in aggressive interactions, even though they may have a quantitative disadvantage [46]. The value of $\hat{\mu}_\lambda$ suggests a net positive pack response to increasing pack abundances over the study period, which suggests positive density-dependence, as for the elk.

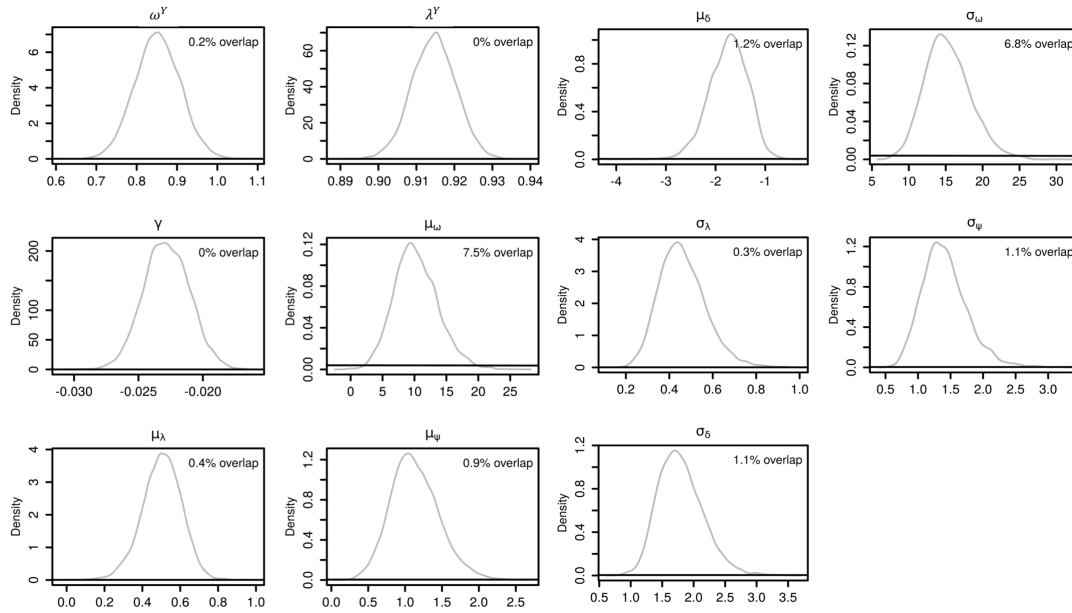


Figure 7.4: Prior- posterior overlap for fixed effects and hyperparameters. The black curve is the prior distribution and grey curve is estimated posterior density. We set $\theta_\mu \sim \mathcal{N}(0, 100^2)$ for $\theta_\mu \in M \cup \{\omega^Y, \lambda^Y, \gamma\}$ and $\theta_\sigma \sim \mathcal{N}^+(0, 100^2)$, for $\theta_\sigma \in \Sigma$.

As $\mu_\psi = 1.14 > 0$, this suggests that there was net positive inter-pack response to increasing pack abundances, with moderate variation around this population mean as seen via σ_ψ . Even though wolf packs are highly territorial, our model might not capture this fully as we are not taking into account that some packs may rarely come into contact with one another, due to low overlapping ranges. It has been noted however that the specific location of the aggressive interaction in relation to pack territories has little to no effect on inter-pack interaction outcomes. Thus the relationship of aggressive interactions to spatial location is quite heterogeneous over time. The interactions of two packs may benefit each of them, perhaps via indirect mutualism (where multiple species benefit from each other's presence indirectly through the presence of another set of species or through environmental factors, rather than through direct interspecies interactions) [276], at specific times depending on pack composition [46].

The value of $\hat{\mu}_\delta$ has multiple interpretations. As a first interpretation it may suggest that there was weak elk predation, with moderate variation around this population mean as

seen via $\hat{\sigma}_\delta$. This magnitude being interpreted as weak is somewhat subjective and is inferred from the following reason. Grey wolves are generalists and so have multiple prey types at any given time. They can also undergo prey switching when certain prey types become scarce [227]. As optimal foraging theory suggests, wolves have a preference for elk, but this decreases as total prey abundance available declines. Prey selection by wolves has been shown to be primarily determined by the within-population vulnerability of elk, where wolves tend to minimise risk of harm from predation [139]. Grey wolves can also shift from hunting to scavenging when their primary prey become rare [261]. Secondly, the percentage of elk hunted by wolf packs has remained around 5% per year despite elk numbers decreasing significantly over the 20 year study period, following an initial increase in elk abundance [254]. This observation and the fact that total wolf abundance rapidly increased up to 2007 and then fell slightly, saturating at around 100 wolves, could also explain the negative mean estimate. The second interpretation is that this parameter may not capture direct predation. Increases in the elk population, at certain times, could have coincided with decreases in the wolf population, thus suggesting that the effect of increasing elk is negative. As in classical predator-prey theory, there are times when predator abundance will be decreasing as prey abundance increases, as there is a delay effect on their dynamics. After 2007, when the overall wolf population was around 170 individuals, abundance decreased significantly and fluctuated close to 100 individuals up to 2016 [254]. Following a rapid increase in abundance from 1997, this lulling period may explain why this parameter is low and negative.

We can observe the realisations of the random effects for each pack through violin plots (showing the estimated posterior density with 0.5-quantiles) in Figure 7.5. Some packs, like pack 6 and 19 for example, have medians close to 0 for both ψ_i and δ_i . Meanwhile others, such as pack 23 and 27, have medians below 0 for δ_i and above 0 for ψ_i . Packs 4 and 28, for example, have random effect medians for ψ_i below 0, indicating negative net effects in relation to other packs present in the system. The resolution of time series data was different for each pack, resulting in varying levels of uncertainty around these median values, as seen in the probability density plots of our posterior estimates in Figure 7.5. Even though the population level means for each random effect may have been positive or negative, these effects varied across all 42 packs, showing that our parameters are able to capture inter-pack heterogeneity when explicitly modelling group dynamics. The relationship between packs cannot be reduced to single time-invariant parameter values as in our model. However, our mean estimates do capture the general relationship between wolf packs and elk, with the changes in both elk and wolf abundance having varying net effects on each pack's dynamics.

This predator-prey system, although highly complex, can offer us insight into how species

may interact with one another, while also explicitly modelling the internal structure of one of the species. These findings could explain how some packs have negative net effects to increases in elk abundance, for example. To quote from [98],

"as the elk population declined wolves killed a larger proportion of the population. Such an inverse density-dependent response is destabilizing, however, predator-prey theory suggests that at low prey densities the total response may become density dependent and thus be regulatory, resulting in persistence of the predator-prey system at a lower prey density than realized in the absence of wolves".

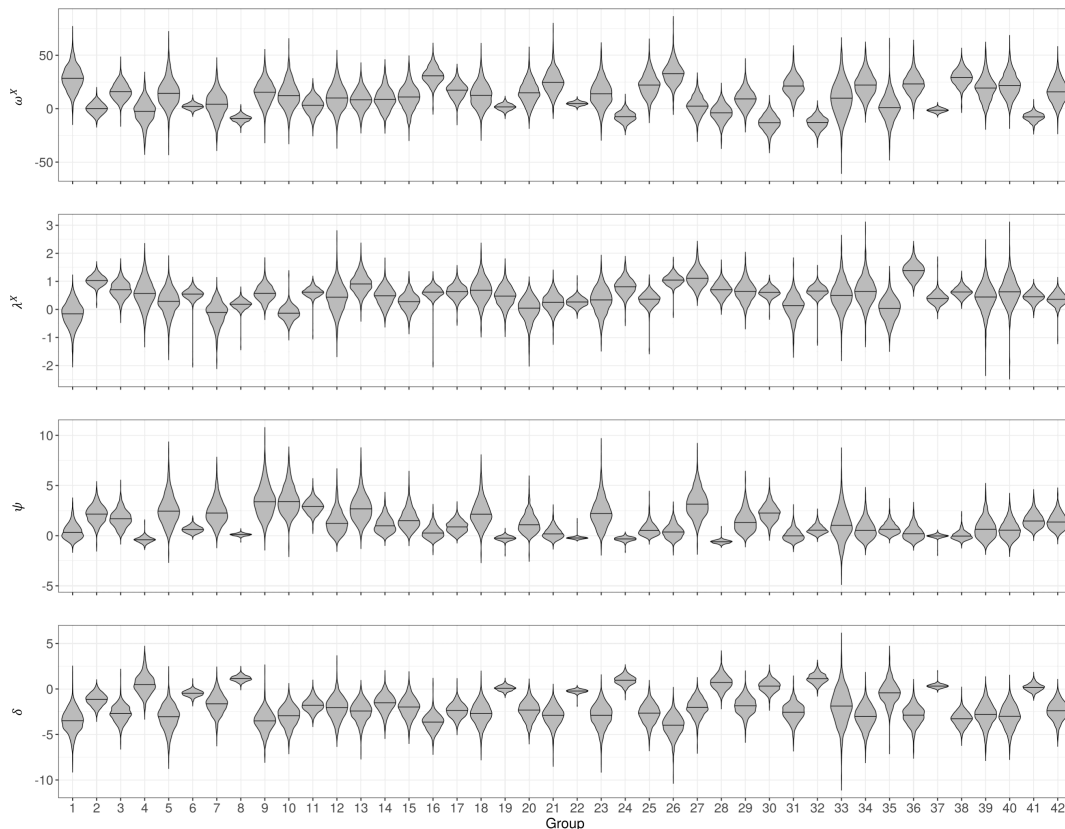


Figure 7.5: Violin plots for $\omega^X := \{\omega_1^X, \dots, \omega_{42}^X\}$, $\lambda^X := \{\lambda_1^X, \dots, \lambda_{42}^X\}$, $\psi := \{\psi_1, \dots, \psi_{42}\}$ and $\delta := \{\delta_1, \dots, \delta_{42}\}$. Each plot shows the posterior density estimates for realisations of the random effects for all 42 wolf packs, with the respective 0.5-quantiles.

7.6. Quantifying Group Interactions

Our modelling framework includes (7.3.7), (7.3.8) and (7.3.11) that respectively capture the effect of changes in abundance of each group with every other group, of each group with an auxiliary population and of an auxiliary population with the main population

of interest. Our aim is to formulate a model that can be used to quantify changes in associations. Our model allows for the modelling of populations where subgroups can disband and reform over time, as is the case with many social animals [217]. As stated in Chapter 3, a crude but effective metric of interactions strength is Pearson's correlation coefficient. In the next section we will discuss such an interaction strength metric in the context of a new, simplified count model. This derivation is a first attempt at deriving such an interaction metric for this type of count time series model.

7.6.1. Correlation Approximation

It is desirable to have analytic results characterising the group correlation structure. However, obtaining such results in the general framework considered thus far is likely to be analytically intractable. To do so would involve deriving the (marginal) temporal group correlation $\rho_{ijt} := \text{Corr}(X_{i,t}, X_{j,t})$, the standard Pearson's correlation between groups i and $j \neq i$ at time t . In order to approximate ρ_{ijt} , by the Law of Total Expectation, we would have to evaluate

$$\begin{aligned} \mathbb{E}[X_{i,t}] &= \mathbb{E}[\mathbb{E}[X_{i,t}|w, \mathcal{H}_{t-1}]] \\ &= \mathbb{E}\left[\exp\left(\omega_i^X + \Lambda_{i,t-1}^X + \Psi_{i,t-1} + \Delta_{i,t}\right)\right] \\ &= \mathbb{E}\left[\exp\left(\omega_i^X\right) (X_{i,t} + 1)^{\lambda_i} \left(\sum_{j \neq i} X_{j,t} + 1\right)^{\psi_i} (Y_t + 1)^{\delta_i}\right]. \end{aligned} \tag{7.6.1}$$

This would involve marginalising the product inside this expectation over w and \mathcal{H}_t . The form of this expectation includes several nonlinearities and approximating it would lead to calculating the expected value of the product of non-independent random variables via sequential Taylor approximations. Even though X_{it} is conditionally Poisson, this does not imply that the marginal distribution of X_{it} is Poisson. In fact it may be a mixture of distributions. This intractability motivated us to approximate ρ_{ijt} under reasonable assumptions. While the general problem seems analytically intractable, it is however possible to derive results which can give insight into the group correlation structure with the addition of some further assumptions. We next outline these assumptions, and show how they allow us to derive an approximation to ρ_{ijt} . Following this, we will then discuss its interpretation as an indicator of interaction, which is in line with the interaction strength metrics as reviewed in [25]. In this section we disregard (7.3.4) and (7.3.5) as being the data generating processes. We will define what these are below for the new model, while emulating the mean process structure of our original model, which will then allow us to derive an approximation of ρ_{ijt} in this context.

Assumption 1: Firstly we assume that

$$\begin{aligned}\ln(Y_t)|w, \mathcal{H}_{t-1} &\sim \mathcal{N}\left(\ln(\mu_t^Y), \ln(\mu_t^Y)\right) \\ \ln(X_{i,t})|w, \mathcal{H}_{t-1} &\sim \mathcal{N}\left(\ln(\mu_{i,t}^X), \ln(\mu_{i,t}^X)\right),\end{aligned}\tag{7.6.2}$$

where $\ln(\mu_t^Y)$ and $\ln(\mu_{i,t}^X)$ are the same as in (7.3.6) and (7.3.9). We assume that both $\ln(X_{i,t})$, $\ln(Y_t)$, $X_{i,t}$ and Y_t have finite moments. Modelling the log of abundance using classical autoregressive models, with standard white noise error, is common in ecological time series analyses [20, 135, 144, 212]. Assuming that the data comes from a log-normal distribution is a somewhat valid assumption when one is modelling multiple species within a community, where there are large population abundances, or, for example, when modelling social animal groups that each comprise hundreds or even thousands of individuals. Recall that

$$\begin{aligned}\ln\left(\mu_{it}^X\right) &= \omega_i^X + \Lambda_{i,t-1}^X + \Psi_{i,t-1} + \Delta_{i,t-1} \\ &= \omega_i^X + \lambda_i^X \ln(X_{i,t-1} + 1) + \psi_i \ln\left(\sum_{j \neq i}^g X_{j,t-1} + 1\right) + \delta_i \ln(Y_{t-1} + 1).\end{aligned}\tag{7.6.3}$$

The elements of $w \cup \mathcal{H}_{t-1}$ are mutually independent. Therefore because of (7.6.3) and the linearity of expectation we have that

$$\begin{aligned}\mathbb{E}[\mathbb{E}[\ln(X_{i,t})|w, \mathcal{H}_{t-1}]] &= \mathbb{E}\left[\omega_i^X + \Lambda_{i,t-1}^X + \Psi_{i,t-1} + \Delta_{i,t-1}\right] \\ &= \mathbb{E}\left[\omega_i^X\right] + \mathbb{E}\left[\lambda_i^X\right] \mathbb{E}[\ln(X_{i,t-1} + 1)] \\ &\quad + \mathbb{E}[\psi_i] \mathbb{E}\left[\ln\left(\sum_{j \neq i}^g X_{j,t-1} + 1\right)\right] \\ &\quad + \mathbb{E}[\delta_i] \mathbb{E}[\ln(Y_{t-1} + 1)].\end{aligned}\tag{7.6.4}$$

Assumption 2: As we are modelling multiple groups of the same species, we further assume a *Heterogeneous Compound Symmetry* (HCS) conditional variance-covariance structure [265, 287], similar to when analysing repeated measurements of clustered data. That is, for $\sigma_{it}^2 := \text{Var}(X_{i,t}|w, \mathcal{H}_{t-1})$, we are assuming that

$$\text{Cov}(X_{i,t}, X_{j,t}|w, \mathcal{H}_{t-1}) = \rho_t \sigma_{it} \sigma_{jt}\tag{7.6.5}$$

where we have that $\rho_{ijt} = \rho_t \in [-1, 1]$ for all $i, j \in \{1, \dots, g\}$, $i \neq j$.

Assumption 3: Deriving the expectation of non-linear functions of random variables can lead to complicated expressions of covariance and correlations. For X a nonnegative random variable with finite moments, we approximate the marginal expectation of $f(X) :=$

$\ln(X + 1)$ using a second order Taylor expansion around $\mathbb{E}[X]$ [45]. We thus have that

$$\mathbb{E}[\ln(X + 1)] \approx f(\mathbb{E}(X)) + \frac{f''(\mathbb{E}(X))}{2} \text{Var}(X) \quad (7.6.6)$$

$$= \ln(\mathbb{E}(X) + 1) + \frac{\text{Var}(X)}{2(\mathbb{E}(X) + 1)^2}. \quad (7.6.7)$$

Assumption 4: Finally, we assume that (7.6.2) satisfies

$$\begin{aligned} \mathbb{E}[\ln(Y_t)|w, \mathcal{H}_{t-1}] &= \ln(\mu_t^Y) \equiv \ln(\mu^Y) \in \mathbb{R}, \\ \mathbb{E}[\ln(X_{i,t})|w, \mathcal{H}_{t-1}] &= \ln(\mu_{i,t}^X) \equiv \ln(\mu_i^X) \in \mathbb{R} \end{aligned}$$

for $i \in \{1, \dots, g\}$, what we will refer to as *conditional constancy*. This then implies that $\rho_t \equiv \rho \in [-1, 1]$, i.e. we are essentially calculating the net group associations/interactions within a population over the time horizon $[0, T]$. This final main assumption is purely a technical one, which will allow us to derive a tractable approximation to the marginal correlation structure between groups. Note that conditional constancy may arise in simpler models such as white noise or moving average models. For $\ln(Z) \sim \mathcal{N}(\mu_z, \sigma_z^2)$, it is well known that

$$\mathbb{E}[Z] = \exp\left(\mu_z + \frac{\sigma_z^2}{2}\right), \quad (7.6.8)$$

$$\text{Var}(Z) = \exp\left(2\mu_z + \sigma_z^2\right) \left(\exp\left(\sigma_z^2\right) - 1\right).$$

It follows from (7.6.2) and (7.6.8) that

$$\mathbb{E}[X_{i,t}|w, \mathcal{H}_{t-1}] = \exp\left(\frac{3 \ln(\mu_i^X)}{2}\right) = \left(\mu_i^X\right)^{\frac{3}{2}}. \quad (7.6.9)$$

Conditional constancy, the Law of Total Expectation and (7.6.9) imply that

$$\mathbb{E}[X_{i,t}] = \mathbb{E}\left[\mathbb{E}[X_{i,t}|w, \mathcal{H}_{t-1}]\right] = \left(\mu_i^X\right)^{\frac{3}{2}}, \quad (7.6.10)$$

where we use the fact that $\mathbb{E}[a] = a$ for $a \in \mathbb{R}$. It follows from (7.6.8), (7.6.10) and the Law of Total Variance [157] that

$$\begin{aligned} \text{Var}(X_{i,t}) &= \mathbb{E}\left[\text{Var}(X_{i,t}|w, \mathcal{H}_{t-1})\right] + \text{Var}\left(\mathbb{E}[X_{i,t}|w, \mathcal{H}_{t-1}]\right) \\ &= \mathbb{E}\left[\exp\left(2 \ln\left(\mu_i^X\right) + \ln\left(\mu_i^X\right)\right) \left(\exp\left(\ln\left(\mu_i^X\right)\right) - 1\right)\right] + \text{Var}\left(\left(\mu_i^X\right)^{\frac{3}{2}}\right) \\ &= (\mu_i^X - 1)(\mu_i^X)^3 =: V_i^X. \end{aligned} \quad (7.6.11)$$

In (7.6.11) we use the fact that the variance of a constant is zero. Analogous expressions for the expectation and variance of Y_t follow similarly. Similarly define $V^Y := (\mu^Y - 1)(\mu^Y)^3$.

It follows from (7.6.5), (7.6.10) and the Law of Total Covariance [157] that

$$\begin{aligned}
 \text{Cov}(X_{i,t}, X_{j,t}) &= \mathbb{E} \left[\text{Cov} (X_{i,t}, X_{j,t} | w, \mathcal{H}_{t-1}) \right] \\
 &\quad + \text{Cov} (\mathbb{E} [X_{i,t} | w, \mathcal{H}_{t-1}] \mathbb{E} [X_{j,t} | w, \mathcal{H}_{t-1}]) \\
 &= \mathbb{E} \left[\rho \sqrt{V_i^X V_j^X} \right] + \text{Cov} \left(\left(\mu_i^X \right)^{\frac{3}{2}}, \left(\mu_j^X \right)^{\frac{3}{2}} \right) \\
 &= \rho \sqrt{V_i^X V_j^X}.
 \end{aligned} \tag{7.6.12}$$

The well known Bienaymé's identity [157] states that for a set of random variables $\{Z_1, \dots, Z_n\}$ with finite moments,

$$\text{Var} \left(\sum_{i=1}^n Z_i \right) = \sum_{i=1}^n \text{Var}(Z_i) + \sum_{\substack{i,j=1 \\ i \neq j}}^n \text{Cov}(Z_i, Z_j). \tag{7.6.13}$$

It then follows from (7.6.11), (7.6.12) and (7.6.13) that

$$\text{Var} \left(\sum_{j \neq i}^g X_{j,t} \right) = \sum_{j \neq i}^g V_j^X + \rho \sum_{\substack{k,j \neq i \\ k \neq j}}^g \sqrt{V_j^X V_k^X}, \tag{7.6.14}$$

for a fixed $i \in \{1, \dots, g\}$. By the Law of Total Expectation, we have that

$$\mathbb{E}[\ln(X_{i,t})] = \mathbb{E}[\mathbb{E}[\ln(X_{i,t}) | w, \mathcal{H}_{t-1}]] \tag{7.6.15}$$

for all $t \in [0, T]$. Using (7.6.15) and our conditional constancy assumption we will now approximate $\ln(\mu_{it}^X)$ by letting the final expression in (7.6.4) be approximately equal to $\ln(\mu_i^X)$. Without our assumptions it may not be true that $\mathbb{E}[\ln(X_{i,t})]$ can be approximated by a constant. Despite this, as a first port of call in deriving the marginal expectations and variances, we will, under our four main assumptions, use our simplified expression as an approximation. We already know the random effects, given by (7.3.2), are Gaussian with their respective means and variances given in (7.3.3). Using (7.6.14), (7.6.15), (7.6.4) and our Taylor approximation (7.6.6) we get that

$$\begin{aligned}
 \ln(\mu_i^X) &\approx \mu_\omega + \mu_\lambda \left(\ln \left(\left(\mu_i^X \right)^{\frac{3}{2}} + 1 \right) + \frac{V_i^X}{2 \left(\left(\mu_i^X \right)^{\frac{3}{2}} + 1 \right)^2} \right) \\
 &\quad + \mu_\psi \ln \left(\sum_{j \neq i}^g \left(\mu_j^X \right)^{\frac{3}{2}} + 1 \right) + \mu_\delta \left(\ln \left(\left(\mu^Y \right)^{\frac{3}{2}} + 1 \right) + \frac{V^Y}{2 \left(\left(\mu^Y \right)^{\frac{3}{2}} + 1 \right)^2} \right) \\
 &\quad + \frac{\mu_\psi}{2 \left(\sum_{j \neq i}^g \left(\mu_j^X \right)^{\frac{3}{2}} + 1 \right)^2} \left(\sum_{j \neq i}^g V_j^X + \rho \sum_{\substack{k,j \neq i \\ k \neq j}}^g \sqrt{V_j^X V_k^X} \right).
 \end{aligned}$$

We can then solve for ρ which gives

$$\rho \approx \tilde{\rho} = -\frac{A_i}{\mu_\psi} - \frac{\mu_\delta B_i}{\mu_\psi} - C_i, \quad (7.6.16)$$

for each $i \in \{1, \dots, g\}$, where

$$\begin{aligned} A_i &:= -D_i \left(\ln(\mu_i^X) - \mu_\omega - \mu_\lambda \left(\ln \left((\mu_i^X)^{\frac{3}{2}} + 1 \right) + \frac{V_i^X}{2 \left((\mu_i^X)^{\frac{3}{2}} + 1 \right)^2} \right) \right), \\ B_i &:= D_i \left(\ln \left((\mu^Y)^{\frac{3}{2}} + 1 \right) + \frac{V^Y}{2 \left((\mu^Y)^{\frac{3}{2}} + 1 \right)^2} \right), \\ C_i &:= \frac{\sum_{j \neq i}^g V_j^X + \ln \left(\sum_{j \neq i}^g (\mu_j^X)^{\frac{3}{2}} + 1 \right) \left(2 \left(\sum_{j \neq i}^g (\mu_j^X)^{\frac{3}{2}} + 1 \right)^2 \right)}{\sum_{\substack{k, j \neq i \\ k \neq j}}^g \sqrt{V_j^X V_k^X}}, \\ D_i &:= \frac{2 \left(\sum_{j \neq i}^g (\mu_j^X)^{\frac{3}{2}} + 1 \right)^2}{\sum_{\substack{k, j \neq i \\ k \neq j}}^g \sqrt{V_j^X V_k^X}}. \end{aligned}$$

7.6.2. Theoretical Interpretation

We interpret $\tilde{\rho}$ as the approximate net group correlation. In order for (7.6.2) to be well defined we assume that $\mu_i^X, \mu^Y > 1$ for all $i \in \{1, \dots, g\}$. This is so the standard deviation terms in (7.6.2) are nonnegative. We also have that

$$\mu_i^X > 1 \implies V_i^X = (\mu_i^X - 1)(\mu_i^X)^3 > 0,$$

and similarly for V^Y . Therefore we have that both C_i and D_i are well defined. In order for $\tilde{\rho}$ to be well defined we assume that $\mu_\psi \neq 0$. In practice, elements of M will not be exactly 0 and so this is reasonable to assume.

As $\tilde{\rho}$ is not indexed by i or t , we thus have g approximations to the net interactions between groups over $[0, T]$. If our underlying assumptions are correct, these should be consistent and not vary significantly. This simple observation gives us a way of testing our assumptions and, where these appear to be valid, we could potentially combine the independent approximations to obtain an improved estimate of the net group correlation. We also note that since this approximation is based on a second-order Taylor expansion

around zero, and other simplifying assumptions, $\tilde{\rho}$ may not be contained within $[-1, 1]$ for certain parameter and mean values. However, should the assumptions hold, this approximation would be an informative measure of net group interactions. In practice, if this approximation resulted in $\tilde{\rho}$ being slightly outside of $[-1, 1]$ we could, for example, take the approximate net group correlation as being given by

$$\tilde{\rho}^* := \begin{cases} 1, & \text{if } \tilde{\rho} > 1 \\ \tilde{\rho}, & \text{if } \tilde{\rho} \in [-1, 1] \\ -1, & \text{if } \tilde{\rho} < -1. \end{cases}$$

As our approximation assumes conditional constancy, it would not be appropriate for the simulation study (see Fig. 7.2) or wolf-elk case study (see Fig. 7.3). In the wolf-elk application we also include a pack formation-splitting data process, which for certain i and t can result in X_{it} being modelled by a degenerate Poisson distribution. Instead, for illustrative purposes we will theoretically interpret $\tilde{\rho}$ in the context of a general predator-prey system, i.e. Y is a population of prey and X is a population of predator groups.

In practice, the signs of the elements of M can be either positive or negative. Note that we exclude the cases where the parameters in M can be zero. Therefore, there are $2^{|M|} = 2^4 = 16$ possible positive-negative parameter combinations. The magnitude of these values can also result in additional scenarios to discuss. So, for brevity and illustrative purposes, we will look at four ecologically meaningful scenarios. We will discuss how the intraspecific and auxiliary coupling parameters (μ_ψ and μ_δ) play a role in determining the sign of $\tilde{\rho}$. In each scenario we assume that $\mu_\omega > 0$ (positive population-level intrinsic growth) and $\mu_\lambda \geq 1$ (positive population density dependence).

Clearly $0 < x < 1$ implies that $\ln(x) < 0$. By monotonicity of \ln ,

$$x > 1 \implies \ln\left(x^{\frac{3}{2}} + 1\right) > \ln(x + 1) > \ln(x) > 0.$$

For $\mu_\lambda \geq 1$, it is then clear to see that

$$\ln(x) - \mu_\lambda \ln\left(x^{\frac{3}{2}} + 1\right) < 0, \tag{7.6.17}$$

for all $x > 0$. It then follows that

$$\mu_i^X, \mu^Y > 0 \implies D_i, A_i, B_i, C_i > 0,$$

for all $i \in \{1, \dots, g\}$. From Fig. 7.6 we can see that if $\mu_\psi > 0$, for each $i \in \{1, \dots, g\}$,

$$\tilde{\rho} > 0 \iff A_i + \mu_\delta B_i + \mu_\psi C_i < 0$$

$$\tilde{\rho} < 0 \iff A_i + \mu_\delta B_i + \mu_\psi C_i > 0,$$

and if $\mu_\psi < 0$, for each $i \in \{1, \dots, g\}$,

$$\tilde{\rho} > 0 \iff A_i + \mu_\delta B_i + \mu_\psi C_i > 0$$

$$\tilde{\rho} < 0 \iff A_i + \mu_\delta B_i + \mu_\psi C_i < 0.$$

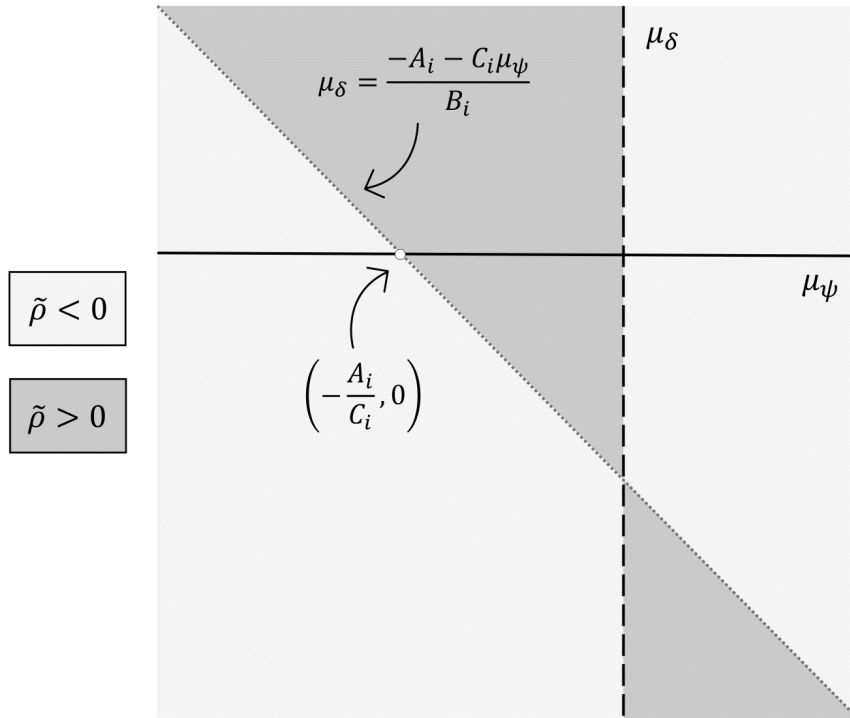


Figure 7.6: Illustration of the μ_ψ - μ_δ parameter space for some fixed $i \in \{1, \dots, g\}$, treating all parameters except μ_ψ and μ_δ as known and fixed. Dark (light) grey shaded areas indicate where $\tilde{\rho} > 0$ ($\tilde{\rho} < 0$). The grey dotted line represents the line $-A_i - \mu_\delta B_i - \mu_\psi C_i = 0$. The black dashed line indicates that $\mu_\psi \neq 0$ (by assumption). The white circle is the point $(\mu_\psi, \mu_\delta) = (-A_i/C_i, 0)$.

Scenario 1: First, suppose $\mu_\delta, \mu_\psi > 0$. The sign of μ_ψ suggests that the effect of increasing group abundance has a net benefit to the mean processes of each group. The prey coupling and benefit of increasing group abundance will be stronger as both of these parameters become large in magnitude. This may arise, for example, in a scenario where the overall predator population is sufficiently large, inter-group responses to increases in predator abundance is strong and the predator is a specialist, i.e. monitors prey availability and is sensitive to abundance changes in their primary prey [8]. As (7.6.17) holds we have that $\mu_\psi, \mu_\delta > 0$ implies that $\tilde{\rho} < 0$ irrespective of the magnitudes of μ_δ and μ_ψ . The sign of μ_δ suggests that there is a positive coupling between predator groups and their prey. Depending on the values of the constant means of the groups in X and Y , the magnitude of $\tilde{\rho}$ will vary. Therefore these group responses may still result in either weak ($\tilde{\rho} \approx 0$) or strong ($\tilde{\rho} \ll 0$) negative interactions. There also could be multiple prey types, for each group. This in turn can allow for a strong numerical response, i.e. a strong change in

predator abundance as a function of change in prey abundance [24]. Even though $\mu_\psi > 0$, which may suggest positive pack correlations, the negative $\hat{\rho}$ could be due to high group numbers and therefore high prey competition, resulting in $C_i \gg 0$, for example.

Scenario 2: Assume $\mu_\psi < 0$. We have two cases to consider for the sign of μ_δ .

(a) Suppose $\mu_\delta > 0$. As is the case in Scenario 1, this means there is a positive coupling between the predator population and their prey. With $\mu_\psi < 0$, the sum of the expression involving A_i and the remaining terms involving B_i and C_i can result in either positive or negative $\tilde{\rho}$ (see Fig. 7.6). For example, if $\mu^Y \gg 0$, a situation may arise where the positivity of the first term dominates the negativity of the sum of the other terms, resulting in $\tilde{\rho} > 0$. This may arise, for example, in a scenario where there is specialist predation and strong inter-group responses to changes in predator abundance (potentially due to strong competition). This can still result in positive interactions among groups, with the prey-coupling potentially compensating for the negative effects of inter-group changes in abundance. This could be explained, for example, by hunting cooperation among certain groups [6]. On the other hand, if there are a larger number of predator groups, we could have that

$$-C_i \ll 0 \implies \tilde{\rho} < 0,$$

as in Scenario 1. This may arise in a situation where there are negative interactions at higher group densities, where strong prey-coupling compensates for the large negative effects of overcrowding, for example. This has been shown mathematically in [145] for a particular spatial model of prey-taxis (where predators have a tendency to move toward regions of highest prey density).

As an example, suppose we observe two groups, X_1 and X_2 , along with their prey Y , over a time horizon of length T . Further suppose we estimate $\mu_\omega = 0.001$, $\mu_\lambda = 1$, $\mu_\psi = -0.62$, $\mu_\delta = 0.0001$, $\mu_1^X = \mu_2^X = 1.5$ and $\mu^Y = 100$. In this case, if we were looked at the (μ_ψ, μ_δ) -parameter space, as in Fig. 7.6, the values of μ_ψ and μ_δ indicate that we have $\tilde{\rho} > 0$. In fact if we calculate $\tilde{\rho}$ using the parameter values we get two estimates which are both approximately 0.745. This implies that the net group correlation was positive and strong (as it is close to unity). For this example, we generated a contour plot (see Fig. 7.7), showing what values of μ_1^X and μ_2^X result in $\tilde{\rho}$ being either in $(0, 1)$ or $(-1, 0)$.

(b) Suppose $\mu_\delta < 0$. This means that as prey abundance increases this will have negative net effects on predator abundance. This may arise in a scenario where there is predator satiation [169]. This is an inverse density-dependent process, where a prey population inundates their predators with more food than they can consume at a certain time. This is

followed by little to no prey reproduction, thus causing large decreases in the numerical responses of the predator.

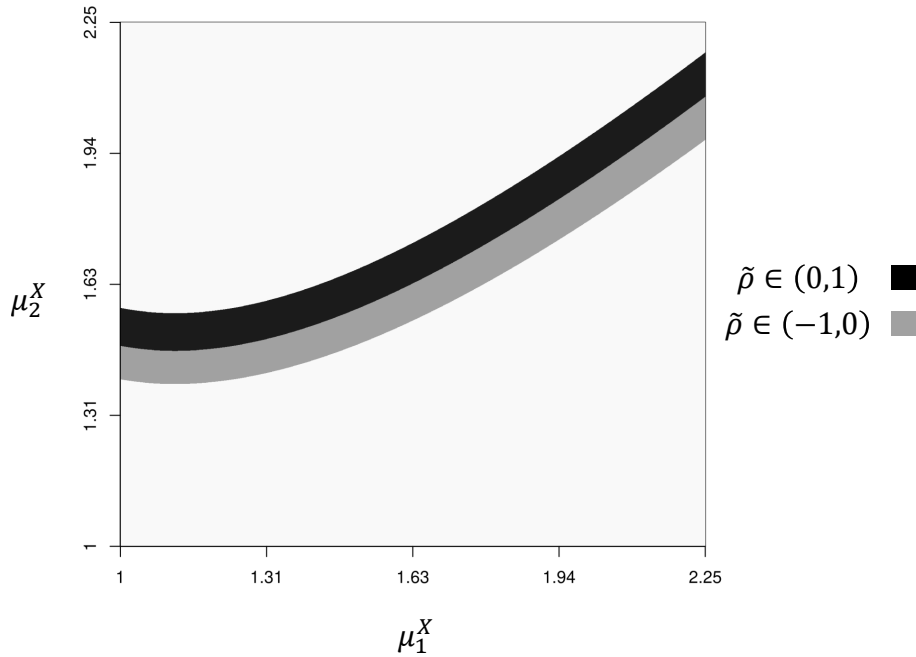


Figure 7.7: Contour plot of $(\mu_1^X, \mu_2^X) \in (1, 2.25]^2$ which result in $\tilde{\rho} \in (0, 1)$ (black) and $\tilde{\rho} \in (-1, 0)$ (dark grey), where $\mu_\delta = 0.0001$, $\mu_\psi = -0.62$, $\mu_\lambda = 1$, $\mu_\omega = 0.001$ and $\mu_Y = 100$.

This can occur via synchronised birth events, herding behaviour or seed masting for example [75, 198, 273]. In this context we could get that

$$\mu^Y \gg 0 \implies \tilde{\rho} < 0.$$

When resources become scarce following rapid decreases in prey, the negative group interactions would be induced in response to resource scarcity. On the other hand, if g and μ^Y were small, and μ_ψ was large enough, it could happen that the expression involving $B_i > 0$ may be large enough to result in $\tilde{\rho} > 0$. This could arise in a scenario where the predator is a generalist, i.e. those that consume numerous species while having little dependence on specific prey types [8], and the prey population being modelled decreases due to environmental disturbances. This would result in positive interactions between groups due to hunting cooperation, in order to switch to alternative prey types.

Scenario 3: Lastly, suppose that

$$\mu_\delta \approx 0, \mu_\psi \gg 0 \implies \frac{\mu_\delta B_i}{\mu_\psi} \approx 0.$$

As mentioned above, the mean parameters in M are not exactly equal to zero, but here we assume μ_ψ is sufficiently large so that the expressions involving B_i adds little contribution

to $\tilde{\rho}$. This implies that there is weak coupling between predator groups and their prey. It also implies that the effect of increasing group constant means increases the mean process of each group. This may arise, for example, in a scenario where predation is generalist. These values also imply that inter-group responses to increases in predator abundance is beneficial, which could have multiple interpretations. If there is weak dependence on changes in both the prey and group abundances, then this could signify that there is prey switching occurring in this system [168, 223]. Having abundant resources means that direct competition may be weak, for example. All the while, the effects of predation could remain sufficiently low for the prey to have minimal impact. There could also be a low number of groups, with small spatial overlapping of territories, and so scarce aggressive interactions. This could consequently lead to competitive effects remaining weak overall and so interactions are deemed beneficial for each group.

We would like to point out that the above interpretations are not exhaustive. Other scenarios can be extrapolated from these parameter values taking various signs and magnitudes. However, based on theoretical and observed phenomena in ecology, we have discussed four plausible scenarios that could occur. In each of these scenarios the sign of $\tilde{\rho}$ can vary, with its magnitude also changing in response to changes in both the magnitudes of elements of M , given in (7.3.3), and the magnitude of the constant means of the groups within X and Y . The strength of group interactions can change depending on the trade-off between processes like resource competition and predation, for example [51]. This dichotomy is not so clear, as we can see in the above scenarios. The sign of $\tilde{\rho}$ is not a direct measure of interaction in the sense of there being strong/weak predation or competition in the system. Incidental events such as indirect mutualism, temperature changes, drought, hunting pressure and other ecological and environmental phenomena, that are not explicitly observed, may also affect the sign of $\tilde{\rho}$.

Demographic and ecological processes, such as those described in the previous theoretical scenarios, can either enhance or inhibit a group's fitness and growth. This can occur due to factors like discounting, where individuals prioritise immediate rewards over future benefits, leading to a reduced investment in cooperative behaviors. For example, an individual with a group may choose to consume resources quickly rather than contributing to the group efforts, such as hunting or reproduction, that would benefit the population in the long run [131]. Additionally, predator interference can further complicate these dynamics, as the presence of other predators can disrupt a main predators foraging abilities. When additional predators are present, prey may become more cautious, reducing their foraging time and thus limiting prey acquisition by a focal predator [54].

In evolutionary game theory, heterogeneous populations can be viewed as comprising

cooperators — those who invest maximally in fitness and survival — and defectors — those who do not contribute to such efforts. Mathematically, it has been established that the ratio of gains to losses from cooperative versus defective interactions must surpass a threshold for cooperation to evolve. Specifically, this ratio must exceed the average degree of nearest neighbors in an evolutionary graph. In this framework, each node reflects an individual in the population, and the edges represent the connections or interactions they have with others. The average degree indicates how many direct interactions each individual has, which ultimately influences the spread of cooperative behavior. If the gains from cooperation outweigh the losses from defection within this population, cooperation can be maintained, thereby enhancing the group’s fitness [175]

In this context, network reciprocity plays a crucial role in sustaining cooperation at the population level [282]. Network reciprocity is a mechanism by which cooperative behavior is sustained in a population through the formation of networks where cooperators are clustered together, providing protection against defectors. In the illustrative scenarios mentioned earlier, the varying interaction strengths, as indicated by $\tilde{\rho}$, must ensure that temporal interactions have a positive effect on the overall population, for cooperation to thrive and for groups to remain cohesive. Simultaneously, these interactions should not be so costly to the overall population that one group could dominate, thereby undermining overall population fitness. Therefore, while we can observe that groups may have a net negative or positive interaction strength over some time horizon, as measured by $\tilde{\rho}$, the individual pairwise interactions could tell us more about how the balance of cooperative and defective behaviors, influenced by demographic and ecological factors, shape such a population’s long-term persistence.

7.7. Summary

In this chapter, we introduced a stochastic framework to analyse the dynamics of animal groups within a population, accounting for group interactions and the influence of an auxiliary population. Our framework does not assume log-Gaussian distributions for abundance counts, a common assumption in species dynamics modeling [144, 292]. We model both observation and latent processes, allowing for overdispersion. We applied this model to a 20-year wolf-elk dataset and confirmed that wolf predation isn’t the primary cause of elk declines, inter-pack dynamics are heterogeneous, and wolf populations in Yellowstone National Park are generalist predators. Inter-pack associations were interpreted to have a weak effect on regulating population abundance. Simulation studies demonstrated the robustness of our model across different contexts. We also derived an approximation to inter-group correlation for a simpler autoregressive model, which captures various predator-prey relationships.

7.8. Appendix

In this appendix we present some plots related to our simulation studies. Fig. 7.8 – 7.12 are boxplots of bias and relative bias for our parameter values over all 100 simulations for each S1 – S5, respectively. Fig. 7.13 – 7.15 are bivariate plots for simulation No. 20 for S2 and S3. The bivariate plots show the marginal (posterior) distribution of the specified parameters along the main diagonal, with bivariate distributions for specified parameter pairs on the off-diagonal. The boxplots show the median of the posterior estimates (bold horizontal line) and the interquartile range with bounds at 25% and 75% quartiles (boxes). The vertical lines indicate the amount of variability beyond the interquartile range. The grey dots represent data points that are outliers with respect to the interquartile range. The boxplots show the estimated posterior density for each parameter and demonstrate when, if present, there was confounding between variables within some HMC runs.

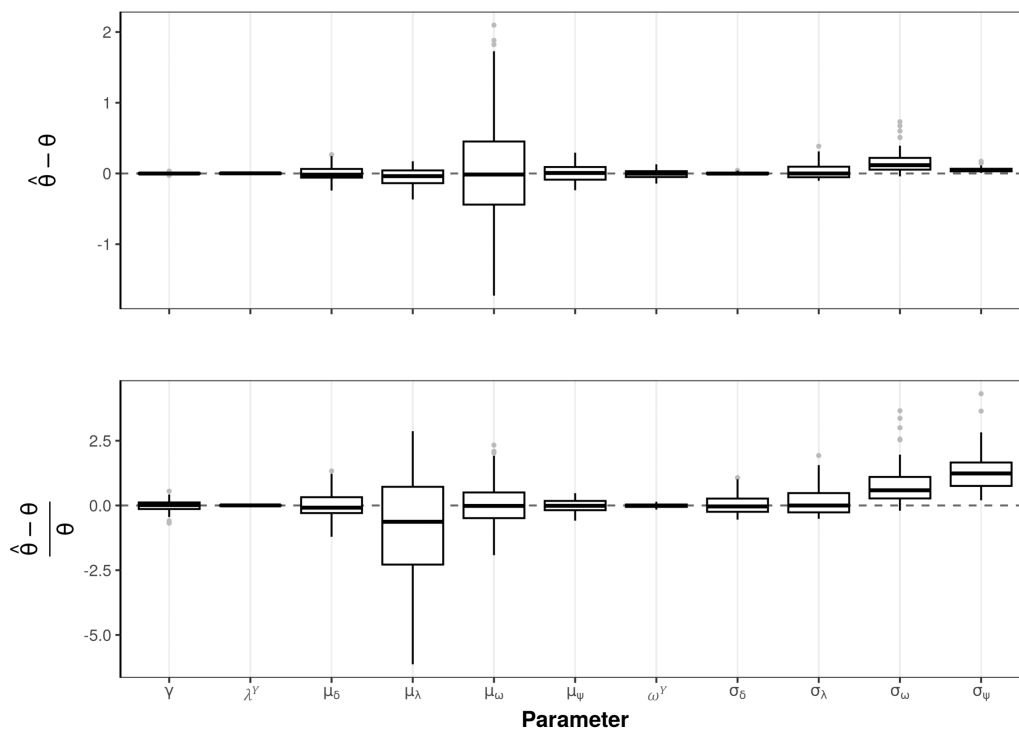
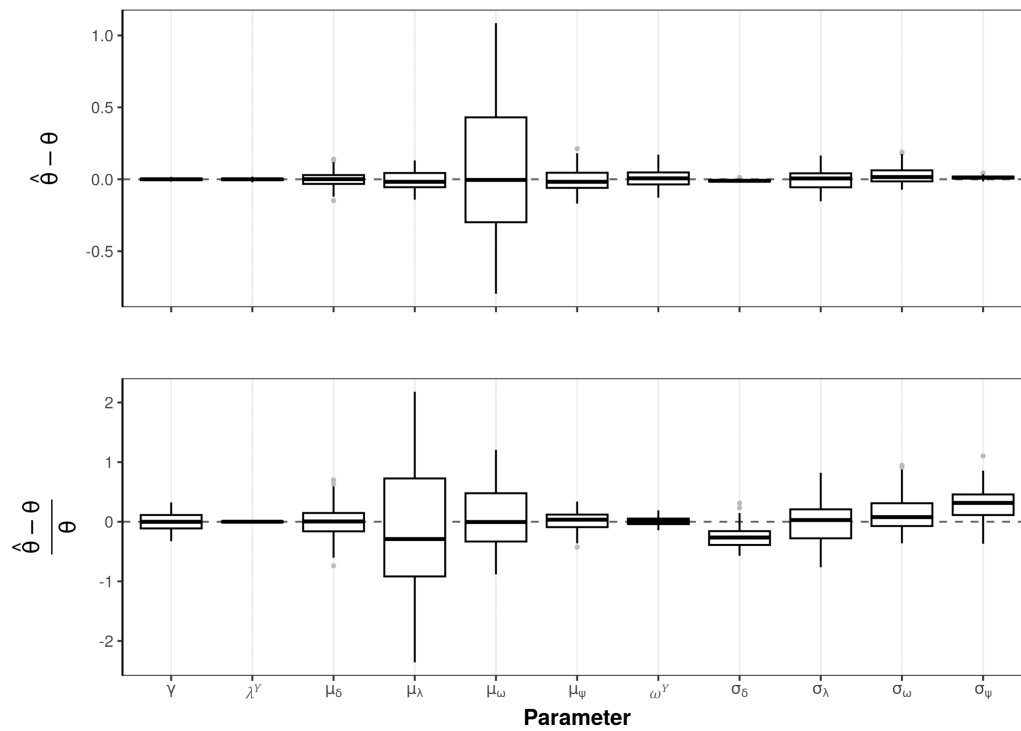
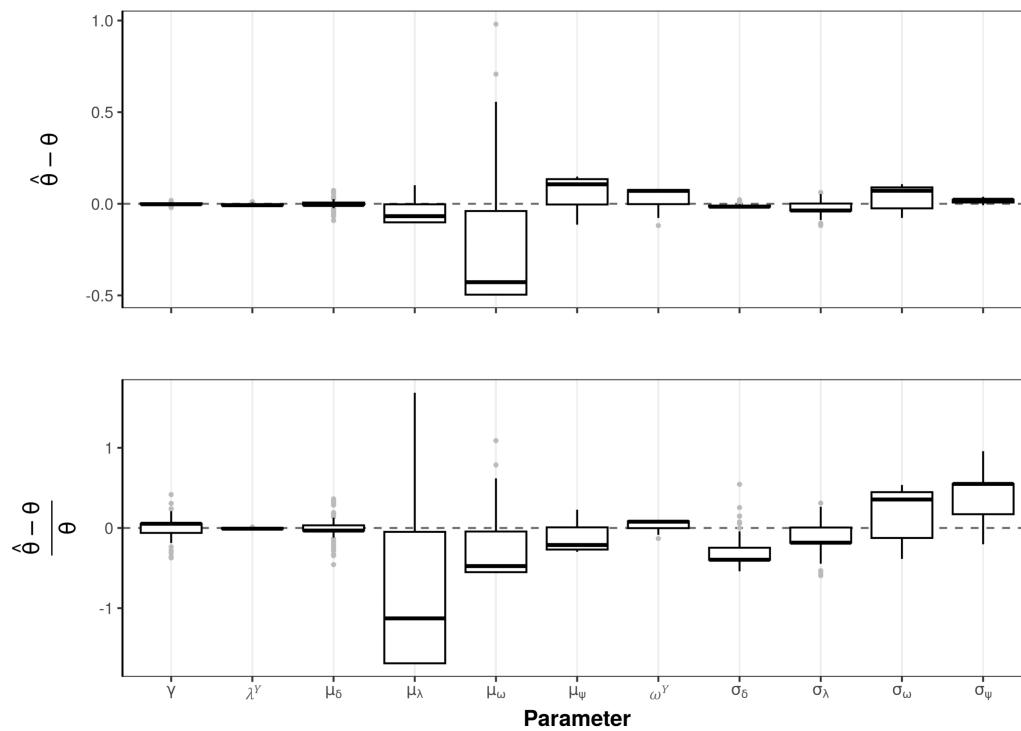
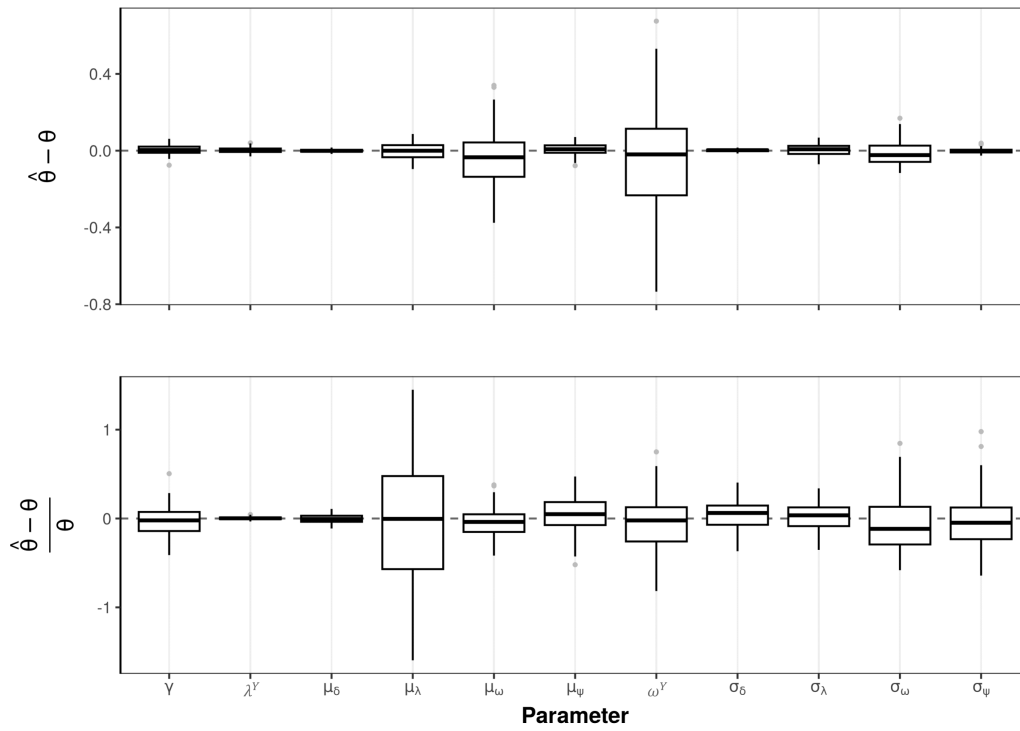
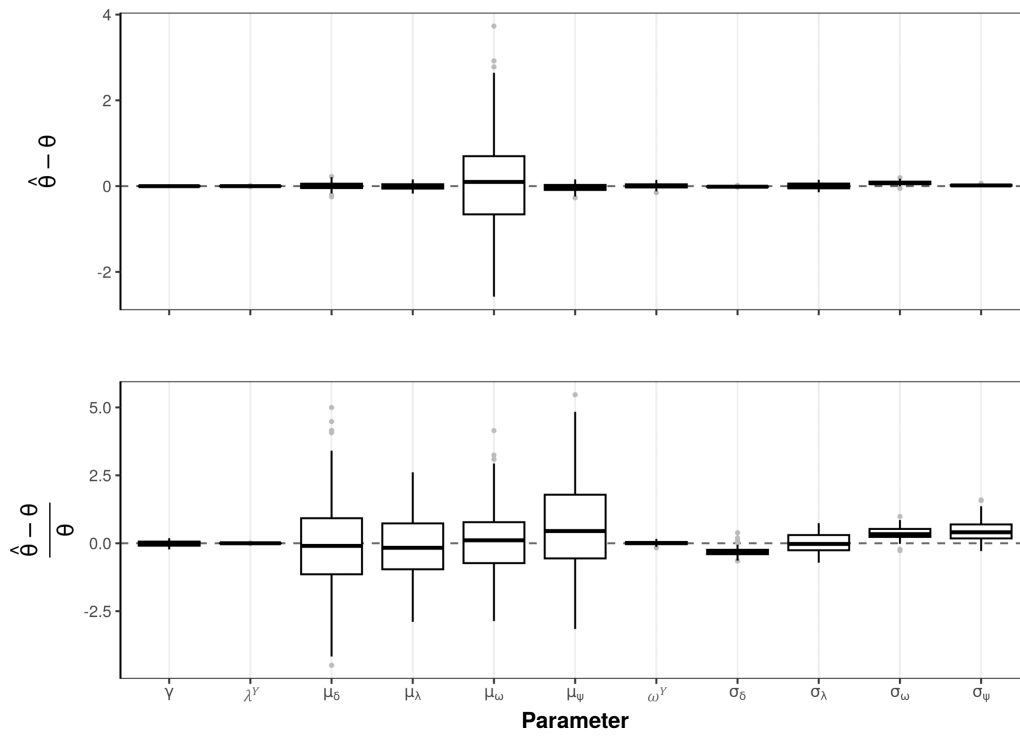
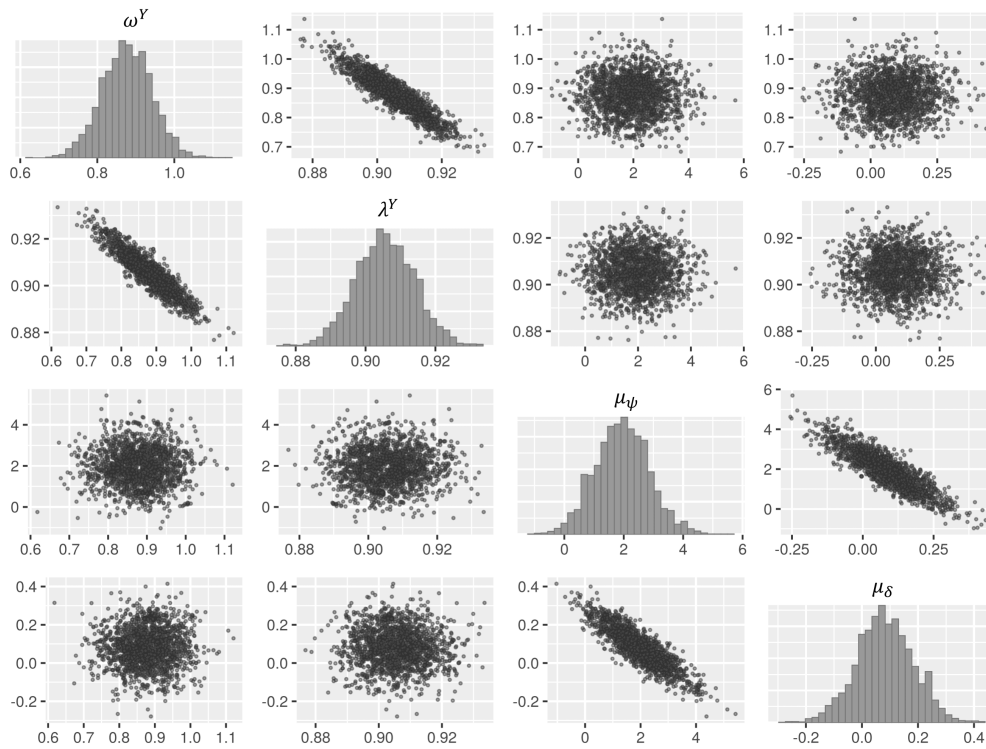
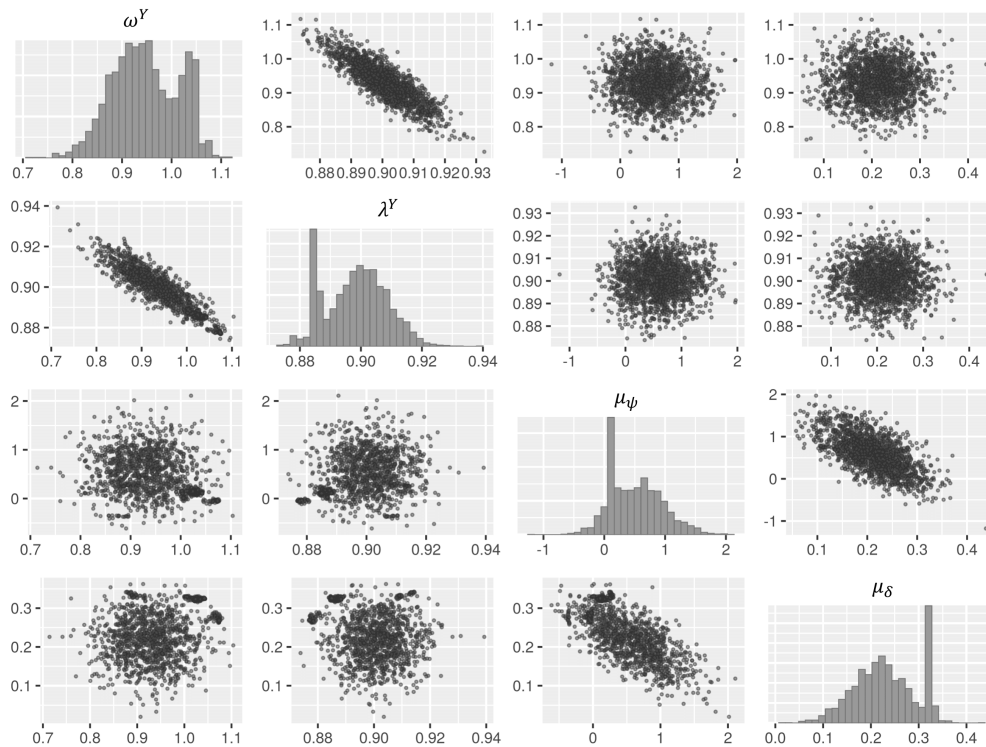


Figure 7.8: Boxplots of bias and relative bias for $\theta \in M \cup \Sigma \cup \{\gamma, \lambda^Y, \omega^Y\}$ for S1.

Figure 7.9: Boxplots of bias and relative bias for $\theta \in M \cup \Sigma \cup \{\gamma, \lambda^Y, \omega^Y\}$ for S2.Figure 7.10: Boxplots of bias and relative bias for $\theta \in M \cup \Sigma \cup \{\gamma, \lambda^Y, \omega^Y\}$ for S3.

Figure 7.11: Boxplots of bias and relative bias for $\theta \in M \cup \Sigma \cup \{\gamma, \lambda^Y, \omega^Y\}$ for S4.Figure 7.12: Boxplots of bias and relative bias for $\theta \in M \cup \Sigma \cup \{\gamma, \lambda^Y, \omega^Y\}$ for S5.

Figure 7.13: Bivariate plots for $\{\omega^Y, \lambda^Y, \mu_\psi, \mu_\delta\}$ from simulation No. 20 for S1.Figure 7.14: Bivariate plots for $\{\omega^Y, \lambda^Y, \mu_\psi, \mu_\delta\}$ from simulation No. 20 for S2.

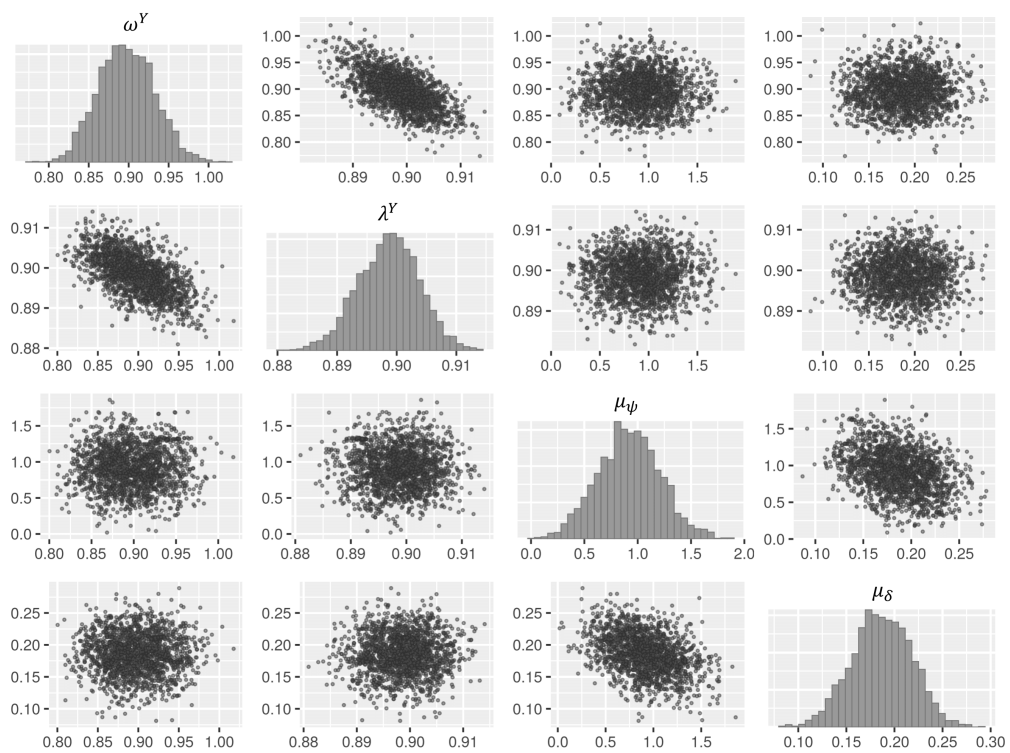


Figure 7.15: Bivariate plots for $\{\omega^Y, \lambda^Y, \mu_\psi, \mu_\delta\}$ from simulation No. 20 for S3.

8. Future Directions

In this thesis we have shown how one can account for various types of internal population heterogeneity when modelling species dynamics in discrete-time. In each chapter we attempted to demonstrate the relevance of our model frameworks and how the results could give us insight into real-world populations that exhibit such ecological complexities. We will now review some of the main results and outline some avenues one could take in relation to the ideas and results in this thesis, to either extend, complement or improve upon such work.

In Chapter 4 we explored a two-patch population model of both passive and density-dependent, cost-free range expansion, motivated by examples based on invasive species, where the dynamics on each patch were modelled by a Ricker map. We provided sufficient conditions for the LAS of the extinction equilibrium, the existence of a patch coexistence equilibrium, weak uniform persistence with respect to one of patches, and strong uniform persistence with respect to both the total population and minimum patch size. One possibility for future work would be to determine if there exist conditions for the existence of a unique positive equilibrium for two coupled Ricker maps with density-dependent dispersal. Following this one could also look at when such an equilibrium is LAS and GAS. This was done for the passive, symmetric dispersal case, as can be seen in [17].

Following the analytical work in Chapter 4, we briefly discussed some ecological scenarios that our model can describe, including transience and spatial synchrony. Finally we applied our model to a case study of plant-host shift, to get some insight into how altering crop types can affect the long term dynamics of an invasive insect. In the context of modelling pest dynamics, one could try extend our model to include stochasticity and detect population outbreaks. For example, this may be done using the Pattern-Based Prediction framework outlined in [219], where the inhomogeneous mean of a count distribution is given by our model equations (4.2.1).

In Chapter 5 we investigated the dynamics of a nonlinear metapopulation model, where the maps describing regional dynamics belong to a general class of bounded population maps and dispersal was density-dependent with a cost across the overall population. We briefly discussed how our model relates to many passive dispersal models. We provided sufficient conditions for the LAS and GAS of the extinction equilibrium. We then derived

conditions for the existence of a positive equilibrium: our proof also described a region in the interior of the nonnegative orthant in which the equilibrium is located. As with the material in Chapter 4, a natural question to ask here is: under what further conditions on both $f_i \in \mathcal{M}$ and d_{ij} satisfying (5.2.1) can one prove either the existence of a unique positive equilibrium or a GAS positive equilibrium? As in [156], it would be interesting to see when (if at all) system (5.2.3) is strongly monotone and if the dichotomous result of [156] holds for some feasible choice of f_i and d_{ij} . In this chapter we also gave a sufficient condition for strong uniform persistence with respect to any norm on \mathbb{R}_+^n and minimum patch size.

We finished Chapter 5 by numerically investigating our model, exploring when various dynamical behaviour arose, for example periodic solutions and chaotic type dynamics. In the context of modelling metapopulations, it would be interesting to see if our results can be specialised to models where there is specific network topologies, i.e. when not all patches/regions are connected via dispersal? This would change the assumption that $d_{ij} \notin \{0, 1\}$ and so more work would be needed to be carried out in order to see if our results can be extended to these cases. In [113] the authors looked at how the strength of passive dispersal between sources and sinks affects the asymptotic total population size when $n = 2$. Another avenue for future work would be to see if the results of [113] could be extended to density-dependent, costly dispersal for $n \geq 2$ when one looks at movement: (i) only between sources; and (ii) between sources and sinks. Both of these extensions have important consequences for ecological corridors and habitat connectivity [93].

In Chapter 6 we explored a linear two-patch population model, where each patch population is partitioned into demographic classes, and there is diffusive dispersal between each of the classes. Given that each patch is a sink, i.e. each isolated population tends to extinction, we gave several sufficient conditions for the asymptotic stability of the zero equilibrium of the coupled model, which is robust to feasible diffusive couplings, also known as robust diffusive stability (RDS). In particular we showed how common linear copositive, quadratic and diagonal Lyapunov functions relate to RDS. Generalising these results for nonlinear matrix models [255] or for diffusively coupled continuous-time systems on proper cones [69] is a natural next step.

In Chapter 6 we also looked at when one can find specific diffusive matrices that induce overall population growth, referred to as diffusive growth. In particular we looked at how the existence of an unstable matrix in the convex hull of our system matrices A and B related to diffusive growth. In [127] the authors investigated how the spectral abscissa of a convex combination of two matrices compared to the convex combination of their individual spectral abscissas. This problem was motivated by a continuous-time structured

population model. Investigating how these results apply to discrete-time models and how do they relate to RDS or diffusive growth would be an interesting route to take. Throughout this chapter we also discussed how our results could be used to study diffusive dispersal for commonly used linear population models in ecology, such as Leslie matrices. Leslie matrix models are used widely in applied ecology for predicting population dynamics. Within the context of our model, one could statistically estimate the entries of the Leslie matrices A and B , by fitting dynamic state-space models to time series data of interest, where A and B are the true generating process for the mean of a count distribution [41]. Then using the results of this chapter, these estimates could be used to infer if diffusive dispersal will result in RDS or help in finding when diffusive growth occurs.

In Chapter 7 we investigated a stochastic time series model of animal groups within a population and an associated auxiliary population. Our aim was to use such time series for inferring interactions among such groups and how the auxiliary population may affect these associations. We then validated this framework under various simulation scenarios to demonstrate parameter estimation and bias, and fitted this model to a real-world predator-prey dataset, in a Bayesian setting. If one was interested in short term predictions one could use observational random effects within our framework in order to account for potential outliers [215]. In this context one may want to reformulate our model into observation and data-generating processes in order to account for imperfect detection and measurement error [201]. One could also, in this case, explicitly account for potential high frequency of zero observations using hurdle or zero-inflated models [124].

In Chapter 7 we were particularly interested in interactions over time. If one was interested not only in the temporal aspect of group interactions, but also their spatial extent, then one could perhaps do this via spatial random effects [150]. One could also incorporate spatiality by introducing a temporally varying network structure into our model. This would be of interest if one was interested in modelling the explicit inflow/outflow of individuals from groups, which could incorporate lone individuals. Perhaps this could be done using, for example, multilayer networks [140] or graphical models [207], where nodes of a spatial graph represent groups or individuals and edges their interactions. We introduced random effects to reduce parameter dimensionality and to model within-population heterogeneity. One way to improve on our work would be to introduce pairwise interaction parameters, either by extending our count time series model, or via the Poisson Lotka-Volterra model of [249]. If both were fitted, then one could select which model is a better fit to the data via methods such as the Bayes factor or using information criteria [176].

Following our simulation and case studies in Chapter 7, we then derived an approximation to the marginal pairwise correlation between groups for a new simpler model, what we

called the net group interaction strength, which quantifies the total interaction strength across all groups over the whole time horizon. Lastly, we discussed the meaning of such an approximation for some theoretical predator-prey scenarios, to show how it can be interpreted. An obvious final question to ask is: it possible to remove the simplifying assumptions that allow for our derivation of $\hat{\rho}$, that is, to derive an analytic expression for the marginal correlation structure of our model, i.e. (7.6.1), without using a second order Taylor approximation and/or the assumptions of log-normality, conditional constancy and heterogenous compound symmetry?

Bibliography

- [1] Miguel A Acevedo and Robert J Fletcher. “The proximate causes of asymmetric movement across heterogeneous landscapes”. In: *Landscape Ecology* 32 (2017), pp. 1285–1297.
- [2] John Aitchison and CH Ho. “The multivariate Poisson-log normal distribution”. In: *Biometrika* 76.4 (1989), pp. 643–653.
- [3] Alexander Aleksandrov and Oliver Mason. “Diagonal stability of a class of discrete-time positive switched systems with delay”. In: *IET Control Theory & Applications* 12.6 (2018), pp. 812–818.
- [4] Richard D Alexander. “The evolution of social behavior”. In: *Annual review of ecology and systematics* (1974), pp. 325–383.
- [5] Res Altwegg et al. “Density-dependent dispersal and the speed of range expansions”. In: *Diversity and Distributions* 19.1 (2013), pp. 60–68.
- [6] Mickaël Teixeira Alves and Frank M Hilker. “Hunting cooperation and Allee effects in predators”. In: *Journal of theoretical biology* 419 (2017), pp. 13–22.
- [7] Elena Angulo et al. “Allee effects in social species”. In: *Journal of Animal Ecology* 87.1 (2018), pp. 47–58.
- [8] Gui Araujo and Rafael Rios Moura. “Individual specialization and generalization in predator-prey dynamics: The determinant role of predation efficiency and prey reproductive rates”. In: *Journal of Theoretical Biology* 537 (2022), p. 111026.
- [9] Steven R Archer et al. “Woody plant encroachment: causes and consequences”. In: *Rangeland systems: Processes, management and challenges* (2017), pp. 25–84.
- [10] O Arino, E Sánchez, and GF Webb. “Necessary and sufficient conditions for asynchronous exponential growth in age structured cell populations with quiescence”. In: *Journal of Mathematical Analysis and Applications* 215.2 (1997), pp. 499–513.
- [11] Vladimir Igorevich Arnold et al. *Dynamical systems V: bifurcation theory and catastrophe theory*. Vol. 5. Springer Science & Business Media, 2013.
- [12] Kenneth J Arrow and Maurice McManus. “A note on dynamic stability”. In: *Econometrica: Journal of the Econometric Society* (1958), pp. 448–454.

-
- [13] Yael Artzy-Randrup and Lewi Stone. “Connectivity, cycles, and persistence thresholds in metapopulation networks”. In: *PLoS Computational Biology* 6.8 (2010), e1000876.
- [14] Alistair G Auffret, Johan Berg, and Sara AO Cousins. “The geography of human-mediated dispersal”. In: *Diversity and Distributions* 20.12 (2014), pp. 1450–1456.
- [15] Piret Avila and Charles Mullan. “Evolutionary game theory and the adaptive dynamics approach: adaptation where individuals interact”. In: *Philosophical Transactions of the Royal Society B* 378.1876 (2023), p. 20210502.
- [16] George Bachman and Lawrence Narici. *Functional analysis*. Courier Corporation, 2000.
- [17] Ignacio Bajo and Alfonso Ruiz-Herrera. “A quantitative approach to the stabilizing role of dispersal in metapopulations”. In: *Mathematical Biosciences* 290 (2017), pp. 49–55.
- [18] Katharine M Banner, Kathryn M Irvine, and Thomas J Rodhouse. “The use of Bayesian priors in Ecology: The good, the bad and the not great”. In: *Methods in Ecology and Evolution* 11.8 (2020), pp. 882–889.
- [19] George Phillip Barker, Abraham Berman, and Robert J Plemmons. “Positive diagonal solutions to the Lyapunov equations”. In: *Linear and Multilinear Algebra* 5.4 (1978), pp. 249–256.
- [20] Frédéric Barraquand and Olivier Gimenez. “Fitting stochastic predator–prey models using both population density and kill rate data”. In: *Theoretical population biology* 138 (2021), pp. 1–27.
- [21] Fethi Belgacem and Chris Cosner. “The effects of dispersal along environmental gradients on the dynamics of populations in heterogeneous environment”. In: *Canad. Appl. Math. Quart* 3.4 (1995), pp. 379–397.
- [22] Michel Benaïm et al. “When can a population spreading across sink habitats persist?” In: *Journal of Mathematical Biology* 88.2 (2024), p. 19.
- [23] Michael F Benard and Shannon J McCauley. “Integrating across life-history stages: consequences of natal habitat effects on dispersal”. In: *The American Naturalist* 171.5 (2008), pp. 553–567.
- [24] Cecilia Berardo et al. “Interactions between different predator–prey states: a method for the derivation of the functional and numerical response”. In: *Journal of mathematical biology* 80.7 (2020), pp. 2431–2468.
- [25] Eric L Berlow et al. “Interaction strengths in food webs: issues and opportunities”. In: *Journal of animal ecology* (2004), pp. 585–598.

-
- [26] Abraham Berman and Robert J Plemmons. *Nonnegative matrices in the mathematical sciences*. SIAM, 1994.
- [27] Sandro Bertolino et al. “A grey future for Europe: *Sciurus carolinensis* is replacing native red squirrels in Italy”. In: *Biological invasions* 16 (2014), pp. 53–62.
- [28] Michael Betancourt. “A conceptual introduction to Hamiltonian Monte Carlo”. In: *arXiv preprint arXiv:1701.02434* (2017).
- [29] Amit Bhaya and Eugenius Kaszkurewicz. “On discrete-time diagonal and D-stability”. In: *Linear Algebra and its Applications* 187 (1993), pp. 87–104.
- [30] F Guillaume Blanchet, Kevin Cazelles, and Dominique Gravel. “Co-occurrence is not evidence of ecological interactions”. In: *Ecology Letters* 23.7 (2020), pp. 1050–1063.
- [31] Timothy C Bonebrake et al. “Managing consequences of climate-driven species redistribution requires integration of ecology, conservation and social science”. In: *Biological Reviews* 93.1 (2018), pp. 284–305.
- [32] Dries Bonte et al. “Costs of dispersal”. In: *Biological reviews* 87.2 (2012), pp. 290–312.
- [33] Jesse B Borden and S Luke Flory. “Urban evolution of invasive species”. In: *Frontiers in Ecology and the Environment* 19.3 (2021), pp. 184–191.
- [34] Mark S Boyce. “Wolves for Yellowstone: dynamics in time and space”. In: *Journal of Mammalogy* 99.5 (2018), pp. 1021–1031.
- [35] Stephen Boyd and Lieven Vandenberghe. *Convex optimization*. Cambridge university press, 2004.
- [36] Christian Braendle et al. “Wing dimorphism in aphids”. In: *Heredity* 97.3 (2006), pp. 192–199.
- [37] Ellen E Brandell et al. “Group density, disease, and season shape territory size and overlap of social carnivores”. In: *Journal of Animal Ecology* 90.1 (2021), pp. 87–101.
- [38] Ellen E Brandell et al. “Patterns and processes of pathogen exposure in gray wolves across North America”. In: *Scientific reports* 11.1 (2021), p. 3722.
- [39] Barry W Brook and Corey JA Bradshaw. “Strength of evidence for density dependence in abundance time series of 1198 species”. In: *Ecology* 87.6 (2006), pp. 1445–1451.
- [40] Jerram L Brown. “Optimal group size in territorial animals”. In: *Journal of Theoretical Biology* 95.4 (1982), pp. 793–810.

-
- [41] Stephen Terrence Buckland et al. “State-space models for the dynamics of wild animal populations”. In: *Ecological modelling* 171.1-2 (2004), pp. 157–175.
- [42] Denise Bunting and Ross A Coleman. “Ethical consideration in invasion ecology: A marine perspective”. In: *Ecological Management & Restoration* 15.1 (2014), pp. 64–70.
- [43] Oscar J Cacho and Susan M Hester. “Modelling biocontrol of invasive insects: An application to European Wasp (*Vespula germanica*) in Australia”. In: *Ecological Modelling* 467 (2022), p. 109939.
- [44] Bob Carpenter et al. “Stan: A probabilistic programming language”. In: *Journal of statistical software* 76 (2017).
- [45] George Casella and Roger Berger. *Statistical inference*. CRC Press, 2024.
- [46] Kira A Cassidy et al. “Group composition effects on aggressive interpack interactions of gray wolves in Yellowstone National Park”. In: *Behavioral Ecology* 26.5 (2015), pp. 1352–1360.
- [47] Hugo Cayuela et al. “Anthropogenic disturbance drives dispersal syndromes, demography, and gene flow in amphibian populations”. In: *Ecological monographs* 90.2 (2020), e01406.
- [48] Yufang Chang et al. “Quadratic stabilization of switched uncertain linear systems: a convex combination approach”. In: *IEEE/CAA Journal of Automatica Sinica* 6.5 (2019), pp. 1116–1126.
- [49] Eric L Charnov. “Optimal foraging, the marginal value theorem”. In: *Theoretical population biology* 9.2 (1976), pp. 129–136.
- [50] Peter Chesson. “Scale transition theory: its aims, motivations and predictions”. In: *Ecological Complexity* 10 (2012), pp. 52–68.
- [51] Peter Chesson and Jessica J Kuang. “The interaction between predation and competition”. In: *Nature* 456.7219 (2008), pp. 235–238.
- [52] Siddhartha Chib and Rainer Winkelmann. “Markov chain Monte Carlo analysis of correlated count data”. In: *Journal of Business & Economic Statistics* 19.4 (2001), pp. 428–435.
- [53] Diana Cole. *Parameter redundancy and identifiability*. Chapman and Hall/CRC, 2020.
- [54] Chris Cosner et al. “Effects of spatial grouping on the functional response of predators”. In: *Theoretical population biology* 56.1 (1999), pp. 65–75.
- [55] RF Costantino et al. “Experimentally induced transitions in the dynamic behaviour of insect populations”. In: *Nature* 375.6528 (1995), pp. 227–230.

-
- [56] David R Cox et al. “Statistical analysis of time series: Some recent developments [with discussion and reply]”. In: *Scandinavian Journal of Statistics* (1981), pp. 93–115.
- [57] GW Cross. “Three types of matrix stability”. In: *Linear algebra and its applications* 20.3 (1978), pp. 253–263.
- [58] Paul Cull. “Local and global stability of discrete one-dimensional population models”. In: *Biomathematics and Related Computational Problems*. Springer, 1988, pp. 271–278.
- [59] Jim M Cushing. “An evolutionary Beverton-Holt model”. In: *Theory and Applications of Difference Equations and Discrete Dynamical Systems: ICDEA, Muscat, Oman, May 26-30, 2013*. Springer. 2014, pp. 127–141.
- [60] Jim M Cushing and Zhou Yicang. “The net reproductive value and stability in matrix population models”. In: *Natural Resource Modeling* 8.4 (1994), pp. 297–333.
- [61] Jim Michael Cushing. *An introduction to structured population dynamics*. SIAM, 1998.
- [62] Jim Michael Cushing. *Matrix Models for Population, Disease, and Evolutionary Dynamics*. Vol. 106. American Mathematical Society, 2024.
- [63] Bertrand Daignan-Fornier, Damien Laporte, and Isabelle Sagot. “Quiescence through the prism of evolution”. In: *Frontiers in Cell and Developmental Biology* 9 (2021), p. 745069.
- [64] Vasilis Dakos et al. “Methods for detecting early warnings of critical transitions in time series illustrated using simulated ecological data”. In: *PloS one* 7.7 (2012), e41010.
- [65] H. V. Danks. *Insect dormancy: an ecological perspective*. English. Ottawa: Biological Survey of Canada (Terrestrial Arthropods), 1987, ix + 439pp. ISBN: 9780969272700.
- [66] Biswa Nath Datta. “Stability and D-stability”. In: *Linear Algebra and its Applications* 21.2 (1978), pp. 135–141.
- [67] Richard A Davis et al. “Count time series: A methodological review”. In: *Journal of the American Statistical Association* 116.535 (2021), pp. 1533–1547.
- [68] Richard A Davis et al. *Handbook of discrete-valued time series*. CRC Press, 2016.
- [69] Patrick De Leenheer. “Stability of diffusively coupled linear systems with an invariant cone”. In: *Linear Algebra and its Applications* 580 (2019), pp. 396–416.

- [70] P. de Valpine et al. “Programming with models: writing statistical algorithms for general model structures with NIMBLE”. In: *Journal of Computational and Graphical Statistics* 26 (2017), pp. 403–417. DOI: 10.1080/10618600.2016.1172487.
- [71] Clarice GB Demétrio, John Hinde, and Rafael A Moral. “Models for overdispersed data in entomology”. In: *Ecological modelling applied to entomology* (2014), pp. 219–259.
- [72] Fabio Dercole, Sergio Rinaldi, et al. “Dynamical systems and their bifurcations”. In: *Advanced methods of biomedical signal processing* (2011), pp. 291–325.
- [73] Robert Devaney. *An introduction to chaotic dynamical systems*. CRC press, 2018.
- [74] Emily Dickinson. *The collected poems of Emily Dickinson*. First Avenue Editions, 2016.
- [75] Odo Diekmann and Robert Planqué. “The winner takes it all: how semelparous insects can become periodical”. In: *Journal of Mathematical Biology* 80.1 (2020), pp. 283–301.
- [76] Xiuyong Ding, Lan Shu, and Changcheng Xiang. “On linear co-positive Lyapunov functions for a special of switched linear positive systems”. In: *Advanced Intelligent Computing: 7th International Conference, ICIC 2011, Zhengzhou, China, August 11-14, 2011. Revised Selected Papers* 7. Springer. 2012, pp. 650–657.
- [77] Diego Felipe Araujo Diniz et al. “Diapause and quiescence: dormancy mechanisms that contribute to the geographical expansion of mosquitoes and their evolutionary success”. In: *Parasites & vectors* 10 (2017), pp. 1–13.
- [78] Richard P Duncan et al. “Eruptive dynamics are common in managed mammal populations”. In: *Ecology* 101.12 (2020), e03175.
- [79] Yoshio Ebihara, Dimitri Peaucelle, and Denis Arzelier. “Analysis and synthesis of interconnected positive systems”. In: *IEEE Transactions on Automatic Control* 62.2 (2016), pp. 652–667.
- [80] Saber Elaydi. *An Introduction to Difference Equations*. Undergraduate Texts in Mathematics. Springer, Berlin, 2005.
- [81] L Mark Elbroch et al. “Recolonizing wolves influence the realized niche of resident cougars”. In: *Zoological Studies* 54 (2015), pp. 1–11.
- [82] Karin Enfjäll and Olof Leimar. “The evolution of dispersal—the importance of information about population density and habitat characteristics”. In: *Oikos* 118.2 (2009), pp. 291–299.

- [83] Anders Eriksson et al. “The emergence of the rescue effect from explicit within- and between-patch dynamics in a metapopulation”. In: *Proceedings of the royal society B: biological sciences* 281.1780 (2014), p. 20133127.
- [84] R Escobedo et al. “Group size, individual role differentiation and effectiveness of cooperation in a homogeneous group of hunters”. In: *Journal of the Royal Society Interface* 11.95 (2014), p. 20140204.
- [85] Lorenzo Farina and Sergio Rinaldi. *Positive linear systems: theory and applications*. John Wiley & Sons, 2011.
- [86] Xavier Fauvergue and Keith R Hopper. “Dispersal of optimal foragers in a patchy environment: Simulations with a mathematical model and tests of predictions in field experiments”. In: *Ecological Modelling* 498 (2024), p. 110887.
- [87] Donald H Feener Jr. “Is the assembly of ant communities mediated by parasitoids?” In: *Oikos* 90.1 (2000), pp. 79–88.
- [88] Mitchell J Feigenbaum. “Quantitative universality for a class of nonlinear transformations”. In: *Journal of statistical physics* 19.1 (1978), pp. 25–52.
- [89] R Fleming et al. “Classes of Schur D-stable matrices”. In: *Linear Algebra and its Applications* 306.1-3 (2000), pp. 15–24.
- [90] Konstantinos Fokianos and Dag Tjøstheim. “Log-linear Poisson autoregression”. In: *Journal of multivariate analysis* 102.3 (2011), pp. 563–578.
- [91] Ettore Fornasini and Maria Elena Valcher. “Stability and stabilizability criteria for discrete-time positive switched systems”. In: *IEEE Transactions on Automatic control* 57.5 (2011), pp. 1208–1221.
- [92] Daniel Franco and Frank M Hilker. “Adaptive limiter control of unimodal population maps”. In: *Journal of theoretical biology* 337 (2013), pp. 161–173.
- [93] Daniel Franco and Alfonso Ruiz-Herrera. “To connect or not to connect isolated patches”. In: *Journal of Theoretical Biology* 370 (2015), pp. 72–80.
- [94] Daniel Franco et al. *A switching feedback control approach for persistence of managed resources*. 2022. DOI: 10.3934/dcdsb.2021109.
- [95] Daniel Franco et al. “Boundedness, persistence and stability for classes of forced difference equations arising in population ecology”. In: *Journal of Mathematical Biology* 79 (2019), pp. 1029–1076.
- [96] Belinda Gallardo and David C Aldridge. “Evaluating the combined threat of climate change and biological invasions on endangered species”. In: *Biological Conservation* 160 (2013), pp. 225–233.

-
- [97] Elizabeth S Garrett and Scott L Zeger. “Latent class model diagnosis”. In: *Biometrics* 56.4 (2000), pp. 1055–1067.
- [98] Robert A Garrott et al. “Apparent competition and regulation in a wolf-ungulate system: interactions of life history characteristics, climate, and landscape attributes”. In: *Terrestrial Ecology* 3 (2008), pp. 519–540.
- [99] Alan E Gelfand and Sujit K Sahu. “Identifiability, improper priors, and Gibbs sampling for generalized linear models”. In: *Journal of the American Statistical Association* 94.445 (1999), pp. 247–253.
- [100] Andrew Gelman. “Prior distributions for variance parameters in hierarchical models (comment on article by Browne and Draper)”. In: *Bayesian Analysis* 1.3 (2006), pp. 515–534. DOI: 10.1214/06-BA117A.
- [101] Andrew Gelman and Donald B Rubin. “Inference from iterative simulation using multiple sequences”. In: *Statistical science* 7.4 (1992), pp. 457–472.
- [102] Andrew Gelman et al. *Bayesian data analysis*. Chapman and Hall/CRC, 1995.
- [103] Stefan AH Geritz and Éva Kisdi. “On the mechanistic underpinning of discrete-time population models with complex dynamics”. In: *Journal of theoretical biology* 228.2 (2004), pp. 261–269.
- [104] Olivier Gimenez, Byron JT Morgan, and Stephen P Brooks. “Weak identifiability in models for mark-recapture-recovery data”. In: *Modeling demographic processes in marked populations* (2009), pp. 1055–1067.
- [105] John L Gittleman. “Carnivore group living: comparative trends”. In: *Carnivore behavior, ecology, and evolution*. Springer, 1989, pp. 183–207.
- [106] Richard Glennie et al. “Hidden Markov models: Pitfalls and opportunities in ecology”. In: *Methods in Ecology and Evolution* 14.1 (2023), pp. 43–56.
- [107] HCJ Godfray and MP Hassell. “Discrete and continuous insect populations in tropical environments”. In: *The Journal of Animal Ecology* (1989), pp. 153–174.
- [108] Isabelle Bueno Silva de Godoy et al. “Plant-host shift, spatial persistence, and the viability of an invasive insect population”. In: *Ecological Modelling* 475 (2023), p. 110172.
- [109] Oscar Godoy et al. “Towards the integration of niche and network theories”. In: *Trends in Ecology & Evolution* 33.4 (2018), pp. 287–300.
- [110] Eben Goodale et al. “Mixed company: a framework for understanding the composition and organization of mixed-species animal groups”. In: *Biological Reviews* 95.4 (2020), pp. 889–910.

-
- [111] DW Goodsman, BJ Cooke, and MA Lewis. “Positive and negative density-dependence and boom-bust dynamics in enemy-victim populations: a mountain pine beetle case study”. In: *Theoretical Ecology* 10.2 (2017), pp. 255–267.
- [112] Purnima Govindarajulu, Res Altwegg, and Bradley R Anholt. “Matrix model investigation of invasive species control: bullfrogs on Vancouver Island”. In: *Ecological Applications* 15.6 (2005), pp. 2161–2170.
- [113] Carolin Grumbach et al. “The effect of dispersal on asymptotic total population size in discrete-and continuous-time two-patch models”. In: *Journal of Mathematical Biology* 87.4 (2023), p. 60.
- [114] Chris Guiver, David Packman, and Stuart Townley. “A necessary condition for dispersal driven growth of populations with discrete patch dynamics”. In: *Journal of Theoretical Biology* 424 (2017), pp. 11–25.
- [115] WSC Gurney, PH Crowley, and RM Nisbet. “Stage-specific quiescence as a mechanism for synchronizing life cycles to seasons”. In: *Theoretical population biology* 46.3 (1994), pp. 319–343.
- [116] M Gyllenberg and GF Webb. “Age-size structure in populations with quiescence”. In: *Mathematical biosciences* 86.1 (1987), pp. 67–95.
- [117] Karl P Hadeler. “Quiescent Phases and Stability in Discrete Time Dynamical Systems”. In: *Discrete & Continuous Dynamical Systems-Series B* 20.1 (2015).
- [118] Karl P Hadeler, Thomas Hillen, and Mark A Lewis. “Biological modeling with quiescent phases”. In: *Spatial ecology*. Chapman and Hall/CRC, 2009, pp. 123–150.
- [119] KP Hadeler. “Quiescence, excitability, and heterogeneity in ecological models”. In: *Journal of mathematical biology* 66 (2013), pp. 649–684.
- [120] KP Hadeler. “Quiescent phases and stability”. In: *Linear algebra and its applications* 428.7 (2008), pp. 1620–1627.
- [121] Christopher Logan Hambric et al. “Minimum number of non-zero-entries in a stable matrix exhibiting Turing instability”. In: *Discrete and Continuous Dynamical Systems-S* 15.9 (2022).
- [122] William D Hamilton. “The genetical evolution of social behaviour. II”. In: *Journal of theoretical biology* 7.1 (1964), pp. 17–52.
- [123] Anna MF Harts, Kim Jaatinen, and Hanna Kokko. “Evolution of natal and breeding dispersal: when is a territory an asset worth protecting?” In: *Behavioral Ecology* 27.1 (2016), pp. 287–294.

-
- [124] John Haslett et al. “Modelling excess zeros in count data: A new perspective on modelling approaches”. In: *International statistical review* 90.2 (2022), pp. 216–236.
- [125] Michael P Hassell, Hugh N Comins, and Robert M May. “Spatial structure and chaos in insect population dynamics”. In: *Nature* 353.6341 (1991), pp. 255–258.
- [126] Michael P Hassell, John H Lawton, and RM May. “Patterns of dynamical behaviour in single-species populations”. In: *The Journal of Animal Ecology* (1976), pp. 471–486.
- [127] Alan Hastings and P van den Driessche. “Inequalities on the spectral abscissa for matrices arising in a stage-structured population model”. In: *Linear Algebra and its Applications* 494 (2016), pp. 90–104.
- [128] Alan Hastings et al. “Chaos in ecology: is mother nature a strange attractor?” In: *Annual review of ecology and systematics* (1993), pp. 1–33.
- [129] Alan Hastings et al. “Effects of stochasticity on the length and behaviour of ecological transients”. In: *Journal of the Royal Society Interface* 18.180 (2021), p. 20210257.
- [130] Alan Hastings et al. “Transient phenomena in ecology”. In: *Science* 361.6406 (2018), eaat6412.
- [131] Christoph Hauert et al. “Synergy and discounting of cooperation in social dilemmas”. In: *Journal of theoretical biology* 239.2 (2006), pp. 195–202.
- [132] Mark Hebblewhite et al. “Density-independent predation affects migrants and residents equally in a declining partially migratory elk population”. In: *Oikos* 127.9 (2018), pp. 1304–1318.
- [133] Julie A Heinrichs, Joshua J Lawler, and Nathan H Schumaker. “Intrinsic and extrinsic drivers of source–sink dynamics”. In: *Ecology and evolution* 6.4 (2016), pp. 892–904.
- [134] Rob Hengeveld. *Dynamics of biological invasions*. Springer Science & Business Media, 1989.
- [135] JM Hilbe. *Modeling Count Data*. Cambridge University Press, 2014.
- [136] Diederich Hinrichsen and Anthony J Pritchard. *Mathematical systems theory I: modelling, state space analysis, stability and robustness*. Vol. 48. Springer Science & Business Media, 2005.
- [137] Roger A Horn and Charles R Johnson. *Matrix Analysis*. Cambridge University Press, 2012.

- [138] Geoffrey R Hosack, Gareth W Peters, and Keith R Hayes. “Estimating density dependence and latent population trajectories with unknown observation error”. In: *Methods in Ecology and Evolution* 3.6 (2012), pp. 1028–1038.
- [139] Sarah R Hoy et al. “Negative frequency-dependent prey selection by wolves and its implications on predator–prey dynamics”. In: *Animal Behaviour* 179 (2021), pp. 247–265.
- [140] Matthew C Hutchinson et al. “Seeing the forest for the trees: Putting multilayer networks to work for community ecology”. In: *Functional Ecology* 33.2 (2019), pp. 206–217.
- [141] Rolf Anker Ims. “On the adaptive value of reproductive synchrony as a predator-swamping strategy”. In: *The American Naturalist* 136.4 (1990), pp. 485–498.
- [142] The MathWorks Inc. *MATLAB version: 9.13.0 (R2022b)*. Natick, Massachusetts, United States, 2024.
- [143] Esperanza C Iranzo et al. “Diffusive dispersal in a growing ungulate population: guanaco expansion beyond the limits of protected areas”. In: *Mammal research* 63 (2018), pp. 185–196.
- [144] Anthony R Ives, Karen C Abbott, and Nicolas L Ziebarth. “Analysis of ecological time series with ARMA (p, q) models”. In: *Ecology* 91.3 (2010), pp. 858–871.
- [145] Hai-Yang Jin and Zhi-An Wang. “Global stability of prey-taxis systems”. In: *Journal of Differential Equations* 262.3 (2017), pp. 1257–1290.
- [146] Wen Jin, Hal L Smith, and Horst R Thieme. “Persistence versus extinction for a class of discrete-time structured population models”. In: *Journal of mathematical biology* 72 (2016), pp. 821–850.
- [147] Charles R Johnson. “Sufficient conditions for D-stability”. In: *Journal of Economic Theory* 9.1 (1974), pp. 53–62.
- [148] Christopher N Johnson, Karl Vernes, and Alison Payne. “Demography in relation to population density in two herbivorous marsupials: testing for source–sink dynamics versus independent regulation of population size”. In: *Oecologia* 143 (2005), pp. 70–76.
- [149] E Jourdain and D Vongraven. “Humpback whale (*Megaptera novaeangliae*) and killer whale (*Orcinus orca*) feeding aggregations for foraging on herring (*Clupea harengus*) in Northern Norway”. In: *Mammalian Biology* 86.1 (2017), pp. 27–32.
- [150] Emily L Kang and Noel Cressie. “Bayesian inference for the spatial random effects model”. In: *Journal of the American Statistical Association* 106.495 (2011), pp. 972–983.

-
- [165] Olga Y Kushel. “Unifying matrix stability concepts with a view to applications”. In: *SIAM Review* 61.4 (2019), pp. 643–729.
- [166] Yuri A Kuznetsov, Iu A Kuznetsov, and Y Kuznetsov. *Elements of applied bifurcation theory*. Vol. 112. Springer, 1998.
- [167] Yousef El-Laham, Mónica Bugallo, and Heather J Lynch. “Switching state-space models for modeling penguin population dynamics”. In: *Environmental and Ecological Statistics* 29.3 (2022), pp. 607–624.
- [168] Edwin van Leeuwen et al. “A generalized functional response for predators that switch between multiple prey species”. In: *Journal of theoretical biology* 328 (2013), pp. 89–98.
- [169] Jussi Lehtonen and Kim Jaatinen. “Safety in numbers: the dilution effect and other drivers of group life in the face of danger”. In: *Behavioral Ecology and Sociobiology* 70 (2016), pp. 449–458.
- [170] Patrick H Leslie. “On the use of matrices in certain population mathematics”. In: *Biometrika* 33.3 (1945), pp. 183–212.
- [171] Chi-Kwong Li and Hans Schneider. “Applications of Perron–Frobenius theory to population dynamics”. In: *Journal of mathematical biology* 44.5 (2002), pp. 450–462.
- [172] Jian Li and Xiang Dong Ye. “Recent development of chaos theory in topological dynamics”. In: *Acta Mathematica Sinica, English Series* 32.1 (2016), pp. 83–114.
- [173] Tien-Yien Li and James A Yorke. “Period three implies chaos”. In: *The theory of chaotic attractors* (2004), pp. 77–84.
- [174] Daniel Liberzon. “Switching in Systems and Control”. In: *Systems & Control: Foundations & Applications*. 2003.
- [175] Erez Lieberman, Christoph Hauert, and Martin A Nowak. “Evolutionary dynamics on graphs”. In: *Nature* 433.7023 (2005), pp. 312–316.
- [176] Fernando Llorente et al. “On the safe use of prior densities for Bayesian model selection”. In: *Wiley Interdisciplinary Reviews: Computational Statistics* 15.1 (2023), e1595.
- [177] Dmitrii Logofet. *Matrices and graphs stability problems in mathematical ecology*. CRC press, 2018.
- [178] Dmitrii O Logofet. “Convexity in projection matrices: projection to a calibration problem”. In: *Ecological Modelling* 216.2 (2008), pp. 217–228.

- [179] Dmitrii O Logofet. “Projection matrices revisited: a potential-growth indicator and the merit of indication”. In: *Journal of Mathematical Sciences* 193 (2013), pp. 671–686.
- [180] Dmitrii O Logofet. “Stronger-than-Lyapunov notions of matrix stability, or how “flowers” help solve problems in mathematical ecology”. In: *Linear algebra and its applications* 398 (2005), pp. 75–100.
- [181] Dmitrii O Logofet and Ekaterina V Lesnaya. “The mathematics of Markov models: what Markov chains can really predict in forest successions”. In: *Ecological modelling* 126.2-3 (2000), pp. 285–298.
- [182] Jürg B Logue et al. “Empirical approaches to metacommunities: a review and comparison with theory”. In: *Trends in ecology & evolution* 26.9 (2011), pp. 482–491.
- [183] Edward N Lorenz. “The problem of deducing the climate from the governing equations”. In: *Tellus* 16.1 (1964), pp. 1–11.
- [184] Dieter Lukas and Tim Clutton-Brock. “Social complexity and kinship in animal societies”. In: *Ecology letters* 21.8 (2018), pp. 1129–1134.
- [185] David J Lunn et al. “WinBUGS—a Bayesian modelling framework: concepts, structure, and extensibility”. In: *Statistics and computing* 10 (2000), pp. 325–337.
- [186] Aleksandr Mikhailovich Lyapunov. “The general problem of the stability of motion”. In: *International journal of control* 55.3 (1992), pp. 531–534.
- [187] Tufail Muhammad Malik. *Microbial quiescence: A survival strategy in environmental stress*. Arizona State University, 2007.
- [188] Julie S Mao et al. “Habitat selection by elk before and after wolf reintroduction in Yellowstone National Park”. In: *The Journal of Wildlife Management* 69.4 (2005), pp. 1691–1707.
- [189] Christian O Marks and Charles D Canham. “A quantitative framework for demographic trends in size-structured populations: analysis of threats to floodplain forests”. In: *Ecosphere* 6.11 (2015), pp. 1–55.
- [190] Oliver Mason, Vahid S Bokharaie, and Robert Shorten. “Stability and D-stability for switched positive systems”. In: *Positive Systems: Proceedings of the third Multidisciplinary International Symposium on Positive Systems: Theory and Applications (POSTA 2009) Valencia, Spain, September 2-4, 2009*. Springer, 2009, pp. 101–109.
- [191] Oliver Mason and Robert Shorten. “On the simultaneous diagonal stability of a pair of positive linear systems”. In: *Linear Algebra and its Applications* 413.1 (2006), pp. 13–23.

- [192] Oliver Mason and Robert Shorten. “Some results on the stability of positive switched linear systems”. In: *2004 43rd IEEE Conference on Decision and Control (CDC)(IEEE Cat. No. 04CH37601)*. Vol. 5. IEEE. 2004, pp. 4601–4606.
- [193] François Massol and Florence Débarre. “Evolution of dispersal in spatially and temporally variable environments: the importance of life cycles”. In: *Evolution* 69.7 (2015), pp. 1925–1937.
- [194] Shuichi Matsumura and Takashi Kobayashi. “A game model for dominance relations among group-living animals”. In: *Behavioral Ecology and Sociobiology* 42 (1998), pp. 77–84.
- [195] Erik Matthysen. “Density-dependent dispersal in birds and mammals”. In: *Ecography* 28.3 (2005), pp. 403–416.
- [196] Robert M May. “Simple mathematical models with very complicated dynamics”. In: *Nature* 261.5560 (1976), pp. 459–467.
- [197] John Maybe and James Quirk. “Qualitative problems in matrix theory”. In: *Siam Review* 11.1 (1969), pp. 30–51.
- [198] Josinaldo Menezes, Enzo Rangel, and B Moura. “Aggregation as an antipredator strategy in the rock-paper-scissors model”. In: *Ecological Informatics* 69 (2022), p. 101606.
- [199] Anna K Miller et al. “The evolutionary ecology of dormancy in nature and in cancer”. In: *Frontiers in Ecology and Evolution* 9 (2021), p. 676802.
- [200] Nicholas J Mills and Wayne M Getz. “Modelling the biological control of insect pests: a review of host-parasitoid models”. In: *Ecological modelling* 92.2-3 (1996), pp. 121–143.
- [201] Niamh Mimmagh et al. “Bayesian multi-species N-mixture models for unmarked animal communities”. In: *Environmental and Ecological Statistics* 29.4 (2022), pp. 755–778.
- [202] Yongyi Min and Alan Agresti. “Random effect models for repeated measures of zero-inflated count data”. In: *Statistical modelling* 5.1 (2005), pp. 1–19.
- [203] Ben A Minter and James P Collins. “Why we need an “ecological ethics””. In: *Frontiers in Ecology and the Environment* 3.6 (2005), pp. 332–337.
- [204] Abhishek Mishra, Partha Pratim Chakraborty, and Sutirth Dey. “Dispersal evolution diminishes the negative density dependence in dispersal”. In: *Evolution* 74.9 (2020), pp. 2149–2157.
- [205] Geert Molenberghs, Geert Verbeke, and Clarice GB Demétrio. “An extended random-effects approach to modeling repeated, overdispersed count data”. In: *Lifetime data analysis* 13 (2007), pp. 513–531.

- [206] Geert Molenberghs et al. “A Family of Generalized Linear Models for Repeated Measures with Normal and Conjugate Random Effects”. In: *Statistical Science* 25.3 (2010), pp. 325–347. ISSN: 08834237.
- [207] Raphaëlle Momal, Stéphane Robin, and Christophe Ambroise. “Accounting for missing actors in interaction network inference from abundance data”. In: *Journal of the Royal Statistical Society Series C: Applied Statistics* 70.5 (2021), pp. 1230–1258.
- [208] William Murdoch, Cheryl J Briggs, and Susan Swarbrick. “Host suppression and stability in a parasitoid-host system: experimental demonstration”. In: *science* 309.5734 (2005), pp. 610–613.
- [209] D Nestel, J Carvalho, and E Nemny-Lavy. “The spatial dimension in the ecology of insect pests and its relevance to pest management”. In: *Insect pest management: field and protected crops*. Springer, 2004, pp. 45–63.
- [210] Arnold J. Nicholson and V. A. Bailey. “The Balance of Animal Populations.—Part I.” In: *Journal of Zoology* 105 (1935), pp. 551–598.
- [211] Martin A Nowak et al. “Evolving cooperation”. In: *Journal of theoretical biology* 299.0 (2012), pp. 1–8.
- [212] Robert O’Hara and Johan Kotze. “Do not log-transform count data”. In: *Nature Precedings* (2010), pp. 1–1.
- [213] Anthony O’Hagan and Luis Pericchi. “Bayesian heavy-tailed models and conflict resolution: A review”. In: *Brazilian Journal of Probability and Statistics* 26.4 (2012), pp. 372–401. DOI: 10.1214/11-BJPS164.
- [214] Akira Okubo, Simon A Levin, et al. *Diffusion and ecological problems: modern perspectives*. Vol. 14. Springer, 2001.
- [215] Thiago de Paula Oliveira and Rafael de Andrade Moral. “Global short-term forecasting of COVID-19 cases”. In: *Scientific reports* 11.1 (2021), p. 7555.
- [216] Peter J Olsoy et al. “Quantifying the effects of deforestation and fragmentation on a range-wide conservation plan for jaguars”. In: *Biological Conservation* 203 (2016), pp. 8–16.
- [217] Daniel Oro. *Perturbation, behavioural feedbacks, and population dynamics in social animals: when to leave and where to go*. Oxford University Press, USA, 2020.
- [218] Otso Ovaskainen et al. “How are species interactions structured in species-rich communities? A new method for analysing time-series data”. In: *Proceedings of the Royal Society B: Biological Sciences* 284.1855 (2017), p. 20170768.

- [219] Gabriel R Palma et al. “Pattern-based prediction of population outbreaks”. In: *Ecological Informatics* 77 (2023), p. 102220.
- [220] Scott D Peacor. “Positive effect of predators on prey growth rate through induced modifications of prey behaviour”. In: *Ecology Letters* 5.1 (2002), pp. 77–85.
- [221] James B Pearson, J Ryan Bellmore, and Jason B Dunham. “Controlling invasive fish in fluctuating environments: Model analysis of common carp (*Cyprinus carpio*) in a shallow lake”. In: *Ecosphere* 13.5 (2022), e3985.
- [222] Rolf O Peterson et al. “Trophic cascades in a multicausal world: Isle Royale and Yellowstone”. In: *Annual Review of Ecology, Evolution, and Systematics* 45.1 (2014), pp. 325–345.
- [223] Sofia H Piltz, Mason A Porter, and Philip K Maini. “Prey switching with a linear preference trade-off”. In: *SIAM Journal on Applied Dynamical Systems* 13.2 (2014), pp. 658–682.
- [224] Stefano Piraino et al. “Reversing the life cycle: medusae transforming into polyps and cell transdifferentiation in *Turritopsis nutricula* (Cnidaria, Hydrozoa)”. In: *The Biological Bulletin* 190.3 (1996), pp. 302–312.
- [225] Martyn Plummer et al. “JAGS: A program for analysis of Bayesian graphical models using Gibbs sampling”. In: *Proceedings of the 3rd international workshop on distributed statistical computing*. Vol. 124. 125.10. Vienna, Austria. 2003, pp. 1–10.
- [226] James A Powell and Barbara J Bentz. “Phenology and density-dependent dispersal predict patterns of mountain pine beetle (*Dendroctonus ponderosae*) impact”. In: *Ecological Modelling* 273 (2014), pp. 173–185.
- [227] Christina Marie Prokopenko. “Hungry wolves and dangerous prey: a tale of prey switching”. PhD thesis. Memorial University of Newfoundland, 2022.
- [228] Timothy Prout and Frances McChesney. “Competition among immatures affects their adult fertility: population dynamics”. In: *The American Naturalist* 126.4 (1985), pp. 521–558.
- [229] H Ronald Pulliam. “Sources, sinks, and population regulation”. In: *The American Naturalist* 132.5 (1988), pp. 652–661.
- [230] RJ Putman. “Ethical considerations and animal welfare in ecological field studies”. In: *Biodiversity & Conservation* 4 (1995), pp. 903–915.
- [231] Lucie Raymond, Manuel Plantegenest, and Aude Vialatte. “Migration and dispersal may drive to high genetic variation and significant genetic mixing: the case of two agriculturally important, continental hoverflies (*E pisyrrhus balteatus* and *S phaerophoria scripta*)”. In: *Molecular ecology* 22.21 (2013), pp. 5329–5339.

- [232] Carolina Reigada et al. “Metapopulation dynamics on ephemeral patches”. In: *The American Naturalist* 185.2 (2015), pp. 183–195.
- [233] Francis J Richards. “A flexible growth function for empirical use”. In: *Journal of experimental Botany* 10.2 (1959), pp. 290–301.
- [234] William Edwin Ricker. “Stock and recruitment”. In: *Journal of the Fisheries Board of Canada* 11.5 (1954), pp. 559–623.
- [235] D Scott Rinnan. “The dispersal success and persistence of populations with asymmetric dispersal”. In: *Theoretical ecology* 11.1 (2018), pp. 55–69.
- [236] Dimitris Rizopoulos, Geert Verbeke, and Geert Molenberghs. “Multiple-imputation-based residuals and diagnostic plots for joint models of longitudinal and survival outcomes”. In: *Biometrics* 66.1 (2010), pp. 20–29.
- [237] António MM Rodrigues and Rufus A Johnstone. “Evolution of positive and negative density-dependent dispersal”. In: *Proceedings of the Royal Society B: Biological Sciences* 281.1791 (2014), p. 20141226.
- [238] Tanya L Rogers, Bethany J Johnson, and Stephan B Munch. “Chaos is not rare in natural ecosystems”. In: *Nature ecology & evolution* 6.8 (2022), pp. 1105–1111.
- [239] Gregory Roth, Paul L Salceanu, and Sebastian J Schreiber. “Robust permanence for ecological maps”. In: *SIAM Journal on Mathematical Analysis* 49.5 (2017), pp. 3527–3549.
- [240] Volker HW Rudolf and Nick L Rasmussen. “Population structure determines functional differences among species and ecosystem processes”. In: *Nature Communications* 4.1 (2013), p. 2318.
- [241] Alfonso Ruiz-Herrera. “Analysis of dispersal effects in metapopulation models”. In: *Journal of mathematical biology* 72 (2016), pp. 683–698.
- [242] Alfonso Ruiz-Herrera. “Metapopulation dynamics and total biomass: understanding the effects of diffusion in complex networks”. In: *Theoretical population biology* 121 (2018), pp. 1–11.
- [243] RA Satnoianu and P van den Driessche. “Some remarks on matrix stability with application to Turing instability”. In: *Linear algebra and its applications* 398 (2005), pp. 69–74.
- [244] Manu E Saunders. “Resource connectivity for beneficial insects in landscapes dominated by monoculture tree crop plantations”. In: *International journal of agricultural sustainability* 14.1 (2016), pp. 82–99.
- [245] Torbjörn von Schantz. “Spacing strategies, kin selection, and population regulation in altricial vertebrates”. In: *Oikos* (1984), pp. 48–58.

-
- [246] Judith Schneider et al. “Molecular assessment of dietary variation in neighbouring primate groups”. In: *Methods in Ecology and Evolution* 14.8 (2023), pp. 1925–1936.
- [247] Sebastian J Schreiber. “Allee effects, extinctions, and chaotic transients in simple population models”. In: *Theoretical population biology* 64.2 (2003), pp. 201–209.
- [248] Sebastian J Schreiber. “Chaos and population disappearances in simple ecological models”. In: *Journal of Mathematical Biology* 42 (2001), pp. 239–260.
- [249] Sebastian J Schreiber. *Coexistence in the face of uncertainty*. Springer, 2017.
- [250] Sarah A Scriven et al. “Barriers to dispersal of rain forest butterflies in tropical agricultural landscapes”. In: *Biotropica* 49.2 (2017), pp. 206–216.
- [251] AN Sharkowskii. “Co-existence of the cycles of a continuous mapping of the line into itself”. In: *Ukrain. MZ* 16.1 (1964).
- [252] Allison K Shaw and Iain D Couzin. “Migration or residency? The evolution of movement behavior and information usage in seasonal environments”. In: *The American Naturalist* 181.1 (2013), pp. 114–124.
- [253] Daniel Simberloff. “Invasive species”. In: *Conservation biology for all* 1 (2010), pp. 131–152.
- [254] Douglas W Smith, Daniel R Stahler, and Daniel R MacNulty. *Yellowstone wolves: Science and discovery in the world’s first national park*. University of Chicago Press, 2020.
- [255] Hal L Smith and Horst R Thieme. *Dynamical systems and population persistence*. Vol. 118. American Mathematical Soc., 2011.
- [256] Iain Stott et al. “On reducibility and ergodicity of population projection matrix models”. In: *Methods in Ecology and Evolution* 1.3 (2010), pp. 242–252.
- [257] David L Strayer et al. “Boom-bust dynamics in biological invasions: towards an improved application of the concept”. In: *Ecology letters* 20.10 (2017), pp. 1337–1350.
- [258] Steven H Strogatz. *Nonlinear dynamics and chaos: with applications to physics, biology, chemistry, and engineering*. CRC press, 2018.
- [259] Lauren L Sullivan et al. “Density dependence in demography and dispersal generates fluctuating invasion speeds”. In: *Proceedings of the National Academy of Sciences* 114.19 (2017), pp. 5053–5058.
- [260] Samir Suweis et al. “Effect of localization on the stability of mutualistic ecological networks”. In: *Nature communications* 6.1 (2015), p. 10179.

-
- [261] Aimee Tallian et al. “Predator foraging response to a resurgent dangerous prey”. In: *Functional Ecology* 31.7 (2017), pp. 1418–1429.
- [262] Yun Tao et al. “Landscape fragmentation overturns classical metapopulation thinking”. In: *Proceedings of the National Academy of Sciences* 121.20 (2024), e2303846121.
- [263] R Core Team et al. “R: A language and environment for statistical computing”. In: *Foundation for Statistical Computing, Vienna, Austria* (2013).
- [264] Gerald Teschl. “Topics in linear and nonlinear functional analysis”. In: *American Mathematical Society* (2020).
- [265] Peter F Thall and Stephen C Vail. “Some covariance models for longitudinal count data with overdispersion”. In: *Biometrics* (1990), pp. 657–671.
- [266] Horst R Thieme. “Discrete-time population dynamics of spatially distributed semelparous two-sex populations”. In: *Journal of Mathematical Biology* 83.2 (2021), p. 18.
- [267] Samuel Thomas and Wanzhu Tu. “Learning Hamiltonian Monte Carlo in R”. In: *The American Statistician* 75.4 (2021), pp. 403–413.
- [268] Eva Thomine et al. “Highly diversified crop systems can promote the dispersal and foraging activity of the generalist predator *Harmonia axyridis*”. In: *Entomol. Gen* 40.2 (2020), pp. 133–145.
- [269] Pat Touhey. “Yet another definition of chaos”. In: *The American Mathematical Monthly* 104.5 (1997), pp. 411–414.
- [270] Arne Traulsen and Christoph Hauert. “Stochastic evolutionary game dynamics”. In: *Reviews of nonlinear dynamics and complexity* 2 (2009), pp. 25–61.
- [271] Justin MJ Travis, David J Murrell, and Calvin Dytham. “The evolution of density-dependent dispersal”. In: *Proceedings of the Royal Society of London. Series B: Biological Sciences* 266.1431 (1999), pp. 1837–1842.
- [272] Justin MJ Travis et al. “Accelerating invasion rates result from the evolution of density-dependent dispersal”. In: *Journal of theoretical biology* 259.1 (2009), pp. 151–158.
- [273] Zivanai Tsvuura et al. “Predator satiation and recruitment in a mast fruiting monocarpic forest herb”. In: *Annals of botany* 107.3 (2011), pp. 379–387.
- [274] Alan Mathison Turing. “The chemical basis of morphogenesis”. In: *Bulletin of Mathematical Biology* 52 (1952), pp. 153–197.

- [275] George AK Van Voorn and Bob W Kooi. “Combining bifurcation and sensitivity analysis for ecological models: Model analysis, and the allegory of the caveEcological Dynamics”. In: *The European Physical Journal Special Topics* 226 (2017), pp. 2101–2118.
- [276] John Vandermeer. “Indirect mutualism: variations on a theme by Stephen Levine”. In: *The American Naturalist* 116.3 (1980), pp. 441–448.
- [277] Nathan Varley and Mark S Boyce. “Adaptive management for reintroductions: updating a wolf recovery model for Yellowstone National Park”. In: *Ecological Modelling* 193.3-4 (2006), pp. 315–339.
- [278] Tom Vogwill, Andy Fenton, and Michael A Brockhurst. “Dispersal and natural enemies interact to drive spatial synchrony and decrease stability in patchy populations”. In: *Ecology Letters* 12.11 (2009), pp. 1194–1200.
- [279] Irina Vortkamp et al. “Multiple attractors and long transients in spatially structured populations with an Allee effect”. In: *Bulletin of mathematical biology* 82 (2020), pp. 1–21.
- [280] John A Vucetich, Rolf O Peterson, and Carrie L Schaefer. “The effect of prey and predator densities on wolf predation”. In: *Ecology* 83.11 (2002), pp. 3003–3013.
- [281] JC Wakefield et al. “Bayesian analysis of linear and non-linear population models by using the Gibbs sampler”. In: *Journal of the Royal Statistical Society: Series C (Applied Statistics)* 43.1 (1994), pp. 201–221.
- [282] Zhen Wang, Attila Szolnoki, and Matjaž Perc. “Rewarding evolutionary fitness with links between populations promotes cooperation”. In: *Journal of theoretical biology* 349 (2014), pp. 50–56.
- [283] Easton R White and Alan Hastings. “Seasonality in ecology: Progress and prospects in theory”. In: *Ecological Complexity* 44 (2020), p. 100867.
- [284] KAJ White and CA Gilligan. “Spatial heterogeneity in three species, plant–parasite–hyperparasite, systems”. In: *Philosophical Transactions of the Royal Society of London. Series B: Biological Sciences* 353.1368 (1998), pp. 543–557.
- [285] Jennifer L Williams and Jonathan M Levine. “Experimental evidence that density dependence strongly influences plant invasions through fragmented landscapes”. In: *Ecology* 99.4 (2018), pp. 876–884.
- [286] Christopher C Wilmers et al. “Trophic facilitation by introduced top predators: grey wolf subsidies to scavengers in Yellowstone National Park”. In: *Journal of Animal Ecology* 72.6 (2003), pp. 909–916.

-
- [287] Russell D Wolfinger. “Heterogeneous variance: covariance structures for repeated measures”. In: *Journal of agricultural, biological, and environmental statistics* (1996), pp. 205–230.
- [288] Abdul-Aziz Yakubu and Carlos Castillo-Chavez. “Interplay between local dynamics and dispersal in discrete-time metapopulation models”. In: *Journal of theoretical biology* 218.3 (2002), pp. 273–288.
- [289] Janica Ylikarjula et al. “Effects of patch number and dispersal patterns on population dynamics and synchrony”. In: *Journal of Theoretical Biology* 207.3 (2000), pp. 377–387.
- [290] P Yodzis. “The compartmentation of real and assembled ecosystems”. In: *The American Naturalist* 120.5 (1982), pp. 551–570.
- [291] Yuval R Zelnik et al. “How collectively integrated are ecological communities?” In: *Ecology Letters* 27.1 (2024), e14358.
- [292] Can Zhou, Masami Fujiwara, and William E Grant. “Finding regulation among seemingly unregulated populations: a practical framework for analyzing multivariate population time series for their interactions”. In: *Environmental and Ecological Statistics* 23 (2016), pp. 181–204.
- [293] Ying Zhou and Mark Kot. “Discrete-time growth-dispersal models with shifting species ranges”. In: *Theoretical Ecology* 4 (2011), pp. 13–25.